Novel approaches to understanding hENT2 and hENT2-related proteins: From novel nuclear variants to global networks

Nuevos enfoques sobre el estudio de hENT2 y proteínas relacionadas: desde nuevas variantes nucleares a redes globales

Natàlia Grañé Boladeras

NOVEL APPROACHES TO UNDERSTANDING hENT2 AND hENT2-RELATED PROTEINS: FROM NOVEL NUCLEAR VARIANTS TO GLOBAL NETWORKS

NATÀLIA GRAÑÉ BOLADERAS

BARCELONA 2012

DEPARTAMENT DE BIOQUÍMICA I BIOLOGIA MOLECULAR
FACULTAT DE BIOLOGIA
UNIVERSITAT DE BARCELONA

NOVEL APPROACHES TO UNDERSTANDING hENT2 AND hENT2-RELATED PROTEINS: FROM NOVEL NUCLEAR VARIANTS TO GLOBAL NETWORKS

"Nuevos enfoques sobre el estudio de hENT2 y proteínas relacionadas: desde nuevas variantes nucleares a redes globales"

Natàlia Grañé Boladeras

Setembre 2012

MEMÒRIA PER OPTAR AL GRAU DE DOCTORA PER
LA UNIVERSITAT DE BARCELONA

PROGRAMA DE DOCTORAT EN BIOMEDICINA
DEPARTAMENT DE BIOQUÍMICA I BIOLOGIA MOLECULAR
FACULTAT DE BIOLOGIA
UNIVERSITAT DE BARCELONA

PRESENTADA PER
NATÀLIA GRAÑÉ BOLADERAS

La interessada,

Natàlia Grañé Boladeras

Vistiplau del director,

Dr. MARÇAL PASTOR ANGLADA
Catedràtic de Bioquímica i Biologia Molecular
Departament de Bioquímica i Biologia Molecular
Universitat de Barcelona

I, a vegades, ens en sortim.
I, a vegades, contra tot pronòstic
una gran bestiesa capgira allò
que crèiem lògic,
Tot fent evident,
que per un moment,
ens en sortim.

- Manel - *Captatio Benevolentiae*

A la meva familia

A la meva mare

Des de que vaig començar a escriure la tesis, ara ja fa uns mesos, he estat evitant aquest moment de sentar-me tranquilament i pensar en lo que han sigut i tot lo que he viscut durant aquests últims 5 anys. Ara que ja no tinc més excuses, em tremola el cos només de pensar en tota la gent amb qui he compartit les diferents etapes, les sensacions viscudes, tan alegries com frustracions, i sincerament puc dir que avui dia sóc molt feliç d'haver viscut aquesta aventura. Així que gràcies a tots vosaltres que ho heu fet possible.

En primer lloc, moltes gràcies a tu, Marçal, per haver-me donat la oportunitat i haver-me "enredat" en aquesta aventura. Moltes gràcies per la teva confiança i el teu suport, crec que n'he après molt de tu, i no només com a científic. Espero que tu també n'estiguis tant content com jo i que ens retrobem en el futur ja sigui col·laborant en ciència o bé fent un cafè (o un "poutine" si et deixes "caure" per Toronto). Gràcies per tot, de debò.

Ara ve lo pitjor, recordar tota la gent que he tingut al meu voltant durant tant de temps i intentar no posar-me massa sentimental. Difícil! Recordo quan vaig començar al lab fent el màster. Recordo el trio Pedro-Ekaitz-Miriam i el bon rotllo que portaveu al lab. Crec que si no fos per vosaltres, mai m'hagués quedat a continuar la tesis. Primer per la vostra qualitat científica, crec que sou genials i que n'he après molt de vosaltres, sobretot per les ganes i l'entusiasme que hi poseu. I després, per la vostra alegria i companyerisme (quantes vegades he creuat la porta del lab demanant-vos socors!). Sens dubte vau ser el millor punt de partida.

Isa, Laia, Itzi… Realment us he trobat molt a faltar aquests últims temps! A part de ser bones companyes, sou unes grans amigues i m'heu alegrat els dies al lab, més del que us imagineu. Des de compartir receptes de cuina, a anar a esquiar tots plegats. Quan miro totes les fotos que tinc, no puc parar de somriure recordant els bons moments. Espero que a totes us vagi tot molt bé en les vostres noves etapes i que ens puguem retrobar en algun moment, en alguna part del món.

Estefi!! Gracias por enseñarme tanto desde el principio, fuiste una gran mentora! Ahora que soy yo la que tiene que explicarle a los "niños" como clonar, me doy cuenta de que sé muchísimo gracias a ti. Estoy muy contenta por vosotros dos y por la nueva etapa que empezasteis, que aunque sean tiempos difíciles, sé que os va a ir todo cada vez mejor. Lore, miLore!! Que puedo decir de ti y sólo ocupar unas líneas?? Intentando ser breve, creo que eres una magnífica persona, excelente compañera de trabajo pero aun mejor amiga! Tienes un gran corazón y tu sonrisa (y risa!) es oro! No los pierdas nunca. Sandreta! Que hagués fet sense tu?? Gràcies per ser tan bona amiga, per tot el suport i per tot el bon vi compartit. Hem viscut grans moments que espero que puguem repetir. Cris!! He rigut tant amb tu!! M'encanta la teva manera de ser, tan natural, sense complexes i tan bona persona. És un luxe tenir-te de companya i amiga. Yeral! La millor col·laboració de RST sens dubte! Frescura, bon humor i hard-work, el cocktail perfecte. Paula, la nota de "color" del lab. Gracias

por tu toque distinto y por tu carácter reposado. Ingrid, sin duda el lab no seria lo mismo sin ti. Gracias por cuidar de todos nosotros cada día.

Valerique, mi gordita! Que decir que no sepas ya? Que te quiero mil, que eres la mejor amiga que se pueda tener y que echo muchísimo de menos nuestras bravas con Voll-Damn! Porqué diablos no las importan aquí?? Igualmente, no seria lo mismo sin ti ;) Lo mismo digo para ti, Isa ("mi Isa" - como se te conoce en el lab). Te echo muchísimo de menos, y solo puedo decirte que gracias, infinitas gracias por ser tan buena amiga (una hermana) durante tantos años. Son muchísimas aventuras vividas juntas e infinitos buenos momentos para recordar. Gracias por haberlos vivido conmigo.

Una no estaria tan a gust a casa si no tingués uns bons veïns, i per sort, nosaltres hem tingut dels millors. Gràcies a tothom del departament, des de la Raquel i el Toni que fan que "màgicament" tot funcioni, a tots els companys de TEC, GMP, MP, TAM, Integrativa i Insulina (sobretodo tú, Vicente, por ser un gran amigo y por todos los momentos vividos dentro y fuera del lab). Un plaer haver compartit la "casa" amb vosaltres durant tot aquest temps.

As all of you know, I had the chance to spend my last year of thesis in Toronto (Canada) and I will actually stay here for the next coming years. So, I have a lot of people here to thank for all the support during all this time. Fist of all, Imogen, a huge thanks for all your support since the very first day, not only in science but also in our personal adventure here in Canada. I do really admire you as a professional, but also as a person. I'm very thankful for the opportunity you give me to continue in this great team and keep on learning from all of you. Zlatina, you already know how thankful we are for all your love and support. It's so wonderful to have a canadian mum that takes care of us. Glad to have you and being part of our new family.

Alex-B & Alex-C!! Guys! You're such great partners! Really, you make my life so easy and so happy. It's a pleasure to work with you cause you're great scientists but also wonderful people (I will never forget that day Alex gave me his cells cause mine were contaminated and I had " a thesis to finish"). So happy to spend some more years with you :) My "kids": Nima, Linda, Maliha & Katerina (If you don't know it yet, I always call you "kids" with all my affection). It's a pleasure to work with you. You all are adorable and great people. A pity that eventually you will leave, but I'm sure you'll be totally successful in your new stages. Nicole, thanks so much for all this time together and all the chatting and laughing shared in "the office". So happy about your new position at YorkU, that's just the beginning of a great career, no doubt! Maria Cristina, so glad you're back to Toronto. This is gonna be a great team definitely! Declan, thank you too for all your help and all the struggling for make the things work. I know we'll get those wonderful results we expect ;)

The same way I thanked my spanish friends and family, I wanna thank my special people in Canada. That's you guys! Graham & Fiona… Thanks so so so much for making our life in Toronto so wonderful! It wouldn't be the same without you. You're one of the main reasons we wanna stay here, cause we love the new family we got here, and you're part of the core. So a very sincere thank you for all your support and love, you're amazing people and we love you.

Finalment, res d'això hagués passat de no ser per la fantàstica família que tinc. Els meus germans per haver sigut sempre al meu costat, per tot el vostre suport i amor incondicional. Sempre heu sigut el meu model a seguir. Estic tan orgullosa de vosaltres, de les persones tan fantàstiques que sou, i me'n alegro moltíssim de que els dos tingueu aquestes grans companyes, Geni (+1) i Vanessa. La única part dolenta de tot plegat és que hagi d'estar lluny de vosaltres, així que ja podeu anar comprant bitllets d'avió! Els meus pares… que puc dir sense posar-me a plorar com una bleda. Us trobo moltíssim a faltar!! No sé si alguna vegada he tingut la ocasió de dir-vos-ho (val la pena fer una tesis només per això), però sou els millors pares que es pot tenir. Per ser tan lluitadors, per no haver-vos rendit mai, per haver-nos-ho donat tot i estimar-nos sense condicions. Crec que podeu estar orgullosos de la família que tenim, és fantàstica. I personalment, mai podré deixar d'agrair-vos tot el vostre suport i amor, per haver estat sempre al meu costat, en lo bo i en lo dolent. I per haver-me ensenyat a ser la persona que sóc avui dia. Us estimo.

Y a ti Luis, mi cielo. No hay palabras para decir todo lo que siento y todo lo que significas para mi. Eres mi amigo, mi amor y mi mayor apoyo. Desde luego, nada de esto valdría la pena si no lo pudiese compartir contigo. Gracias por todo este tiempo a mi lado, por todo el cariño, por todos los ánimos, sobretodo en la recta final. Me haces ser mejor persona. Te quiero.

List of figures

List of tables

.index

I. Introduction

1 BIOLOGICAL RELEVANCE OF NUCLEOSIDES

Nucleosides are glycosylamines consisting of a nucleobase bound to a ribose or deoxyribose sugar via a beta-glycosidic bond (King *et al*. 2006). Nucleosides are named according to the base they contain, either a purine (adenine, guanine or hypoxanthine) or a pyrimidine (cytosine, thymine or uracil). Purine nucleosides are adenosine, guanosine and inosine, while pyrimidine nucleosides are cytidine, thymidine and uridine (figure 1). A nucleoside differs from a nucleotide in lacking a phosphate. Nucleosides can be phosphorylated by specific kinases in the cell on the primary alcohol group of the sugar, producing nucleotides, which are the molecular building-blocks of DNA and RNA (Kalckar 1950).

Nucleosides are molecules of remarkable importance for the cell due to the several essential processes that are involved in. Scientific interest in nucleosides dates from 1920s when Cerecedo (1927) conducted studies on thymidine and uracil metabolism. Since then, nucleoside research has been diversified to understand their role in the purinergic signalling via adenosine receptors (Geiger *et al.* 1985; Endres *et al*. 2004; Aymerich *et al*. 2005), the energetic metabolism involving ATP and GTP (Griffith & Jarvis 1996; Baldwin *et al*. 1999; Cabrita *et al*. 2002; Kong *et al*. 2004), neuronal and cardioprotection modulated by adenosine during periods of hypoxia or ischemia (Angelakos & Glassman 1961; Rose *et al*. 2010; Takahashi *et al*. 2010), and nucleoside-derived drugs as therapeutic agents in anticancer and antiviral treatments (Wiley *et al*. 1982; Pastor-Anglada *et al*. 1998; Xia *et al.* 2007).

Nucleos(t)ides can be produced by *de novo* synthesis pathways, in particular in the liver, but they are more abundantly supplied via ingestion and digestion of nucleic acids, also known as the salvage pathway (Cabrita *et al*. 2002). *De novo* synthesis is an anabolic route that represents a high cost of energy to the cell and there are certain cell types that lack that pathway, such as protozoan parasites, mammalian enterocytes or bone marrow cells (King *et al.* 2006; Cui *et al*. 2001; Leung *et al*. 2001). Therefore, the salvage pathway acquires a crucial role as the main via of entrance of nucleosides (Murray 1971).

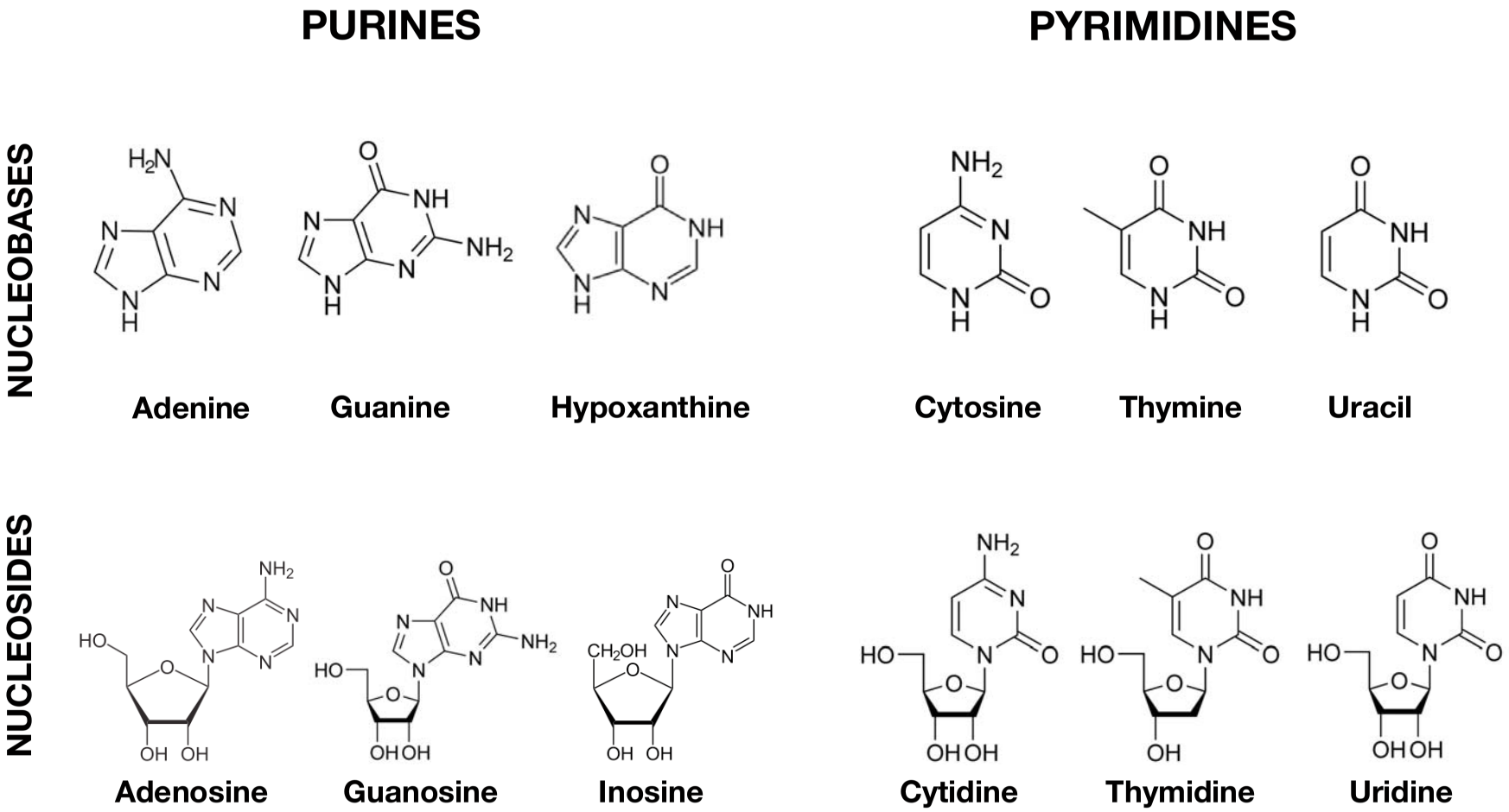

Figure 1. The purine and pyrimidine nucleobases and nucleosides. Purine nucleobases are adenine, guanine and hypoxanthine while purine nucleosides are adenosine, guanosine and inosine. Pyrimidine nucleobases are cytosine, thymine and uracil while pyrimidine nucleosides are cytidine, thymidine and uridine.

In the salvage pathway, after degradation of nucleic acids obtained through diet or already existing in the organism, nucleotides are broken down into molecules of nucleosides and phosphate by membrane-bound and soluble nucleotidases, which are present at the cell surface and the extracellular environment (Yegutkin 2008). Given their hydrophilic nature, nucleosides require of specialised class of integral membrane proteins to be internalized and incorporated to the salvage pathway. Those proteins are known as Nucleoside Transporters (NT) (Molina-Arcas *et al*. 2009).

2 NUCLEOSIDE TRANSPORTERS

Nucleoside participation in cell physiology lies on their bioavailability either inside the cell or at the extracellular environment. Modulating nucleoside flux across the plasma membrane is a mechanism to regulate those pathways where nucleosides are involved in. A clear example is the adenosine, a nucleoside that depending on its concentration levels will selectively bind to adenosine receptors, which have different affinity to such substrate. As consequence, adenosine will trigger different pathways and cell responses depending on its presence at the extracellular space (Choi *et al.* 2004; Beal *et al*. 2004; Elwi *et al*. 2006; Naydenova *et al*. 2008; Huber-Ruano *et al*. 2010).

Furthermore, the effectiveness of anticancer and antiviral treatments using nucleoside analogs will also depend on the capacity of the cell to internalize those substrates. This capacity is different depending on the cell type and environmental conditions of the target, conditioning the responsiveness promoted by the treatment (Griffith & Jarvis 1996; Pastor-Anglada *et al.* 2005). Since nucleosides are hydrophilic molecules barely diffused across the plasma membrane, nucleoside transporters become crucial pieces in cell physiology but also as pharmacogenomic targets (Pastor-Anglada *et al.* 2005; King *et al*. 2006; Molina-Arcas *et al*. 2009). These examples illustrate the relevance of the study of nucleoside transporters to understand their nature and figure out their mechanisms of regulation, as well as their expression profiles.

First evidences of nucleoside and nucleobase transporters date back to the 1990s, when multiple carriers were recognized as such, being responsible of either equilibrative facilitated diffusion or concentrative Na^+/co-transport (Griffith & Jarvis 1996). Based on their kinetic features, nucleoside transporters were classified into two different families: the Equilibrative Nucleoside Transporters (ENT), codified by the SLC29 gene family, and the Concentrative Nucleoside Transporters (CNT), codified by the SLC28 gene family. Although both types of proteins apparently transport the same substrates, ENTs and CNTs are structurally unrelated, as we will clarify in the coming sections. In addition, ENT family is restricted to eukaryotes, whereas CNT family members are also found in eubacteria (Griffith & Jarvis 1996; King *et al*. 2006). These transporters also show some differences in substrate selectivity, kinetics, regulation and subcellular distribution, a fact that explains this multiplicity of nucleoside transporters (Zhang *et al*. 2007; Pastor-Anglada *et al*. 2008; Young *et al*. 2008). For instance, in polarized kidney cells, CNTs seem to be localized primarily to the apical membrane, whereas ENTs proteins are mainly basolateral. Such distribution might facilitate the transepithelial flux of nucleosides (Errasti-Murugarren *et al*. 2008; Rius *et al*. 2010).

2.1 CONCENTRATIVE NUCLEOSIDE TRANSPORTERS

The SLC28 gene family codifies for the concentrative nucleoside transporters. Those proteins mediate a secondary active nucleoside transport against its concentration gradient, coupled to a cation symport (Na^+ or H^+) in a unidirectional manner (King *et al*. 2006). Despite five different functional units were initially identified based on their kinetics, only three isoforms have been cloned in mammals to date: CNT1 (Q. Q. Huang *et al*. 1994; Ritzel *et al*. 1997), CNT2 and CNT3 (Ritzel *et al*. 2001; Hu *et al*. 2006).

The main difference among CNTs is their substrate specificity and selectivity. All of them transport uridine with values of the affinity constant (K_m) between 20-80 μM but none is capable of transporting nucleobases (C. Chang *et al*. 2004). CNT1

mediates pyrimidine uptake, while CNT2 internalize purines. On the contrary, CNT3 shows a higher selectivity and transports both purines and pyrimidines (figure 2d). Some studies showed that CNT1 could also translocate adenosine but it is currently believed that this nucleoside would interact with CNT1 and act as inhibitor (Lai *et al*. 2002; Larráyoz *et al*. 2004). Besides differences in substrate selectivity, CNTs also differ in their stoichiometry of sodium ions required for the symport. It has been demonstrated that CNT3 uses two Na^+ per nucleoside translocated (Ritzel *et al*. 2001), while CNT1 and CNT2 activity is coupled to only one cation (Che *et al*. 1995; Larráyoz *et al*. 2004)

CNTs tissue distribution also differs depending on the isoform. CNT1 is predominantly localised in the liver, kidney, intestine and brain (Pennycooke *et al*. 2001). In contrast, CNT2 is broadly distributed, compared to CNT1, and it is also found in heart, skeletal muscle, pancreas, placenta, cervix, prostate and lung. CNT3 has a broad tissue distribution as well and it is localised in mammary glands, pancreas, bone marrow, trachea, intestine, liver, lung, placenta, prostate, testis, brain and heart (Che *et al*. 1995; Gray *et al*. 2004).

2.2 CNT STRUCTURE

First CNTs bidimensional models proposed a 14 transmembrane domain structure with both intracellular N- and C-extremes (Wang *et al*. 1997). Nonetheless, further studies supported the existence of 13 transmembrane domains with a N-linked glycosylation sites within their C-terminal region, which has been the accepted model to date (figure 2a) (J. Wang *et al.* 1997; Hamilton *et al*. 2001; Gray *et al*. 2004). In this model, the N- and C-termini are long sequences that extend into the intracellular and extracellular environments respectively, suggesting a possible region for regulation or even protein-protein interactions (Huber-Ruano *et al*. 2010; Pinilla-Macua *et al*. 2012), although those regions are not present in prokaryotes.

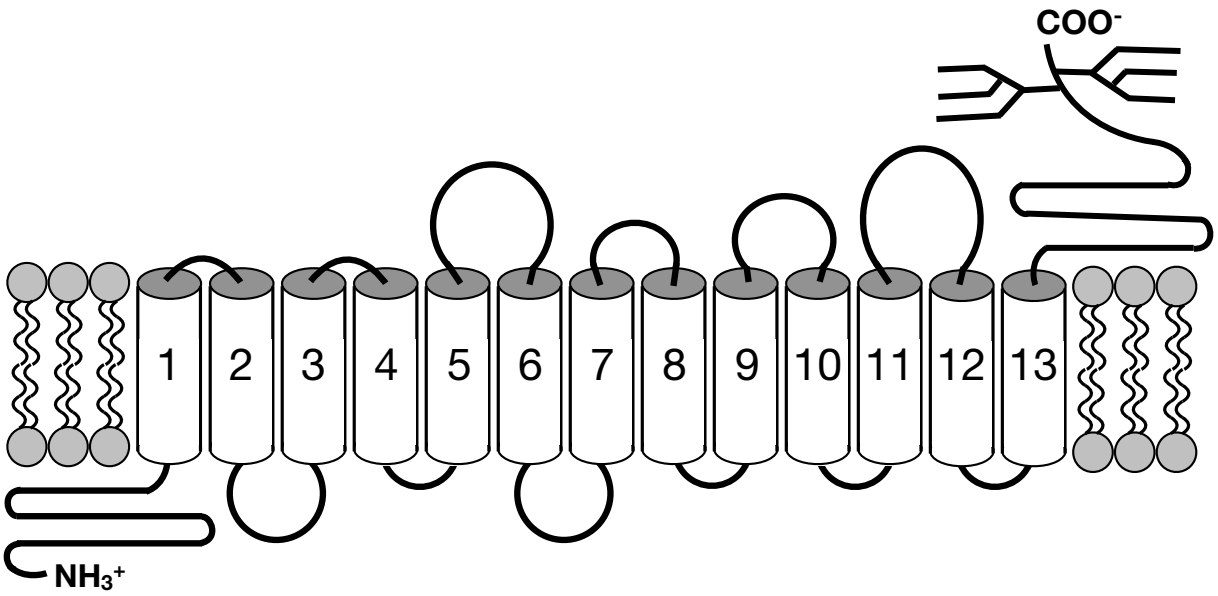

a)

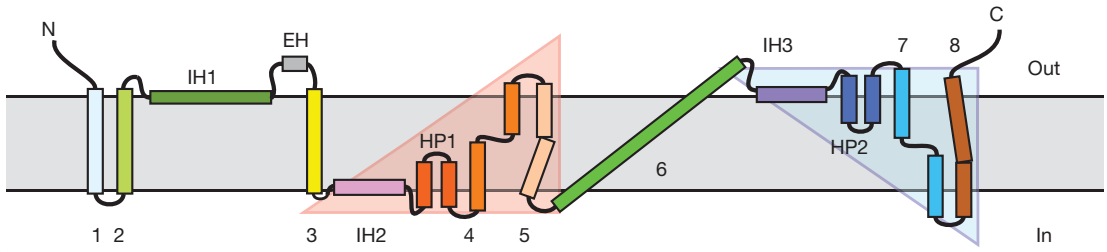

b)

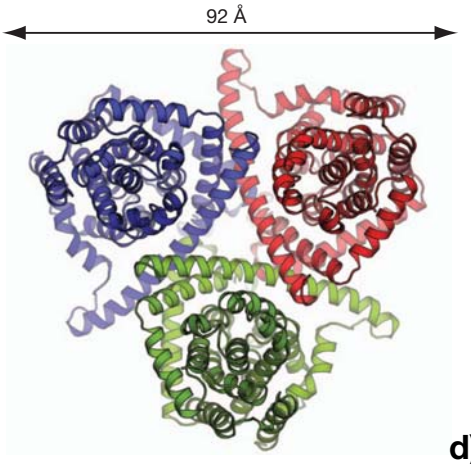

c)

d)

CONCENTRATIVE NUCLEOSIDE TRANSPORTERS		
GENE	**PROTEIN**	**SUBSTRATE (K_m)**
SLC28A1	hCNT1	Urd - 50 μM Tyd - 6 μM Cyd - 34 μM
SLC28A2	hCNT2	Ado - 8 μM Guo - 21 μM Ino - 4.5 μM Urd - 80 μM
SLC28A3	hCNT3	Ado - 15.1 μM Guo - 43 μM Ino - 52.5 μM Urd - 21.6 μM Tyd - 21.2 μM Cyd - 15.4 μM

Figure 2. CNTs structural and kinetic features. (a) The 2D topology proposed for concentrative nucleoside transporters, which contains 13 transmembrane domains as well as the intracellular N- and extracellular glycosylated C-termini. (b) Schematic representation of vcCNT topology. The group of helices under the pink triangular background is related to the group of helices under the cyan triangular background by two-fold pseudo-symmetry, with the symmetry axis parallel to the membrane. (c) Cartoon representation of the vcCNT trimer viewed from the cytoplasm. Individual protomers are coloured blue, red and green. (d) Kinetic properties of the three members of the CNT family. Figures *b* and *c* are adapted from Johnson *et al.* 2012.

Recently, it has been presented the crystal structure of a concentrative nucleoside transporter from *Vibrio cholerae* (39% identical to hCNT3) in complex with uridine, which, like its human orthologues, uses a sodium-ion gradient for nucleoside transport (Johnson *et al*. 2012). This work reveals that the protein contains eight transmembrane helices (figure 2b) and predicts three more amino-terminal transmembrane helices for hCNTs (a total of 11), in contrast of what has been accepted to date. Furthermore, crystallisation of vcCNT provides, for first time, evidences of homotrimers of a nucleoside transporter (figure 2c).

In addition, chimeric and also mutational studies provided relevant information about critical residues for substrate selectivity, such as Ser319, Ser353, Leu354 and Gln320 in CNT1, as well as Gly313, Met314, Thr347 and Val348 in CNT2 (Hamilton *et al*. 2001; J. Wang *et al*. 1997). There is also some data regarding structural elements that may determine CNTs stability, sorting and trafficking to the membrane. For instance, the Gly476 in transmembrane domain 11, the glutamate-enriched region between residues 21 and 28 or the potential protein kinase CK2 domain that led to a loss of brush border-specific sorting (Z. Tackaberry *et al*. 2006; Pinilla-Macua *et al*. 2012)

2.3 EQUILIBRATIVE NUCLEOSIDE TRANSPORTERS

The SLC29 gene family codifies for the equilibrative nucleoside transporters. Those proteins mediate a bidirectional passive nucleoside transport in either direction down the substrate concentration gradient (Cabrita *et al*. 2002). These transporters show a broad substrate selectivity but a relative low affinity compared to CNTs (K_m around 40-710 μM). Unlike the CNTs, there are no ENT homologues identified in bacteria, however, they have been found in the majority of eukaryotic species, such as fungi, protozoans, nematodes, insects and plants (Acimovic & Coe 2002).

A total of four members of the ENT family have been identified in mammals to date: ENT1-ENT4. These proteins are classified according to their sensitivity to the inhibitor nitrobenzylthioinosine (NBTI), a structural analog of adenosine. Thereby, ENT1 is historically known as *es* (**e**quilibrative **s**ensitive - to NBTI) transporter (nanomolar IC_{50} values), while ENT2 is *ei* (**e**quilibrative **i**nsensitive - to NBTI) transporter (IC_{50} values above 10 μM). ENT3 and ENT4 were further identified (Baldwin *et al*. 2004). ENT3 is able to transport adenosine and its activity is not inhibitable by NBTI nor Dipyridamole. On the other hand, ENT4 seems to participate in serotonin translocation and it is partially inhibited by Dipyridamole or Dilazep, but not by NBTI. In both cases, ENT3 and ENT4 activities are pH-dependent (Baldwin *et al*. 2005; Barnes *et al*. 2006).

ENT1 was the first member of the ENT family to be cloned from human erythrocytes (Griffiths, Beaumont, *et al*. 1997a). As we already mentioned, ENT1 is highly sensitive to NBTI at nanomolar concentrations, but also to other molecules such as the coronary vasodilators Dilazep, Dipyridamole and Draflazine (Hyde *et al*. 2001; Aguayo *et al*. 2005). ENT1 is responsible of the uptake of both purines and pyrimidines, with K_m affinity values between 40-580 μM (figure 3c). However, although ENT1 has never been described as a nucleobase transporter (Ward *et al*. 2000; Beal *et al*. 2004), recent evidences demonstrated a significant activity as nucleobase transporter (Yao *et al*. 2011). Regarding its expression and distribution, ENT1 is ubiquitously expressed in mammal tissues (Pennycooke *et al*. 2001; Jennings *et al*. 2001) and, despite it could be thought to be exclusively localized at the plasma membrane, there are some evidences that suggested its presence at the mitochondrial membrane (Lai *et al*. 2004; E.-W. Lee *et al*. 2006).

ENT2 was the next ENT member to be cloned. It was actually cloned in two different labs simultaneously, in 1997 from cDNA of human placenta (Griffiths, Yao, *et al*. 1997b), and also in 1998 from cDNA of human leukaemia CEM cells (Crawford *et al*. 1998). When ENT2 sequence was analyzed, it was observed around 50% identical to ENT1 in mammals. Surprisingly, the C-terminus of ENT2 protein was nearly identical to a smaller protein previously cloned and identified as a growth factor-induced

delayed early response gene, named HNP36 and reported to be located at the nuclear periphery (Williams *et al*. 1995). HNP36 sequence analysis suggested that this protein would be originated from a second start codon within the ENT2 open reading frame. Despite its function still remains unknown, it was demonstrated that only the full length protein conferred uridine transport activity to the cells (Crawford *et al*. 1998).

ENT2 transports a broad range of purine and pyrimidine nucleosides, although with a lower apparent affinity than ENT1, except in the case of inosine (Beal *et al*. 2004). However, ENT2 differs from ENT1 in also being able to transport efficiently a wide range of purine and pyrimidine nucleobases (Crawford *et al*. 1998; Yao *et al*. 2002). ENT2 mRNA is expressed in a wide range of tissues including brain, heart, placenta, thymus, pancreas, prostate and kidney, but is particularly abundant in skeletal muscle (Griffiths, Yao, *et al*. 1997b; Crawford *et al*. 1998; Pennycooke *et al*. 2001).

ENT3 was first described in 2001 and characterized more recently (Hyde *et al*. 2001; Acimovic & Coe 2002; Baldwin *et al*. 2005). In contrast to the SLC29 gene family members ENT1 and ENT2, ENT3 has been mostly found in intracellular structures. Indeed, ENT3 was initially localized in lysosomes (Baldwin *et al*. 2005) but later it was shown that it is more likely to be expressed in mitochondria, where it may play a role in the mitochondrial toxicity of certain nucleoside-derived drugs (Govindarajan *et al*. 2009; Kang *et al*. 2010). However, recent evidences have suggested that ENT3 is also able to localize to the plasma membrane, although this has only been seen in placental cell lines (Govindarajan *et al*. 2009).

Like the other ENT family members, ENT3 isoform has a broad tissue distribution. It also shares structural characteristics and a preference for purine and pyrimidine nucleosides and nucleobases (Baldwin *et al*. 2005). On the other hand, ENT3 activity appears to be proton dependent in such a way that pH has an effect on its uptake capacity. This fact suggests a plausible evolution to adapt itself to the acidic pH of the lysosomal lumen (Baldwin *et al*. 2005). Unlike the other ENT family members, ENT3 is the first nucleoside transporter related to a genetic human disease.

The H syndrome (OMIM 612391) is a recently described syndrome caused by mutations in the SLC29A3 gene that encodes for hENT3. The H syndrome is an autosomal recessive disorder that is characterized by hyperpigmentation, histiocytosis, hypertrichosis and short stature (Huber-Ruano *et al*. 2012).

The last member of the ENT family identified to date is ENT4 (Acimovic & Coe 2002). First ENT4 characterization assays revealed its functionality as a nucleoside transporter by translocating adenosine, despite its low affinity to the substrate (Baldwin *et al*. 2005). Further studies corroborated previous observations and clarified the fact this transport activity occurs under acidic pH conditions (Barnes *et al*. 2006; H. Li *et al*. 2008; M. Zhou *et al*. 2010). However, controversy still exists since parallel characterization assays suggested ENT4 as a plasma membrane monoamine transporter and so renamed as PMAT, supported by the fact that hENT4 shares a 18% of identity with hENT1 (K. Engel *et al*. 2004). Despite its functionality is not accurate yet, ENT4 has a broad distribution in tissues such as brain, skeletal muscle, kidney, heart and liver, just like the other ENT proteins.

2.4 ENT STRUCTURE

ENTs are proteins of 450 amino acids approximately. The two dimensional topology predicted for these transporters is made up of 11 transmembrane domains, with the N-terminus facing the cytosolic side and the C-terminus in the extracellular space. Their predicted structure also has an intracellular loop between transmembrane domains 6 and 7, and a potential glycosylation site in the first extracellular loop between transmembrane domains 1 and 2 (figure 3a) (Griffith *et al*. 1996).

In order to understand the mechanisms by which ENTs are regulated and they interact with and translocate the substrates, several studies performed chimeric and site directed mutagenesis assays with ENT proteins. Unfortunately there is not much known regarding the residues involved in the substrate recognition and translocation. As with the mammalian CNTs, no crystallographic models of the ENTs have been presented to date, probably due to the challenges associated with acquiring sufficient

protein to conduct structural analyses, what makes it difficult to elucidate structural relevances or mechanisms.

Similar to the CNT family, ENTs are proposed to form a pore through which nucleosides and nucleobases are translocated. There are some evidences obtained from nucleoside transporters of *Leishmania donovani* parasite (LdNT) that suggested that this pore is lined by transmembrane domains 1, 2, 4, 5, 8, 10 and 11 (figure 3b) (Arastu-Kapur *et al*. 2005, Valdés *et al*. 2009). This studies also identified some residues that might play a key role in substrate affinity such as Met_{33}, Leu_{92} and Gly_{179} (hENT1), Gly_{183} and Cys_{337} (LdNT1), Asp_{389} and Arg_{393} (LdNT2), and an exofacial Cys_{140} (rENT1). Further studies performed with *Plasmodium falciparum* ENT1 indicated that the transmembrane domain 11 is an alpha helix indeed, and supported the proposal of that domain lines the translocation pore (Riegelhaupt *et al*. 2010). Other works described transmembrane domains 3-6 to be implicated in substrate translocation in hENT1 (Sundaram *et al*. 2001), leaving the controversy regarding which transmembrane domains comprise this pore unresolved (Sengupta & Unadkat 2004). However, a very recent mutational study supported the notion that helices 1, 2 and 7 constitute the extracellular gate of LdNT1.1 (Valdés *et al*. 2012).

There are several studies that described which residues are involved in inhibitor binding or at least might play a key role in ENTs sensitivity to those compounds. Residues better characterised in ENTs inhibition are Trp_{29}, Met_{33}, Leu_{92}, Gly_{154} and Gly_{179}, Ser_{160}, Asn_{338} and Leu_{442}. (Vickers *et al* 1999; Hammond 2000; Sengupta *et al*. 2002; Visser *et al*. 2002; Endres *et al*. 2004; Sengupta & Unadkat 2004; Endres & Unadkat 2005; Reyes & Coe 2005; Paproski *et al*. 2008). With regards to trafficking and sorting, Gly_{184} has been implicated in trafficking to the plasma membrane while the sequence PEXN (residues 71-74) has been proposed to be involved in mitochondrial targeting (Sengupta *et al*. 2002; E.-W. Lee *et al*. 2006) On the other hand, a dileucine motif at the N-terminus of ENT3 has been suggested to determine its lysosomal sorting (Baldwin *et al*. 2005).

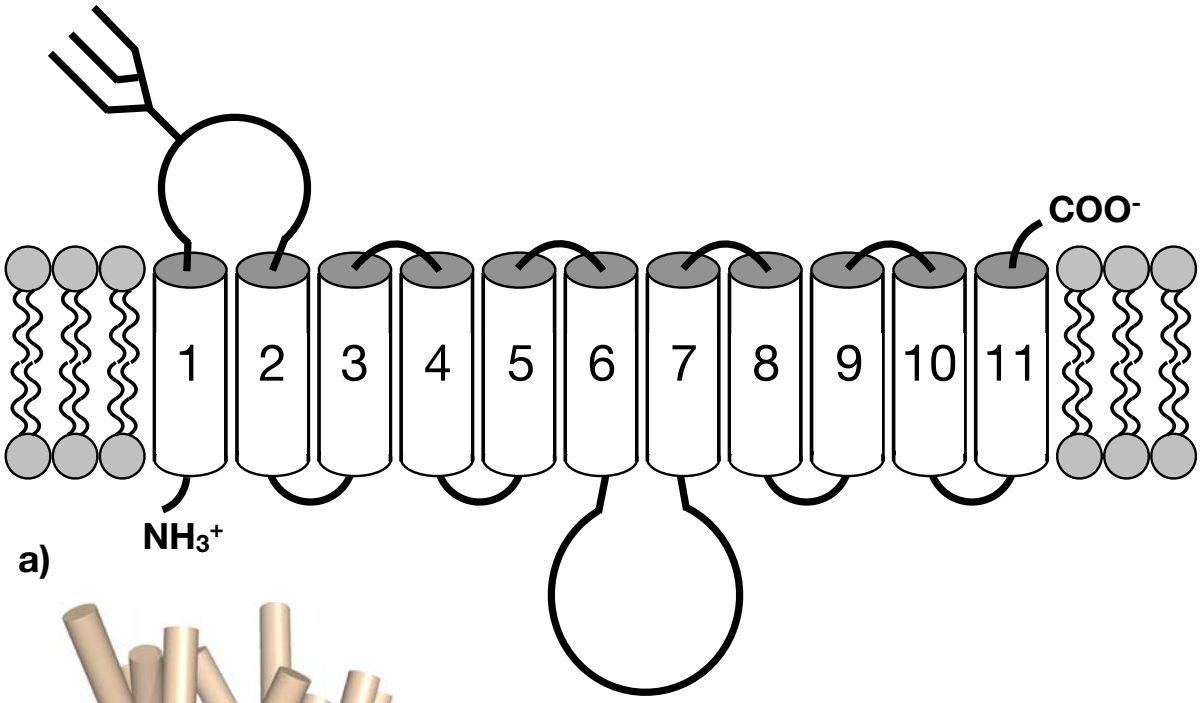

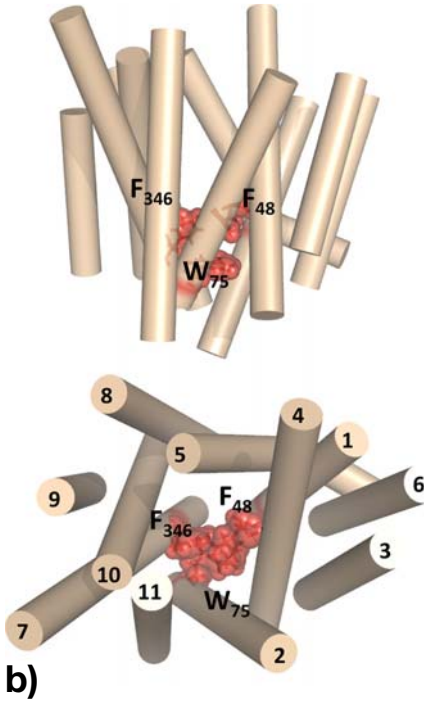

EQUILIBRATIVE NUCLEOSIDE TRANSPORTERS			
GENE	**PROTEIN**	**SUBSTRATE (K_m)**	**INHIBITOR (IC_{50})**
SLC29A1	hENT1	Ado - 40 μM Guo - 140 μM Ino - 170 μM Urd - 260 μM Tyd - 30 μM Cyd - 580 μM	NBTI - 0.4 nM Dipyridamole - 5 nM
SLC29A2	hENT2	Ado - 100 μM Guo - 2700 μM Ino - 50 μM Urd - 250 μM Tyd - 710 μM Cyd - 5610 μM Nucleobases	NBTI - 2.8 μM Dipyridamole - 356 nM

c)

Figure 3. ENTs structural and kinetic features. (a) The 2D topology proposed for equilibrative nucleoside transporters, which contains 11 transmembrane domains as well as the intracellular N- and extracellular C-termini. It also has a potential glycosylation site on the first extracellular loop and a remarkable intracellular loop between TM6-TM7. (b) Proposed ab initio model of LdNT1.1 showing side (top panel) and cytosolic (bottom panel) views. The model pictures a cluster of three aromatic residues (Phe_{48}, Trp_{75} and Phe_{436}) that may interact to close an extracellular gate formed by TM1, TM2 and TM7. Figure adapted from Valdés *et al*. (2009). (c) Kinetic properties of the two members of the ENT family best characterized to date.

3 NUCLEOSIDE ANALOGS AS THERAPEUTIC AGENTS

As previously mentioned, nucleoside transporters in addition to transporting their natural substrates, nucleosides and nucleobases, they also have the capacity of internalizing nucleoside analogs used as therapeutic agents. This kind of drugs are frequently used in treatments of different kinds of cancer such as leukemia, lymphomas and solid tumors, or viral infections like HIV and Hepatitis B. Nucleoside transporters are also clinically relevant given the fact they are the targets in some treatments for cardiovascular and neurological disorders and parasitic infections (Galmarini *et al*. 2002; Galmarini *et al*. 2003). However, since there are big differences in NTs expression among the different tissues and population, the pharmacokinetics of such drugs may be compromised depending on the target and the patient profile (Balnave *et al*. 1981).

As happens with nucleosides and nucleobases, there are two types of nucleoside analogs (NA): pyrimidines such as Cytarabine, Gemcitabine or Capecitabine; and purines like Fludarabine, Cladribine or Clorafabine (figure 4) (Damaraju *et al*. 2003). One of the first nucleoside analogs to be developed was Cytarabine (deoxycytidine-1-*β*-D-arabinofuranosylcytosine), also known as AraC (Wiley *et al*. 1982). This NA is mainly internalized by hENT1, although there are some evidences of its transport via hCNT1 (Hubeek *et al*. 2005; Chow *et al*. 2005). It is widely used to treat haematological malignancies such as acute lymphoblastic leukemia, chronic myelocytic leukemia, erythroleukemia and mantle-cell lymphoma (Lamba 2009). However, since this drug is rapidly metabolised into uracil, Cytarabine is continuously administrated intravenously in order to be effective. Unfortunately, this treatment may result in acquired resistance (Bardenheuer *et al*. 2005) by the elimination of the drug from inside the cell via multidrug resistant transporters (Reid *et al*. 2003; Eckford & Sharom 2009).

Gemcitabine (2', 2'-difluorodeoxycytidine - dFdC), is another pyrimidine nucleoside analog currently used in the chemotherapeutic treatment of cancers such as pancreatic carcinoma, non-Hodgkin's lymphoma, non-small lung, cervical, bladder

and breast cancer (Pérez-Torras *et al*. 2008; Okazaki *et al*. 2010; Farrell *et al*. 2009; O'Reilly 2009; Maase 2001; Oguri *et al*. 2007). Gemcitabine is mainly internalized by hENT1, although it can also be transported by hENT2 and to a lesser extent by hCNT1 and hCNT3 (Santini *et al*. 2011). Like Cytarabine, Gemcitabine is also deaminated and therefore administrated intravenously (Clarke *et al*. 2002; Gilbert *et al*. 2006; Giovannetti *et al*. 2008). Once inside the cell, Gemcitabine is phosphorylated into its di- and triphosphate forms (Kroep *et al*. 2002). The diphosphate metabolite acts as an inhibitor of the ribonucleotide reductase enzyme, which participates of the synthesis of natural nucleotides (dNTPs). Since the cell runs out of dNTPs, the triphosphate metabolite of Gemcitabine (dFdCTP) is subsequently incorporated into DNA (Prakasha Gowda *et al*. 2010). Due to its two fluorine groups (F), dFdCTP is not able to create a phosphodiester bond with a subsequent nucleotide, such a way it prevents the elongation of the DNA chain and promotes DNA disintegration and cell death (Fowler *et al*. 2008). Gemcitabine is also considered a radiosensitizer (Mornex & Girard 2006) since its incorporation into the DNA chain makes the DNA fragile and highly susceptible to breakage by radiation (Doyle *et al*. 2001).

Cladribine and Fludarabine, two adenosine analogs, are also used in cancer treatment, specially in leukemias and lymphomas (Ross *et al*. 1993; Pastor-Anglada *et al*. 2004). As the previous examples, these drugs are also incorporated into DNA and RNA during its synthesis as a triphosphate metabolite (Lotfi *et al*. 2001; Mackey *et al*. 2005). In addition, they suppress DNA synthesis by inhibiting DNA polymerases, or DNA repair mechanisms (Robak *et al*. 2006). Cladribine uptake is mediated via ENT1 and ENT2 mainly, although rCNT2 has also been reported to translocate this drug (Gerstin *et al*. 2002; Molina-Arcas *et al*. 2005). In the case of Fludarabine, ENT1 and ENT2, together with CNT1-3, are responsible for its internalization (Molina-Arcas *et al*. 2005; Tsang *et al*. 2008).

THERAPEUTIC NUCLEOSIDE ANALOGS

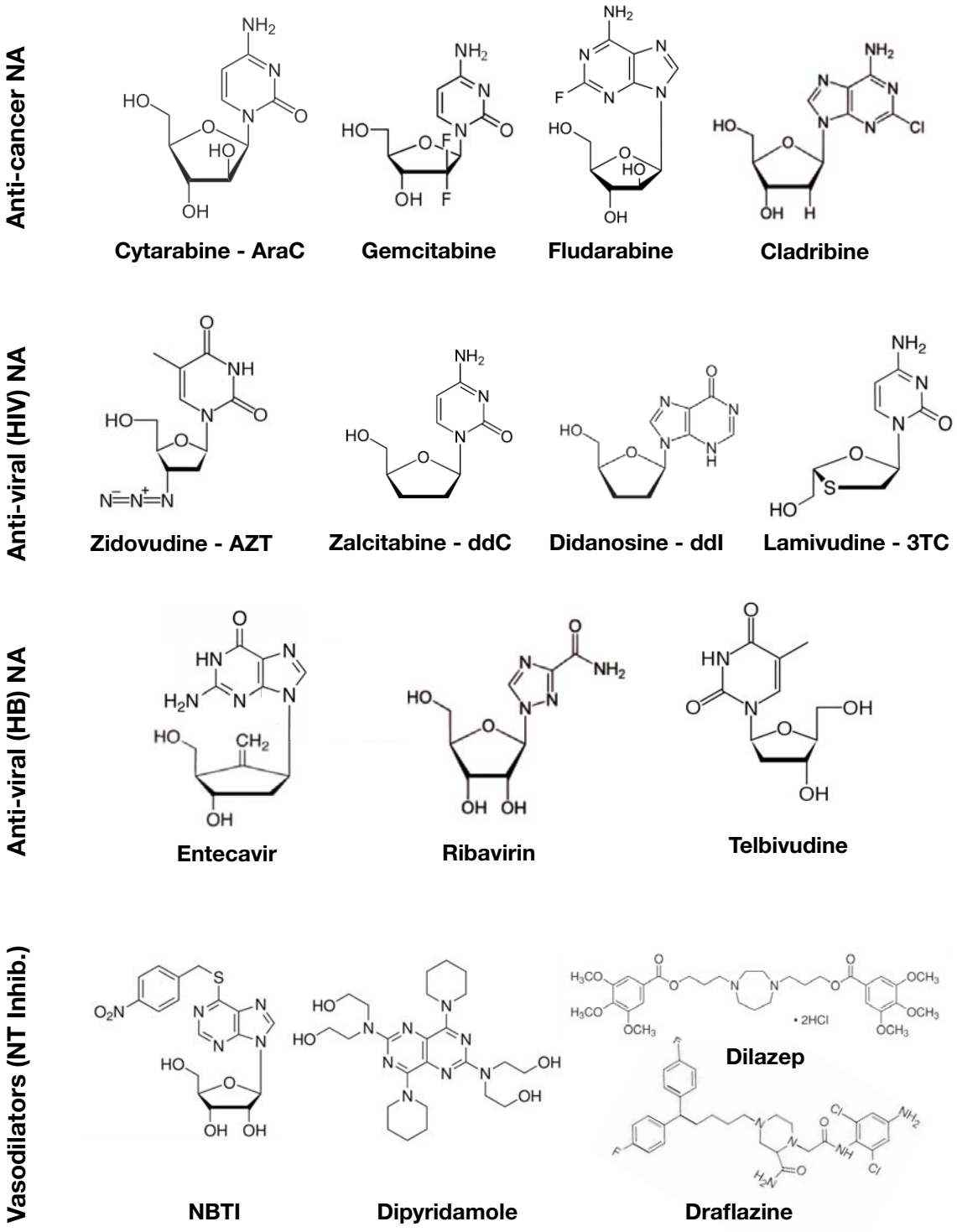

Figure 4. Therapeutic Nucleoside Analogs (NA). First line shows NA used in anti-cancer treatments for leukemias, lymphomas and solid tumors. Second line shows NA used in treatments for HIV. Third line shows anti-viral NA used in Hepatitis B patients. Fourth line shows NT inhibitors commonly used as vasodilators.

hENT2 plays a crucial role in Fludarabine uptake in Chronic Lymphocytic Leukemia (CLL) patients. As reported, sensitivity of CLL cells to this drug was initially correlated with ENT-type transport activity (Pastor-Anglada *et al*. 2004). However, studies using polyclonal antibodies against ENT1 and ENT2 epitopes revealed a significant correlation between ENT2 protein expression and Fludarabine uptake, as well as *ex vivo* sensitivity of CLL cells (Molina-Arcas *et al.* 2005). Furthermore, a recent study in Mantle Cell Lymphoma (MCL) cells described SLC29A2, gene that encodes for hENT2 protein, as one of the five predictor genes that compose a new quantitative gene expression-based model developed to predict survival in MCL patients (Hartmann *et al*. 2008). Despite the biological foundation of the hENT2 correlation remains unclear, it suggests an important role of this transporter in the clinical outcome of MCL patients.

Nucleoside-derived drugs are also commonly used in anti-viral therapies, specially in HIV and Hepatitis B patients (Zoulim 2005; Perez-Bercoff *et al*. 2007). Some examples are represented in figure 4 (Vivet-Boudou *et al*. 2006; Menéndez-Arias 2008; Endres *et al*. 2009). As happens with the other NA described, these anti-viral drugs are tri-phosphorylated and incorporated into the host DNA, preventing the incorporation of the viral DNA and also promoting host DNA disintegration and cell apoptosis. In addition, these nucleoside analogs also inhibit the reverse transcriptase, which is the enzyme that synthesises viral DNA (Cherry & Wesselingh 2003). Similar to Fludarabine treatment, hENT2 seems to represent an important route for cellular uptake of NA used on HIV therapy since hENT2 can transport AZT, unlike hENT1, and also exhibits a much greater capacity to transport ddC and ddI (Beal *et al*. 2004)

Based on their role as adenosine transporters, NTs have become clinical targets in cases of cardio- and neuropathies. NT inhibitors like dilazep, dipyridamole and draflazine (figure 4) (Sundaram *et al.* 1998; Hammond 2000; Musa *et al*. 2002; Paproski *et al*. 2008) have been commonly used to inhibit adenosine uptake and increase its extracellular levels promoting vasodilation and/or inhibition of platelet aggregation (Van Belle 1993; Dunwiddie & Diao 2000; Visser, Zhang, *et al*. 2005b; Noji *et al*. 2004; Chakrabarti & Freedman 2008; Young *et al*. 2008). Following this line,

since parasites are unable to synthesise their own nucleosides, nucleoside salvage pathways have been an important target in developing new drug therapies against infection by *Plasmodium falciparum* (malaria), *Trypanosoma brucei* (African trypanosomiasis) and *Toxoplasma gondii* (toxoplasmosis) (De Koning *et al*. 2003; Safarjalani *et al*. 2003; Quashie *et al*. 2008; Aly *et al*. 2010; Landfear 2010; Riegelhaupt *et al*. 2010).

4 REGULATORY MECHANISMS OF NUCLEOSIDE TRANSPORTERS

Most processes in cells do not take place independently of one another or at constant rate. Instead, the catalytic activity of enzymes or the assembly of a macromolecular complex is so regulated that the amount of reaction product or the appearance of the complex is just sufficient to meet the needs of the cell. This fine regulation also occurs to membrane proteins, and nucleoside transporters in particular. Regulation may occur at different points of the life span of a protein, either before the gene transcription or during / after the protein translation.

4.1 TRANSCRIPTIONAL REGULATION

Transcriptional regulation determines levels of protein expression and it is conducted by multiple protein-binding DNA sequences such as promoters and other types of control elements, together with those regulatory proteins known as transcriptional factors, either activators or repressors. Several examples of transcription regulation of membrane proteins have been described, like the case of the glucose transporter (GLUT4), the Aquaporin water channel (AQP2) or the human Na^+/H^+ exchanger 3 hNHE3, among many others (Nelson *et al*. 1998; Malakooti *et al*. 2006; McGee *et al*. 2008; M.-J. Yu *et al*. 2009b).

Regarding nucleoside transporters, some studies described how hCNT1 is transcriptionally regulated by HNF-4α and bile acids, and also rCNT2 regulation via TGF-ß (Valdés *et al*. 2006; Klein *et al*. 2009). Certainly, ENT1 is the nucleoside transporter most studied regarding transcriptional regulation. Some evidences suggested that ENT1 promoter could be upregulated by the transcription factors Sp1 (zinc-finger specificity protein-1) and MAZ (myc-associated zinc protein) (Abdulla & Coe 2007). More recent studies have been focused on cellular pathways that would be involved in ENT1 regulation finding that the activation of JNK-cJun pathway negatively regulates mENT1 (Leisewitz *et al*. 2011), and that PPARα and γ activation or overexpression resulted in higher hENT1 transport activity (Montero *et al*. 2012).

Due to the neuro- and cardioprotective role of adenosine in cases of ischemia or hypoxia, different research groups studied the NTs regulation in these situations. These studies described how mENT1 and mENT2 promoters were down-regulated by hypoxia inducible factor 1 (HIF-1), as well as during cerebral ischemia (Chu *et al*. 2012). In both situations, ENTs downregulation promote an increasing of extracellular adenosine levels, which has a protective effect on the cell by activation of adenosine receptors (Chaudary *et al*. 2004; Eltzschig *et al*. 2005; Löffler *et al*. 2007).

Other physiological situations have also been involved in changes on ENTs expression. For instance, high-glucose levels, together with its subsequent increasing of NO production, reduces SLC29A1 promoter activity via MAP kinases (Puebla *et al*. 2008; Farias *et al*. 2010). In addition, studies on Inflammatory Bowel Disease (IBD) patients, described a change in mRNA expression of both hENT1 and hENT2, in such a way that hENTs expression levels were significantly higher in IBD patient samples than in healthy intestinal tissue, suggesting a dysregulation on hENTs mRNA levels due to that disease (Wojtal *et al*. 2009).

4.2 PROTEIN SYNTHESIS AND POST-TRANSLATIONAL MODIFICATIONS

Once a protein has been synthesised from its codifying mRNA sequence, the cell promotes the proper folding and, in many cases, modifies residues or cleaves the polypeptide backbone to generate the final protein (Castro-Fernández *et al*. 2005; J.-C. Wu *et al*. 2006). Nucleoside transporters, in order to be properly functional, must be delivered to a particular cell membrane and reach their correct location. The following sections will discuss those processes involved in nucleoside transporter synthesis, modification, sorting and trafficking necessary to be functional proteins.

4.2.1 Protein synthesis and sorting:

After being exported from the nucleus to the cytosol, nuclear-encoded mRNA transcripts are translated into proteins on cytosolic ribosome. There are two main pathways regarding membrane protein synthesis and sorting. The first general process involves targeting of a protein to the membrane of an intracellular organelle and can occur either during or soon after synthesis of the protein by cytosolic translation at the ribosome. Those nascent proteins contain a targeting sequence that leads their sorting to a specific organelle such as endoplasmic reticulum (ER), mitochondria, chloroplasts, peroxisomes or nucleus, and insertion of the protein into the lipid bilayer of the membrane (figure 5) (Lodish *et al*. 2007).

The second general sorting process is known as the secretory pathway and applies to proteins that initially are targeted to the ER membrane and whose final destination is the ER itself, the Golgi apparatus, lysosomes and membranes of those organelles and the plasma membrane. In the secretory pathway proteins are transported by small vesicles that bud from the membrane of one organelle and then fuse with the membrane of the next organelle in the pathway (figure 5) (Lodish *et al*. 2007). In order for those proteins to leave the ER, they must be incorporated into a coatomer protein II (COPII) vesicle, which traffics the protein to the Golgi apparatus (Barlowe 1998; Watson & Stephens 2005; M. C. S. Lee & Miller 2007). The COPII coat is a protein complex formed by several subunits like Sar1, a GTPase that initiates the

membrane curvature (Bonifacino & Glick 2004; Bielli *et al*. 2005) and also recruits the other COPII members (Bi *et al*. 2002; Futai *et al*. 2004). Several studies defined two ER export signals recognised by COPII complex: the diacidic and the di-hydrophobic motifs, both of them usually localised in cytosolic regions of the protein (X. Wang *et al*. 2004; Mikosch *et al*. 2006; Zuzarte *et al*. 2007). The diacidic motifs are typically made up of two acidic amino acid residues separated by another amino acid (X) in such motifs as ((D/E)-X- (D/E)) (Sevier *et al*. 2000; X. Wang *et al*. 2004; Hanton *et al*. 2005). Di-hydrophobic motifs are usually made up of two phenylalanine, leucine or tyrosine residues (FF, LL or YY) (Wendeler *et al*. 2007). Some works described associations between COPII vesicle components and serotonin transporter (SERT) (Chanrion *et al*. 2007) or the GABA transporter 1 (GAT1) (Farhan *et al*. 2007), suggesting these proteins participate of the secretory pathway.

A recent study observed the intracellular N-terminal tail of rCNT2 to be implicated in its plasma membrane sorting (Pinilla-Macua *et al*. 2012). However, very few is known regarding ENTs targeting motifs. The RXXV motif for hENT1 and a dileucine repeat for hENT2 present in the extracellular C-terminus were suggested to be crucial for basolateral sorting in renal epithelial cells. In addition, the dileucine repeat was implicated in surface expression of hENT2, which was drastically reduced when those residues were mutated (Mangravite *et al*. 2003).

Despite no association of COPII complex and ENTs has been confirmed, sequence analysis of the intracellular regions of hENT2 suggests several putative ER export motifs, all of them conserved in both mENT2 and hENT2:

- DED diacidic motifs between TM8-9
- ERE diacidic motifs between TM10-11
- Sequences present it the intracellular loop between TM6-7:
    - YY - di-hydrophobic residues 221 - 222
    - ELE - diacidic motifs 234 - 236
    - LL - di-hydrophobic residues 241 - 242
    - DLDLEKEPESEPD (DXDXEXEXEXEXD) - acidic motifs 261 - 273

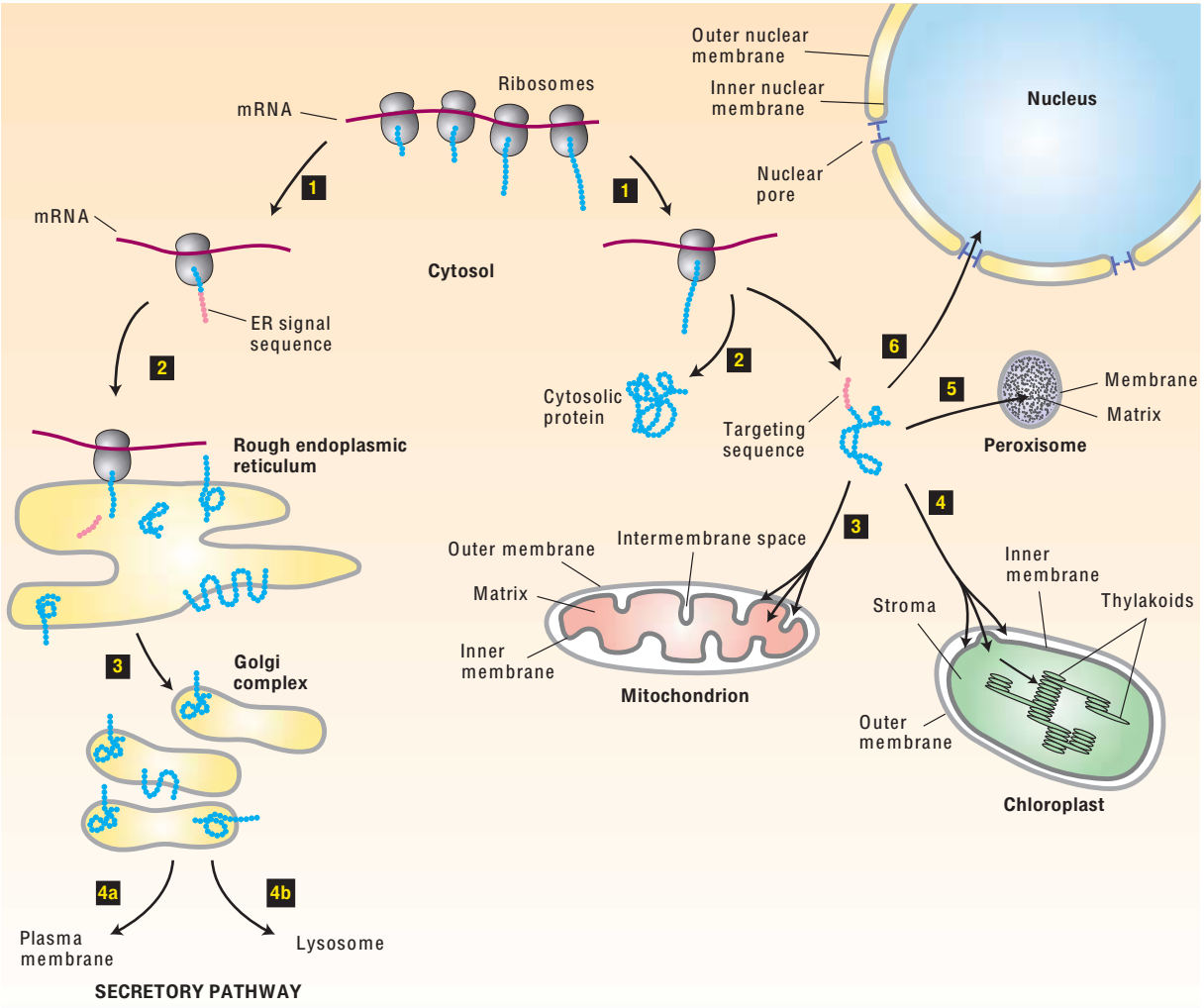

Figure 5. Protein synthesis and sorting pathways. Nuclear-encoded mRNA transcripts are translated into proteins on cytosolic ribosomes after being exported from the nucleus (step 1). Nascent proteins with an ER targeting sequence (pink) are directed to the ER, where translation is completed (step 2 - left). These proteins can move via COPII vesicles to the Golgi complex (step 3 - left) and be further delivered to the plasma membrane (step 4a) or lysosomes (step 4b). Proteins lacking an ER signal sequence are completed on free ribosomes and released to the cytosol (step 2 - right). Depending on whether they contain an organelle-specific targeting sequence (pink) or not, proteins will remain soluble at the cytosol or be imported into mitochondria, chloroplasts, peroxisomes or the nucleus, or any of these organelle membranes (steps 3 to 6 - right). Figure adapted from Lodish *et al.* (2007).

4.2.2 The Golgi apparatus and glycosylation:

Most of the proteins synthesised on the rough ER undergo glycosylation in the ER and Golgi. Carbohydrate chains in glycoproteins may be attached to the hydroxyl group in serine and threonine or to the amide nitrogen of asparagine. These are referred to as O-linked and N-linked oligosaccharides, respectively (Keller & Simons 1997). The more common N-linked oligosacharides are larger and more complex, containing several branches in mammalian cells. Its biosynthesis begins in the rough ER with addition of a preformed precursor containing 14 residues ($Glucose_3$-$Mannose_9$-N-$Acetylglucosamine_2$). The entire 14-residue precursor is transferred to and asparagine in the tripeptide Asn-X-Ser and Asn-X-Thr (where X is any amino acid except proline) (Helenius & Aebi 2001; Suzuki & Lennarz 2002; Molinari 2007). Once the protein reaches the Golgi apparatus, the oligosaccharide chain is modified and the glycosylation process is then completed allowing the protein to be sorted to its final destination (Cheung & Reithmeier 2007).

The oligosaccharides attached to glycoproteins serve various functions. For example, some proteins require N-linked oligosaccharides in order to fold properly in the ER. When glycosylation fails, those proteins remain misfolded in the rough ER (Buck *et al*. 2004; F. Zhou *et al*. 2005; Cheung & Reithmeier 2007). In addition to promote proper folding, N-linked oligosaccharides also confer stability on many secreted glycoproteins. When those proteins are non-glycosylated due to mutations in their asparagine residues, they have been shown to be less stable and degraded faster than their glycosylated forms (Martínez-Maza *et al*. 2001; Cai *et al*. 2005). For instance, it has been observed that glycosylation in glucose transporters GLUT1 and GLUT4 enhances their folding and conformational stability as well as cell surface expression (Tortorella & Pilch 2002).

Oligosaccharide on certain cell-surface glycoproteins also play a role in cell-cell adhesion. For example, CAMs (cell adhesion molecules) in leukocytes interact with certain CAMs found in endothelial cells lining blood vessel (Lodish *et al*. 2007). On the other hand, N-liked glycosylation in aquaporin (AQP) transporters has been shown to

play a role in exiting the Golgi apparatus and proper trafficking to the plasma membrane (Martínez-Maza *et al*. 2001; Tortorella & Pilch 2002; Hendriks *et al*. 2004; Buck *et al.* 2004; Cai *et al*. 2005). Same evidences were found in the case of the human organic anion transporter (hOAT4) and the human norepinephrine transporter (NET) (Nguyen & Amara 1996; F. Zhou *et al*. 2005).

Some other cases have been described, in which glycosylation appeared to be crucial for the proper functionality and activity of some transporters located at the plasma membrane. For instance, ABC transporters were observed to be incapable to transport substrate in the absence of glycosylation (Draheim *et al.* 2010). The same effect was shown for the case of the GABA transporters (Bennett & Kanner 1997). In addition, some glycoproteins have two or more glycosylation sites like the urea transporter (UT)-A1, which each one is glycosylated to a different extent (G. Chen *et al*. 2006).

Since glycosylation is highly important for the physiology of a protein, those cases in which glycosylation can not be executed properly, many diseases have been attributed to (Sturiale *et al*. 2005; Freeze & Aebi 2005; Kaji *et al*. 2007). An example of such a disease is congenital muscular dystrophy which results from the lack of glycosylation inalpha-dystroglycan (Matsumoto *et al*. 2005).

In the case of ENTs, two dimensional models predicted N-glycosylation sites in the extracellular loop between transmembrane domains 1 and 2, in the Asn_{48} for ENT1 and Asn_{48} and Asn_{57} in the case of ENT2 (Boleti *et al*. 1997). Those residues were confirmed by mutational studies in both transporters. For ENT1, it seems that its glycosylation is involved in nucleoside transport and/or inhibitor binding affinity, as well as maintaining ENT1 structure (Vickers *et al*. 1999; Sundaram *et al*. 2001; Ward *et al*. 2003; Reyes & Coe 2005; Amanchy *et al*. 2007). Mutation of the N-linked glycosylation sites in ENT2 showed disrupted plasma membrane localization suggesting that this modification is need for proper targeting and/or trafficking (Ward *et al*. 2003).

4.2.3 Phosphorylation/ dephosphorylation:

Reversible phosphorylation of proteins is an important regulatory mechanism that occurs in both prokaryotic and eukaryotic organisms, in which kinases are the enzymes that phosphorylate proteins while phosphatases dephosphorylate them. This is a fast and reversible regulatory mechanism that takes place after proteins are released from the ER and Golgi apparatus (Procino *et al*. 2003). It is based on the balance between phosphorylation and dephosphorylation of proteins and participates in multiple signalling and regulatory pathways within the cell physiology (Newton 2003). Reversible phosphorylation results in a conformational change in the structure of many enzymes and receptors, causing them to become activated or deactivated, what is also known as switching proteins “on” or “off” (Olsen *et al*. 2006).

Phosphorylation usually occurs on serine (S), threonine (T) and tyrosine (Y) residues by adding a phosphate molecule to a polar R group of such amino acid residue (Amanchy *et al*. 2007) either directly from ATP or GTP molecules, or via interaction with another phosphorylated protein that transfers its phosphate group (Butt & Pitman 2005). This enzymatic reaction can turn a hydrophobic portion of a protein into a polar and extremely hydrophilic region, specially when it is phosphorylated at multiple sites, in such a way that introduces a conformational change in the protein with its subsequent effects. For instance, in response to extracellular stimuli, many plasma membrane receptors are phosphorylated at multiple tyrosine residues changing its conformation in order to recruit other proteins. Those proteins are subsequently phosphorylated, starting a cascade of phosphorylation events that define the beginning of a signalling pathway (figure 6a) (Salazar & Höfer 2009). On the other hand, phosphorylation may regulate the activity of transcription factors at several levels, such as subcellular localization, DNA binding affinity and transcriptional activity (figure 6b). Furthermore, multisite phosphorylation can also regulate protein stability since it may lead to ubiquitination of the target protein and its degradation by the proteosome (figure 6c) (Salazar & Höfer 2009).

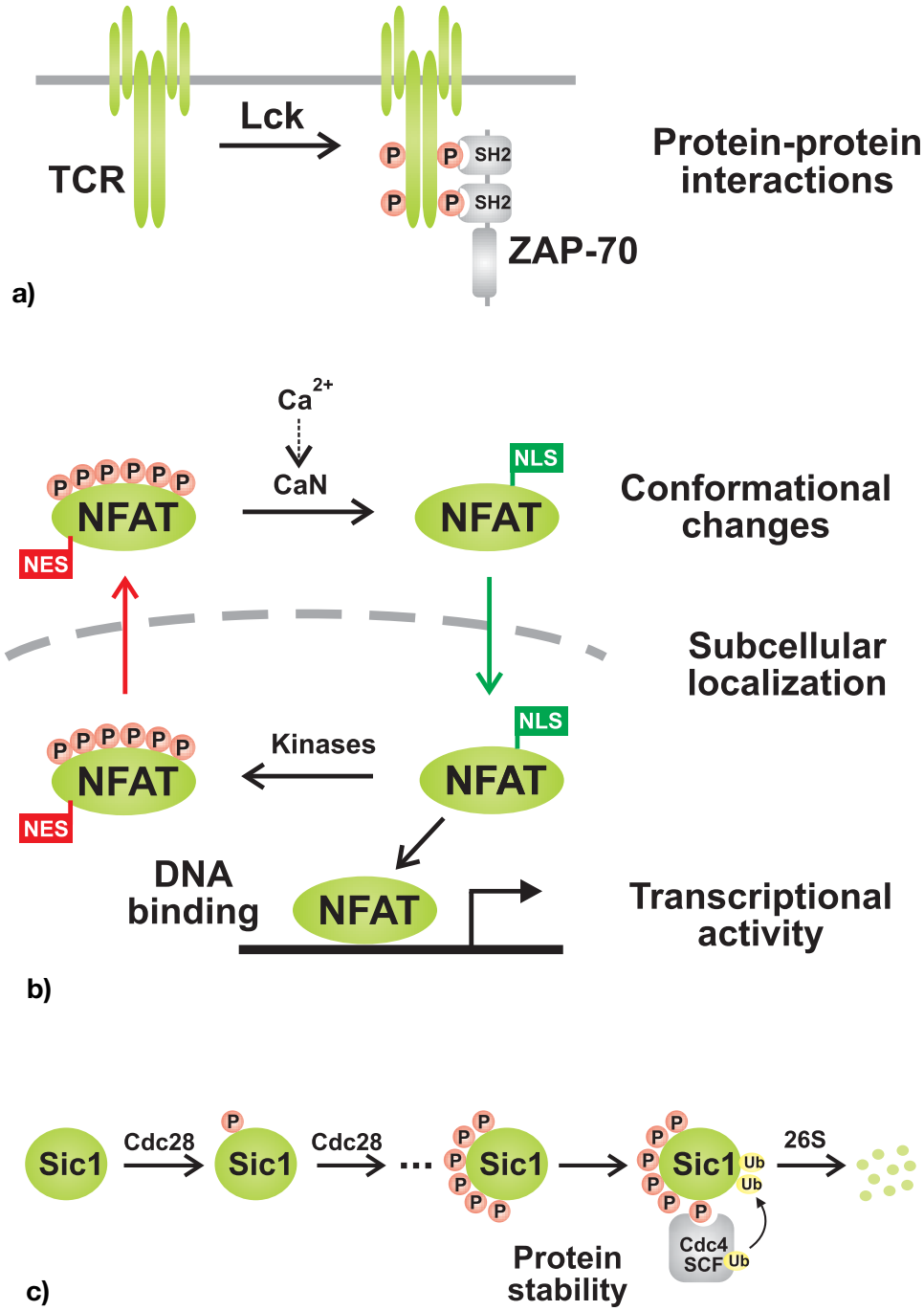

Figure 6. Prototypical examples of protein regulation by phosphorylation. (a) Receptor proteins. Binding of a high-affinity ligand to the T-cell receptor (TCR) leads to its own phosphorylation and recruiting of ZAP-70 kinase triggering a signalling cascade. (b) Transcription factors. Dephosphorylation of the nuclear factor of activated T-cells (NFAT) by calcineurin (CaN) induces a conformational change that exposes a nuclear localization signal (NLS), leading to its translocation to the nucleus to bind DNA with maximal transcriptional activity. (c) The cell-cycle inhibitor Sic1 requires phosphorylation by the cyclin-dependent kinase Cdc28 on at least six sites before it can be ubiquitinated by the Cdc4 / SCF complex and degraded by the 26S proteasome. Figure adapted from Salazar & Höfer (2009).

In those cases where a protein is phosphorylated at multiple sites, it is more important the number and the order of the reactions rather than the type of site (S, T or Y) since that will determine the biological effects of the conformational changes. Therefore, multisite phosphorylation can occur in a variety of ways: *sequential* - following the order appeared in the protein sequence; *random* - phosphate groups added in random order; *cyclic* - once all residues are phosphorylated, the last one becomes the first to be dephosphorylated generating a cycle; *hierarchical* - one event can not happen before another one is done due to conformational inaccessibility; and *compensatory* - when a target site is unavailable another site is phosphorylated causing the same biological effect (Salazar & Höfer 2009; Levy *et al*. 2010; Edwards *et al*. 1999).

Several examples have been described regarding regulation of transporters by phosphorylation. For instance, the aquaporin protein 2 (AQP2), which is trafficked to the plasma membrane when it is phosphorylated by PKA at Ser_{256}. However, when PKC is the kinase involved, AQP2 is internalized by endocytosis (van Balkom *et al*. 2002). A similar situation happens to the serotonin transporter (SERT), which reduces its transport activity by phosphorylation on a serine residue, and increases its internalization after a subsequent threonine is phosphorylated (Jayanthi *et al*. 2005). On the contrary, in the case of the γ-aminobutyric acid (GABA) transporter GAT1, the conformational change produced by phosphorylation slows down its internalization (Law *et al*. 2000). An interesting example, also associated with the plasma membrane, is the endothelial nitric oxide synthase (eNOS), where phosphorylation in Ser_{635} and Ser_{1179} activates its activity and production, while Ser_{116} and Ser_{617} have negative regulatory effects (Bauer *et al*. 2003).

Regarding ENTs being regulated by phosphorylation, barely few is known about the mechanism to date. However, there are strong evidences that suggest these transporters might be regulated by phosphorylation either in terms of trafficking and activity. Three putative kinases have been described to play a role in ENTs regulation: CKII, PKA and PKC. Putative CKII phosphorylation sites were predicted in both ENT1 and ENT2 sequences (Kiss *et al*. 2000; Stolk *et al*. 2005; Robillard *et al*. 2008). In one

of those studies, a mENT1 splice variant (mENT1b) was identified and predicted to have a potential CKII phosphorylation site at Ser_{254}, within the large intracellular loop located between TM 6 and 7 (Kiss *et al*. 2000; Handa *et al*. 2001). Further analysis of nucleoside uptake and inhibitor sensitivity of both mENT1 isoforms (mENT1a or wild type and mENT1b) correlated CKII phosphorylation with a major presence of the transporters at the membrane, an increasing in substrate translocation and changes in NBTI sensitivity (Bone *et al*. 2007).

PKC and PKA have also been studied regarding their role in ENTs regulation. First evidences suggesting the involvement of those kinases in ENTs regulation date from 1998 (Sen *et al.* 1998), but it was not until 2002 that the first work came up demonstrating hENT1 regulation by PKC (Coe *et al.* 2002). In that work, PKC activation is shown to increase hENT1 nucleoside transport activity by the activation of the transporter at the cell surface. Further studies corroborated ENT1 regulation by PKC via adenosine receptors and the MAP kinases pathway (Grden *et al*. 2008). Latest data supported a role for PKA and PKC in the phosphorylation of ENT1 within the intracellular loop and showed that PKA can phosphorylate multiple sites within this loop, while PKC specifically targets serines 279 and 286 and threonine 274, proving for the first time a direct *in vitro* phosphorylation of ENT1 by PKA and PKC (Reyes *et al*. 2011).

Despite there are no specific studies of PKA/PKC phosphorylation on ENT2, a recent work performed by Lu *et al.* (2010), revealed how adenosine accumulation, due to chronic morphine treatment, was attributable to the alteration of adenosine uptake via ENT2. Changes in PKC activity were correlated with the attenuation of ENT2 function and thereby an accumulation of extracellular adenosine (G.Lu *et al*. 2010).

4.2.4 Protein trafficking to the plasma membrane and other organelles:

After membrane proteins are synthesised and matured along its passage through the ER and Golgi apparatus, they are trafficked to its final destination via the secretory pathway (Aridor & Traub 2002). Those vesicles, which have been originated

at the ER and Golgi, move along the cellular cytoskeleton, interacting either with filaments of actin or microtubulues (Stamnes 2002; Salmon *et al*. 2002; Rodriguez *et al*. 2003; Racine *et al*. 2007).

The cytoskeleton is formed by two main structures, actin filaments and microtubules. Actin is a highly conserved protein and it participates in maintaining the cell shape and in cell mobility as well (van den Ent *et al*. 2001; Otterbein *et al*. 2002; Roffers-Agarwal *et al*. 2005). The particularity of actin filaments is the tight networks they form closely associated and lying just beneath the plasma membrane (Tseng *et al*. 2005). In fact, there is a constant communication between plasma membrane components and actin cytoskeleton mediated by Phosphatidylinositol 4,5-bisphosphate (PtdIns-4,5-P2). The interactive signalling regulates, for instance, the cytoskeleton remodelling during membrane invagination during endocytosis or the signalling cascades via protein-protein interactions (Sechi & Wehland 2000; Robertson *et al*. 2009, Saarikangas *et al*. 2010). On the other hand, microtubules are cylindric structures constituted by dimers of α- and β-tubulin (Diaz-Font & Beales 2008). These structures also participate of the transport of vesicles and organelles within the cell (Tietz *et al*. 2006).

Once those vesicles are released from the Golgi apparatus, a set of small GTP-binding proteins, known as Rab proteins, participate in the targeting of the vesicles to the appropriate target membrane (Lodish *et al*. 2007). Shortly after a vesicle buds off from the donor membrane, the vesicle coat disassembles to uncover a vesicle-specific membrane protein known as v-SNARE. Likewise, each type of target membrane in a cell contains specific t-SNARE membrane proteins. After Rab-mediated docking of a vesicle on its target membrane, the interaction of both cognate SNAREs brings the two membranes close enough together that they can fuse (Fletcher *et al*. 2000; Leabu 2006; Lodish *et al.* 2007; Pocard *et al*. 2007). Following the vesicle fusion with its target membrane, SNARE proteins dissociate and are recycled back to the ER to join more vesicular structures and traffic other proteins (Bonifacino & Glick 2004).

Several studies have described the role of vesicular trafficking and interactions with the cytoskeleton for some transporters at the plasma membrane. For instance, the kidney anion exchanger 1 (kAE1) has been suggested to interact with actin indirectly, what helps to stabilise kAE1 at the basolateral cell surface (Keskanokwong *et al*. 2007). Actin has also been involved with both serotonin (SERT) and dopamine (DAT) transporters, which seemed to co-localize at the cell surface (Ukairo *et al*. 2005; Gill *et al*. 2008). On the other hand, microtubules have also been related to some transporters such as the glucose transporter GLUT4. Depolymeration of microtubules resulted in a decrease in GLUT4 translocation to the plasma membrane and therefore glucose uptake (Fletcher *et al*. 2000). A similar case was described for the Na^+/H^+ exchanger (NHE3), where inhibition of microtubule polymerization after treatment with colchicine resulted in the loss of translocation of the transporter to the plasma membrane (Sabolić *et al*. 2002).

A recent study identified the mechanism involved in hENT trafficking to the plasma membrane. In that case, hENT1 is trafficked in association with microtubules and incorporated in the plasma membrane where it subsequently undergoes clathrin-mediated endocytosis and recycling (Nivillac *et al*. 2011). On contrary, there is no information currently available regarding ENT2 and the mechanism involved in its trafficking to the plasma membrane. However, there are some evidences that described the participation of RS1 in CNTs transport to the plasma membrane (Errasti-Murugarren *et al*. 2012). RS1 is a transporter regulator initially identified as a short-term post-transcriptional regulator of the high-affinity Na^+-coupled glucose transporters (SGLTI) (Korn 2001) that coordinately down-regulates the localization and activity at the plasma membrane of the three members of the CNT family, probably acting as inhibitor of their exocytosis (Errasti-Murugarren *et al*. 2012).

ENTs have been observed to be located at the plasma membrane as well as the mitochondria (Mangravite *et al*. 2003; E.-W. Lee *et al*. 2006), but they have also been described to be present at the nuclear membrane. Mani *et al*. (1998) demonstrated the presence of functional hENT1 and hENT2 in nuclear envelopes and endoplasmic reticulum of cultured human choriocarcinoma BeWo cells, by functional

reconstitution in proteoliposomes (Mani *et al*. 1998). In fact, a spliced variant of ENT2, named HNP36, had been previously described as a delayed-early response gene located at the nuclear membrane (Williams & Lanahan 1995). The lipid bilayer nuclear envelope (NE) comprises the outer nuclear membrane (ONM) and the inner nuclear membrane (INM). The ONM is contiguous to the ER membrane, whereas the INM has a different protein composition and is associated with underlaying chromatin and lamina. The INM and ONM are joined at the NPC, which form aqueous channels embedded in the NE (Stewart 2007). There is no evidence to predict whether ENTs would be located at the INM or ONM, however there is a well described mechanism of trafficking for membrane proteins from ER to the INM known as the INTERNET pathway (Y.-N. Wang *et al*. 2010).

Nuclear translocation of INM proteins is a related example for studying the nuclear trafficking of integral membrane proteins. Multiple mechanisms of nuclear transport, which depend on the unique characteristics of the INM proteins, have been reported, including simple or gated lateral diffusion, veiscle fusion events and classical Nuclear Pore Complex (NPC)-mediated nuclear import (Zuleger *et al*. 2008). The rules governing the targeting of integral membrane proteins to the INM depend on several characteristics, such as the size of the extralumenal domain, the involvement of the Nuclear Localization Signals (NLS) and the affinity of the NLS for the karyopherins/importins. Proteins are the targeted to the INM of the NE through the OMN and NPC. The INM targeting process for the ER-to-NE transport of integral membrane proteins is known as the INTERNET pathway, standing for the INtegral Trafficking from the ER to the NE Transport (Y.-N. Wang *et al*. 2010) (figure 7).

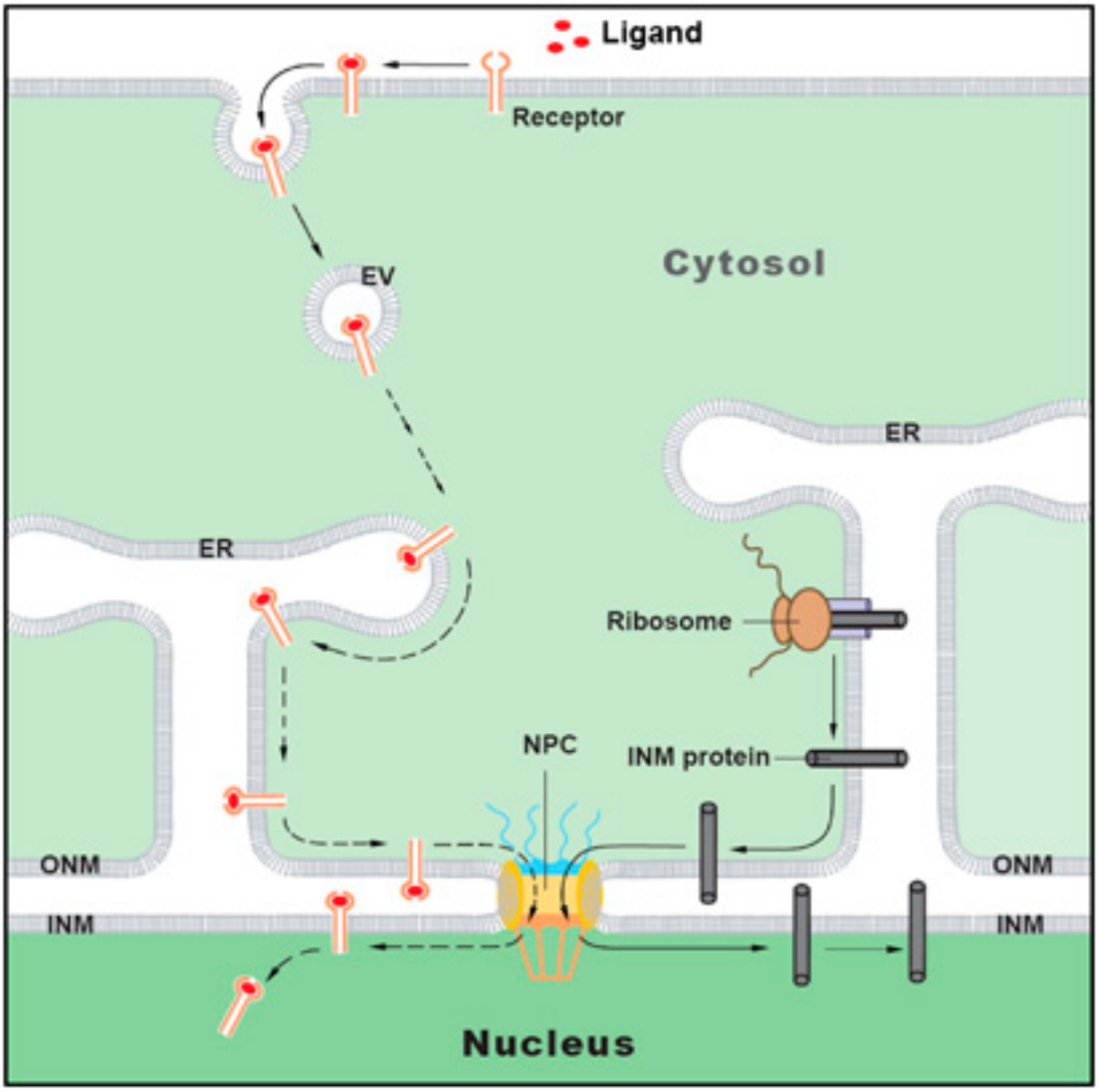

Figure 7. A model of integral trafficking from the ER to the NE transport (INTERNET). Integral INM proteins initially inserted into the ER membrane are targeted to the INM of the NE through the ONM and NPC. This INTERNET model may be involved in the nuclear transport of other integral membrane proteins such as cell surface EGFR RTKs. Figure adapted from Wang *et al*. (2010).

5 ALTERNATIVE SPLICING

5.1 ALTERNATIVE SPLICING MECHANISM

Alternative splicing is a process by which the exons of the RNA produced by transcription of a gene (a primary gene transcript of pre-mRNA) are reconnected in multiple ways during RNA splicing. The resulting different mRNAs may be translated into different protein isoforms, thus a single gene may code for multiple proteins (Black 2003).

The splicing model accepted to date consists in that once the pre-mRNA has been transcribed from the DNA (it includes several introns and exons), the exons to be retained in the mRNA are determined during the subsequent splicing process. However, a very recent model described that in the human genome, splicing occurs predominantly during transcription, becoming a co-transcriptional splicing (Tilgner *et al*. 2012). Anyway, the regulation and selection of splice sites is done by trans-acting splicing activators and splicing repressor proteins. Splicing of mRNA is performed by a RNA and protein complex known as the spliceosome, containing snRNPs designated U1, U2, U4, U5 and U6 (U3 is not involved in mRNA splicing) (figure 8) (Ritchie *et al*. 2009). U1 binds to 5' GU and U2 binds to the branch region with the assistance of the U2AF protein factors. The complex at this stage is known as the spliceosome A complex. Formation of the A complex is usually the key step in determining the end of the intron to be spliced out, and defining the end of the exon to be retained (Matlin *et al*. 2005). The U4, U5, U6 complex binds, and U6 replaces the U1 position. U1 and U4 leave and the remaining complex performs two transesterification reactions. In the first transesterification, 5' end of the intron is cleaved from the upstream exon and joined to the branch site by a 2',5'-phosphodiester bond. In the second transesterification, the 3' end of the intron is cleaved from the downstream exon, and the two exons are joined by a phosphodiester bond. The intron is then released in lariat form and degraded (Black 2003; Ritchie *et al*. 2009).

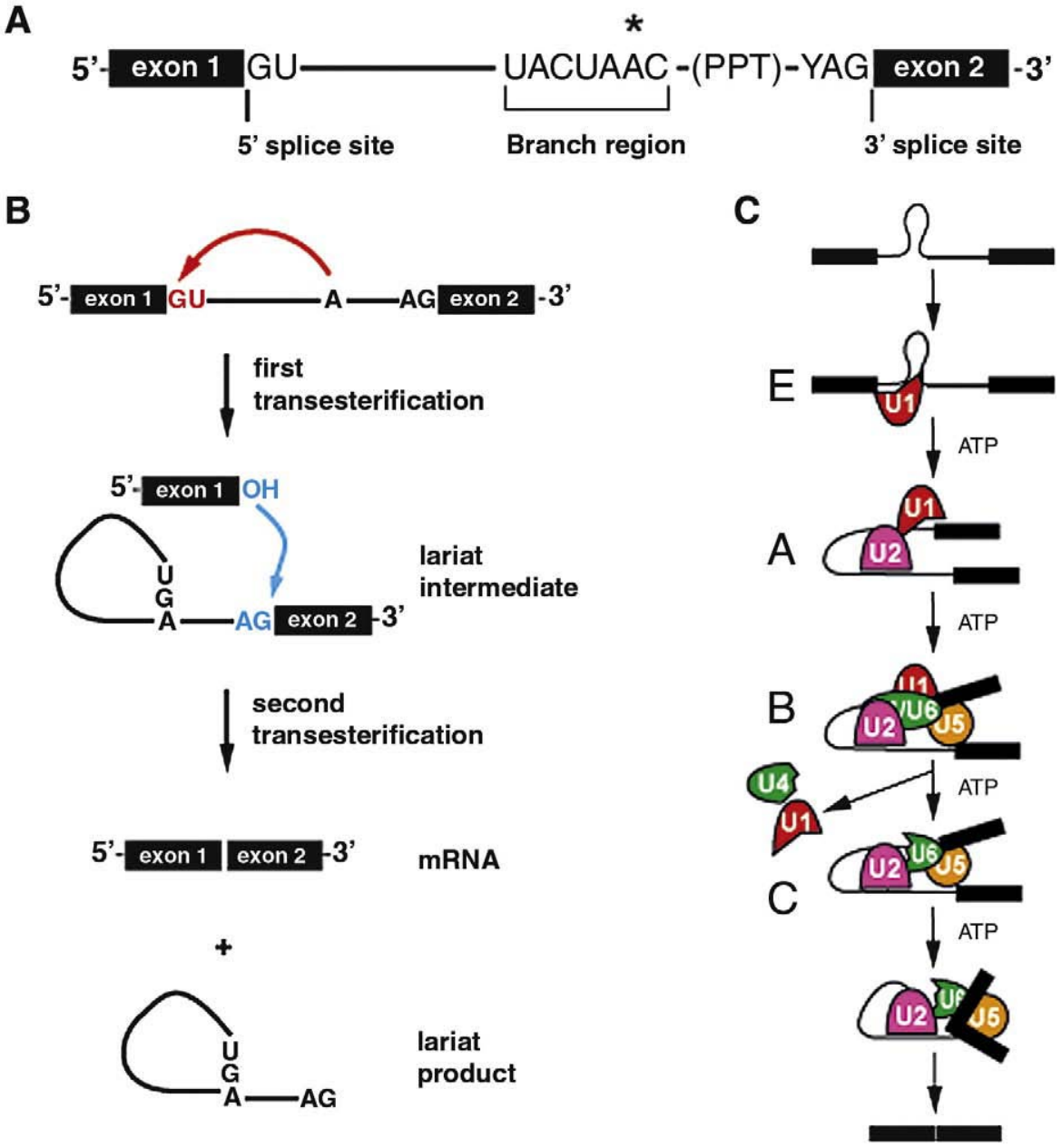

Figure 8. Splicing of pre-mRNA by the spliceosome. (a) Intron structure highlighting conserved sequences at the 5′ and 3′ splice sites, the optimal branch sequence, and metazoan polypyrimidine tract. The preferred branch adenosine is indicated (*). (b) Sequential transesterification reactions catalyzed by the spliceosome. (c) Stepwise assembly of the spliceosome on a pre-mRNA showing sequential association of U1, U2, U4/U6·U5 snRNPs with the intron. Figure adapted from Ritchie *et al.* (2009).

Alternative splicing is one of the most important mechanisms to generate a large number of mRNA and protein isoforms from the surprisingly low number of human genes. Unlike promoter activity, which primarily regulates the amount of transcripts, alternative splicing changes the structure of transcripts and their encoded proteins. Together with nonsense-mediated decay (NMD), at least 25% of all alternative exons are predicted to regulate transcript abundance. Molecular analyses during the last decade demonstrate that alternative splicing determines the binding properties, intracellular localization, enzymatic activity, protein stability and post-translational modifications of a large number of proteins. The magnitude of the effects ranges from a complete loss of function or acquisition of a new function to very subtle modulations, which are observed in the majority of cases reported (figure 9). Alternative splicing factors regulate multiple pre-mRNAs and recent identification of physiological targets showed that a specific splicing factor regulates pre-mRNAs with coherent biological functions. Therefore, evidences are now supporting that alternative splicing coordinates physiologically meaningful changes in protein isoform expression and is a key mechanism to generate the complex proteome of multicellular organisms (Stamm *et al*. 2005).

Figure 9 (next page). Generation of complex protein expression patterns by alternative splicing. Cells are indicated as large squares; the cell nucleus is indicated as a large circle. Three genes are shown in the nucleus and are indicated by different colors. Proteins generated by these genes are shown in the same color on the right of each cell. Boxes indicate exons, horizontal lines show introns. Small ellipses indicate proteins. Each gene has an alternative spliced exon (AE1, AE2 and AE3) and splicing regulation is achieved by regulatory proteins 1 (yellow) and 2 (green) that activate an exon after binding to the appropriate enhancer (yellow or green square in the exon). (a) None of the splicing regulatory proteins is expressed, leading to skipping of all alternative exons. (b) Only the splicing regulatory protein 1 is expressed, resulting in the inclusion of AE1 and the expression of transmembrane protein (red). Binding to exon AE2 cannot activate the inclusion of this exon, as additional factors are needed (green).

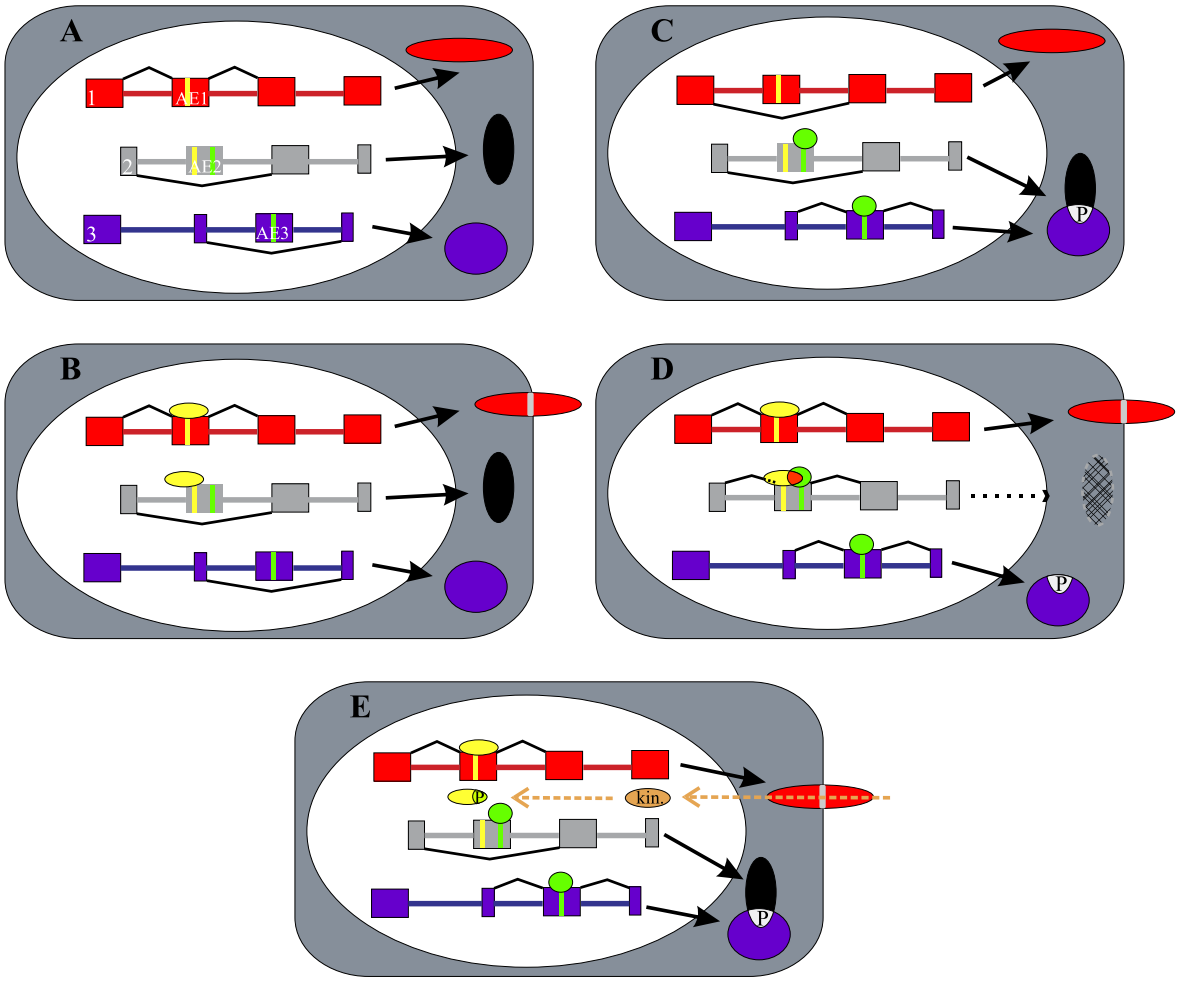

(c) Only the splicing regulatory protein 2 is expressed. It induces the alternative exon AE3 that encodes a phosphorylation site, which results in the binding of the protein encoded by gene 2 to the one made by gene 3. (d) Both splicing factors 1 and 2 are expressed.AE2 is activated because the binding of both factors is stabilized by the protein–protein interaction (red area between the splicing factors). Since exon AE2 encodes a premature stop codon, no protein is made (dashed circle). (e) External signals can change splice-site selection. In this example, an ion influx into the cell (orange dashed line) activates a kinase (kin) that phosphorylates the yellow splicing factor 2. As a result, exon AE2 is skipped and protein is made. Figure adapted from Stamm *et al*. (2005).

5.2. REGULATION AND DYSREGULATION OF ALTERNATIVE SPLICING

Organisms regulate alternative splice site selection by changing the concentration and activity of splicing regulatory proteins. This is achieved by *de novo* protein synthesis, by regulation of the intracellular localization and by phosphorylation (Stamm 2002). Since splice sites are highly degenerated, protein complexes forming on the pre-mRNA help in the high-fidelity recognition of exons. Serine/arginine-rich (SR) proteins and hnRNPs are the major classes of proteins identified in these complexes. They generally possess RNA- binding and protein-interaction domains that allow weak, transient binding between protein and pre-mRNA as well as between proteins. The combination of these multiple weak interactions ultimately leads to the proper recognition of exons by the spliceosome (Smith & Valcárcel 2000; Maniatis & Tasic 2002). Phosphorylation can either increase or decrease alternative exon usage, which most likely reflects that it can both promote and inhibit protein-protein interactions. Protein phosphatases cause the dephosphorylation of SR-proteins, what is necessary for the transesterification reaction (Cao *et al*. 1997).

Studies of the SR-protein class of regulators identified different kinases, such as MAPK (Al-Ayoubi *et al*. 2012), and protein phosphatase 1 as the molecules that control reversible phosphorylation, which regulates not only splice site selection, but also the localization of SR-proteins and mRNA export. The involvement of protein phosphatase 1 explains why second messengers like cAMP and ceramide that control the activity of this phosphatase influence alternative splicing. The emerging mechanistic links between splicing regulatory proteins and known signal transduction pathways now allow in detail the understanding how cellular signals modulate gene expression by influencing alternative splicing. This knowledge can be applied to human diseases that are caused by the selection of wrong splice site (Stamm 2008; Novoyatleva *et al*. 2008).

Since a fine-tuned balance of factors regulates splice site selection, a disturbance of this balance can cause human disease by leading to distinct products of gene expression (Tazi *et al*. 2009; J.-Y. Wu *et al*. 2003). Antagonistic splice variants of

genes involved in differentiation, apoptosis, invasion and metastasis often exist in a delicate equilibrium that is found to be perturbed in tumours. In several recent examples, splice variants that are over-expressed in cancer are expressed as hyperoncogenic proteins, which often correlate with poor prognosis, thus suggesting improved diagnosis and follow up treatment. Global gene expression technologies are just beginning to decipher the interplay between alternatively spliced isoforms and protein-splicing factors that will lead to identification of the mutations in these trans-acting factors responsible for pathogenic alternative splicing in cancer (Venables 2006; Venables *et al*. 2009).

Research during the last few years identified a number of low–molecular-mass chemical substances that can change alternative exon usage. Most of these substances act by either blocking histone deacetylases or by interfering with the phosphorylation of splicing factors. How the remaining large number of these substances affect splicing is not yet fully understood. The emergence of these low-molecular-mass substances provides not only probes for studying alternative pre-mRNA splicing, but also opens the door to the possible harnessing of these compounds as drugs to control diseases caused by the selection of ‘wrong’ splice sites (Garcia-Blanco *et al*. 2004; Hagiwara 2005; Sumanasekera *et al*. 2008).

5.3 ALTERNATIVE SPLICING VARIANTS OF NUCLEOSIDE TRANSPORTERS

For nucleoside transporters, very few spliced variants have been described to date and their roles as novel functional transporters remain unclear. For the SLC28 family, the Concentrative Nucleoside Transporters, one spliced variant has been described for the CNT3 family member (Errasti-Murugarren *et al*. 2009). In this case, the novel protein does not reach the cytoplasmic membrane but it is retained at the endoplasmic reticulum, except when in a polarized system. This variant seems to be functional although its role inside the cell remains unclear.

In the case of ENTs more variants have been previously described. For mENT1, the first variant was described in 2000, and is a protein which is identical to the wild type isoform but with 2 extra amino-acids in the internal loop. This addition results in the protein acquiring a new putative CK2 phosphorylation site that makes the protein functional but less active than the wild type (Kiss *et al*. 2000). In 2008, a novel variant was found in which exon 11 had been skipped resulting in the protein missing the last three transmembrane domains. This protein reaches the plasma membrane and is as active as the wild type but less sensitive to the inhibitor NBMPR (Robillard *et al*. 2008). Intriguingly, no spliced variants have been described for hENT1 to date. In contrast, many polymorphic variants have been analyzed, in which some cases regulation by CK2 is altered (Handa *et al*. 2001; Bone *et al*. 2007), or where the functionality as a nucleoside transporter is modified (Osato *et al*. 2003; Fukuchi *et al*. 2010; Kim *et al*. 2011).

ENT2 is the nucleoside transporter with the most spliced variants described so far. In 2005, a rbENT2 protein isoform was described, which was missing 41 residues but was still functional (S. K. Wu *et al*. 2005). Previously, in 2003, a hENT2 spliced variant was found, which possessed a 40 base pair deletion in exon 9 resulting in a 301 amino acid protein named hENT2A (Mangravite *et al*. 2003). This protein never reached the plasma membrane but stayed in an intracellular location within vesicular structures, and consequently no transport activity was determined. The most interesting ENT2 spliced variant found to date, due to its novel location, is the HNP36 protein, which is a 36 KDa hydrophobic nucleolar protein described as a mitogenic delayed-early response gene (Williams & Lanahan 1995; Crawford *et al*. 1998).

II. Research Objectives

Nucleoside transporters, besides internalizing their natural substrates, are responsible for the uptake of some anticancer and antiviral nucleoside-derived drugs. Nucleoside-based therapies might associate with chemoresistance and, among other factors, impaired drug uptake into the target cell may be a major cause of unsuccessful therapies. hENT2 plays an important role in leukemias and lymphomas, such as Chronic Lymphocytic Leukemia (CLL) (Pastor-Anglada *et al*. 2004), due to the fact that hENT2 mediates the cytotoxic effect of fludarabine, a major choice in CLL treatment. In addition, hENT2 has also been identified as one of the five genes that allow to predict positive outcome in Mantle Cell Lymphoma (MCL) patients (Hartmann *et al*. 2008). Thus, it is clear the relevance of nucleoside transporters, specially hENT2, in anticancer therapies. However, hENT2 mRNA levels did not show any correlation with protein expression and transport activity in CLL (Molina-Arcas *et al*. 2003), suggesting, among other possibilities, that not all the mRNA expressed would be translated into protein (Molina-Arcas *et al*. 2003). This would be consistent with different hENT2 transcripts of still unknown function.

Understanding how a protein implicated in drug uptake and action is regulated is the first step to figure out new strategies to improve nucleoside-based therapies. ENTs have been suggested to be regulated by phosphorylation, and despite some work described the effects of phosphorylation on ENT1 (Stolk *et al*. 2005; Bone *et al*. 2007; Coe *et al*. 2002; Grden *et al*. 2008; Reyes *et al*. 2011), there are very few studies about the biological effects of phosphorylation on ENT2. Moreover, as introduced above, sets of genes might have prognostic value and this anticipates unknown relationships among genes that may help to build up novel gene networks. Elucidating the connection of our target gene in a global gene network, or picturing different protein-protein interactions that regularly take place in the cell, should provide us with valuable information to spot hENT2, in our case, in a wide image of the cell physiology and its functioning and regulation.

Based on these issues, the specific objectives of this dissertation were:

1. To Identify and characterise novel splice variants of the human Equilibrative Nucleoside Transporter 2 (hENT2).

2. To study the phosphorylation status of hENT2 and the role phosphorylation might play in transporter trafficking and activity.

3. To perform a large-scale screening for hENT2 protein-protein interactions using the Membrane Yeast Two-Hybrid (MYTH) technique.

4. To identify putative novel gene networks involving nucleoside transporters (a transportome approach) and their role in the pharmacogenetic response of solid tumors to drug therapy.

III. Materials and Methods

6 CELL CULTURE

6.1 INTRODUCTION

Cell culture is the complex process by which cells are grown outside of their natural environment, in a proper atmosphere that provides the conditions need to conserve their physiological, biochemical and genetic properties. Experimenting with cell culture provides notable advantages to the biomedical research since it allows the study and analysis of relatively homogenous cell populations.

Culture prepared directly from tissues of a specific organism is called primary cell culture. Likewise, established or immortalised cell lines can be generated by acquiring the ability to proliferate indefinitely either through random mutation or deliberate modification, such as artificial expression of the telomerase gene. Numerous cell lines were well established as representative of particular cell types. Cell lines are better conserved than primary cell culture and they also allow to perform long term experiments. However, since they lost the proliferation control, they also lost some particular cell features becoming less differentiated than the original tissue.

Depending on their capacity of adhesion to the different culture support surface, cells can be grown in suspension or as monolayer. In the last case, cells depend on the binding to the surface and do not start to proliferate until being attached to the support. Generally, cells coming from organs grow in monolayer, while blood cells usually grow in suspension. However, some certain cell lines can form multiple layers or even grow in both ways, monolayer and suspension.

6.2 CELL CULTURE TECHNIQUE

Working with cell culture entails the maintaining of strict sterile conditions. Therefore, it is need to always work in laminar flow cabinets sterilized with ultraviolet

light (UV) and autoclaved material sprayed with ethanol 70%. Cell culture material includes:

i. Laminar flow cabinet with UV system, vacuum system for liquids aspiration and Bunsen burner.
ii. Cell culture incubator with a controlled atmosphere at 37ºC, 5% CO_2 and 95% relative humidity.
iii. Cryogenic equipment: -20ºC and -80ºC freezers, liquid nitrogen tank and a freezing container providing the critical 1ºC/min cooling rate required for successful cryopreservation of cells.
iv. Thermostated bath at 37ºC.
v. Sterilizing material: ethanol 97%, filter pump and autoclave system.
vi. Inverted optical microscope.
vii. Neubauer chamber for cell counting.
viii. Other material: pipette controller, plates, flasks etc.

6.3 CELL LINES CULTURE

Cell line maintaining involves the use of culture medium with all the nutrients required for the cell growing. Those media are regularly supplemented with serum and other components to compensate the lack of growing factors and aminoacids like glutamine. Antibiotics and antimycotics are often added to the medium to prevent infections.

Basic cell culture maintaining involves plating part of a grown culture with high density of cells to a new plate or flask with fresh medium to guarantee its viability. Despite cells are immortalized and they could keep on dividing indefinitely, this plating process might cause an undesired accumulation of mutations and senescence of the cells. Therefore, it is needed to amplify and freeze some aliquots of cells of low passages.

6.3.1 Detaching and plating:

In order to detach cells from their growing support and plate them in a new surface we need the use of substances such as trypsin or EDTA. Trypsin is a proteolytic enzyme belonging to the group of serine proteases that breaks the intercellular bindings. EDTA is a chelant molecule that retains Ca^{2+} ions required for cell-cell adhesion.

This process needs to be done inside a laminar flow cabinet in sterile conditions. Once cells reach a certain confluence, depending on the cell line type, we aspirate the medium and add sterile PBS to remove any trace of serum left. Some serum components might interfere with the trypsin action, so it is important to ensure cells are clean before adding trypsin. Subsequently, we aspirate PBS and add the minimum volume of trypsin required for the correct disaggregation of cells. Trypsin volume depends on the size of the support. Incubation at 37ºC during trypsin treatment might be recommended depending on the cell type. Once confirming a correct disaggregation under the microscope, the next step is to add new fresh medium supplemented with serum to inactivate the enzymatic activity of the trypsin. Mechanical disaggregation with a pipette is recommended.

Afterwards, cells may be frozen in aliquots and kept at -80ºC or seeded on new plates or flasks. If the purpose is just to do a regular maintaining of the culture, cells are diluted and plated on a new flask with fresh medium. Dilution factor will depend on the cell type. If the aim is to seed cells for a particular experiment, then it is need to count the density of cells with the Neubauer chamber and dilute the cells to a specific density to plate them according to the design of the experiment.

6.3.2 Freezing and thawing:

Cell freezing requires the use of cryoprotectant agents like glycerol or DMSO that promote the cell viability after freezing. Freezing medium composition may vary depending on the researcher but in our particular case we used FBS with 10% DMSO.

Cryoprotectant agents are toxic for the cell at room temperature when their concentration is more than 2%. Therefore, it is very important to reduce the contact time of the cells with these compounds and proceed rapidly.

After trypsinization, cells are centrifuged at 2500 x g for 3-5 minutes. Then media is removed and cells are resuspended in freezing medium and aliquoted (2,000,000 cells/tube) in 2ml cryotubes. Rapidly, cryotubes are introduced into the freezing container at -80ºC for a minimum of 4h and a maximum of 1 month. Cryotubes are lately conserved in a liquid nitrogen tank for years if wished.

Cell lines and media used in this dissertation are described in table 1.

6.4 CYCLOHEXIMIDE TREATMENT

Cycloheximide (CHX) is an inhibitor of protein biosynthesis in eukariotic organisms, produced by the bacterium *Streptomyces griseus*. CHX exerts its effect by interfering with the translocation step in protein synthesis thus blocking translational elongation. CHX is widely used in biomedical research to inhibit protein synthesis in eukaryotic cells studied *in vitro*. It is inexpensive and works rapidly. Its effects are rapidly reversed by simply removing it from the culture medium.

CHX may be used to distinguish between proteins translated in the mitochondria and proteins translated in the cytosol. mRNA translated in cytosol or ER from mRNA derived from the nucleus will not be expressed in the presence of CHX. Conversely, translation using mitochondrial ribosomes is unaffected by CHX and mitochondrial genes will continue to be expressed. CHX can also be used in molecular biology to determine the half-life of a protein treating cells with CHX in a time-course experiment and analyzing the protein expression by immunoblotting. In this thesis we mainly used CHX for two different purposes: to reduce protein background at the ER in immunocytochemistry assays, and to block the NMD pathway and determine mRNA surveillance.

Table 1. Cell lines and media used

Cell line	Origin	Source	Medium
HeLa	Human cervix, epithelial adenocarcinoma	ATCC[K]: CCL-2	DMEM + 10%FBS + 1% Gln + 1% Anti
HEK-293	Human embryonic kidney, epithelial	ATCC[K]: CRL-1573	DMEM + 10%FBS + 1% Gln + 1% Anti
MCF7	Human mammary gland, epithelial adenocarcinoma	ATCC[K]: HTB-22	DMEM + 10%FBS + 1% Gln + 5% Anti
BeWo	Human placenta, epithelial choriocarcinoma	ATCC[K]: CCL-98	DMEM - F12 + 10%FBS + 1% P/S Medium needs to be replaced daily
PanC-1	Human pancreas duct, epithelioid carcinoma	Dr. A. Mazo	DMEM + 10%FBS + 1% Gln + 1% Anti
BxPC3	Human pancreas, epithelial adenocarcinoma	Dr. A. Mazo	DMEM + 10%FBS + 1% Gln + 1% Anti
NP9	Human pancreas, epithelial adenocarcinoma	Dr. A. Mazo	DMEM - F12 + 10%FBS + 1% Anti
NP29	Human pancreas, epithelial adenocarcinoma	Dr. A. Mazo	DMEM - F12 + 10%FBS + 1% Anti
NP31	Human pancreas, epithelial adenocarcinoma	Dr. A. Mazo	RPMI 1640 + 10%FBS + 1% Gln + 1% Anti
AGS	Human stomach, epithelial gastric adenocarcinoma	ATCC[K]: CRL-1739	F12-K + 10% FBS + 1% Gln + 1% Anti
SNU-1	Human stomach, epithelial gastric adenocarcinoma	ATCC[K]: CRL-5971	RPMI 1640 + 10%FBS + 1% Gln + 1% Anti
SNU-5	Human stomach, epithelial gastric adenocarcinoma	ATCC[K]: CRL-5973	IMDM + 20% FBS + 1% Gln + 1% Anti
MKN-45	Human stomach, epithelial gastric adenocarcinoma	DSMZ[L]: ACC 409	RPMI 1640 + 10%FBS + 1% Gln + 1% Anti
KATO III	Human stomach, epithelial gastric adenocarcinoma	ATCC[K]: HTB-103	IMDM + 20% FBS + 1% Gln + 1% Anti
Mz-ChA-1	Human gallbladder, epithelial adenocarcinoma	Dr. A. Knuth	RPMI 1640 + 1% GlutaMAX™-1 + 1% Sodium Pyruvate + 1% MEM non-essential aa + 1% Gln + 1% P/S + 10% FBS heat inactivated
Mz-ChA-2	Human gallbladder, epithelial adenocarcinoma	Dr. A. Knuth	
SK-ChA-1	Human bile duct, epithelial carcinoma	Dr. A. Knuth	
TFK-1	Human bile duct, epithelial carcinoma	DSMZ[L]: ACC 344	RPMI 1640 + 10%FBS + 1% Gln + 1% Anti
EGI-1	Human bile duct, epithelial carcinoma	DSMZ[L]: ACC 385	DMEM + 10%FBS + 1% Gln + 1% Anti

Gln: L-Glutamine; Anti: Antibiotic-antimycotic; P/S: Penicillin-Streptomycin

Common CHX concentrations used in biology research are within the range of **1 - 20 µg/ml**. The classical protocol used for CHX treatment starts preparing the necessary volume of medium pre-warmed at 37ºC, and adding the volume of CHX stock needed to get a desired final concentration. Following, old medium is removed from the cell culture and replaced by the fresh medium with CHX incorporated. Since CHX is a photosensitive molecule, we recommend to work with lights off inside the cabinet. After **3 hours** incubating the cells at **37ºC** with CHX, treatment is removed and cells are ready to continue with the following steps of the experiment.

6.5 TRANSIENT TRANSFECTION FOR HETEROLOGOUS GENE EXPRESSION IN CELLS

Transfection is the process of deliberately introducing nucleic acids into cells, specifically for non-viral methods in animals cells. Other terms are used when transfection is virus-mediated (transduction), or when is a non-viral DNA transfer in bacteria or non-animal eukaryotic cells (transformation). Genetic material, such as supercoiled plasmid DNA or siRNA constructs, are transfected into animal cells by typically opening transient pores in the cell membrane to allow the material uptake.

Transfection can be carried out by using calcium phosphate, by electroporation, or by mixing a cationic lipid with the material to be transfected in order to produce liposomes, which will fuse with the cell membrane and deposit their cargo inside. Since it is an aggressive technique for the cell, transfection can result in unexpected morphologies and abnormalities in target cells.

For most experimental applications, it is sufficient if the transfected genetic material is only transiently expressed. Since the DNA introduced in the transfection process is usually not integrated into the nuclear genome, the foreign DNA will be diluted through mitosis or degraded. If desired, a stable transfection where the transfected material is incorporated into the cell genome must occur.

To accomplish this, a marker gene is co-transfected, like the neomycin resistance gene. That gene gives the cell some selectable advantage, such as resistance toward the toxin geneticin. Some of the transfected cells will, by chance, have integrated the foreign genetic material into their genomes. If the toxin is then added to the cell culture, only those few cells with the marker gene integrated into their genomes will be able to proliferate, while other cells will die. After applying this selective stress for some time, only cells with a stable transfection remain and can be further cultivated.

6.5.1 Calcium phosphate transfection:

This method is based on the precipitated formed from calcium chloride and the DNA in a phosphate saline solution. Those aggregates are incorporated inside the cell by endocytosis or even phagocytosis. Calcium attached to the DNA protects it from being degraded by nucleases. Size and quality of those aggregates are critical for this protocol, therefore little changes in the pH might increase the efficiency drastically. Before transfecting DNA into a determined cell line, pH optimization needs to be done to ensure a maximum efficiency of the experiment. Transfection efficiency can be analyzed using a GFP vector to determine the percentage of transfected cells at any pH. The same way, GFP plasmid can be used as positive control for any transfection assay.

For this kind of transfection method, cells must be around 40-60% confluent. First, old medium is removed and replaced by fresh new medium properly supplemented according to the cell line requirements. Following, transfection mixed is prepared in a sterile tube, adding the different components according to that order:

1st. Sterile water and DNA sample
2nd. Transfection calcium buffer
3rd. Transfection phosphate buffer

Reagents are mixed by bubbling and incubated at room temperature for 15 minutes to form the DNA-calcium aggregates. Then, the transfection mix is added drop by drop to the cell culture and it is incubated overnight at 37ºC. Transfection medium is removed the following day and cells can be assayed within 24 - 72 hours after transfection.

DNA used in transfection protocols should be obtained from a maxi-prep, since the concentration and the quality of the DNA is better than a mini-prep. The amount of the DNA added to the transfection mix is 0.35 µg/cm^2, considering the surface of the cell culture support (plates or wells). The volume of the transfection mixed added cannot exceed 10% of the total volume of the medium added to the cell culture (table 2).

Table 2. Conditions of calcium-phosphate transfection mix

Culture Vessel	DNA	Sterile water	Calcium buffer	Phosphate buffer	Culture medium
24-well plate	0.7 µg	12.5 µl	12.5 µl	25 µl	0.5 ml
6-well plate	3.5 µg	50 µl	50 µl	100 µl	2 ml
60-mm plate	7 µg	125 µl	125 µl	250 µl	5 ml
100-mm plate	21 µg	250 µl	250 µl	500 µl	10 ml
150-mm plate	52 µg	0.75 ml	0.75 ml	1.5 ml	30 ml

6.5.2 Lipofectamine® 2000 transfection:

Lipofectamine® 2000 transfection is based on the formation of complexes from a cationic lipid and DNA producing liposomes. Those liposomes will fuse with the cell membrane internalizing the genetic material into the cytoplasm. The mortality rate of that technique is even higher than using calcium-phosphate, therefore initial culture should be at 75-90% of confluence before transfection. However, the efficiency of transfection is also higher using lipofectamine® and it also allows the transfection of siRNAs.

Once cells are ready to be transfected, first step is to remove the old culture medium and replace it by fresh new non-supplemented medium, since antibiotics and serum might interfere in the liposomes formation. In one sterile tube, lipofectamine® and non-supplemented medium are mixed and incubated at room temperature for 5 minutes. In another sterile tube, DNA is added to non-supplemented medium (table 3). Both preparations are eventually mixed adding the lipofectamine® to the DNA tube. After mixing, this transfection mix is incubated for 20 minutes at room temperature and added to the cell culture. Cells are incubated for 4 hours at 37ºC. Afterwards, transfection mix is replaced by fresh medium properly supplemented. Cells can be assayed within 24 - 72 hours after transfection.

Table 3. Conditions of lipofectamine® 2000 transfection mix

Culture Vessel	DNA	Non-sup. medium	Lipofect.	Non-sup. medium	Culture medium
24-well plate	0.8 µg	50 µl	2 µl	50 µl	0.5 ml
6-well plate	4 µg	200 µl	10 µl	200 µl	2 ml
60-mm plate	8 µg	0.5 ml	20 µl	0.5 ml	5 ml
100-mm plate	24 µg	1.5 ml	60 µl	1.5 ml	15 ml
150-mm plate	60 µg	3 ml	150 µl	3 ml	30 ml

7 CYTOTOXICITY ASSAYS

Cytotoxicity assays are performed to determine the cell-killing property of a chemical compound without defining any specific cellular death mechanism. There are several methods commonly used to detect cell viability, in our case we used the MTT assay.

7.1 CELL SEEDING AND TREATMENT

To perform this kind of experiments cells are seed on 96-well plates with the help of a multichannel pipette to ensure each well has the same amount of cells. Next

day, once cells are settled onto the well surface, treatments are administrated for 24-72h depending on the experiment. Afterwards, cell viability is determined by MTT assay.

There is a specific strategy when applying the treatments in order to get reliable results. As shown in figure 10, the first two columns are the control samples, which the treated samples will be relativized to. By control it is understood non-treated cells, only the solvent of the drug will be administrated in case that is not water. A total of 10 different doses can be administrated in one experiment, considering each column one single dose. (D1-D10). Doses are usually distributed starting from the more diluted (D1) to the more concentrated (D10). Quadruplicates are required to reduce the error of the experiment, therefore, lines A-D belong to one experiment and lines E-H belong to another experiment. As a summary, one 96-well plate allows us to analyze 10 doses of two different compounds at once.

7.2 MTT ASSAY

The MTT assay is a colorimetric assay for measuring the activity of cellular enzymes that reduce the tetrazolium dye, MTT (3-(4,5-Dimethylthiazol-2-yl) -2,5diphenyltetrazolium bromide), from a yellow tetrazole to its insoluble purple formazan in living cells. This assay measures cellular metabolic activity via NAD(P)H-dependent cellular oxidoreductase enzymes and reflects the number of viable cells. MTT assays can be used to measure cytotoxicity (loss of viable cells) or cytostatic activity (shift from proliferative to resting status) of different compounds and drugs.

Detection of the formazan precipitates requires a solubilizing solution able to lysate the cellular membrane and also to dissolve the produced salts, generating a homogeneous purple solution. Common solubilizing agents are DMSO, acidified ethanol solution, or a solution of SDS in HCl. The absorbance of this coloured solution can be quantified by measuring at certain wavelength between 500-600 nm with an ELISA plate reader.

The first step of the protocol followed in this thesis is to remove the cell medium containing the treatments. MTT is added to the cells dissolved in non-supplemented culture medium at a final concentration of 0.75 mg/ml. Cells are incubated at 37ºC between 45 minutes and 3h, depending on the cell line. Reaction is done when purple precipitates are noticeable at the bottom of the control wells. Afterwards, MTT solution is carefully removed. Since MTT is a colorimetric assay it is extremely important to make sure there are no drops of medium inside the wells as that would compromise the absorbance readings. Following, 100 µl of DMSO are added to each well to solubilize the formazan product with the help of a shaker. Finally, plates are read at 550 nm with an ELISA plate reader. Results are relativized to the control samples, considering those points 100% of viability.

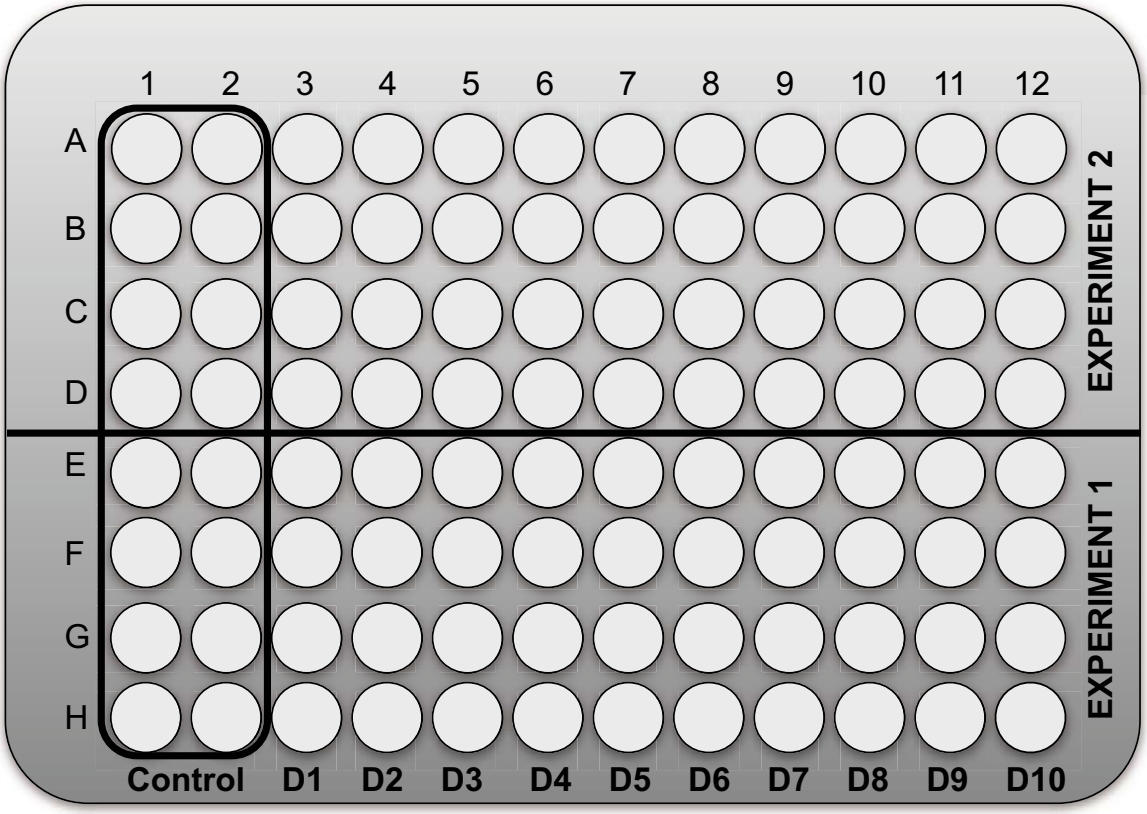

Figure 10. Representation of treatments distribution in a 96-well plate. Since each point requires quadruplicates, lines A-D belong to experiment 1 while lines E-H belong to experiment 2. The first two columns have the control points, what means non-treated cells. Only the solvent of the drug will be administrated to the control wells in case that is not water. Columns 3-12 are used for 10 different drug concentrations, applying the lower dose on column 3 (D1) and the highest dose on column 12 (D10).

8 NUCLEOSIDE UPTAKE MEASURING

The process of measuring the nucleoside uptake in mammalian cells basically consists in incubating cells with a known concentration of cold substrate plus a proper proportion of radio-labelled substrate. Once cells are incubated during the required time, uptake is stopped by removing the radioactive medium and washing cells with a cold stop solution. Afterwards, cells are lysed and measured its up-taken radioactivity, corresponding to the amount of substrate internalized by the cell.

For the experiment designing, there are some important considerations to take into account, like the fact that the total concentration of substrate (cold and radio-labelled together) should be within the range of the Km of the studied transporter. The assay must always be performed in initial velocity conditions, ensuring the transporter is not saturated. Therefore, it is recommended to perform a previous time-course assay.

As we explained in the introduction section, there are two main families of nucleoside transporters according to their sodium-dependent activity. To evaluate the transport activity of CNTs, it is needed to use a transport medium containing NaCl. Unlike the case of ENTs, where a choline-based buffer is used instead. Regarding the total ENT activity, the use of specific inhibitors will allow to discern between ENT1 and ENT2 activity. The difference between transport activity using choline buffer and choline buffer with NBTI 1 μM, reflects the activity due to ENT1 transporter. When medium contains dipyridamole 10 μM, the transport activity detected is non-specific of ENTs. Subtracting ENT1 and non-specific values to the total of ENT activity, ENT2 transport activity is then obtained.

8.1 MAMMALIAN CELLS TRANSPORT ASSAY

In our group, transport assays with mammalian cell lines are performed in 24-well plates (figure 11). Each column of the plate represents quadruplicates of the same

experimental point. There are three different conditions to be analyzed in every experiment: without inhibitors (1), with NBTI 1 µM (2) and with dipyridamole 10 µM (3). Using that deign of the plate, we can perform two different experiment at once.

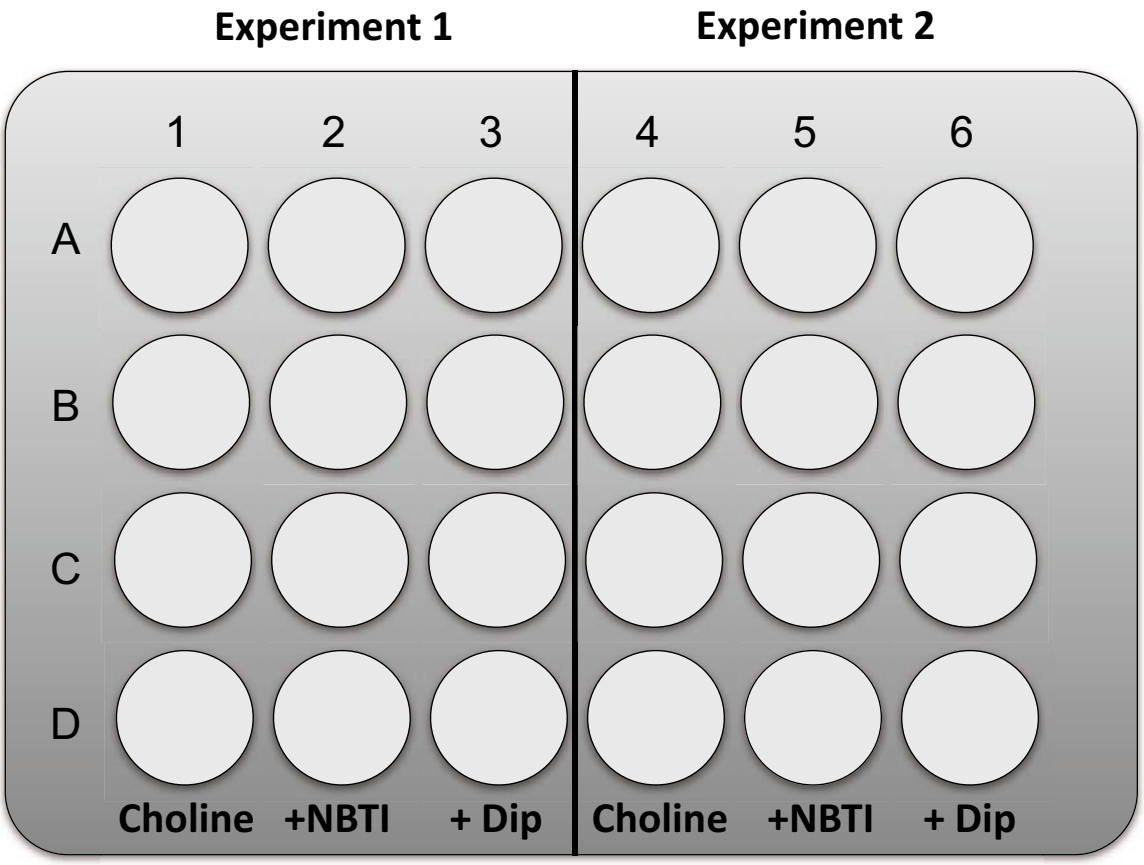

Figure 11. Representation of a 24-well plate distribution for transport assays. Each column represents quadruplicates of the same experimental point. Three conditions are tested in every assay: no inhibitors (1, 4), NBTI 1 µM (2, 5) and dipyridamole 10 µM (3,6). This particular design allows us to perform two different experiments at once. Subtracting values from columns 2 and 3, 5 and 6 to 1 and 4 respectively, ENT1 and ENT2 activity values will be obtained separately.

To perform the experiment, cells are first washed twice with choline buffer pre-warmed at 37ºC. Following, cells are incubated for 1 minute with the radioactive solution, which has a final substrate concentration of 1 µM and 1 µCi/ml of radioactivity, with or without inhibitors. In total, 250 µl of transport solution are added to each well. Reaction is stopped by washing the samples twice with 1 ml of cold stop buffer. It is important to aspirate all the medium left to remove all the radioactivity not incorporated by cells. At that point, cells can by lysed directly or kept in the -20ºC freezer to continue with the protocol another day.

Cells need to release all the radioactive substrate incorporated in order to determine their transport activity. Therefore, samples are incubated with 100 µl/well of lysis solution for 30 minutes - 1 hour with horizontal shaking. Afterwards, lysates are homogenized by pipetting and transferred into a scintillation vial containing scintillation liquid. A 10 µl aliquot of each well has to be kept to quantify the concentration of total protein, 90 µl will then be used for radioactivity quantification. Scintillation liquid is required to convert the energy released during radioactivity decay in light, which is detected by the scintillation counter.

Radioactivity values associated to each sample in disintegrations per minute (DPM), are relativized to the respective concentration of protein. This calculation is required to correct possible differences in the number of cells per well, either intra- or inter-experiment. Calculations to be done are:

$$Activity(pmol/mgprot) = \frac{DPMsample \times 10^3}{AE \times Vsample \times [prot(\mu g/\mu l)]}$$

Where AE is the specific activity of the radioactive transport medium expressed in DPM/pmol.

8.2 OOCYTES TRANSPORT ASSAY

An oocyte is an immature ovum, or egg cell from *Xenopus laevis*. This cells are commonly used in transport assays due to its clear background for most of the human proteins. In order to work with oocytes, first it is needed to clone the gene of interest into a proper vector suitable to generate cRNA. Unlike cell lines, genetic material transfected into oocytes is usually cRNA instead of DNA.The reason is because DNA should be injected into the nucleus to be expressed starting from the gene transcription. Due to its difficulty, a better efficiency is obtained when cRNA injected at the cytosol, ready to be translated.

To perform an *in vitro* transcription, a T7 promoter sequence has to be introduced before the start codon of our gene of interest. In our case, we cloned the hENT2 genes into the pBSxG vector, which contains a T7 promoter region before its multi-cloning site. cRNA transcripts were subsequently generated according to the mMessage mMachine® Kit manufacturer's protocol. The concentration and size of the RNA transcripts was determined using a spectrophotometer and agarose gel electrophoresis.

Xenopus laevis oocytes were used for heterologous hENT2 expression since they lack endogenous nucleoside transport activity. Oocytes were removed from adult female frogs by Dr. WJ Brad Hanna, from University of Guelph. After extraction, stage V-VI oocytes were stored overnight at 18-20 ºC in ND96 medium. Follicle layers were removed by treating the oocytes with collagenase Type I (1 mg/ml) for 20-40 minutes in calcium-free saline. For injections, 75 ng of cRNA were injected into 15-20 oocytes per treatment per trial using a nanoinjector. Following injection, oocytes were kept at room temperature for 72 hours in ND96 medium. In order to have a good maintaining, medium has to be changed daily and necrotic oocytes have to be removed since they release cytotoxic material.

To assess transport activity, oocytes are incubated for 60 minutes at room temperature in 200 µl of choline chloride transport buffer containing 10 µM of substrate and 0.1 mCi/ml of [^{3}H] radio-labelled substrate. Following incubation, extracellular

substrate is removed using three rapid 1 ml washes with cold choline chloride buffer containing dipyridamole 10 µM. Each single oocyte is then placed into a separate scintillation vial containing 200 µl of SDS 1% (w/v). Vials are subjected to vigorous shaking for 45 minutes to dissolve the oocyte. Finally, 2 ml of scintillation fluid is added to each vial followed by scintillation counting. In that case, results are expressed as Cpm/oocyte.

9 PROTEIN EXPRESSION ANALYSIS

Cellular lysates are obtained from cells seeded on 60, 100 or 150 mm plates depending on the purpose of the experiment. In this thesis, we used two different types of protein extraction methods depending if our aim was to study the expression of proteins from a total fraction of the extract, or enriched membrane proteins.

9.1 PROTEIN EXTRACTION FROM CELLULAR LYSATES

9.1.1 Protein extraction with NP-40 buffer:

The reagent used for this kind of extraction is NP-40 or Nonidet P-40 (octyl phenoxypolyethoxyethanol), a non-ionic, non-denaturing detergent. Nonidet P-40 is frequently abbreviated as NP-40, but should not be confused with a different detergent by the same name (NP-40, nonyl phenoxypolyethoxyethanol), which is not powerful enough to break the nuclear membrane, but can break the cytoplasmic membrane.

Lysis buffer is composed by NP-40 1% buffer (see recipes section - appendix II), and a cocktail of protease inhibitors and sodium orthovanadate. Volumes may vary depending on the surface of the plate where cells are seeded, as we describe in table 4. Protease inhibitor cocktail solution is ten times concentrated, and it is obtained by dissolving one tablet in 1 ml of NP-40 1% buffer.

Table 4. NP-40 lysis buffer composition			
Component	**60 mm plate**	**100 mm plate**	**150 mm plate**
NP-40 1% buffer	160 µl	400 µl	1,120 µl
10X Protease inhibitor cocktail	20 µl	50 µl	140 µl
Na_2VO_3 10 mM	20 µl	50 µl	140 µl
Total volume	200 µl	500 µl	1,400 µl

All the process has to be done on ice, keeping cells and proteins at 4ºC to avoid protein degradation. First, old culture medium is aspirated and cells are carefully washed with PBS twice. At this point, plates can be kept at -80ºC to proceed later on with the extraction. Lysis buffer is added to the plate and cells are detached by using a plastic scrapper. Cells are collected with the pipette and transferred to an eppendorf tube. Cells suspension is then mixed by vortexing first and placed on ice for 10-20 minutes. Cells are disrupted by homogenizing with a 1 ml syringe and a 26g needle. Cells homogenate is then centrifuged at 8,000 rpm for 5 minutes at 4ºC. Cell debris pelleted is discarded and the supernatant, which contains the total protein extract, can be kept either at 4ºC or -20ºC.

9.1.2 Isolation of crude membrane proteins:

This protocol must be performed on ice to keep samples at 4ºC all the time. After washing the cell plates with PBS (see 6.3.1), lysis buffer supplemented with protease inhibitor cocktail, is added to the cell plates; 200 µl for 60 mm plates and 500 µl for 100 mm plates. According to the protocol described in 6.3.1 section, cells are detached using a scrapper and homogenized by vortexing and using a 26g needle. Cells are then centrifuged at max speed for 30 minutes at 4ºC. Cell debris is discarded and supernatant is following ultra-centrifuged at 54.000 rpm for 1 hour and 30 minutes at 4ºC. Supernatant is discarded and the transparent pellet is resuspended in crude membranes solubilizing buffer; 50 µl for proteins coming from a 60 mm plate, and 100 µl for 100 mm plates.

9.2 DETERMINATION OF PROTEIN CONCENTRATION

In the present thesis, two different methods have been used to quantify protein concentration; BCA method was used to determine to concentration of samples obtained during transport assays, while Bradford method was used for the other experiments.

9.2.1 BCA method:

The bicinchoninic acid assay (BCA assay) is a biochemical assay for determining the total concentration of protein in a solution (0.5 µg/ml to 1.5 mg/ml). The total protein concentration is exhibited by a change of color of the sample from green to purple in proportion to the protein concentration, which can then be measured using colorimetric techniques.

Firstly, the peptide bonds in protein reduce Cu^{2+} ions from the cupric sulphate to Cu^{+}. The amount of Cu^{2+} reduced is proportional to the amount of protein present in the solution. Next, two molecules of bicinchoninic acid chelate each Cu^{+} ion, forming a purple-coloured product that strongly absorbs light at a wavelength of 562 nm. The amount of protein present in a solution can be quantified by measuring the absorption spectra and comparing with a protein solution of known concentrations.

For the standard curve, a serial of dilutions are made from the commercial albumin stock present in the BCA assay kit, using the same buffer used during the protein extraction. Duplicates of 10 µl of each standard curve dilution and protein sample are dropped on a 96-well plate. Commercial A:B solutions are mixed with the proportion of 50:1, and 200 µl/well are added to the 96-well plate. The plate is gently shaken and incubated at 37ºC for 30 minutes. Afterwards, the plate is room tempered for 10 minutes and absorbance is measured using an ELISA device at 562 nm. Software used for protein quantification is called Magellan, from TECAN®.

9.2.2 Bradford method:

The Bradford assay is a colorimetric protein assay based on an absorbance shift of the dye Coomassie Brilliant Blue G-250, in which under acidic conditions the red form of the dye is converted into its blue form to bind to the assayed protein. During the formation of this complex, two types of bond interactions take place: the red form of Coomassie dye first donates its free electron to the ionizable groups on the protein, which causes a disruption of the protein native state, consequently exposing its hydrophobic pockets. These pockets on the protein tertiary structure bind non-covalently to the non-polar region of the dye via van der Waals forces, positioning the positive amine groups in proximity with the negative charge of the dye. The bond is further strengthened by the ionic interaction between the two. The binding of the protein stabilizes the blue form of the Coomassie dye; thus the amount of the complex present in solution is a measure for the protein concentration, and can be estimated by use of an absorbance reading.

To perform this assay, the commercial Bradford dye reagent is diluted 1:4 with distillate water. 1 ml of this solution is added to each plastic cuvette suitable for spectrophotometer. Depending on the sample to be measured, 2 - 10 µl of protein are added to the cuvettes in duplicates. In parallel, a standard curve is made using a solution of BSA (Bovine Serum Albumin). Cuvettes are then mixed and after 5 minutes the absorbance of the standard curve and also the sample is read at 595 nm.

9.3 BIOTINYLATION OF MEMBRANE PROTEINS

Biotinylation is the process of covalently attaching biotin to a protein, nucleic acid or other molecule. Biotinylation is rapid, specific and is unlikely to perturb the natural function of the molecule due to the small size of biotin. Biotin is a vitamin that binds to streptavidin and avidin with an extremely high affinity, fast on-rate, and high specificity, and these interactions are exploited in many areas of biotechnology to isolate biotinylated molecules of interest. Biotin-binding to streptavidin and avidin is

resistant to extremes of heat, pH and proteolysis, making capture of biotinylated molecules possible in a wide variety of environments. Also, multiple biotin molecules can be conjugated to a protein of interest, which allows binding of multiple streptavidin or avidin protein molecules and increases the sensitivity of detection of the protein of interest.

In this thesis we used biotinylation to label membrane proteins exclusively and purify them using streptavidin beads. This protocol has to be realized under cool temperatures, using ice specially during the first steps to avoid protein degradation. To perform that kind of technique, a minimum of 5 x 150 mm plates seeded with cells are required to guarantee a decent quantity of protein obtained.

Culture plates with cells seeded on it are carefully washed twice with PBS-Ca/Mg. Presence of calcium and magnesium minimizes cell detaching. Cells are then incubated with a sulfo-NHS-LC-biotin 500 µM dissolved in PBS-Ca/Mg for 30 minutes at 4ºC and with soft shaking. Biotin has to be first dissolved in dimetilformamide and then diluted in PBS to be used right away. Biotin solution is then aspirated and cells are washed with a solution of PBS-Ca/Mg with glycine 100 mM for 15 minutes three times. Following, cells are lysed using 750 µl of NP-40 lysis buffer (supplemented with protease inhibitors and Na_2VO_3) and shaked for 15 minutes. Cells are detached using a plastic scrapper and homogenized by vortexing and using a 26g needle. Homogenate is centrifuged at max speed for 30 minutes at 4ºC. The supernatant is considered the “homogenate” fraction, including total protein but the nuclear fraction. At this point, homogenate fraction can be kept at -80ºC to continue or repeat the protocol another day.

Streptavidin-agarose beads are washed with NP-40 buffer twice, centrifuging tubes at 2,500 rpm for 5 minutes. Once beads are ready, 500 µg of homogenate fraction are incubated with 30 - 50 µl of streptavidin beads solution for 1 hour and 30 minutes at room temperature using an orbital rotator. Following, samples are centrifuged at 2,500 rpm for 5 minutes at room temperature (same conditions for the following washes). In this case, the supernatant is considered the intracellular fraction,

while the pellet contains the streptavidin beads linked to biotin-bound membrane proteins. Streptavidin beads are then washed with 1 ml of NP-40 1% buffer, followed by two washes with biotinylation washing buffer 2 and three washes with biotinylation washing buffer 3.

Finally, membrane proteins are disrupted from streptavidin-biotin beads by adding 20 µl of protein loading buffer 5x and 30 µl of ddH_2O, and incubating samples for 30 minutes at room temperature in an orbital rotator. Samples are then boiled for 5 minutes at 95ºC (or 30 minutes at 37ºC in case of HA-tagged proteins) and centrifuged at max speed for one minute to obtain the membrane fraction (supernatant) separated from the streptavidin-biotin beads (pellet). Samples are then ready to be analyzed by SDS-PAGE electrophoresis and Western-Blot.

9.4 ELECTROPHORESIS IN SDS-PAGE

SDS-PAGE, sodium dodecyl sulfate polyacrylamide gel electrophoresis, describes a technique widely used in biochemistry and other fields to separate proteins according to their electrophoretic mobility, which is a function of the length of a polypeptide chain and its charge, and no other physical features. SDS is an anionic detergent applied to linearize proteins and to impart a negative charge to them. In most proteins, the binding of SDS to the polypeptide chain imparts an even distribution of charge per unit mass, thereby resulting in a fractionation by approximate size during electrophoresis.

In SDS-PAGE, proteins migrate through an electric field across the acrylamide matrix pores, which size depends on the percentage of acrylamide present in the gel. The system we use is a discontinuous electrophoresis where samples must first cross a stacking gel, with a lower percentage of acrylamide (5%) and lower pH (pH 6.8) that promotes proteins alignment before moving into the running gel. Running gel has a higher percentage of acrylamide (10-15%) and a pH of 8.8. Higher concentrations of

acrylamide are used to get a proper separation of small proteins, while lower concentrations are used for bigger proteins.

Table 5. Electrophoresis gel composition

Running gel	**10% Acrylamide**		**12% Acrylamide**		**15% Acrylamide**	
Components	**Small gel**	**Large gel**	**Small gel**	**Large gel**	**Small gel**	**Large gel**
ddH_2O	5 ml	15 ml	4.5 ml	13.5 ml	3.75 ml	11.25 ml
Solution A*	2.5 ml	7.5 ml	3 ml	9 ml	3.75 ml	11.25 ml
Solution B*	2.5 ml	7.5 ml	2.5 ml	7.5 ml	2.5 ml	7.5 ml
APS 10%	50 µl	150 µl	50 µl	150 µl	50 µl	150 µl
TEMED	10 µl	30 µl	10 µl	30 µl	10 µl	30 µl
Stacking gel	**Small gel**			**Large gel**		
ddH_2O	2.3 ml			6.9 ml		
Solution A*	0.67 ml			2 ml		
Solution C*	1 ml			3 ml		
APS 10%	30 µl			90 µl		
TEMED	5 µl			15 µl		

* Electrophoresis Solutions described in recipes section - Appendix II

Acrylamide gels are made according to the instructions describe in table 5. For small gels we use the Mini Protean II system (Bio-Rad), and for large gels, The Sturdier Vertical Gel Slab SE 400 (Hoefer). Gels can be made right before use or up to 24 hours in advance, being kept at 4ºC in humid conditions. Before running the electrophoresis gel, samples must be denaturalised by adding a proportional volume of protein loading buffer 5x (PLB 5x) and heating samples either at 95ºC for 5 minutes or 37ºC for 30 minutes. Samples and protein marker are load into the gel wells and running buffer is added to the electrophoresis system. Small gels usually run at 120 V for approximately 1.5 hours, and large gels run at 200 V for 3.5 hours, depending on the percentage of acrylamide of the gel.

9.4.1 Coomassie staining:

In those cases where protein electrophoresis does not continue with a transference to a nitrocellulose membrane to analyze protein expression by immunodetection, and only presence or absence of protein wants to be detected, protein staining can be applied. We also use protein staining to isolate a gel band containing some protein to be further detected and analyzed by mass spectrometry.

There are plenty of protein staining systems, however the most common probably is the Coomassie Brilliant Blue G-250, which binds to proteins nonspecifically. That is a fast and cheap method in which all proteins present in the acrylamide gel are stained with a similar intensity. The main disadvantage of this method is a low sensitivity compared with other staining methods, like silver staining.

Staining solution can be prepared in the same lab, however the reagents used are toxic by inhalation and also a destaining step is required, increasing the timing to detect proteins. In this thesis we used a commercial solution, PageBlue™ Protein Staining solution, ready-to-use, with a higher sensitivity and no destaining required. Staining protocol according to manufacturer's instructions.

9.5 WESTERN-BLOT TECHNIQUE

The Western-Blot or immunoblot is a widely accepted analytical technique used to detect specific proteins in the given sample of tissue homogenate or extract. It uses a previous gel electrophoresis to separate denatured proteins by length of the polypeptide (see section 9.4). The proteins are then transferred to a membrane, typically nitrocellulose or PVDF, where they are detected by using specific antibodies against the target protein.

9.5.1 Transference:

Once proteins are separated by electrophoresis (see section 9.4), the gel is dismounted from the electrophoresis system and equilibrated with transfer buffer, previously prepared. Acrylamide gel is then cut to discard the stacking gel and also parts of the gel where there are no proteins or not the target protein. Nitrocellulose membrane is also cut according the final size of the gel and equilibrated with transfer buffer as well.

For the transference we use a Trans-Blot® semi-dry electrophoretic transfer cell (Bio-Rad). Transfer montage is made as described in figure 12: nitrocellulose membrane is close to the positive pole of the transfer cell with the acrylamide gel on top, both of them surrounded by 3 layers of Whatman paper. Transference is ran at 20 V for 1 hour.

9.5.2 Ponceau staining:

Ponceau S is a sodium salt of a diazo dye that is commonly used to prepare a stain for rapid reversible detection of protein bands on nitrocellulose or PVDF membranes from Western-Blot technique, as well as on cellulose acetate membranes. A Ponceau S stain is useful because it does not appear to have a deleterious effect on the sequencing of blotted polypeptides and is therefore one method of choice for locating polypeptides on Western-Blot for blot-sequencing. It is also easily reversed with water washes, facilitating subsequent immunological detection. The stain can be completely removed from the protein bands by continued washing.

In our case, we use Ponceau stain to confirm that transference step worked successfully and we can continue with the immunodetection. To stain a nitrocellulose membrane with Ponceau, first the membrane is shortly washed with ddH_2O to remove all the transfer buffer present on it. Then, the membrane is incubated with the Ponceau solution for one minute. Ponceau solution can be recycled and reused as many times

as we consider. Membrane is then washed with ddH_2O until protein bands are perfectly defined. Washings can continue until staining fades completely.

9.5.3 Immunodetection:

Detection of the protein of interest contained in a nitrocellulose membrane is performed by the sequential incubation of two different antibodies. Primary antibody is the one that recognises the target protein specifically, while secondary antibody detects the primary antibody based on the animal used to produce the primary antibody. Secondary antibody is usually conjugated to horseradish peroxidase (HRP), which promotes a luminescence reaction in proportion to the amount of protein.

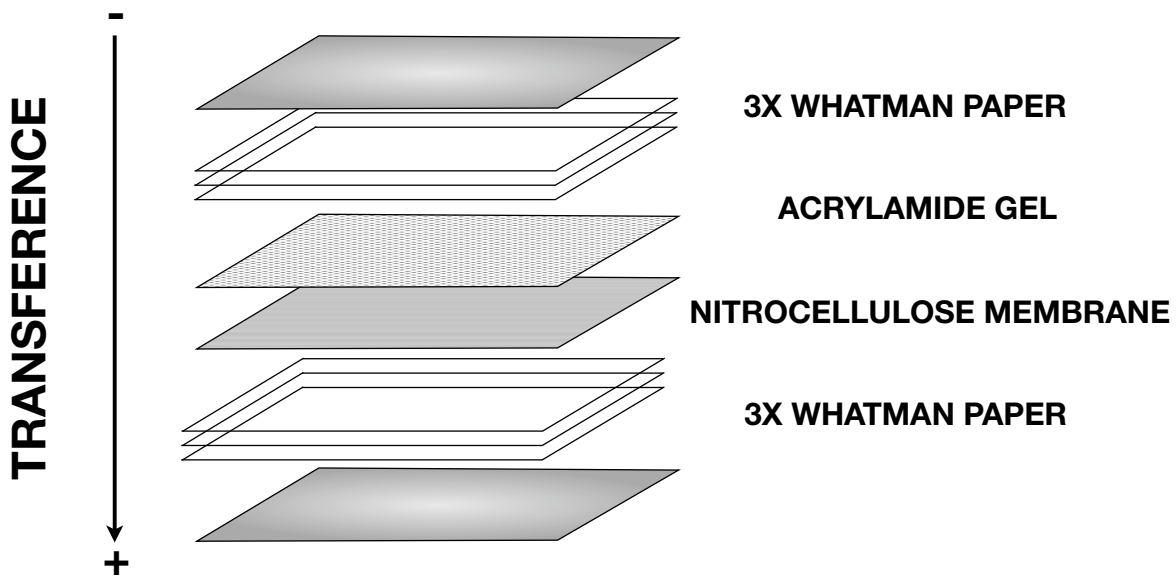

Figure 12. Mounting sequence for protein transference in Wester-Blot technique.

Before starting with the immunodetection, nitrocellulose membrane is incubated with a blocking solution of skimmed milk 5% (w/v) in TBS-T for one hour at room temperature with shaking, to block the nonspecific binding points of the proteins present in the membrane. Following, membrane is incubated with the primary antibody diluted in skimmed milk 1% (w/v) in TBS-T. Incubation may be during 1 hour at room temperature although we recommend to incubate it at 4ºC overnight for better results. Afterwards, membrane is washed with TBS-T buffer for 10 minutes three times. Membrane is then incubated with the secondary antibody, also diluted in skimmed milk 1% (w/v) in TBS-T, at room temperature for 1 hour. Finally, the membrane is washed once with TBS-T and twice with TBS for 10 minutes each washing.

9.5.4 Antibodies used:

Antibodies used in this thesis are summarized in table 6 with recommended dilutions and other indications.

Table 6. Features of antibodies used

Protein	Company	Specie	Dilution*	Reactivity
ENT2	Abcam	Rabbit	1:1000 (WB); 1:100 (ICC)	Mouse, human
FLAG	Abcam	Mouse	1:5000 (WB); 1:500 (ICC)	FLAG tag
HA	Roche	Rat	1:2000 (WB), 1:200 (ICC)	HA tag
NPC	Abcam	Mouse	1:5000 (WB); 1:500 (ICC)	Mouse, human, rat
Anti-mouse	Bio-Rad	Goat	1:2000 (WB)	Mouse
Anti-rabbit	Bio-Rad	Goat	1:2000 (WB)	Rabbit
Anti-rat	Abcam	Goat	1:5000 (WB)	Rat

* WB: Western-Blot; ICC: Immunocytochemistry

9.5.5 ECL developing:

Detection of the protein of interest is mediated by the peroxidase (HRP) conjugated to the secondary antibody, generating a luminescence reaction that is

visualised by autoradiography. ECL solution is prepared following manufacturer's instructions, usually mixing 1:1 the two solutions provided in the commercial kit. Nitrocellulose membrane is incubated with ECL mix for 1 minute at room temperature. Afterwards, liquid excess is removed and membrane is introduced inside a plastic transparent cover to be fixed in a cassette suitable for film exposure. Exposure time may vary from 1 minute to 1 hour depending on the sample and the antibody. Film is developed in a dark room following the protocol provided by the facility service.

9.6 PROTEIN DETECTION AND ANALYSIS BY MASS SPECTROMETRY

The following protocol was designed and performed by Declan Williams, PhD student from Dr. Michael Siu's lab of Chemical Department and CRMS of York University, Toronto, Canada.

Protein disulfide bonds were reduced with dithiothreitol, alkylated using iodoacetamide then digested with trypsin. Tryptic ENT phosphopeptides were separated over an acetonitrile gradient and analyzed using multiple reaction monitoring (MRM) and MRM-initiated enhanced product ion scans on a Tempo nanoflow HPLC-4000 QTRAP (AB Sciex). Transitions for MRM experiments included mass-to-charge values of all fully tryptic phosphopeptides, their y-ions and the mass-to-charge values of the phosphopeptides following neutral loss of phosphoric acid from serine and threonine or phosphate from tyrosine residues.

10 IMMUNOCYTOCHEMISTRY

Immunocytochemistry (ICC) is a common laboratory technique that uses antibodies that target specific peptides or protein antigens in the cell via specific epitopes. These bound antibodies can be detected using secondary antibodies conjugated to different fluorophores (different Alexa Fluor® in our case), which are detected in a fluorescence or confocal microscope. ICC allows researchers to evaluate

whether or not cells in a particular sample express the antigen in question. In cases where and immunopositive signal is found, ICC also allows researchers to determine which sub-cellular compartments are expressing the antigen.

To perform ICC assays, cells are previously seed on 100 mm coverslips contained in a 24-well plate (one coverslip per well). Cells can then be transfected or treated according to the design of the experiment. In order to have a nice and good quality of images at the microscope, it is recommended to not have highly confluent cells, since shape and morphology would be harder to appreciate. It is also recommended to treat cells with cycloheximide for 3 hours to reduce synthesis at ER background (see section 6.4). ICC protocol consists of a series of incubations with different reagents. Before incubating cells, we recommend to transfer the coverslips with cells seeded on to a new 24-well plate to avoid contaminations and cross reactions between the ICC reagents and the old culture medium. Cells are incubated with 500 µl/well of different solutions with soft horizontal agitation, following the order described below (table 7).

After incubations and treatments, last step is to mount coverslips on a proper support to be analyzed under fluorescence or confocal microscope. To that purpose, it is required the use of any aqueous Mowiol mounting medium. A drop of mounting medium is placed on a glass slide ensuring there are no air bubbles on top. Coverslip is carefully taken from the 24-well plate with tweezers and gently dropped upside down on top of the mounting medium. That process is repeated for each coverslip. Slides are left to dry overnight on the bench. It is very important to keep the samples out of light at anytime to not excite the fluorophores and loose signal. Slides can be analyzed right away or kept at 4ºC for future studies with the microscope.

Table 7. Immunocytochemistry protocol

Step	Solution	Time	Notes
Washing	PBS - Ca/Mg	2 X 5 min	Ca/Mg help to avoid cell detaching
Fixing	PFA 4% in PBS	15 - 30 min	Toxic if swallowed, absorbed or inhaled. Work in hood
Washing	PBS	3 X 5 min	Afterwards, plate can be kept at 4ºC with NaN_3 0.3% in PBS
Incubation	NH_4Cl 50 mM in PBS	10 min	To reduce autofluorescence
Incubation	Glycine 20 mM in PBS	10 min	To remove traces of other reagents and solutions
Permea-bilization	Triton® X-100 0.1% in PBS	10 min	To permeabilize cells
Washing	PBS	3 X 5 min	To remove detergent traces
Blocking	FBS 10% in PBS	30 min	To block non-specific bindings of the antibodies
Antibody*	1st antibody in FBS 10%	1 hour	Antibodies must be first centrifuged for 5 minutes at max speed 4ºC to avoid aggregates. Check table 8.
Washing	PBS	3 X 5 min	Coverslips are transferred to the 24-well plate
Antibody*	2nd antibody in FBS 10%	45 min	Coverslips must be protected from light for next steps
Washing	PBS	3 X 5 min	Plate should be wrapped in aluminium foil
Treatment	Check table 8		Optional treatments to stain cells apart from the antibodies
Washing	PBS	3 X 5 min	Optional after treatment if required

* 25 µl of antibody solution are dropped on plastic paraffin film. Coverslips are placed on it upside down for the incubation.

Table 8. Immunocytochemistry antibodies dilutions and treatments

Treatment	Dilution	Time	Notes
Anti-FLAG*	1:500	1 hour	Mouse monoclonal antibody
Anti-HA*	1:200	1 hour	Rat monoclonal antibody
Anti-NPC*	1:500	1 hour	Mouse monoclonal antibody that targets nuclear membrane
DoMo 555	1:300	45 minutes	Donkey anti-mouse (red). No cross-reaction with rat
DoRa 488	1:300	45 minutes	Donkey anti-rat (green). No cross-reaction with mouse
GoMo 488	1:300	45 minutes	Goat anti-mouse (green)
GoMo 546	1:300	45 minutes	Goat anti-mouse (red)
WGA	1:200 in PBS	10 minutes	Plasma membrane. Requires washing
MitoTracker ®	1:1000 in non-supplemented culture medium	45 minutes at 37ºC	Mitochondria. Treatment must be applied before the fixing step. Washing required
DAPI	300 nM in PBS	5 minutes	Nuclei. Requires washing
TO-PRO®-3	1:1000 in PBS	10 minutes	Nuclei. Last step before mounting. No washing required

* Antibodies dilution in ICC is usually 10X concentrated than the one used in WB

11 MOLECULAR BIOLOGY TECHNIQUES

11.1 TRANSFORMATION IN COMPETENT CELLS

In molecular biology, transformation is the genetic alteration of a cell resulting from a direct uptake, incorporation and expression of exogenous genetic material (DNA) from its surrounding taken up through the cell membrane. Transformation occurs naturally in some species of bacteria, but it can also be effected by artificial means in other cells. For transformation to happen, bacteria must be in a state of competence, which occurs as a time-limited response to environmental conditions such as starvation and cell density.

In this thesis, we used two different cell system to work on molecular biology: bacteria (prokaryotic) and yeast cells (eukaryotic). Protocols used for each case are described below.

11.1.1 Transformation in bacteria cells:

Bacterial transformation may be referred to as a stable genetic change brought about by the uptake of naked DNA (DNA without associated cells or proteins), and competence refers to the state of being able to take up exogenous DNA from the environment. Artificial competence can be induced through laboratory procedures that involve making the cell passively permeable to DNA by exposing it to conditions that do not normally occur in nature. Typically, the cells are incubated in a solution containing divalent cations, most commonly calcium chloride solution under cold conditions, and then exposed to a pulse of heat shock.

The surface of bacteria such as *E. coli* is negatively charged due to phospholipids and lipopolysaccharides on its cell surface, and the DNA is also negatively charged. One function of the divalent cation is to shield those charges by coordinating the phosphate groups and other negative charges, thereby allowing a DNA molecule to adhere to the cell surface. It is suggested that exposing the cells to

divalent cations in cold condition may also change or weaken the cell surface structure of the cells making it more permeable to DNA. The heat-pulse is thought to create a thermal imbalance on either sides of the cell membrane, which forces the DNA to enter the cells through either pores or the damaged cell wall.

The protocol used in this thesis is based on the instructions from the manufacturer that provides commercial competent cells (see commercial references section - appendix II). All material used has to be previously autoclaved and all the protocol must be done under sterile conditions, commonly under a flame. Commercial competent cells are thawed on ice and gently mixed with the pipette tip. Cells are aliquoted in 15 µl of cell mix for each transformation into 1.5 ml microcentrifuge tubes on wet ice.10-50 ng of DNA is then added to each reaction tube by mixing gently and incubated on ice for 30 minutes.

After incubation, cells are heat-shocked for 45 second at 42ºC, by using either a water bath or a dry thermo-block. Tubes are immediately placed back on ice for two more minutes. 100 µl of pre-warmed medium (LB in our case) is added to each transformation mix, and cells are then incubated at 37ºC for one hour at 225 rpm. Cells are then centrifuged at max speed for 15 seconds and all the supernatant but 40 µl is removed. Pelleted cells are resuspended in this 40 µl left and plated on pre-warmed selective plates (LB plus the proper antibiotic). It is recommended to plate half of the transformation mix to keep some cells in case the incubation does not work. Cells can be kept at 4ºC and be plated during the next days.

In case the DNA used for transformation comes from a mutagenesis PCR reaction, volumes of the protocol must be readjusted to ensure a better transformation efficiency. Modifications are: 50-75 µl of competent cells per reaction, 10 µl of the PCR product as DNA to be transformed, heat-shock for 1 minute 45 seconds, 1 ml of LB added after the heat-shock, centrifugation for 1 minute, 800 µl of LB removed from the supernatant and all the transformed cells should be plated at once.

11.1.2 Transformation in yeast cells:

Most species of yeast, including *Saccharomyces cerevisiae*, may be transformed with exogenous DNA in the environment or under laboratory conditions. Exposing intact yeast cells to alkali cations such as those of caesium or lithium allows the cells to take up plasmid DNA. Later protocols adapted this transformation method, using lithium acetate, polyethylene glycol, and single-stranded DNA (ssDNA). In these protocols, the ssDNA preferentially binds to the yeast cells wall, preventing plasmid DNA from doing so and leaving it available for transformation. The protocol we used is a DTT-based adaptation of a lithium acetate protocol described in Snider *et al*. (2010).

Yeast cells coming from a stationary phase culture are aliquoted in 250 µl per reaction into a 1.5 ml microcentrifuge tube. Stationary phase cells may come from either an overnight culture, cells on a plate (resuspending 2 colonies per 100 µl of medium) or a glycerol stock. Tubes are pulse spun down at max speed and supernatant is then removed. 100 µl of fresh yeast transformation buffer (see recipes section - appendix II) are added to each tube together with 100-300 ng of DNA, and gently mixed by pipetting. Cells are heat-shocked at 42ºC for 30 minutes at 225 rpm. Samples are then spun down at max speed for 1 minute and supernatant is discarded. Finally, pelleted cells are resuspended in 100 µl of sterile NaCl 0.9%, plated on a proper selective medium and incubated at 37ºC for 2-3 days.

11.2 EXTRACTION OF PLASMID DNA

Transformation in bacteria cells allows to maintain and amplify DNA plasmids. After transfection, cells must grow to a certain volume in order to extract the amplified DNA. For that, a single colony is picked up and growth in 3 ml of liquid medium, in our case LB plus a proper antibiotic (commonly ampicillin or kanamycin) at 37ºC overnight at 225 rpm. Depending on the desired amount of DNA to be obtained, after this overnight incubation, bacteria culture can be scaled up to 100 - 250 ml and incubated with for another overnight at the same conditions.

There are different commercial DNA extraction protocols depending on the amount and purity of the DNA obtained. Mini-prep protocols start from a 3 ml culture and the amount of DNA obtained is around 10 - 40 μg. Maxi-prep protocols start from a 100 - 250 ml culture and the yield is around 100 - 500 μg of DNA, depending on the plasmid features and the starting volume. Timing required for each protocol is quite different, such a way that mini-prep protocol is performed within 30 minutes - 1 hour, while maxi-prep requires 4 - 6 hours depending on the number of samples. There are also differences on the purity of the DNA obtained, where samples obtained from a maxi-prep are more pure and clean from salts since the maxi-prep protocol has an extra purification step than the mini-prep protocol. Therefore, we regularly use the mini-prep protocol when DNA obtained will be used for molecular biology purposes, and maxi-prep samples when DNA will be transfected into mammalian cells for cell culture experiments.

Both mini-prep and maxi-prep protocols are based on an ionic column exchange. First steps are meant to break the cell membranes to release all the genetic material. From here, DNA is bound to the ionic column to be washed from other bacterial material and eluted using ddH_2O or elution buffer. In both case, we always follow the manufacturer's instructions provided with the kit.

11.3 GENETIC ENGINEERING TECHNIQUES

11.3.1 PCR reaction:

The polymerase chain reaction (PCR) is a biochemical technique used in molecular biology to amplify a single or a few copies of a piece of DNA across several orders of magnitude, generating thousands to millions of copies of a particular DNA sequence.

The method relies on thermal cycling, consisting of cycles of repeated heating and cooling of the reaction promoting DNA melting and enzymatic replication of the

DNA. Primers (short DNA fragments) containing sequences complementary to the target region, along with a DNA polymerase, are key components to enable selective and repeated amplification. As PCR progresses, the DNA generated is itself used as template for replication, setting in motion a chain reaction in which the DNA template is exponentially amplified. PCR can be extensively modified to perform a wide array of genetic manipulations.

Almost all PCR applications employ a heat-stable DNA polymerase, such as Taq polymerase, an enzyme originally isolated from the bacterium *Thermus aquaticus*. This DNA polymerase enzymatically assembles a new DNA strand from DNA building-blocks, the nucleotides, by using single-stranded DNA as template and DNA oligonucleotides (also called DNA primers), which are required for initiation of DNA synthesis. The vast majority of PCR methods use thermal cycling to a defined series of temperatures steps. These thermal cycling steps are necessary first to physically separate the two strands in a DNA double helix at a high temperature, in a process called DNA melting. At a lower temperature, each strand is then used as template in DNA synthesis by the DNA polymerase to selectively amplify the target DNA. The selectivity of PCR results from the use of primers that are complementary to the DNA region targeted for amplification under specific thermal cycling conditions.

The typical PCR thermal cycling steps are (figure 13):

A. *Initialization step*: Heating the reaction for 5-10 minutes to activate the polymerase.
B. *Denaturation step*: It causes DNA melting of the DNA template by disrupting the hydrogen bonds between complementary bases, yielding ssDNA molecules.
C. *Annealing step*: It allows annealing of the primers to the ssDNA template. Annealing temperature depend on the composition and length of the primer but it is usually comprised between 55 and 68ºC. The polymerase binds to the primer-template hybrid to begin DNA formation.

D. *Extension/elongation step:* The temperature at this step depends on the DNA polymerase used. Taq polymerase is commonly used at 72ºC. DNA polymerase synthesizes a new DNA strand complementary to the DNA template by adding dNTPs in 5' to 3' direction. The extension time depends on both the DNA polymerase speed (e.g Taq polymerase usually works at 1 Kb/min) and the length of the DNA fragment to be amplified.
E. *Final elongation:* Optional step to ensure that any remaining ssDNA is fully extended.
F. *Final hold:* To inactivate the enzyme with cold temperatures and stop the reaction.
G. *Storage:* Short-term storage of the reaction.

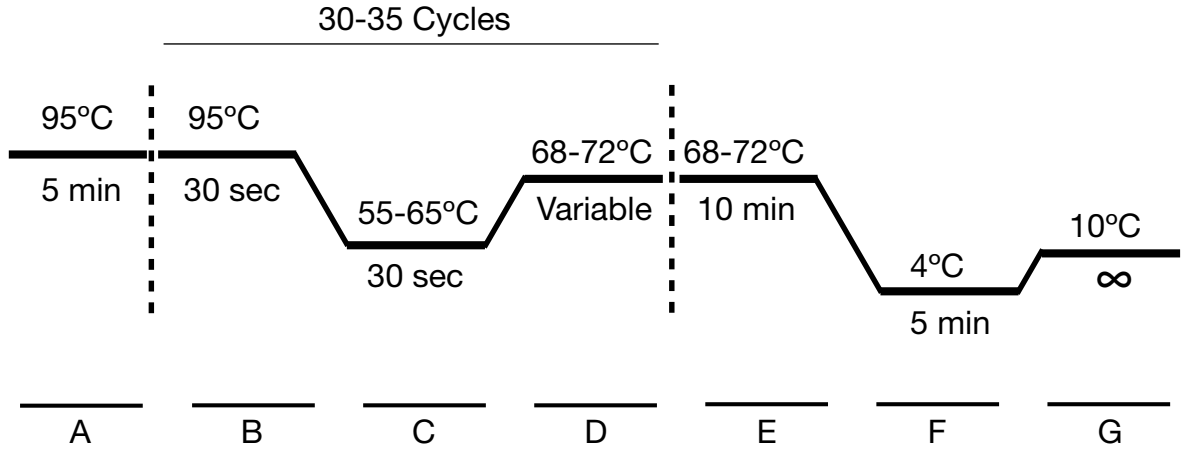

Figure 13. Representation of the thermal cycling of a standard PCR reaction.

Primers designing is also a clue step to optimise a PCR reaction. Pairs of primers should have similar melting temperatures since annealing in a PCR occurs for both simultaneously. This temperature depends on the length of the primer, usually around 20 nucleotides, and the composition of guanines and cytosines, which should not be higher than 55-60%. When designing a pair of primers it is also important to double-check they do not hybridise at multiple regions of the DNA template to avoid secondary PCR products.

In this thesis, the polymerases we used for all the molecular biology work are the Taq polymerase and the Pfu polymerase (see commercial references section - appendix II). To perform the reactions we followed the specific indications provided by the manufacturer. Sequences of the primers used in this thesis are detailed in the appendix I section (table 20).

11.3.2 Site-directed mutagenesis:

Site-directed mutagenesis is a molecular biology technique often used in biomolecular engineering, in which a mutation is created at a defined site in a DNA molecule. In general, this form of mutagenesis requires the wild type gene sequence to be known. It is commonly used in protein engineering. The basic procedure consists of the synthesis of a short DNA primer. This synthetic primer contains the desired mutation and is complementary to the template DNA around the mutation site so it can hybridise with the gene of interest. The mutation may be a single base change, multiple base changes, deletion or insertion. The single-stranded primer is then extended using a DNA polymerase, which copies the rest of the gene.

In this thesis, we used site-directed mutagenesis to insert the HA tag used for the study of the hENT2 spliced variants (figure 14). Bold letters represent the HA tag amino acid sequence. Below the HA sequence, there is the sequence of nucleotides that correspond to the peptide above. The strategy used for PCR generation and insertion of the HA tag was to perform regular mutagenic PCR amplifications adding 3 new amino acids every time, so after 3 PCRs we would have the HA tag incorporated in our construct.

The polymerase used for the site-directed mutagenesis PCR reactions was the PfuTurbo® polymerase. The primers we designed are detailed in the appendix I section (table 21). The particularity of the primers used is that the forward and reverse sequences are exactly complementaries, such a way both oligonucleotides include the regions to be inserted. Since the polymerase finishes the reaction at the same point it started, the gene of interest is amplified together with the plasmid.

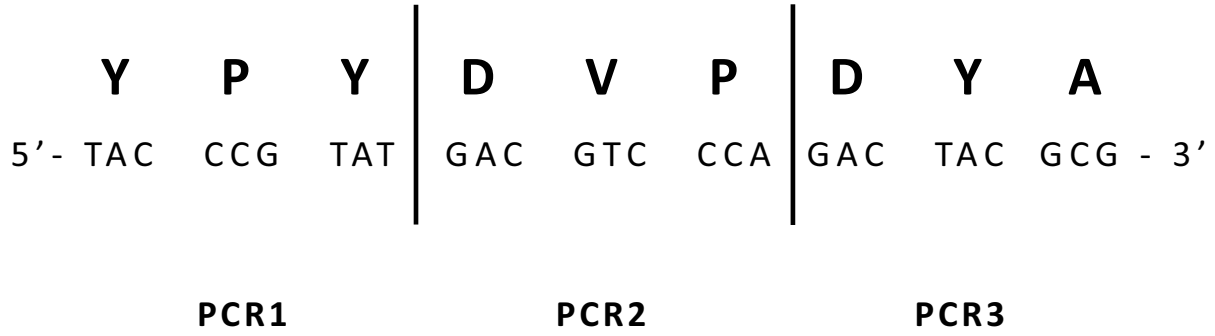

Figure 14. Strategy for HA tag cloning.

After the PCR reaction, samples are treated with the endonuclease DpnI, a restriction enzyme that degrades methylated DNA at 37ºC for one hour. As a consequence, template DNA is degraded while the PCR product remains intact since only the DNA coming from bacteria (template from a mini-prep) is methylated. PCR product with the site-directed mutation incorporated is transformed into bacteria cells to be amplified (see section 11.1.1). Thermal cycling conditions used for this reaction are detailed in figure 15.

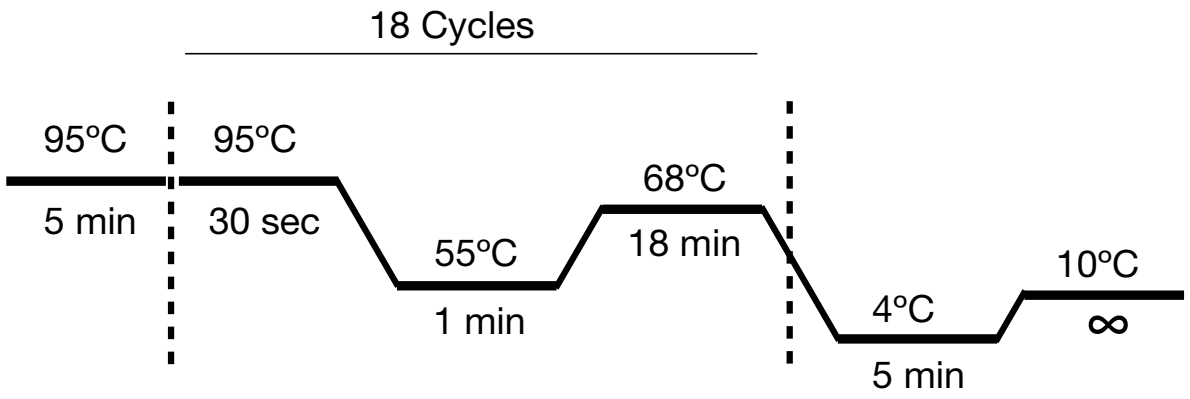

Figure 15. Representation of the thermal cycling of a site-directed mutagenesis PCR reaction.

11.3.3 Digestion with restriction endonucleases:

A restriction enzyme or endonuclease is an enzyme that cuts DNA at specific recognition nucleotide sequences known as restriction sites. Such enzymes, found in bacteria and archaea, are thought to have evolved to provide a defense mechanism against invading viruses. Isolated restriction enzymes are used to manipulate DNA for different scientific applications.

Restriction enzymes are used to assist insertion of genes into plasmid vectors during gene cloning. For optimal use, plasmids that are commonly used for gene cloning are modified to include a short polylinker sequence, called multiple cloning site (MCS), rich in restriction enzyme recognition sequences with the particularity that those enzymes cut only once inside the vector. To clone a gene fragment into a vector, both plasmid DNA and gene insert are cut with the same restriction enzymes, and then glued together with the assistance of an enzyme known as DNA ligase.

Protocols used for digestion with restriction enzymes are the ones provided by the manufacturer. Usually those protocols demand to incubate a certain amount of DNA, from 100 ng to 10 μg, with a proper number of enzymatic units (1 unit digests 1 μg of DNA in 1 hour) for 1-3 hours at 30-37ºC, depending on the enzyme. In case of double digestions, it is recommended to find a common reaction buffer where both enzymes have a high activity.

11.3.4 DNA visualization and extraction with agarose gel:

Agarose gel electrophoresis is a method used to separate a mixed population of DNA and RNA fragments by length, to estimate the size of DNA and RNA fragments or visualise the different products generated after a PCR reaction. Nucleic acid molecules are separated by applying an electric field to move the negatively charged molecules through an agarose matrix. Shorter molecules move faster and migrate farther than longer ones because shorter molecules migrate more easily through the pores of the gel. Percentage of agarose used may vary depending on the size of the

molecule of interest. Gels with 1% of agarose are commonly used for 1-3 Kb molecules. For shorter molecules, less than 1 kb, 1.5% of agarose is recommended. On contrary, 0.7% of agarose is frequently used for molecules of more than 3 kb size.

After the electrophoresis is completed, the molecules in the gel can be stained to make them visible. The most common dye used to make DNA or RNA bands visible for agarose gel electrophoresis is ethidium bromide (EtBr). It fluoresces under UV light when intercalated into the major groove of DNA or RNA. By running DNA through an EtBr-treated gel and visualizing it with UV light, any band containing more than 20 ng of DNA becomes distinctly visible. EtBr is a known mutagen and safer alternatives are nowadays available, such as SYBR® Safe. SYBR® Safe is a variant of SYBR® Green, a product provided by Invitrogen, that has been shown to have low enough levels of mutagenicity and toxicity to be deemed nonhazardous waste under U.S. Federal regulations. It has similar sensitivity levels to EtBr but is significantly more expensive.

Agarose gels are made by melting the agarose powder in TAE buffer using a microwave. SYBR® Safe is added after the solution as cooled down to 50ºC approximately and poured to a cast with a comb. While gel is solidifying, DNA samples are prepared by adding a proportion of commercial gel loading dye 6x. Samples are then load into the wells and run at 100 V for 1 - 2 hours. DNA ladders are used to identify the size of the DNA bands. If desired, DNA bands can be extracted from the agarose gel by using a commercial gel extraction kit, following the manufacturer's instructions.

11.3.5 DNA ligation:

DNA ligases are a specific type of enzyme, a ligase, that facilitates the joining of DNA strands together by catalysing the formation of a phosphodiester bond. DNA ligases have become an indispensable tool in modern molecular biology research for generating recombinant DNA sequences by inserting a DNA fragment digested with restriction enzymes into a plasmid. When performing a ligase reaction, it is

recommended to try different molar rates vector : insert. Calculations to determine the amount of DNA needed are the following:

$$\frac{ng.Vector \times Kb.Insert}{Kb.Vector} \times molar.rate\frac{insert}{vector} = ng.Insert$$

Reaction components are the digested vector, the DNA insert digested if needed, enzyme T4 DNA ligase, reaction buffer 10x and ddH_2O to the minimum final volume possible. Reaction is incubated at 16ºC overnight and transformed into bacteria cells afterwards (see section 11.1.1).

11.3.6 Vectors and plasmids:

In molecular biology, a vector is a DNA molecule used as a vehicle to transfer foreign genetic material into another cell. Common to all engineered vector are an origin of replication, a multicloning site (MCS) and a selectable marker gene. Plasmids are double-stranded circular DNA sequences that are capable of automatically replicating in a host cell. Plasmid vectors consist of an origin of replication that allows for semi-independent replication of plasmid in the host and also the transgene insert. MCS has the particularity that the restriction enzyme sites present there are not found in any other region of the vector (see section 11.3.3). The selectable marker is usually an antibiotic resistance gene (most frequent are ampicillin and kanamycin) that allows to select only those cells which have incorporated the plasmid. More complex plasmids include other sophisticated systems, such as the Lac Z promoter, which is activated by IPTG, or the GFP sequence to generate fusion proteins.

The plasmids used in this thesis are (figure 16):

A. *pGemT easy*: a commercial vector product of Promega that is ready to ligate PCR products with an extra adenosine added in both edges by the polymerase as default. Suitable for bacteria but not mammalian cells.

B. *pCDNA3.1*: Vector used for transient expression in mammalian cells. We cloned hENT2 isoforms from pGemT easy vector to pCDNA3.1 by digesting with ApaI and PstI restriction enzymes.

C. *pBSxG*: Vector used for cRNA transcription. We cloned hENT2 isoforms into it by adding SmaI (blunt ends) sites at both edges of hENT2 ORFs and digesting the vector with StuI (blunt ends too), since it is known that cRNA is more stable when flanked by ß-globin UT region.

D. *pTLB-1*. Vector used for the MYTH screening. hENT2 was cloned by adding PstI and StuI sites at both edges of its ORF.

11.3.7 Clone screening by PCR:

Screening by PCR is a strategy used for the cloning of hENT2 isoforms. After transforming hENT2 mixed isoforms to bacteria cells we obtained a total of 360 colonies, each one containing one single molecule of hENT2. Optimizing the sequencing of such amount of samples, we first performed a screening by PCR of all of them. We grew each colony in 100µL of LB-Ampicilin in 96 wells plates overnight at 37ºC. Next day, we pooled 5µL of the 8 wells from the same column (figure 17) and ran a PCR amplifying hENT2 using those DNA pools as template. Afterwards, we ran the PCR products in a 1% agarose gel to visualise which columns might contain interesting isoforms of hENT2, which were further sequenced. This method allowed us to discard a big number of repetitive molecules and select a smaller number of samples to de sequenced, thereby optimising time and expenses.

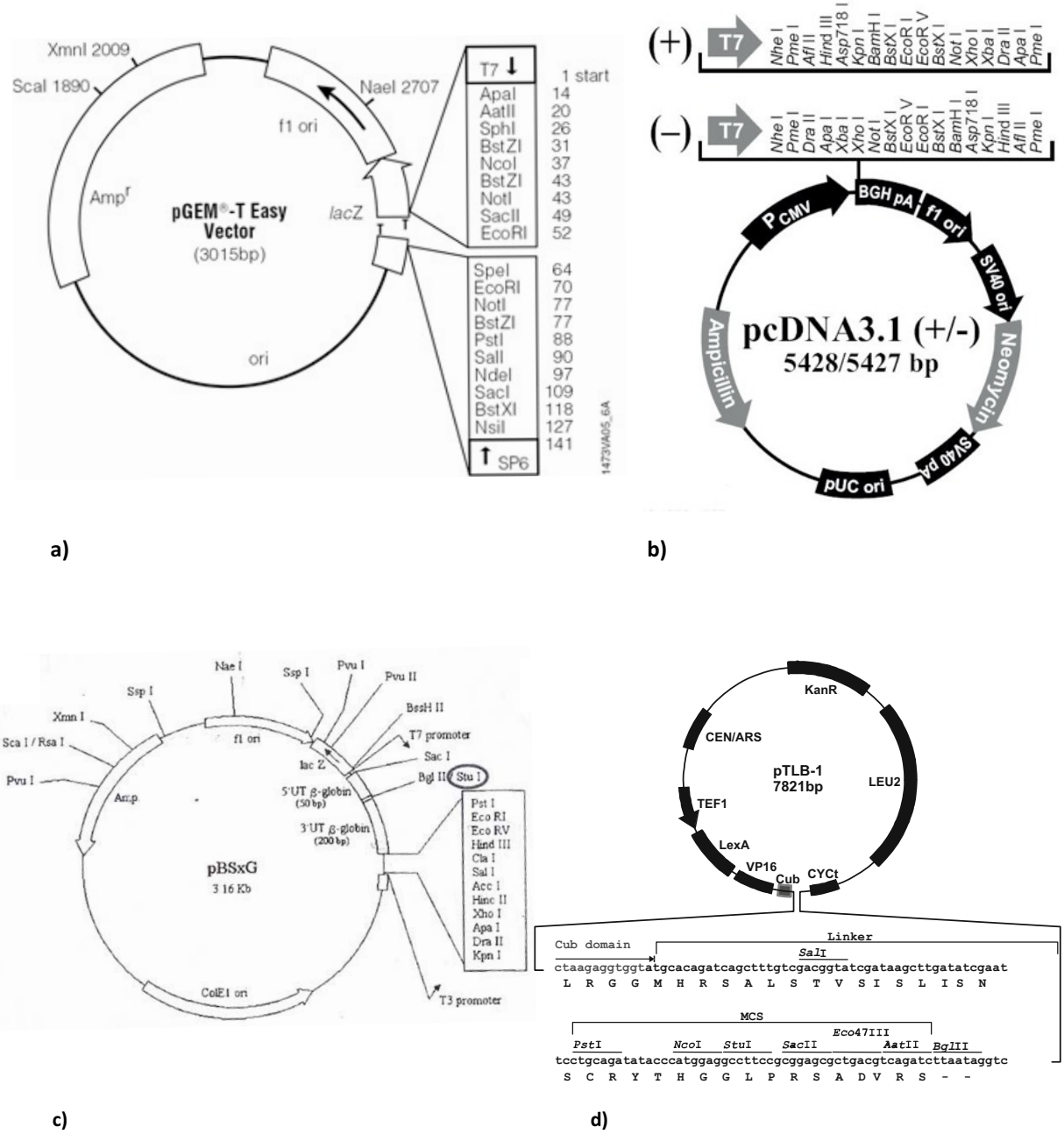

Figure 16. Plasmid vectors used in this thesis.

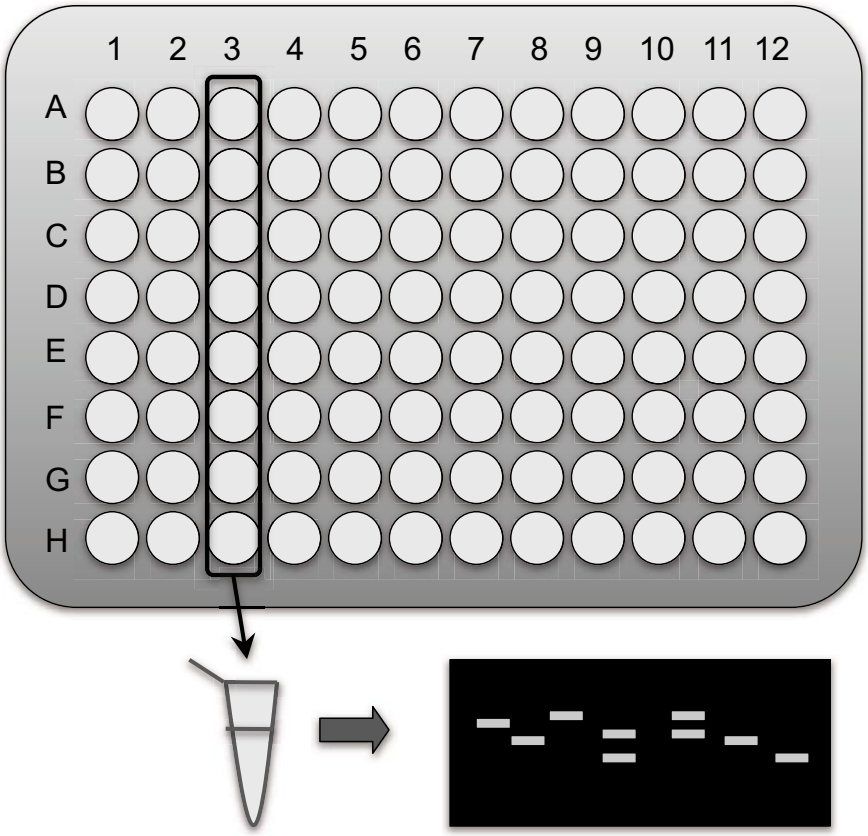

Figure 17. Screening by PCR. We make a pool of the 8 wells of each column and then we perform a PCR reaction for each DNA mix. In the agarose gel, each lane shows the PCR products obtained from its corresponding mix. Then, we select those columns where we noticed one or more products of interest to be sequenced.

11.3.8 DNA sequencing by PCR:

DNA sequencing by PCR is based on the usage of dNTPs labelled with fluorochromes. Those dNTPs lack its 3'-hydroxyl group what terminates the elongation step in the PCR reaction. This way, DNA fragments of different sizes are generated according to the moment in which the labelled dNTP was incorporated. Billions of different DNA fragments are then separated by size using capillary electrophoresis. Once the DNA molecule reaches the bottom of the capillary, it is excited by a laser emitting fluorescence at certain wave length. Since the four dNTPs (A, G, C, T) are differently labelled, as a result we obtain an electropherogram that will determine the sequence of the analyzed DNA sample.

To perform this reaction we need a rate of 100 ng of DNA per Kb of the sample, considering the size of the vector plus the insert. Following the manufacturer's instructions, we use the BigDye® Terminator v3.1 Cycle Sequencing Kit: 1 μl of ready reaction mix, 3 μl of BigDye® sequencing buffer, 1 μl of 20 μM primer, DNA and ddH_2O up to a final volume of 20 μl. The PCR program used is: 96 ºC for 1 min, 25 cycles of 96 ºC for 10 s, 50 ºC for 5 s and 60 ºC for 4 min, and a final step of 4 ºC for 5 min. Once the reaction is done, samples are processed and analyzed by the Scientific and Technical Services of the UB (CCiTUB)[M].

11.4 RNA EXTRACTION AND MANIPULATION

11.4.1 RNA extraction from cell culture:

RNA extraction is the purification of RNA from biological samples. This procedure is complicated by the ubiquitous presence of ribonuclease enzymes in cells and tissues, which can rapidly degrade RNA. For the RNA extraction we used the commercial kit "SV Total RNA isolation System" from Promega following the manufacturer's instructions. This method is based on the disruptive properties, at the same time than protective, of the association of SDS with guanidinium thiocyanate and the capacity of ß-mercaptoethanol to inactivate the ribonucleases.

11.4.2 cDNA synthesis by reverse transcription:

In the field of molecular biology, a reverse transcriptase is a DNA polymerase enzyme that transcribes single-stranded RNA into single-stranded DNA, also known as cDNA. To perform that reaction we used a commercial reverse transcription kit following the manufacturer's instructions. This reaction basically contains the reaction buffer, dNTP mix 100 mM, random primers, the MultiScribe™ reverse transcriptase and RNase inhibitor. The thermal cycle conditions are 25ºC for 10 min, 37ºC for 120 min, 85ºC for 5 min and short-term storage at 4ºC.

11.5 REAL-TIME PCR REACTION

Real-time polymerase chain reaction is a laboratory technique based on the PCR, which is used to amplify and simultaneously quantify a targeted DNA molecule. For one or more specific sequences in a DNA sample, real-time PCR enables both detection and quantification. The quantification can be either an absolute number of copies or a relative amount when normalised to a DNA input or additional normalising genes. The procedure follows the general principle of PCR; its key feature is that the amplified DNA is detected as the reaction progresses in real time. Two common methods for detection of products are: non-specific fluorescent dyes that intercalate with any double-stranded DNA, and
sequence-specific DNA probes consisting of oligonucleotides that are labeled with a fluorescent reporter which permits detection only after hybridisation of the probe with its complementary DNA target.

11.5.1 TaqMan® reagents:

TaqMan® probes are hydrolysis probes that are deigned to increase the specificity of real-time PCR assays. The Taqman® probe principle relies on the 5' -> 3' exonuclease activity of Taq polymerase to cleave a dual-labeled probe during hybridisation to the complementary target sequence and fluorophore-based detection. The resulting fluorescence signal permits quantitative measurements of the accumulation of the product during the exponential staged of the PCR.

TaqMan® probes consist of a fluorophore (e.g. FAM or VIC) covalently attached to the 5'-end of the oligonucleotide probe and a quencher (e.g. TAMRA or MGB) at the 3'-end (figure 18). The quencher molecule quenches the fluorescence emitted by the fluorophore when excited by the cycler's light source via Fluorescence Resonance Energy Transfer (FRET). As long as the fluorophore and the quencher are in proximity, quenching inhibits any fluorescence signals. TaqMan® probes are designed such that they anneal within a DNA region amplified by a specific set of primers. As the Taq polymerase extends the primer and synthesises the nascent

strand, the 5' -> 3' exonuclease activity of the polymerase degrades the probe that has annealed to the template. Degradation of the probe releases the fluorophore from it and breaks the close proximity to the quencher thus relieving the quenching effect and allowing fluorescence of the fluorophore. Hence, fluorescence detected is directly proportional to the fluorophore released and the amount of DNA template present in the sample.

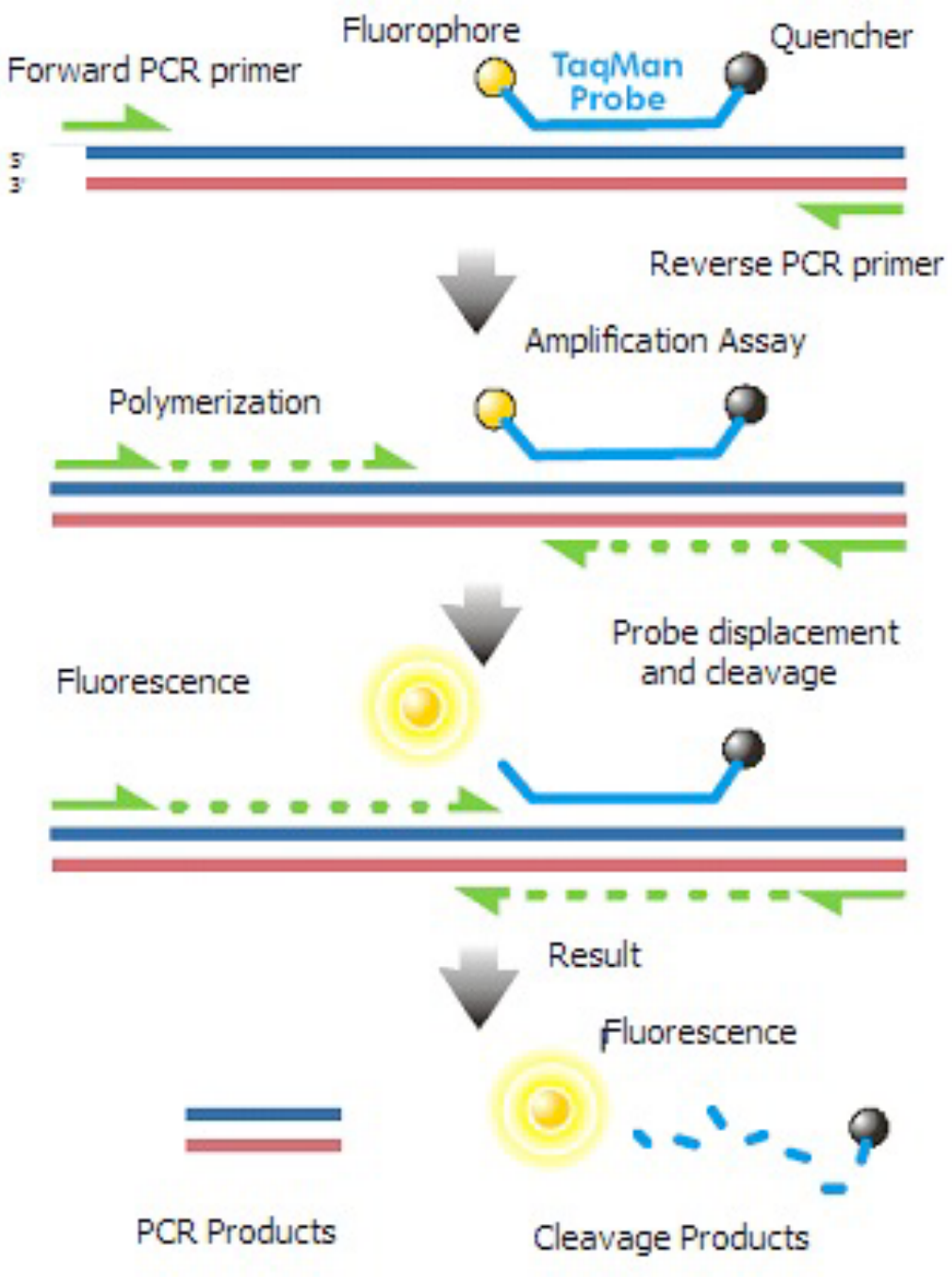

Figure 18. Real-time PCR using TaqMan® probes.

TaqMan® is a product of Applied-Biosystems. Commercial and customised probes are provided by them together with the master mix 2x necessary to perform the reaction. Housekeeping genes commonly used are GAPDH, GUSB and 18S. The thermal cycler conditions are provided within the device software also supplied by Applied-Biosystems. Protocols to perform the reaction and the thermal cycler functioning are provided by the manufacturer.

11.5.2 SYBR® Green reagents:

SYBR® Green is an asymmetrical cyanine dye used as a nucleic acid stain in molecular biology. SYBR® Green bind to DNA and the resulting DNA-dye-complex absorbs blue light (λmax = 497 nm) and emits green light (λmax = 520 nm). The stain is used as a dye for the quantification of double stranded DNA in real-time PCR causing fluorescence of the dye. An increase in DNA product during PCR leads to an increase of fluorescence intensity and is measured at each cycle, thus allowing DNA concentrations to be quantified (figure 19). However, dsDNA dyes such as SYBR® Green will bind to all dsDNA PCR products, including nonspecific PCR products such as primer dimer. This can potentially interfere with, or prevent, accurate quantification of the intended target sequence.

To perform a real-time PCR using SYBR® Green as a detector, first it is needed to design a set of primers to amplify the gene of interest, ensuring they do not amplify secondary products by running a regular PCR reaction and visualizing the results on an agarose gel. If it the purpose of the experiment is to analyze different genes within the same sample, amplicons of each set of primers must have the same length, 150 - 200 bp, hence an increase in fluorescence signal is caused by a higher number of copies instead of being consequences of a longer amplicon. The protocol used in SYBR® Green is similar to the one for TaqMan® probes by using a master mix 2x with all the reagents incorporated. This master mix is provided by Applied-Biosystems together with the protocol directions. The same device used in TaqMan® can also be used for detecting SYBR® Green reactions since the software contemplates both protocols.

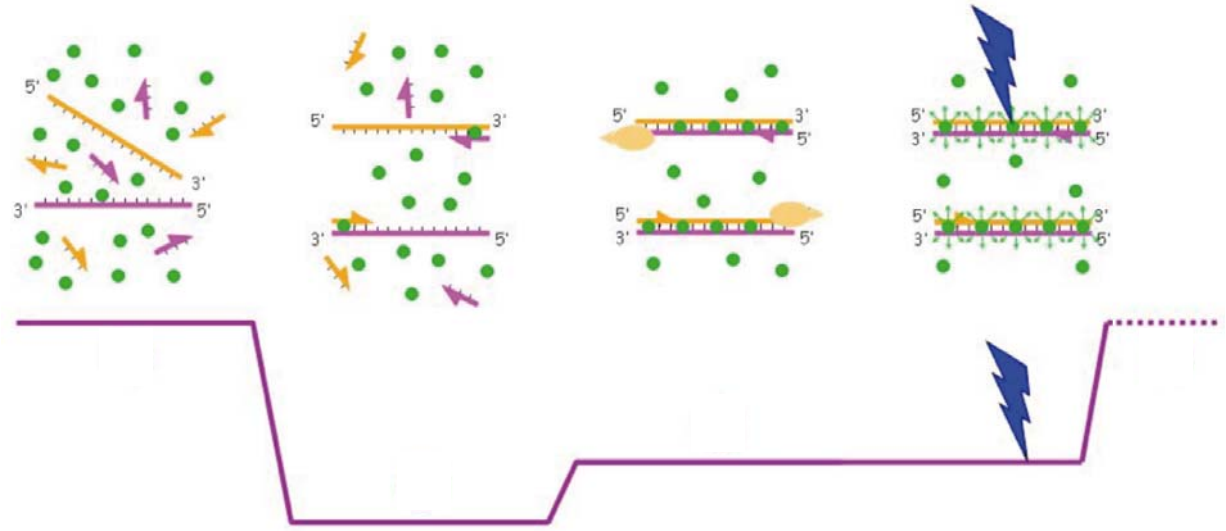

Figure 19. Real-time PCR using SYBR® Green dye.

11.5.3 Microfluidic cards (TLDA):

The Applied-Biosystems Low Density Array (microfluidic card) screens multiple samples against custom-selected gene panels, providing a cost-effective solution to validating the expression of large numbers of genes using smaller numbers of samples. Up to 380 genes can be rapidly examined on the same array using the well-established TaqMan® gene expression reagents. These are predesigned real-time PCR assays available for human, mouse, and rat gene expression research.

The TaqMan® Assay can be customised to a design of 6 configurations: from 11 genes with 4 replicates run on 8 samples, to 380 genes with no replicates run on a single sample. The Low Density array minimises reagent consumption, as reaction volumes of ~ 2 µl not only reduce the cost in terms of consumables but also limit the amount of RNA required per experiment.

To perform an analysis using TLDAs, cDNA samples must be prepared according to the protocol provided by the manufacturer. Those samples are load into

the microfluidic cards using the ports disposed at one of the sides (figure 20). Cards are then centrifuged to equally distribute the cDNA sample among the different spots, each one containing one validated TaqMan® probe, according to the customised design of the card. Microfluidic cards are then placed into the thermal cycle device to detect the fluorescence signals as the PCR reaction progresses.

11.5.4 Real-time PCR calculations:

The method of DNA quantification by real-time PCR relies on plotting fluorescence against the number of cycles on a logarithmic scale. A threshold for detection of DNA-based fluorescence is set slightly above background, at the beginning of the exponential stage of the amplification curve. The number of cycles at which the fluorescence exceeds the threshold is called the cycle threshold, Ct, which is the value used for analysing the results. Calculation steps are the following:

1. Determine a Ct average for each target gene (Ct_x) and each housekeeping gene (Ct_{HK})
2. Calculate ΔCt for each target gene: $\Delta Ct = Ct_x - Ct_{HK}$
3. Calculate the standard error (SE) of the experiment for each sample:

$$SE_{\Delta Ct} = \sqrt{(SE_x)^2 + (SE_{HK})^2}$$

4. Calculate ΔΔCt by subtracting ΔCt values from a control or non-treated sample to a treated (or condition 1) sample:

$$\Delta\Delta Ct = \Delta Ct_{treatment\ 1} - \Delta Ct_{control}$$

5. Calculate the relative expression of each sample:

$$\text{Relative expression} = 2^{-\Delta\Delta Ct}$$

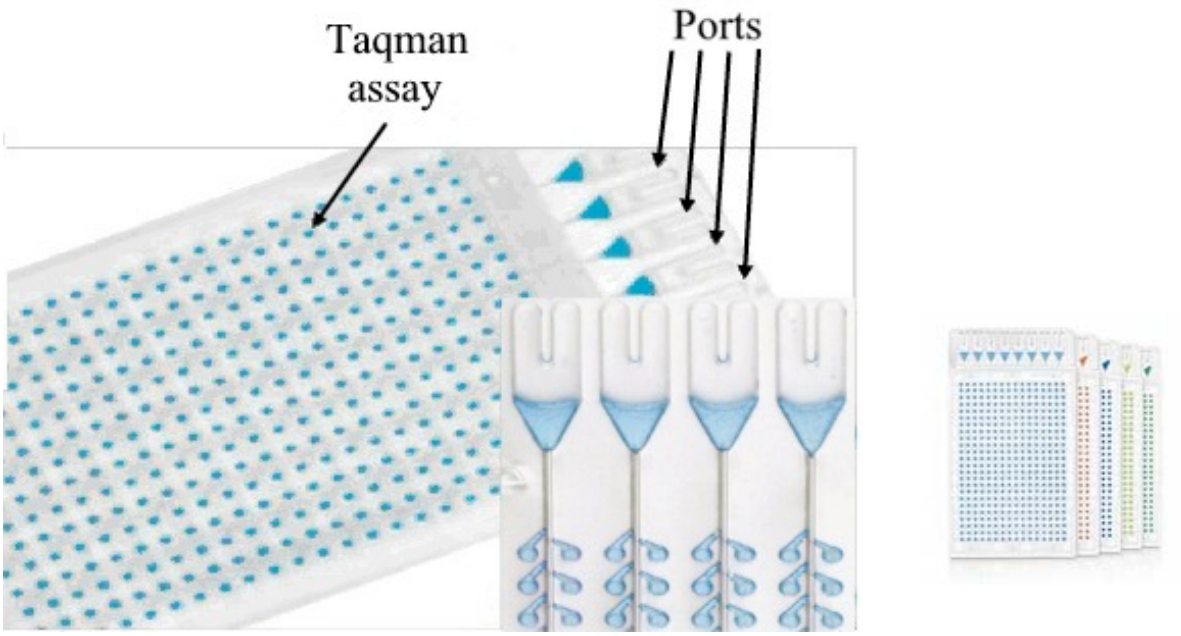

Figure 20. TaqMan® Low density arrays from Applied-Biosystems.

12 MEMBRANE YEAST TWO-HYBRID (MYTH) TECHNIQUE

Recent research has begun to elucidate the global network of cytosolic and membrane protein interactions. The resulting interactome map facilitates numerous biological studies, including those for cell signalling, protein trafficking and protein regulation. Due to the hydrophobic nature of membrane proteins such as tyrosine kinases, G-protein coupled receptors, membrane bound phosphatases and transporters it is notoriously difficult to study their relationship to signalling molecules, the cytoskeleton, or any other interacting partners. Although conventional yeast-two hybrid is a simple and robust technique that is effective in the identification of specific protein-protein interactions (PPI), it is limited in its use for membrane proteins (Kittanakom *et al*. 2009).

Membrane proteins make up approximately one-third of all proteins in a cell, having important functions in signalling, cell structure, and, as discussed before, transport. Membrane proteins are distributed ubiquitously and understanding their PPIs has important implications in medicine since many membrane proteins are drug targets (A. Engel & Gaub 2008).

In 1994 a split-ubiquitin based method was established by Johnsson and Varshavsky (1994), when they discovered that ubiquitin, split into two moieties, can re-associate due of the high affinity of the moieties for each other. These two halves were named N_{ub} for N-terminal half of ubiquitin, and C_{ub} for C-terminal half of ubiquitin (Johnsson & Varshavsky 1994). These researchers fused cDNAs encoding a library of proteins to the N-terminal moiety called N_{ub}. Two variants of N_{ub} are used. N_{ub}I refers to the wild type form bearing Ile13. The N_{ub}G form bears an Ile13 Gly substitution. This substitution ensures that the affinity between C_{ub} and N_{ub} is decreased such that if the bait and prey interact, C_{ub} and N_{ub}G will be forced together and ubiquitin-specific proteases will recognize the complete ubiquitin molecule and cleave off the reporter protein from C_{ub}, which can be detected through selective screening (Johnsson & Varshavsky 1994).

This simple, but elegant method for the detection of protein-protein interactions for integral membrane proteins was later adapted for high-throughput screens and this system came to be known as Membrane Yeast-Two Hybrid, MYTH (figure 21). The membrane protein of interest is bound to the C or N-terminal moiety of C_{ub}. C_{ub} is fused to transcription factors, which consist of DNA-binding domain LexA from *Escherichia coli* and VP16 from the herpes simplex virus. This C_{ub} fusion protein is known as the bait. The prey is a N_{ub}G-fused cDNA library. Both the N_{ub}G and C_{ub} fusion proteins are co-expressed in yeast. If an interaction takes place with the bait and the prey, ubiquitin-specific proteases will recognize the complete ubiquitin molecule and cleave off the transcription factors from C_{ub}. The transcription factors then translocate to the nucleus and activate the reporter genes: LacZ, His3, Ade2 (Snider *et al*. 2010). While MYTH is, by far, the best tool available for examining PPIs of membrane proteins, it does have disadvantages: A high number of false positives can arise during screening, although

this can be somewhat alleviated by making more stringent growing conditions for the yeast, as well as performing subsequent bait dependency tests to confirm the validity of the interaction. The putative interacting preys are re-screened against the bait as well as non-interacting artificial bait and if an interaction occurs with the artificial bait, it is said to be a false positive and the putative prey protein is discarded (Iyer *et al*. 2005).

Therefore, MYTH technique adapts the principle of split ubiquitin for use as a potent *in vivo* sensor of protein-protein interactions, allowing large-scale screening for interactors of full-length membrane proteins, from a range of organisms, using *Saccharomyces cerevisiae* as a host. The followed protocol has been adapted from the one described by Snider *et al.* in 2010, which describes a protocol for MYTH bait generation, validation and library screening. The entire MYTH procedure can generally be completed in 4-6 weeks.

12.1 BAIT GENERATION AND VALIDATION

When using MYTH, the bait must be cloned into an appropriate vector for tagging and expression. Currently, a wide variety of bait vectors are available, allowing for both N- and C-terminal tagging, and expression under the control of the promoters of different strengths. In our case, we cloned hENT2 into pTLB1 vector since our transporter has its N-terminal intracellular. Restriction enzymes sites were added at both edges of the hENT2 sequence and amplified by PCR. That PCR product was then digested and ligated inside the pTLB1 vector, ensuring hENT2 gene was in reading frame with the C_{ub} sequence.

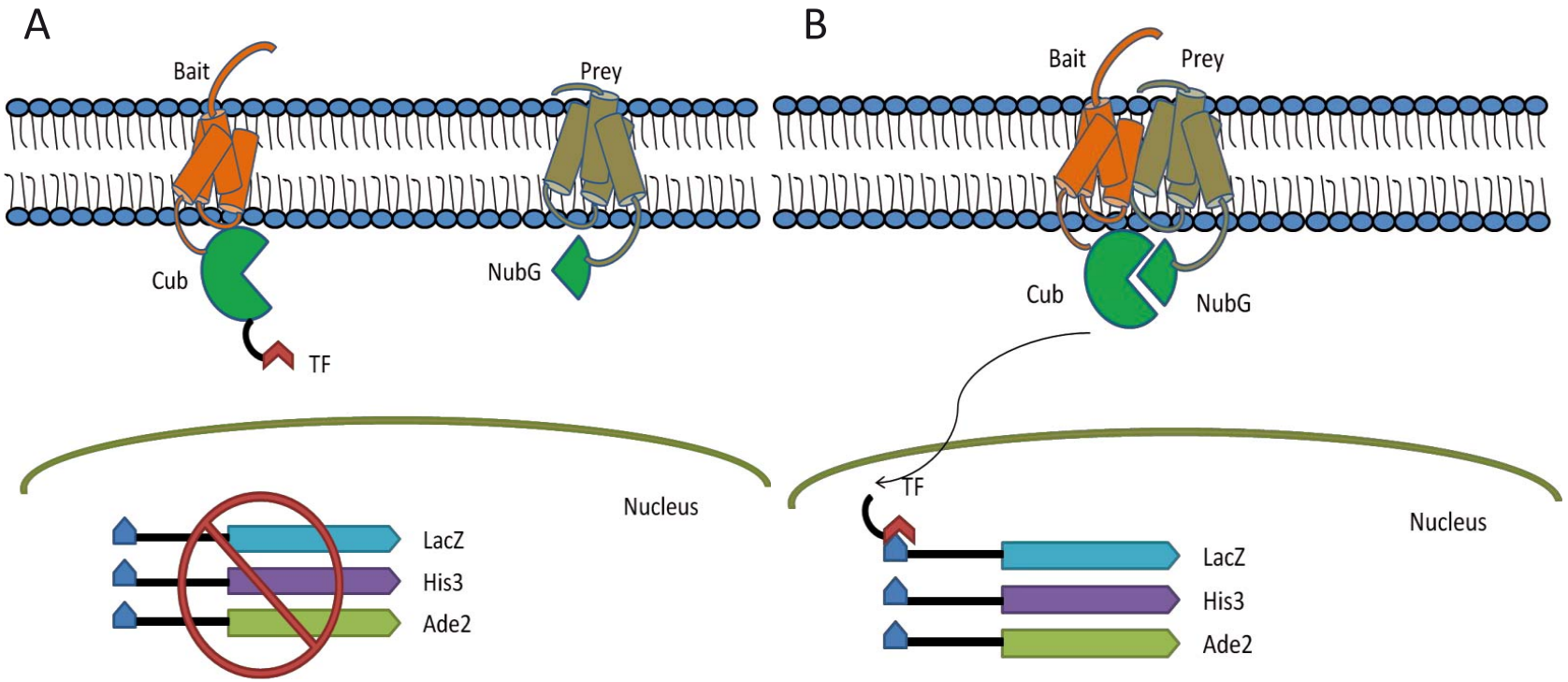

Figure 21. MYTH. Split-ubiquitin based Membrane Yeast Two-Hybrid (MYTH). The protein of interest (Bait) is fused to the C-terminal half of ubiquitin (C_{ub}), while the Prey protein is one of a number of different proteins from a cDNA library, which is subsequently attached to the N-terminal half of ubiquitin ($N_{ub}G$). (a) If no interaction between the bait and the prey takes place, then the reporter system will not be turned on. (b) Only when an interaction takes place are the two halves of ubiquitin forced together resulting in ubiquitin specific proteases cleaving off the transcription factor attached to C_{ub} and turning on the reporter system.

Following, ligation product was transformed into *E. coli* competent cells and grown on specific selection medium, LB-kanamycin, for plasmid propagation. Plasmid DNA was isolated using a mini-prep commercial kit following manufacturer's protocol. Afterwards, bait construct is transformed into a proper MYTH reporter strain, NMY51 in our case. Transformed cells are plated onto appropriate solid selective medium, SD-Leu, and grown at 30ºC for 2-3 days. Molecular cloning steps are widely described in section 11, Molecular Biology Techniques. Medium recipes and product references are found in Snider *et al*. (2010).

Before being used in screening, baits must be validated to ensure that they do not activate the reporter system in the absence of an interacting prey ("self-activate"). Only baits that meet this criteria are suitable for screening. The level of self-activation is assessed using the N_{ub}G/I control test, in which the bait is transformed with both interacting N_{ub}I (positive) and noninteracting N_{ub}G (negative) control preys and grown on selective medium. A bait must grow on selective medium in the presence of the positive control, but not in the presence of the negative control, to be suitable for MYTH. If a bait shows self-activation, the stringency of the selective medium can be improved by the inclusion of up to 100 mM of the His3-competitive inhibitor 3-amino-1,2,4-triazole (3-AT). Note that if 3-AT is found to be necessary at these steps, it must be included at the same concentration throughout the entire screening process.

For the N_{ub}GI control test, yeast cells containing the bait plasmid are transformed with 100-200 ng appropriate N_{ub}I and N_{ub}G control prey plasmids using the protocol described in section 11.2 and plated onto SD-WL selection medium plates for 2-3 days. Following, one single colony of each plate is resuspended in 100 µl of sterile 0.9% NaCl and diluted serially producing dilutions of 1:10, 1:100 and 1:1,000. 2.5 µl of each undiluted and diluted cells are spotted onto the following transformation and interaction selective media plates:

- SD-WL	- SD-WLAH + 3-AT 25 mM
- SD-WLAH	- SD-WLAH + 3-AT 50 mM
- SD-WLAH + 3-AT 10 mM	- SD-WLAH + 3-AT 100 mM

Note: SD = Synthetic dropout medium; - WL = Dropout mix minus tryptophan and leucine; - WLAH = Dropout mix minus tryptophan, leucine, adenosine and histidine; 3-AT = 3-amino-1,2,4-triazole.

Plates are incubated at 30ºC for 3-4 days. Afterwards, positive (N_{ub}I) and negative (N_{ub}G) controls must be compared. Ideally, all transformed strains should show comparable growth on transformation selection medium (SD-WL), but only bait strains containing N_{ub}I control preys should grow on interaction selection medium (SD-WLAH ± 3-AT). Baits containing N_{ub}G control preys that grow on interaction selection medium are said to be self-activating and are not suitable for screening.

12.2 LIBRARY SCREENING: LARGE-SCALE TRANSFORMATION AND PREY PLASMID RECOVERY

When carrying out a screening, it is important to calculate the number of individual prey transformants, or coverage, obtained. This is best carried out by plating a small aliquot of the transformation mix onto appropriate transformation selection medium (SD-WL) to select for prey transformation (but not bait-prey interaction) and the counting of colonies after growth. The level of coverage deemed acceptable will ultimately depend on both the complexity of the library being screened and the individual goals of the experimenter. As a general guideline, however, it is typically tried to obtained coverage equal to at least twice the complexity of the prey library being used.

For the large-scale screening, a single colony of validated bait strain (freshly streaked from the glycerol stocks grown on a SD-L plate) is inoculated into 4 ml SD-L medium and incubated overnight at 30ºC with shaking. This overnight culture is used to

inoculate 200 ml SD-L to an initial OD_{600} of 0.15 and incubate it at 30ºC until a target OD_{600} of 0.6-0.7 is reached (approximately 4-5 hours). This grown 200 ml culture is then divided in 4 x 50 ml screw-cap sterile tubes and centrifuged at 700g for 5 minutes at 4ºC. Each pellet is then resuspended in 30 ml sterile ddH_2O by vortexing briefly and centrifuged again at 700 g for 5 minutes at 4ºC. From here, the yeast transformation protocol described in section 11.1.2 is followed up-scaling volumes to adapt it to the large scale-transformation, where 10 µg of prey library are used for each 50 ml screw-cap tube.

Eventually, pellets are resuspended in 4.9 ml of sterile NaCl 0.9%. Starting with 100 µl of cell suspension, 1:10, 1:100 and 1:1,000 serial dilutions are prepared with NaCl 0.9%. 100 µl of both 100X and 1,000X dilutions are plated onto transformation selection medium SD-WL and incubated at 30ºC for 3-4 days. Once grown, these plates can be used to calculate the total number of transformants obtained by counting colonies and using the following equation:

Total transformants = Number of Colonies on Plate X Dilution Factor X 49

The remaining 4.8 ml of cell suspension are then equally divided and plated onto large 150 mm plates containing appropriate solid interaction selection medium. If 3-AT was found to be necessary in the N_{ub}GI control test, it has to be then included in the medium at the required concentration. Plates are incubated at 30ºC for 3-4 days or until distinct, moderate-to-large-sized single colonies appear. Each single colony is resuspended in 100 µl of sterile NaCl 0.9% and spotted (2.5 µl) onto appropriate interaction selection medium + X-Gal. Plates are once more incubated at 30ºC for 3-4 days. Afterwards, only colonies that show both blue colour and robust growth are further analyzed.

To recover the positive prey plasmids for further analysis, those robustly growing blue colonies have to be first grown in 4 mL of SD-W medium at 30ºC overnight. Following, plasmid DNA from the cultures are isolated using a commercial mini-prep kit according to manufacturer's manual. One modification has to be done

though; after initial resuspension, a small volume of 0.5 mm soda lime glass beads has to be added and vortexed vigorously for 5 minutes to ensure sufficient lysis of the yeast cells.

Once prey plasmid DNA from yeast are obtained, they are following transformed into a competent *E. coli* strain suitable for plasmid propagation (protocol described in section 11.1.1). DNA plasmid is then isolated from the transformed *E. coli* using the commercial kit (as per the manufacturer's instructions).

12.3 BAIT DEPENDENCY TESTING AND SEQUENCING

On completion of screening and identification of candidate interactors spurious hits can be ruled out using the bait dependency test. In this test, isolated prey plasmids are transformed back into the original bait, as well as into an unrelated control bait, and cells are grown on selective medium. Only specific interactors, capable of activating the reporter system in the original bait, but not in the unrelated bait, are considered for further analysis.

To perform this confirmation test, prey plasmid DNA obtained from *E. coli* mini-prep are transformed into both the original bait strain and an unrelated control bait strain, and plated onto appropriate transformation selection medium (SD-WL), following by incubation at 30ºC for 3-4 days. Three individual colonies from each transformation plate are resuspended in 100 µl sterile NaCl 0.9% and spotted (2.5 µl) each onto appropriate interaction selection medium + X-Gal. Plates are incubated at 30ºC for 3-4 days. After that timing, growth of specific preys in both the original bait and control bait stain are compared. Preys that cause growth and blue coloration with both the control and the original bait strain are considered spurious, likewise those preys that do not reproduce growth and blue colour in the original bait strains. Preys that cause growth and blue coloration in the original but not the control bait strain are considered specific.

Positive and specific original bait preys are then sequenced using the $N_{ub}G$ forward internal sequencing primer. In our case, the library used was $N_{ub}G$-X, so the primer used for sequencing is 5′-CCGATACCATCGACAACGTTAAGTCG-3′. Protocol followed for sequencing is described in section 11.3.8. Once results are obtained, last step is to analyze those sequences by using BLAST[F] open source software.

13 PROTEIN EXPRESSION IN BACTERIA

Protein expression is a subcomponent of gene expression. It consists of the stages after DNA has been transcribed to mRNA. The mRNA is then translated into polypeptide chains, which are ultimately folded into proteins. There are many ways to induce foreign DNA to a cell for expression, and there are many different host cells which may be used for expression. The best expression system of choice depends on the gene involved. Nonetheless, bacterial expression has the advantage of easily producing large amounts of protein, which is required for X-ray crystallography or nuclear magnetic resonance experiments for structure determination, together with other purposes.

E. coli is one of the most widely used expression hosts, and DNA is normally introduced in a plasmid expression vector. The techniques for overexpression in *E. Coli* are well developed and work by increasing the number of copies of the gene, or increasing the binding strength of the promoter region so assisting transcription. For example, a DNA sequence for a protein of interest could be cloned or sub-cloned into a high copy-number plasmid containing the lac promoter, which is then transformed into *E. coli*. Addition of IPTG, a lactose analog, activates the lac promoter and causes the bacteria to express the protein of interest.

13.1 SYNTHESIS OF ENT2 INTRACELLULAR LOOP PEPTIDES

Plasmids containing either the intracellular loop (residues 217 to 289) sequence of hENT2 or mENT2 (preceded by His and Ubiquitin tags) were synthesized by DNA 2.0[G] such that, once translated, the resulting peptides are:

hENT2:
MHHHHHHMQIFVKTLTGKTITLEVEPSDTIENVKAKIQDKEG
IPPDQQRLIFAGKQLEDGRTLSDYNIQKESTLHLVLRLRGGL
VPRGS**HLKFARYYLANKSSQAQAQELETKAELLQSDENG**
IPSSPQKVALTLDLDLEKEPESEPDEPQKPGKPSVFTVFQ
KI

mENT2:
MHHHHHHMQIFVKTLTGKTITLEVEPSDTIENVKAKIQDKEG
IPPDQQRLIFAGKQLEDGRTLSDYNIQKESTLHLVLRLRGGL
VPRGS**HLKFARYYLTEKLSQAPTQELETKAELLQADEKNG**
VPISPQQASPTLDLDPEKEPEPEEPQKPGKPSVFVVFRK

The portion of the peptide corresponding to the ENT2 intracellular loop is indicated in bold. Plasmids were transformed into *Escherichia coli* DH5α bacteria followed by plating onto kanamycin (50 µg/ml) plates. Following overnight incubation at 37ºC a single colony was inoculated into 3 mL LB containing 50 µg/ml of kanamycin and grown at 37ºC for 8 hours. The resulting starter culture was subsequently transferred to 50 ml LB containing 50 µg/ml kanamycin and allowed to grow for a further 14 hours before being transferred to 1L of M9 minimal medium.

When the bacterial culture reached an OD_{600} = 0.7, IPTG 1 mM was added to induce protein expression. Bacteria were induced at 37ºC for 2 hours and then pelleted at 7000 x g for 20 minutes. Pellets were resuspended in 30 ml T300 and passed through a French press (5 times) to lyse bacteria and release the protein. Unbroken cell debris was pelleted at 16,000 rpm for 20 minutes.

His-Ubiquitin tagged peptides were extracted from the supernatant (obtained from the previous centrifugation step) using standard nickel affinity chromatography methods. Briefly, following preparation of the column with $NiCl_2$ 50 mM, protein was bound at a rate of 2 ml/min. The column was then washed at a rate of 5 ml/min first with 100 ml T300 and then with 100 ml T300 buffer supplemented with imidazole 10 mM. Bound protein was eluted from the column using 50 ml T300 buffer supplemented with EDTA 20 mM. Presence of the peptide was confirmed using a 10% SDS gel and Coomassie blue staining.

The 50 ml sample was then concentrated at 4000 x g to 4mL using Microcon YM-3 columns (Millipore) and subjected to further purification by fast protein liquid chromatography (FPLC) using a Sephadex S-100 16/60 column (GE Biosciences). The resulting elution fraction was concentrated to 5ml using Microcon YM-3 columns.

14 *IN VITRO* PHOSPHORYLATION ASSAYS

In vitro phosphorylation studies were conducted using 10 µg of the ENT2-loop peptide or Histone H1 as positive control, which was treated with PKC (0.02 units), PKA (2500 units), CKII (500 units) or CamKII (0.02 units) and [γ-32P]-ATP (0.25 mCi/ml; for autoradiography) or non-radiolabeled ATP (for mass spectrometry). Following a 2 hour incubation at 30ºC, samples were mixed with an appropriate volume of protein loading buffer and boiled at 90ºC for 10 minutes. Protein samples were separated by 10% SDS-PAGE for 3.5 hours at 200 V.

Following separation, 16kDa bands representing phosphorylated or non-phosphorylated mENT2 and hENT2 peptides were visualised using coomassie blue stain. Gels containing radiolabeled protein were dried and subjected to autoradiography using standard imaging film in cassettes lined with a ^{32}P intensifying screen for one hour at room temperature or overnight at -80ºC. Gels containing non-radiolabeled samples were prepared for mass spectrometry analysis.

IV. Results and Discussion

15 IDENTIFICATION AND CHARACTERIZATION OF 3 NOVEL NUCLEAR SPLICED VARIANTS OF THE HUMAN EQUILIBRATIVE NUCLEOSIDE TRANSPORTER 2 (hENT2)

15.1 IDENTIFICATION AND CLONING OF NOVEL ALTERNATIVE SPLICING VARIANTS OF hENT2

Previous work described the existence of two spliced variants of the human equilibrative nucleoside transporter 2 (hENT2) (Williams & Lanahan 1995; Mangravite *et al*. 2003). Our research also produced evidence for other variants. Therefore, our first aim was to identify and clone the various isoforms (figure 22).

We designed a set of primers based on the published hENT2 sequence (NM001532) and used these to amplify the complete ORF from the cDNA generated from mRNA isolated from the breast cancer cell line MCF7. The conditions used for the PCR reaction are outlined in table 9.

Table 9. PCR amplification of hENT2

Primer 5' – FL4F	5'-CTTTCACCCCAGGCGCATCCG		
Primer 3' – FL5R	5'-GGATCTCAGCTCCGGAAGG		
Reaction Mix	Taq polymerase buffer 10X …….. 5 μl Primer 5' (20 μM) …… 1 μl Primer 3' (20 μM) …… 1 μl dNTPs (2.5 mM) …….. 4 μl DMSO …… 4 μl $MgCl_2$ (25 mM) ……. 3 μl DNA ……..…..…. 50 ng *FastStart Taq High Fidelity* ……..…. 2.5 U MilliQ water …… to a final volume of 50 μl		
PCR Parameters	Denaturation:	94ºC	30s
(35 cycles)	Annealing:	58ºC	30s
	Extension:	72ºC	1min 45 s

PCR products were analyzed by standard agarose electrophoresis and initial amplifications resulted in four different products being amplified which ranged in size from 1000 and 1500 bp (figure 22b). We surmised that the largest band was likely to correspond to the wild type (wt) isoform of hENT2 (1456 bp). To ensure that as many isoforms as possible were included in our analysis, we repeated the PCR reaction using four different sources of MCF7 cDNA coming from four different cell batches. We extracted PCR products for cloning by cutting the appropriate section of each lane as shown in figure 22d. PCR products were ligated into the vector pGemT Easy and transformed into competent *E. coli* DH5α bacteria as described in the materials and methods section.

Cloning resulted in a total of 360 colonies, which were screened by PCR as described in materials and methods. From the colonies isolated, a total of 33 sequences were confirmed to be the full-length hENT2 wt isoform, and 77 appeared to be spliced variants of hENT2. Results are shown in table 10, where we describe the most relevant isoforms identified, based on their prevalence, and the structure of their translated proteins.

Our approach allowed us to analyze 360 samples and identify as many different isoforms as possible (figure 23). We analyzed 45 DNA pools and 16 candidates were chosen to be sequenced, resulting in a total of 128 different samples of which 110 sequences turned out to be hENT2, 45 candidates from the upper bands and 65 from the lower bands.

To help understand the nature, similarities and differences among the splice variants, we classified the identified isoforms into different groups depending on the putative proteins generated by the ORFs. We noted that two variants would generate putative proteins containing the first 6 transmembrane domains of the full-length hENT2 protein. One of those variants has been previously defined as hENT2A (Mangravite *et al*. 2003). This spliced variant was previously reported as being a protein that did not reach the plasma membrane but which remained in an intracellular location with a vesicular distribution. These data suggested that the isoform we designated as 17G was likely to be a new potential cytoplasmic variant.

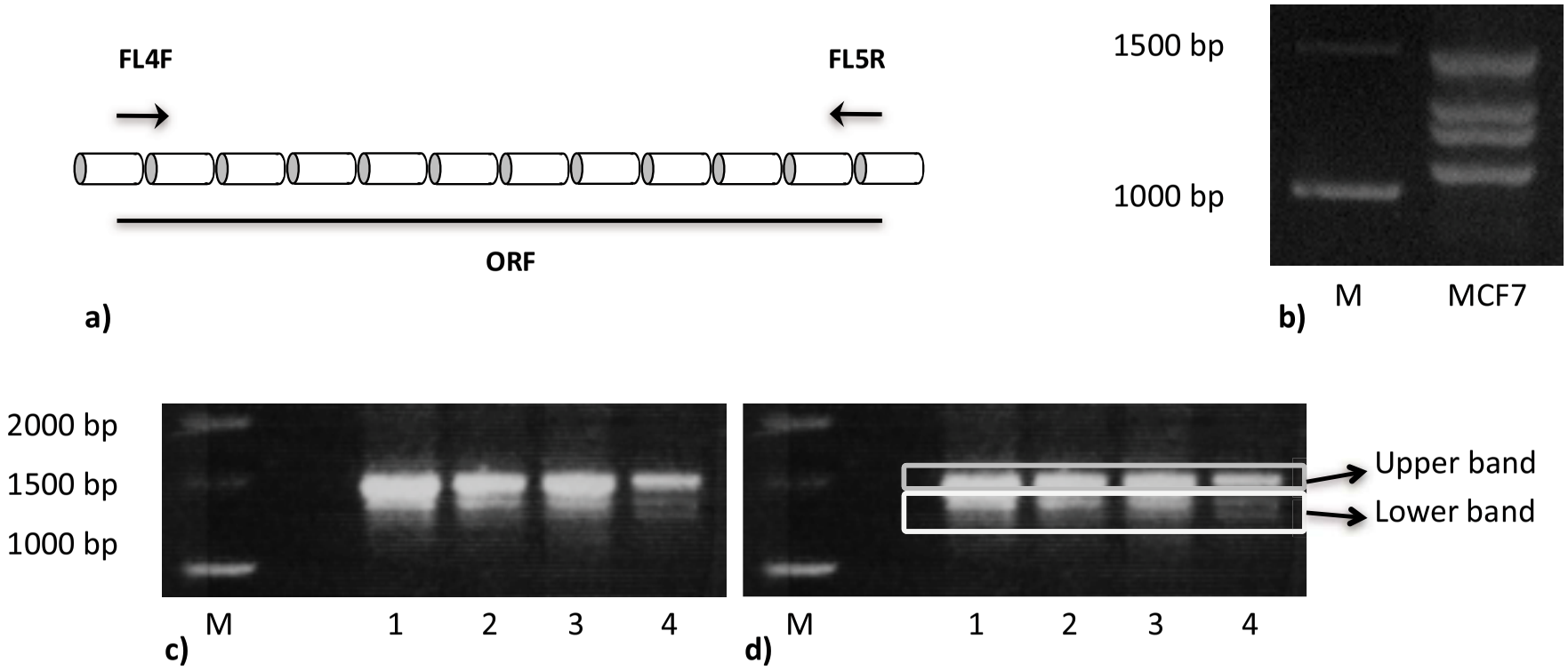

Figure 22. Amplification of the hENT2 gene from MCF7 cDNA. (a) hENT2 transcript pattern comprised of 12 exons. Sites of PCR primers are shown above and the open reading frame (ORF) is shown as black line representing a 456 aa protein. (b) PCR amplification of MCF7 cDNA resulted in four products of different molecular weight. (c) PCR amplification of four different samples of MCF7 cDNA (lanes 1-4) resulted in the same pattern of products. (d) Strategy used to extract the DNA by cutting each lane in 2 parts: upper band and lower band.

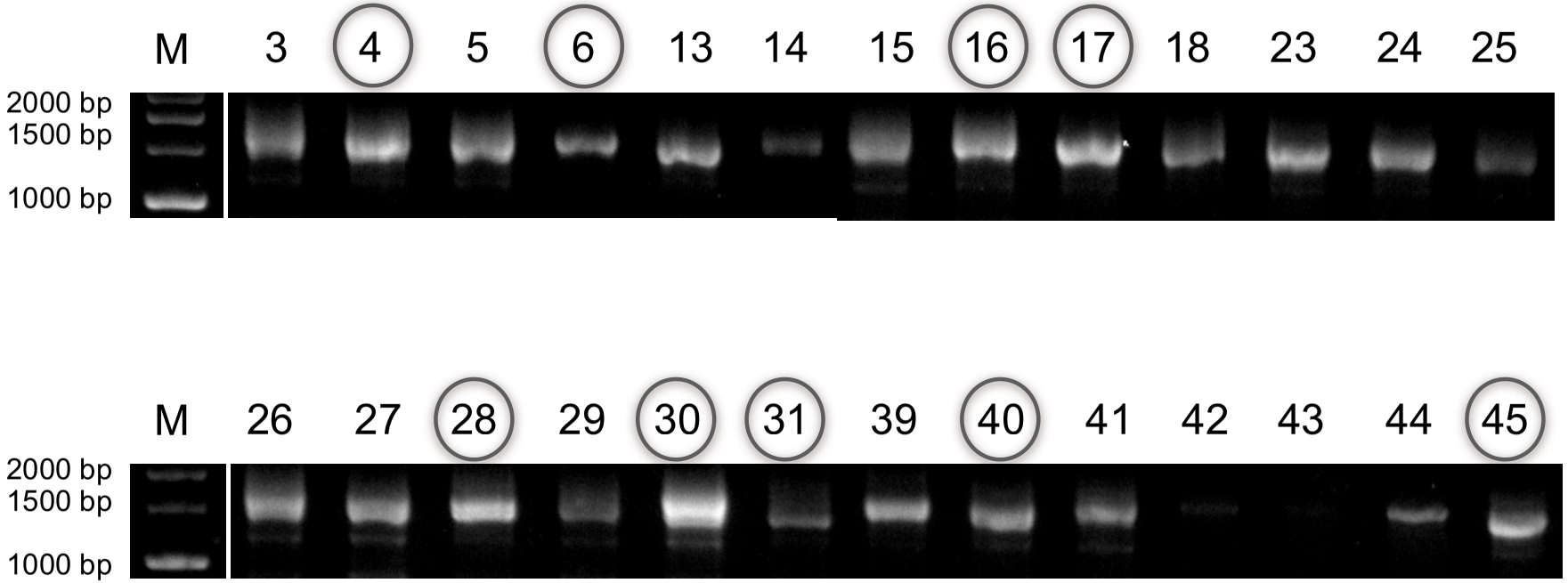

Figure 23. Screening by PCR. Results obtained from the PCR screening of samples from lower bands. Based on the different patterns observed, a total of 16 DNA pools were chosen to be sequenced, samples highlighted with a circle together with lanes 2, 8, 10, 20, 22, 34 and 35 (not shown) from upper bands.

Table 10. Splicing variants of hENT2

Sample	Deletion	Name DB	Prevalence	Protein	TM Domains	Localization
10C	-	NM001532	33/45	456 aa	1 - 11	PM
22C	40 bp in exon 9	AF401235	7/45 + 7/65	301 aa	1 - 6	Intracellular
17G	Exon 8	-	10/65	361 aa	1 - 6	Intracellular?
22E	68 bp in exon 4	X86681	2/65	336 aa	4 - 11	Nuclei
4A	Exon 2	-	5/65	336 aa	4 - 11	Nuclei
16D	Exon 4	-	6/65	302 aa	5 - 11	Nuclei ?
45F	Exons 2 and 4	-	9/65	302 aa	5 - 11	Nuclei ?
30D	247 bp (e3,e4,e5)	-	3/65	302 aa	5 - 11	Nuclei ?
4D	Exon 2 + 40 bp exon 9	-	6/65	181 aa	4 - 6	?
45C	Exons 2 and 8	-	2/65	241 aa	4 - 6	?
31F	Ex.2 + ex.4 + 40 bp ex.9	-	2/65	147 aa	5 - 6	?

Features described in table 10: *Sample*, identifier; *Deletion*, region of gene deleted compared to hENT2 wt; *Name DB*, reference found in GenBank[A] database for the transcript; *Prevalence*, number of repetitions found during the screening; *Protein*, length in amino acid of putative protein product based on analyses using Clone Manager software[B]; *TM Domains*, putative transmembrane domains based on analysis using TMHMM 2.0 software[C] ; *Localization*, confirmed or proposed cellular localization of the protein.

In addition, we identified a variant whose transcript was previously named as X86681 and which is described as missing 68 bp in exon 4 resulting in a translated protein of 36 KDa. This variant is described as a hydrophobic nucleolar protein (HNP36) comprising 326 amino acids (Williams & Lanahan 1995). However, according to our studies using the ORF Finder software from NCBID (see figure 60 - appendix I) or the Clone Manager software[B], the transcript would result in a protein of 336 amino acids.

We identified a novel spliced variant in which exon 2 had been skipped resulting in a predicted ORF of 336 amino acids which is identical to our analysis of the actual structure of HNP36 protein (figure 24). We also detected three more variants, which would produce a translated protein containing only the last 7 transmembrane domains (TMD) of the wild type protein. This structure consists of one less TMD than HNP36, indicating the possibility of the existence of another nuclear variant. The existence of different spliced variants of the same protein suggests a multitude of ways of regulating the protein and perhaps multiple roles.

```
X86681          1 mspgpffsitmasvcfinsfsavlqgslfgqlgtmpstystlflsgqglagifaalamllsmasgvdaetsalgyfitpyvgilmsivcy
4A              1 mspgpffsitmasvcfinsfsavlqgslfgqlgtmpstystlflsgqglagifaalamllsmasgvdaetsalgyfitpyvgilmsivcy
HNP36           1 ----------masvcfinsfsavlqgslfgqlgtmpstystlflsgqglagifaalamllsmasgvdaetsalgyfitpyvgilmsivcy

X86681          91 lslphlkfaryylankssqaqaqeletkaellqsdengipsspqkvaltldldlekepesepdepqkpgkpsvftvfqkiwltalclvlv
4A              91 lslphlkfaryylankssqaqaqeletkaellqsdengipsspqkvaltldldlekepesepdepqkpgkpsvftvfqkiwltalclvlv
HNP36           81 lslphlkfaryylankssqaqaqeletkaellqsdengipsspqkvaltldldlekepesepdepqkpgkpsvftvfqkiwltalclvlv

X86681         181 ftvtlsvfpaitamvtsstspgkwsqffnpiccfllfnimdwlgrsltsyflwpdedsrllpllvclrflfvplfmlchvpqrsrlpilf
4A            181 ftvtlsvfpaitamvtsstspgkwsqffnpiccfllfnimdwlgrsltsyflwpdedsrllpllvclrflfvplfmlchvpqrsrlpilf
HNP36         171 ftvtlsvfpaitamvtsstspgkwsqffnpiccfllfnimdwlgrsltsyflwpdedsrllpllvclrflfvplfmlchvpqrsrlpilf

X86681         271 pqdayfitfmllfavsngylvsltmclaprqvlpherevagalmtfflalglscgaslsflfkall
4A             271 pqdayfitfmllfavsngylvsltmclaprqvlpherevagalmtfflalglscgaslsflfkall
HNP36          261 pqdayfitfmllfavsngylvsltmclaprqvlpherevagalmtfflalglscgaslsflfkall
```

Figure 24. Alignment of three predicted ORF for hENT2 spliced variants. Predicted protein for the transcript X86681 according to ORF Finder from NCBI[D] and Clone Manager[B] software. Predicted protein for our novel variant 4A also consisting of 336 aa. HNP36 protein sequence as described (Williams & Lanahan 1995) comprised of 326 aa, lacking the 10 first residues of X86681 and 4A.

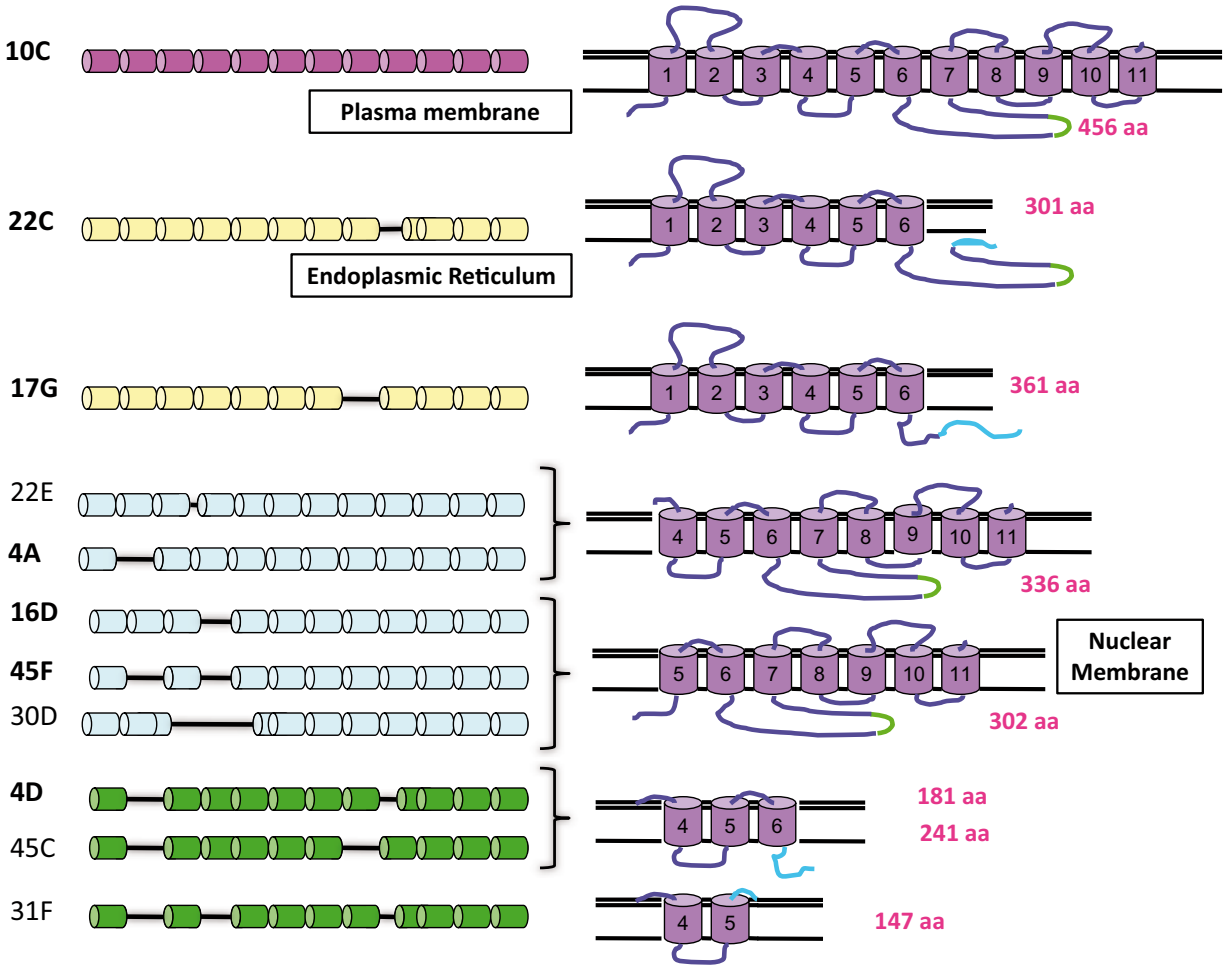

Figure 25. Representation of hENT2 splicing variants and their putative proteins. *Left* (Transcripts): Wild type isoform is represented in pink. Variants with deletions at the end of the transcript generating putative proteins missing the C-terminal TMDs are shown in yellow. Variants with deletions at the beginning of the transcript generating putative proteins missing the N-terminal TMDs are shown in blue. Variants with deletions at both the N and C-termini of the transcript, generating small putative proteins containing only the central TMDs are shown in green. *Right* (Proteins): The epitope within the large intracellular loop between TMD 6 and 7 which is recognized by the anti-hENT2 antibody is shown in green. The region of putative protein in which the sequence varies from the wild type protein due to a frame shift because of a deletion is shown in light blue.

We also identified three spliced variants with deletions at both ends of the transcript resulting in small proteins consisting of only 3 transmembrane domains. It is unlikely that these variants would reach the plasma membrane or be functional based on their short structure. However, since these small variants were well represented in the total pool, we speculate that they may play a regulatory function.

We continued further studies on the 6 more prevalent identified variants together with the wild type isoform, as indicated in table 10. To conduct expression and functional assays, we cloned the splice variants into pCDNA3.1, which is a vector suitable for heterologous expression.

15.2 PROTEIN EXPRESSION OF hENT2-HA TAGGED SPLICED VARIANTS

Following cloning of the putative newly identified spliced variants for the hENT2 gene, we determined whether these variants were translated into proteins or not. Since commercial antibodies against the hENT2-loop will recognize many variants, and are therefore not able to help us to distinguish between them, we decided to insert an HA-tag into the variants so each potential protein would be detected individually in a heterologous system. The HA tag consists of a 9 amino acids sequence from the human influenza hemagglutinin protein and reliable commercial antibodies against this sequence are readily available. Since this is a very small tag, we presume it will not interfere with the sorting and function of the protein, which is a potential problem of much larger tags such as GFP.

Before starting the cloning, we analyzed in depth all the theoretical ORF contained in our transcripts in order to add the tag into a proper position. We found that some of the variants included more than one ORF, such as a variant which could produce a protein of 143 aa or another of 120 aa, both of them repeated in some of the cases. Since we could not ensure which ones would be synthesized in advance, we decided to generate all the required constructs to analyze all these theoretical ORF (figure 26).

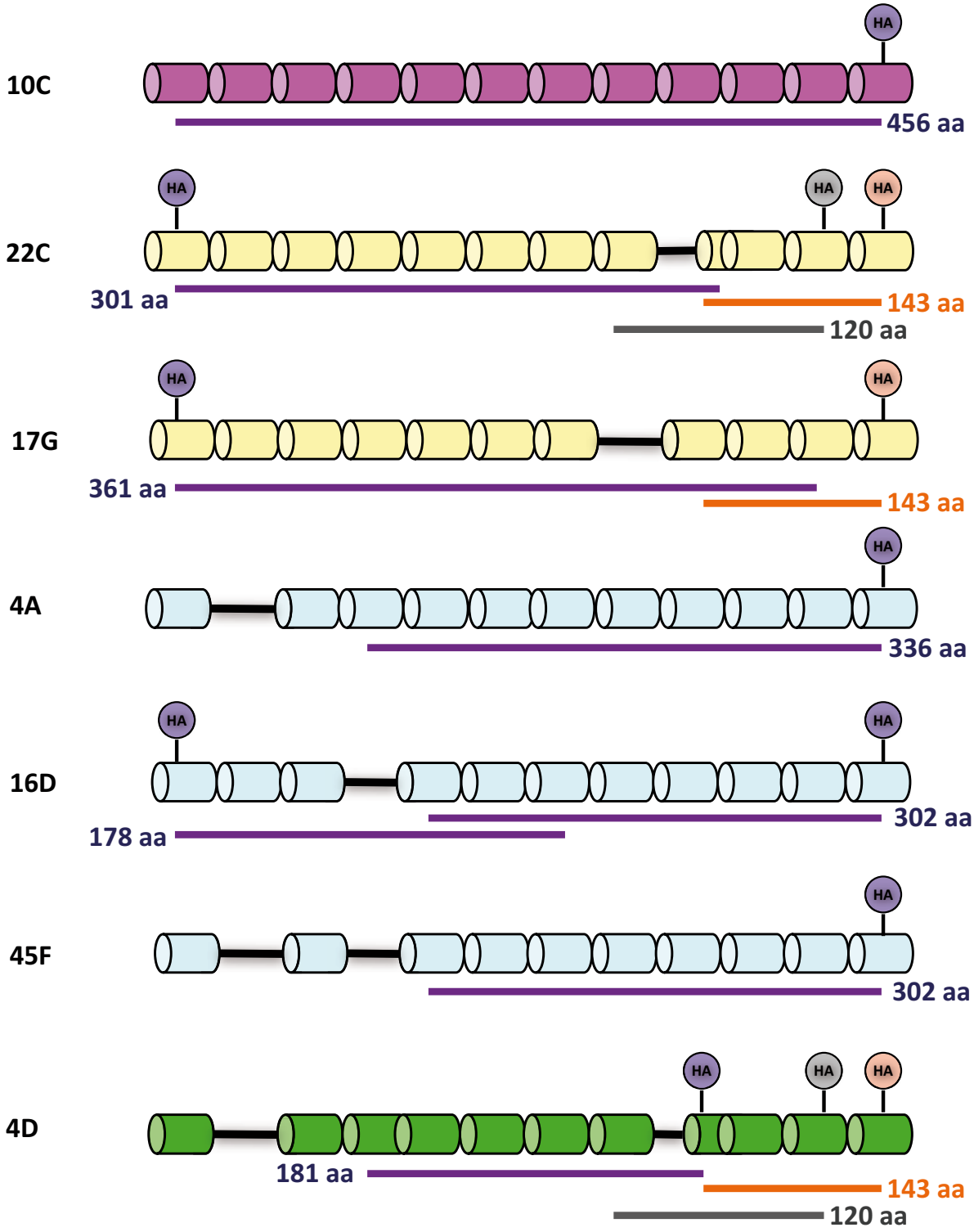

Figure 26. Open Reading Frames (ORF) for each transcript and positions of their HA tag. In purple are shown the ORFs that would be translated into proteins with a similar or partial structure with respect to the wild type isoform. Samples 22C, 17G and 4D have a common ORF with a 143 aa protein. In the same way, isoforms 22C and 4D share a potential ORF for a protein of 120 aa. HA tags were inserted in specific positions to be in frame with only one ORF at a time so we would know which possible protein had been synthesized.

For that purpose we designed a set of 26 primers, including forward and reverse oligonucleotides, classified in 4 groups: Initial HA, to add the tag at the beginning of the ORF (exon 1), Final HA, to add the tag at the end of the ORF (exon 12), 4D HA, specific for the 181 aa protein from the 4D sample (exon 9), and P120 HA, for those that might produce the 120 aa protein (exon 11) (table 21 - appendix I). As a result, we obtained a total of 13 hENT2-HA constructs, all of which were verified by sequencing (table 11).

Table 11. hENT2-HA constructs

Sample	Protein	HA position	Name
10C	456 aa	Exon 12	F10C-HA
22C	301 aa	Exon 1	I22C-HA
	143 aa	Exon 12	F22C-HA
	120 aa	Exon 11	P22C-HA
17G	361 aa	Exon 1	I17G-HA
	143 aa	Exon 12	F17G-HA
4A	336 aa	Exon 12	F4A-HA
16D	302 aa	Exon 12	F16D-HA
	178 aa	Exon 1	I16D-HA
45F	302 aa	Exon 12	F45F-HA
4D	181 aa	Exon 9	4D-HA
	143 aa	Exon 12	F4D-HA
	120 aa	Exon 11	P4D-HA

Once we had generated the hENT2-HA constructs, we determined which proteins could be synthesized by transfecting the constructs into HEK-293 cells, using lipofectamine® 2000. Total protein was extracted 36 hours later with NP-40 buffer. We then denatured the samples and separated them by SDS-PAGE followed by immunoblotting using a commercial anti-hENT2 antibody and an anti-HA antibody (figure 27a). Results show the presence of the wild type isoform together with the putative nuclear variants: 4A, 16D and 45F. The molecular weight of these variants corresponds to the expected values of approximately 36KDa for 4A (HNP36), and 32 KDa for 16D and 45F since they have one transmembrane domain less. The results using the anti-hENT2 antibodies confirm that that antibody can recognize these variants as expected since they possess the conserved intracellular loop between TMD 6 and 7, which contains the epitope against which the antibody has been designed.

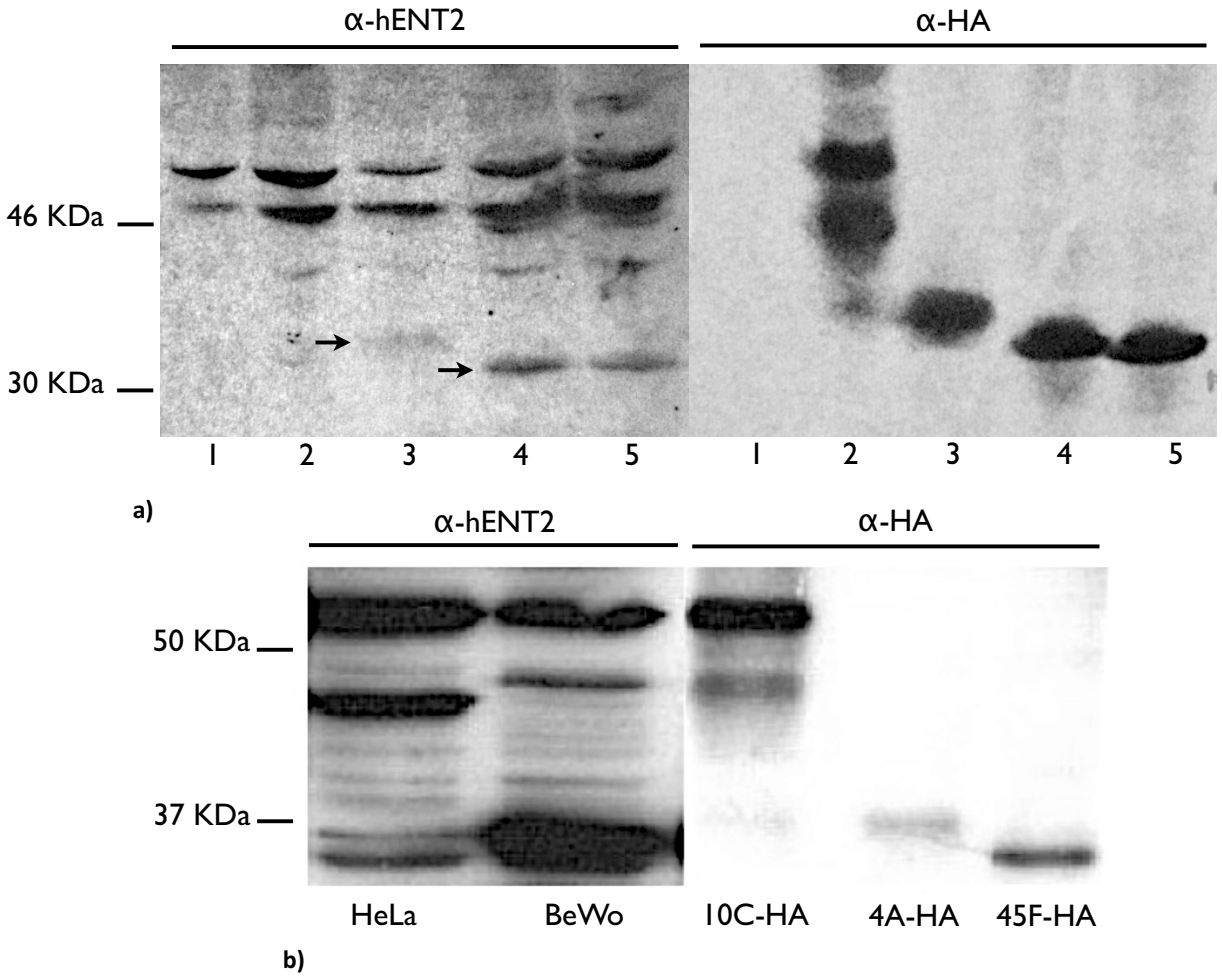

Figure 27. Immunoblots of endogenous hENT2 and hENT2-HA proteins. (a) WB of total protein extracted with NP-40 extraction buffer from HEK-293 cells transfected with different constructs: pCDNA3.1 (lane 1), F10C-HA (lane 2), F4A-HA (lane 3), F16D-HA (lane 4) and F45F-HA (lane 5). Membranes were incubated with antibodies anti-hENT2 and anti-HA tag. (b) Comparison of endogenous hENT2 total protein extracted from HeLa and BeWo cells versus total protein extracted from HeLa cells transfected with 3 HA-tagged hENT2 isoforms.

We also wanted to investigate the presence of the putative nuclear variants in a homologous system using endogenous extracted protein. Since BeWo cell line was described to express ENTs transporters at the nuclear membrane (Mani *et al*. 1998), we analyzed the expression of endogenous hENT2 isoforms in both BeWo and HeLa cells. We compared the protein pattern of BeWo with HeLa cells transfected with the wt-HA and two tagged variants and confirmed that BeWo cells have high expression levels of both splice variants which are presumed to be located at the nuclear membrane.

The putative ER variants, 22C and 17G, could not be detected by immunoblotting (data not shown). Similarly, the 4D truncated proteins of 143 aa and 120 aa, and the 178 aa protein derived from a 16D ORF, could not be detected even when using special nitrocellulose membranes for small molecular weight peptides. Before concluding that these proteins are not synthesized by transient overexpression, we decided to continue with immunocytochemistry (ICC) assays to confirm immunoblotting results and also determine the cellular localization of proteins we have confirmed are synthesized.

For ICC assays, both HeLa and HEK-293 cells were seeded on glass coverslips (12 mm diameter) in a 24-well plate. We transfected the cells with constructs and fixed the cells after 36 hours according to the protocol described in materials and methods section. Initially, we used the anti-HA antibody to confirm expression of the proteins. As previously noted with immunoblotting, we did not detect the putative ER variants 22C and 17G, neither for the proteins of 143 aa and 120 aa. In contrast, we confirmed protein synthesis in the cases of the wild type isoform (F10C-HA) which is apparently localized at the plasma membrane, and also for the potential nuclear variants: F4A-HA, F16D-HA and F45F-HA (figure 28), which seemed to be located at the nuclear periphery according to the nucleoplasma staining with DAPI. The I16D-HA and 4D-HA constructs appeared to be present in some kind of intracellular vesicles that do not reach neither the cytoplasmic nor the nuclear membrane. These vesicles did not co-localize with mitochondria, as detected by Mitotracker®, so we presume they may be lysosomal-like structures that degrade mis-folded proteins.

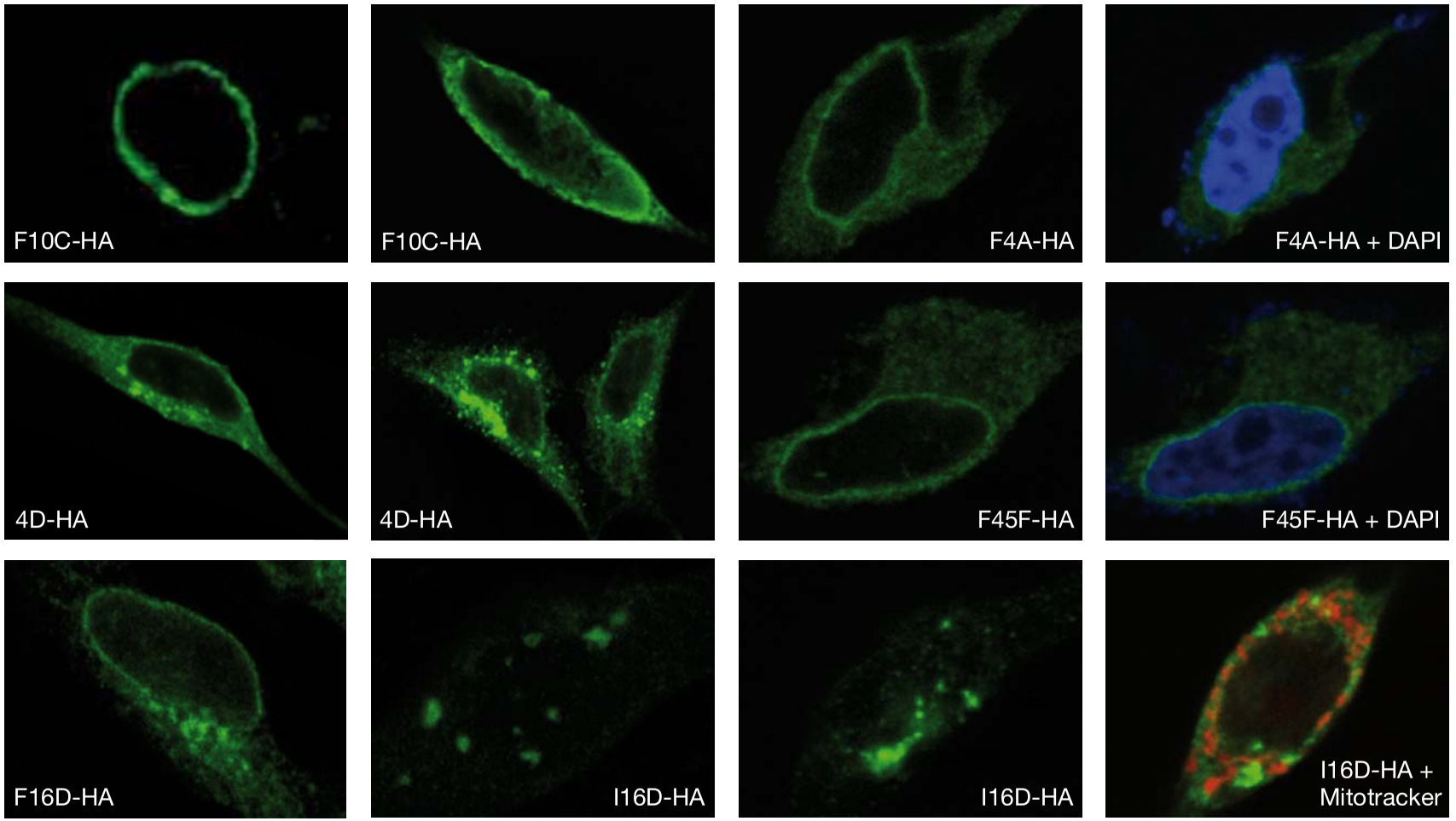

Figure 28. Distribution of hENT2-HA and its spliced variants in human cells. Immunocytochemistry of HeLa cells transfected with hENT2-HA and its spliced variants. F10C-HA samples belong to the wild type isoform of the gene, which appears to be located to the plasma membrane. F4A-HA, F16D-HA and F45F-HA are those variants predicted to be located at the nuclear membrane which is confirmed with DAPI staining. 4D-HA isoform was found in some intracellular vesicles, which may be lysosomes as for I16D-HA, since vesicles did not co-localize with mitochondria detected by MitoTracker® probe.

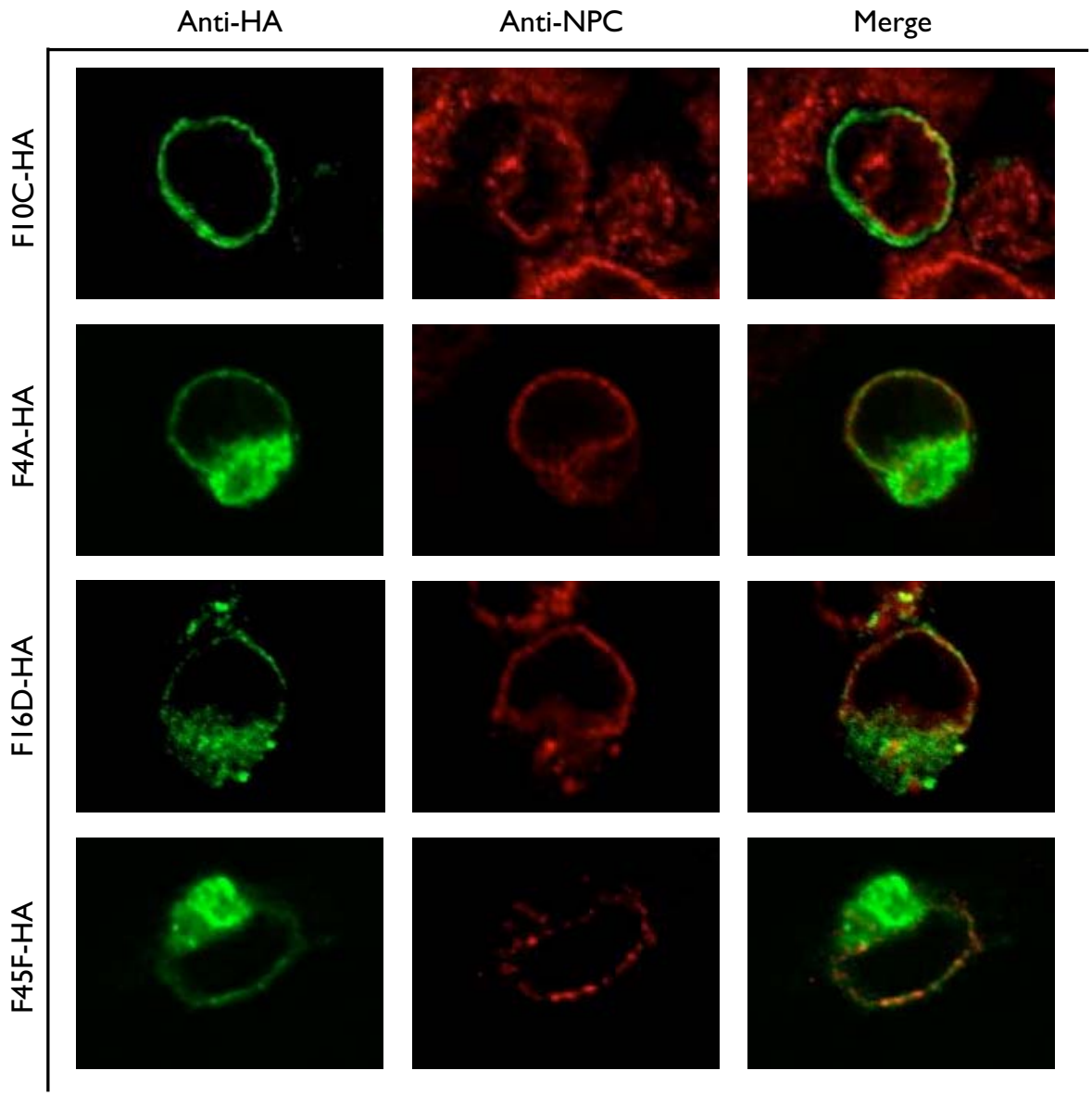

Figure 29. Co-localization of hENT2-HA nuclear variants with the nuclear membrane in human cells. We transfected HEK-293 with the wild type isoform F10C-HA, together with the nuclear variants F4A-HA, F16D-HA and F45F-HA. As shown, the wild type isoform is not present at the nuclear membrane, unlike the nuclear variants which clearly co-localize with the NPC.

To confirm that our novel nuclear variants are located at the nuclear membrane, we repeated the ICC transfecting only the wild type isoform and the three nuclear variants with the HA tag. We immunodetected the HA tag and the Nuclear Pore Complex (NPC), a nuclear membrane marker (figure 29), at the same time. Results confirmed the co-localization between the hENT2 variants 4A, 16D and 45F and the NPC proteins located at the nuclear membrane but not for the wild type isoform, 10C.

15.3 NUCLEAR SPLICED VARIANTS mRNA SURVEILLANCE

Our results thus far were obtained in a heterologous system where we over-expressed the various constructs. Unfortunately, we have not been able to detect them in a homologous system. Therefore, we must confirm that our observations to date are not an artefact due to over-expression and that maybe these proteins would never be synthesized at all because the mRNAs decay before being translated.

It is well known that all eukaryotic cells conserve the nonsense mediated decay (NMD) pathway, which detects and degrade mRNA transcripts that contain premature termination codons (PTC). These PTCs may be generated either by mutations, transcriptional mistakes or errors during mRNA processing, like the alternative splicing phenomenon. Failure to recognize and degrade these mRNA transcripts can result in the production of truncated proteins, which may be harmful to the organism since they might turn out to be some sort of deleterious dominant-negative or gain of function effects.

The NMD pathway is linked to the synthesis of proteins as it detects the PTC once the ribosome binds to the mRNA and the translation starts. One way to find out whether our novel spliced variants are degraded or not by that system, is to block the NMD pathway and determine if there is an accumulation of the mRNA afterwards. That would mean that the transcript is indeed degraded by that pathway and results obtained so far are a consequence of the over-expression protocol.

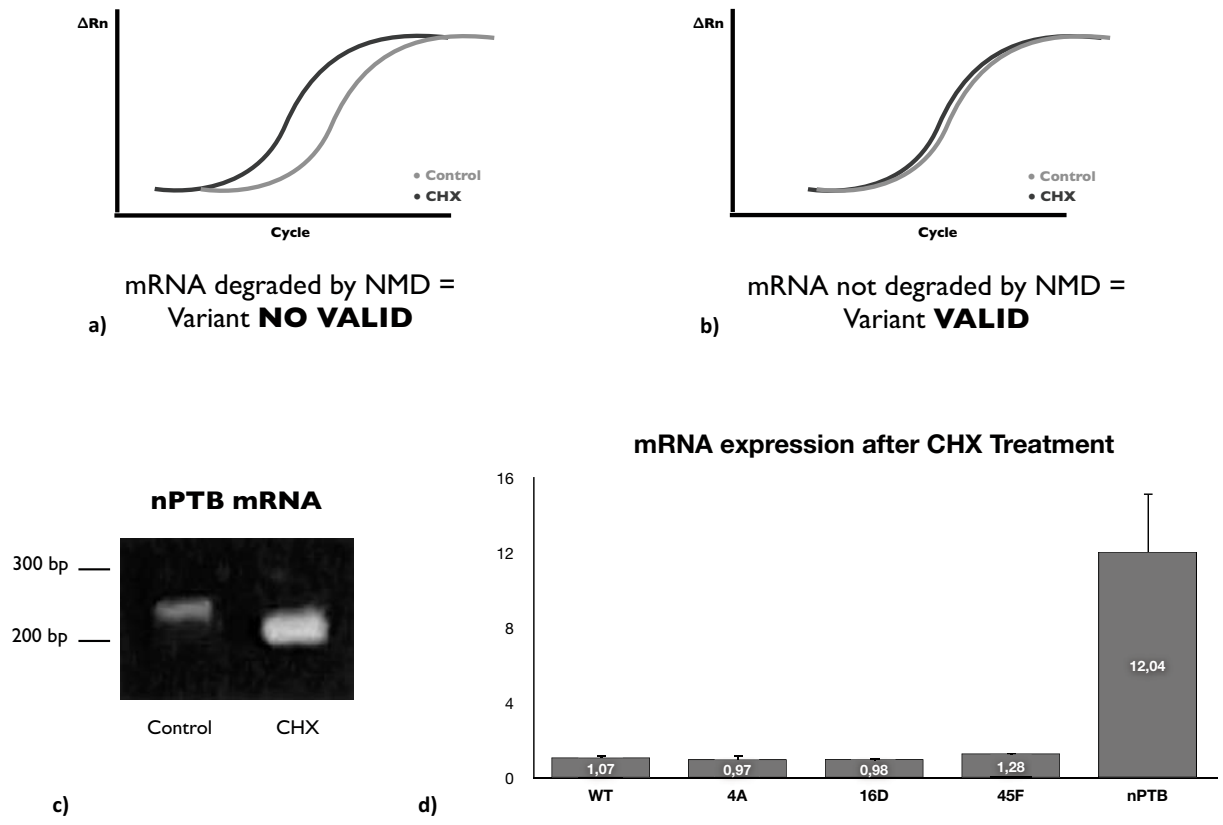

Figure 30. NMD pathway analysis. (a) Example of a realtime PCR profile for mRNA degraded by the NMD pathway where its expression increases after the treatment with CHX. (b) Example of a realtime PCR profile for a mRNA not degraded by the NMD pathway where the expression level is the same before and after the treatment with CHX. (c) PCR amplification of the nPTB gene was used as a positive control. (d) Results of realtime analysis of the hENT2 spliced variants. The four isoforms, wild type plus three nuclear variants, have the same expression before and after the treatment with CHX, what means they are usually translated into proteins since they are not degraded by the NMD pathway. Last bar represents the expression of our control gene, nPTB, which increases its expression 12-fold after the treatment indicating this mRNA is regularly degraded by the NMD pathway.

To block the NMD pathway, we treated HEK-293 cells with cycloheximide (CHX) (20 µg/mL for 6 hours) to inhibit protein synthesis and the NMD machinery. We then extracted the RNA from control (DMSO) and treated samples (CHX) and generated cDNA to analyze the expression of the transcripts and determine if there is any increase in the mRNA levels before and after treatment (figure 30a and 30b). As a positive control we used the nPTB gene, which has been previously described to have an alternative splicing variant where exon 10 is skipped leading to degradation of the variant mRNA by the NMD pathway (Boutz *et al*. 2007). As shown (figure 30c), we observed an increase of the smallest transcript of nPTB gene (corresponding to the exon 10-skipped variant) after treatment with CHX, confirming the involvement of the NMD pathway.

Once we had validated this technique, we analyzed the expression of our variants before and after the treatment. For this, we designed a set of primers such that each couple would amplify only one isoform specifically. We used these primers to detect the levels of these transcripts by real time PCR with SYBR Green®. Results (figure 30d) show that neither the wild type isoform nor the three nuclear variants experience any change in their expression levels after treatment with CHX, which means these mRNAs are not degraded by NMD pathway, so they appear to be translated into proteins in a homologous system. On the contrary, our positive control, nPTB exon 10 skipped variant, showed elevated mRNA expression levels by about 12-fold when we blocked the NMD pathway, which confirms its degradation by this system.

15.4 FUNCTIONAL CHARACTERIZATION OF hENT2 NUCLEAR VARIANTS

After confirming the expression and localization of our novel spliced variants, we continued with their functional characterization. The first assay we performed was a transport assay using transiently transfected HeLa cells and constructs of the wild type isoform and the three variants (figure 31a). As expected, we only observed a significant increase in uptake in HeLa cells transfected with the wild type isoform. Interestingly, we observed an increase of ENT2 activity while ENT1-dependent uptake decreased. However, we did not see any change in uptake with the nuclear variants which is consistent with their presence at the nuclear membrane instead of the cytoplasmic membrane.

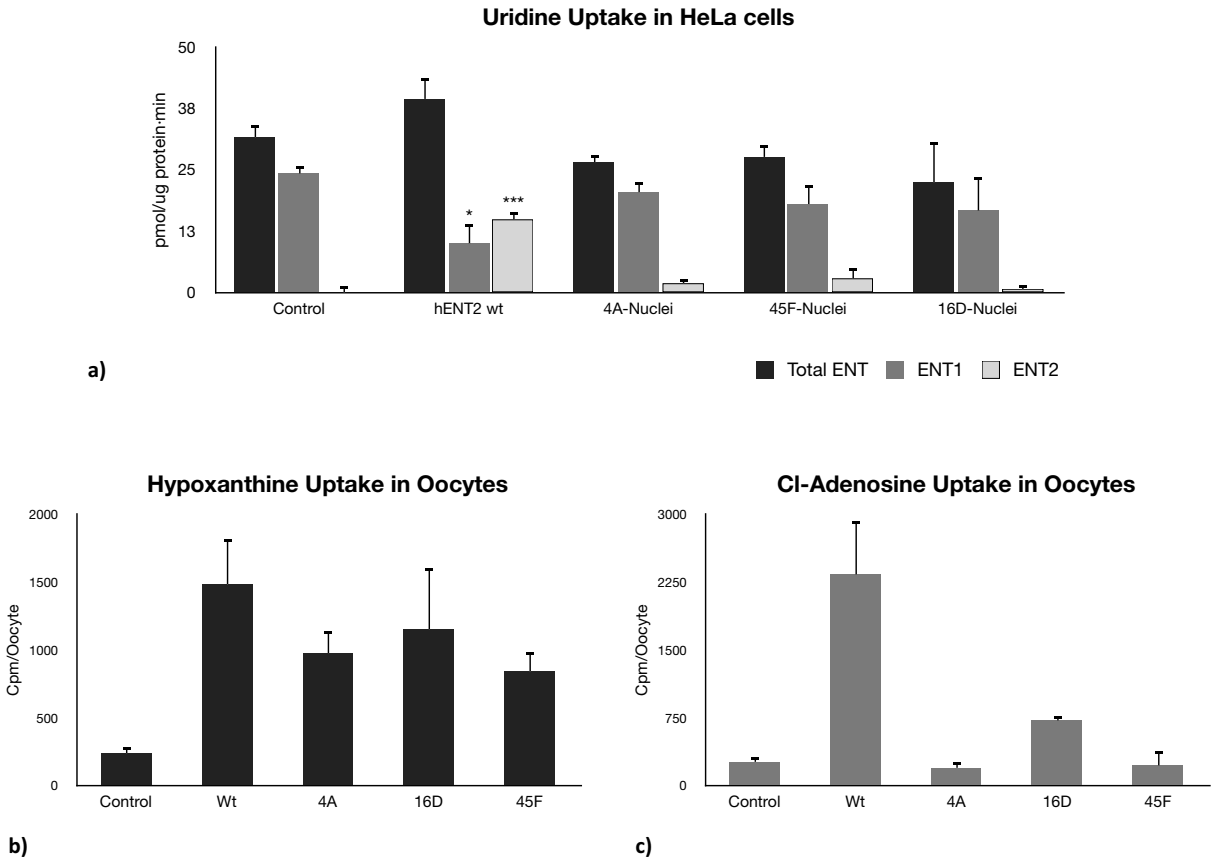

Figure 31. Transport assays of hENT2 and its nuclear variants. (a) Uridine transport assays performed in HeLa cells transfected with four isoforms together with the empty vector as a control (pCDNA3). Transfection of the wild type isoform led to ENT2-dependent uptake while ENT1-dependent uptake decreases. Presence of nuclear variants leads to no increase in ENT2-dependent uptake and there is no change in ENT1-dependent uptake. (b) Hypoxanthine transport assays in oocytes injected with hENT2 wild-type (wt) or the splice variants (4A, 16D, 45F) and water as a control. (c) Chloro-adenosine uptake in oocytes injected with hENT2 wt, three nuclear variants and water as a control.

To determine if the nuclear variants were functional or not, we attempted to purify nuclei from BeWo cells to conduct transport assays since this cell line appears to express nuclear variants (figure 27). Unfortunately, despite trying different protocols, we were unable to obtain a pure fraction of functional nuclei. Nuclei preparations were either contaminated with mitochondria or the nuclear membranes were damaged affecting the functionality of proteins present within them. We therefore decided to purify nuclei from *Xenopus laevis* oocytes injected with our variants. Surprisingly, we observed a significant uptake of hypoxanthine in the oocytes injected with hENT2 wild type as well as the putative nuclear isoforms (figure 31b). We hypothesize that the sorting signal that usually sends the spliced variants to the nuclear membrane in human cells, is not recognized in oocytes and they therefore reach the plasma membrane resulting in measurable uptake.

Transport results with injected oocytes are still preliminary and need to be repeated to confirm the results. However, a priori, the nuclear variants appear to be functional for hypoxanthine uptake although they would have less capacity to translocate the substrate, either because there is less protein reaching the membrane or the transporter variant has less affinity for the substrate than the wild type isoform. We repeated the assay with the same samples but using chloro-adenosine as a substrate. We observed that the nuclear variants do not transport the nucleoside compared to the nucleobase hypoxanthine. This difference could be explained by the lack of the first transmembrane domains in these variants which would be determinant for interaction and recognition of the substrate (Yao *et al*. 2001; Yao *et al*. 2002). Transport assays with the ENT1/2 inhibitor dipyridamole were also performed but data were equivocal so we could not determine whether nuclear variants are sensitive to this inhibitor.

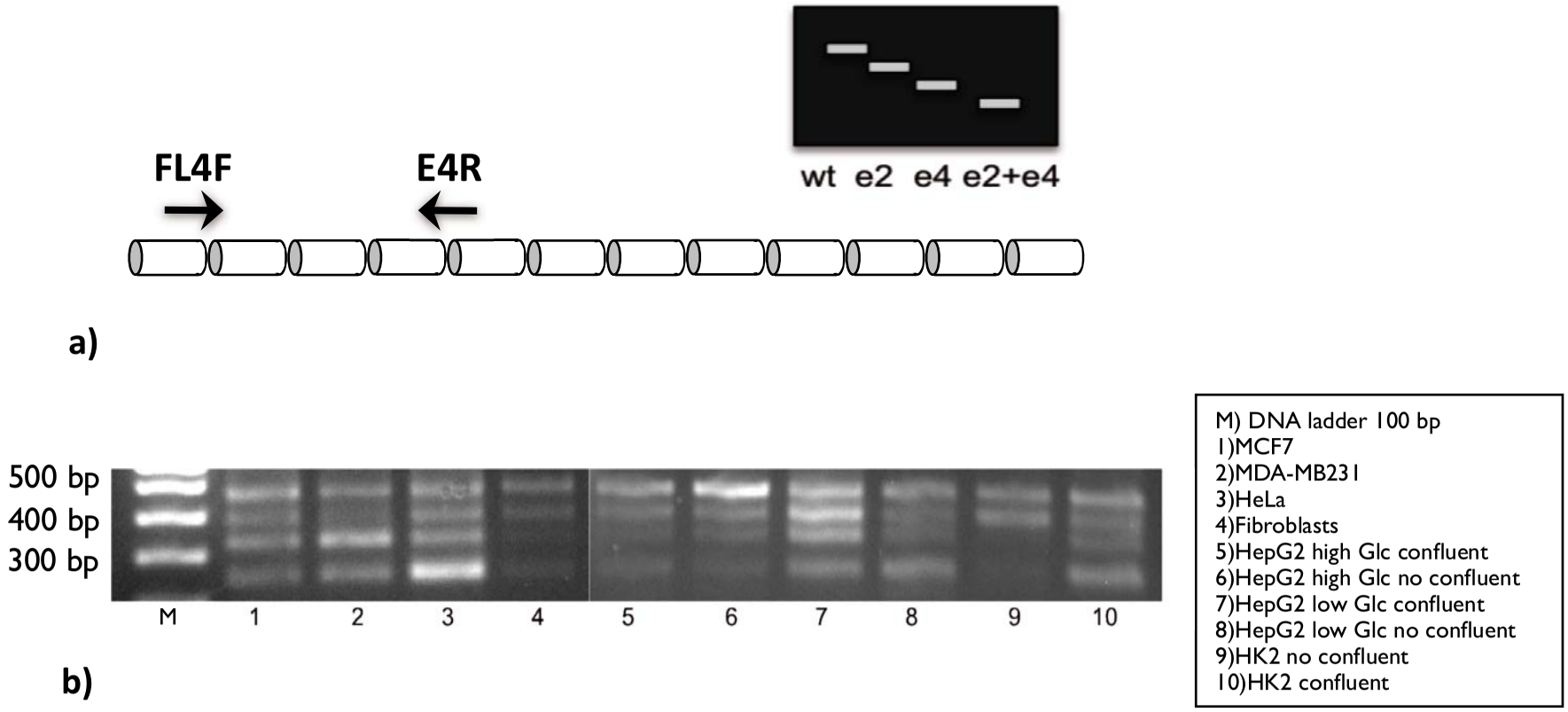

Figure 32. hENT2 mRNA expression in different cell lines and conditions. (a) Strategy used to detect four isoforms of hENT2. (b) Expression of those isoforms in different cell lines and different conditions. Profile changes between samples (i.e. lane 3 and 6) and also depending on the growth conditions like lane 9 and 10, where HK2 non-confluent cells do not express 16D and 45F isoforms (e4 and e2+e4), while the same cell line when highly confluent expresses all four.

15.5 EXPRESSION ANALYSIS OF hENT2 NUCLEAR VARIANTS

After confirming that the nuclear variants were functional, we asked the question as to whether they are constitutively expressed in a range of tissues and cell lines, and if there is any regulation of their expression depending on the growth conditions. To answer this question, we selected two primers (FL4F and E4R) that amplify the region between exon1 and exon 5 in such a way that each variant produces a product of a unique molecular weight making presence of each variant easy to distinguish (figure 32a). We conducted PCR analyses with these conditions using a battery of different cDNAs as templates. This set of cDNA samples was derived from cell lines of different origin (mammary, uterus, fibroblasts, liver and kidney) and some cell lines had been exposed to different growth conditions (e.g. high/low glucose and confluent or not).

Our results (figure 32b) suggest that the four isoforms are extensively expressed. However, some of them show a different pattern of expression: HeLa cells seem to express more 45F than the other three variants unlike MCF7 cells, where this variant is less expressed. We also note a different expression pattern depending the condition used to grow the cells: the clearest case is the HK2 cells which only seem to express the wt and 4A isoforms when cells are not confluent, but express all four variants when the cells reach confluence. These results provide some evidences of a possible regulation of these variants depending on the needs of the cell.

After this qualitative analysis, we performed relative screening in three different cell lines using real-time PCR analysis to better understand the relevance of the presence of each isoform within a single cell type and between cell types. We used three cell lines with different origins: HEK-293 from kidney, NP31 from pancreas and TFK-1 from gallbladder. We analyzed the results using as a reference the wild type isoform of each sample (figure 33a) to compare the relative expression of each isoform within the same sample, and used HEK-293 values as a control (figure 33b) to analyze the expression of the same transcript among samples. Our data suggest that HEK-293 and NP31 have a similar pattern of expression where the wild type isoform is the prevalent form present. The only difference between the cell types is the overall expression levels, where NP31 have greater expression for all the transcripts compared to HEK-293. TFK-1 has highly expressed nuclear variants, about 3 to 10-fold greater than the wild type.

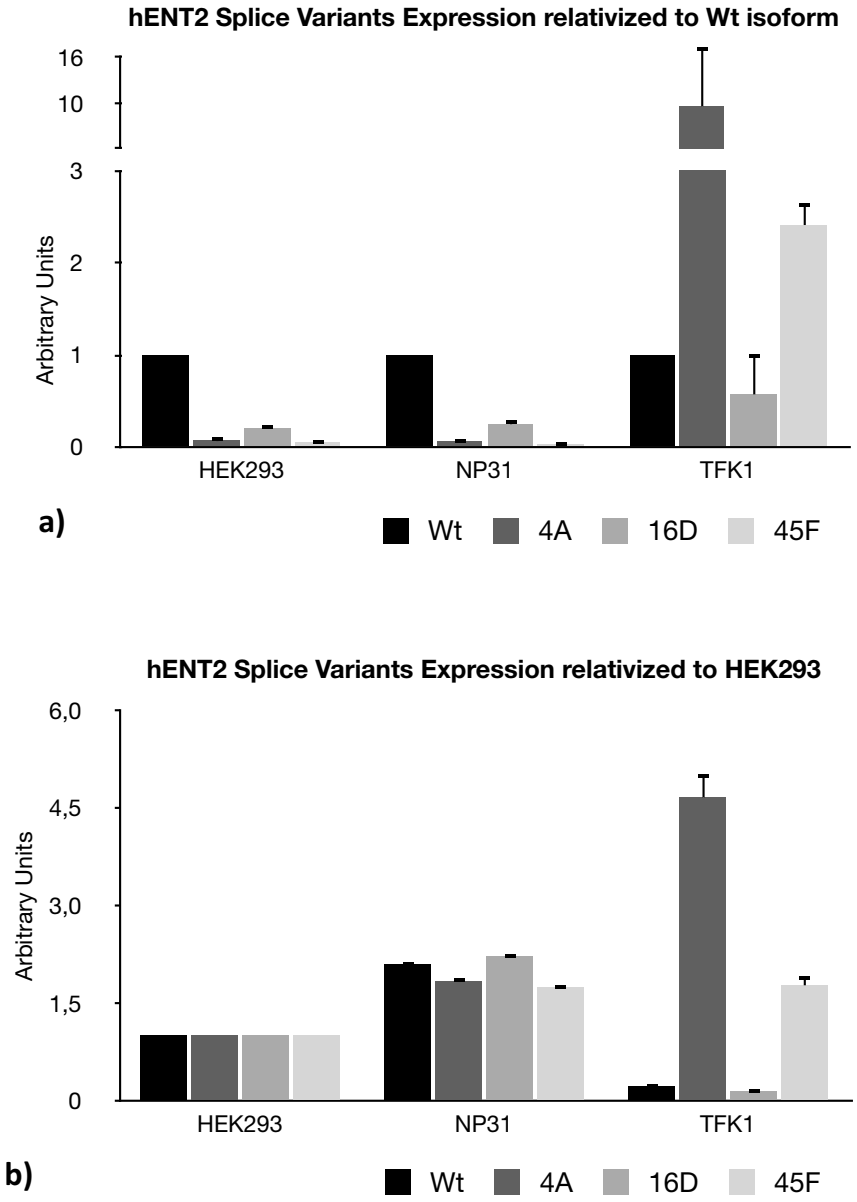

Figure 33. hENT2 mRNA expression detected by relative real-time PCR in three different cell lines. (a) Expression levels of hENT2 isoforms using the wt as a reference within each sample. (b) Expression levels of hENT2 isoforms using HEK-293 values as a reference for each transcript.

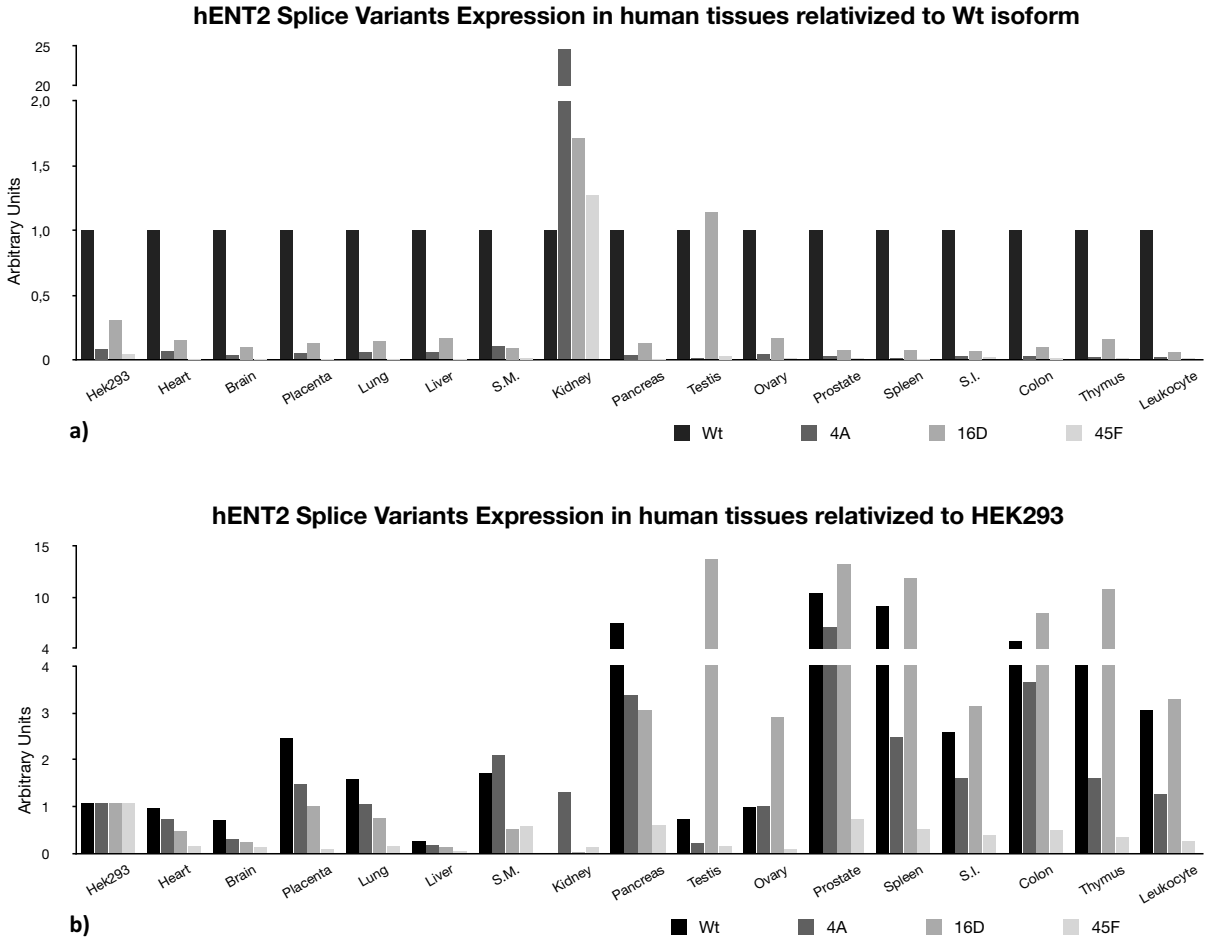

Figure 34. hENT2 mRNA expression in different human tissues (a) Expression levels of hENT2 isoforms using the wt as a reference within each sample. (b) Expression levels of hENT2 isoforms using HEK-293 values as a reference for each transcript. Samples: S.M = Skeletal Muscle; S.I = Small Intestine.

A second relative screening was performed using a commercial multiple tissue cDNA panel as a template. Samples are from human tissues free of genomic DNA, ensuring that all signals generated are from actual mRNA transcripts. In most of these samples, the wild type isoform is the predominant form except in kidney, where the three nuclear variants are more highly expressed than the wild type, and in testis in where the 16D nuclear variant has a similar expression to that of the wt isoform (figure 34a). When comparing samples to HEK-293 values (figure 34b), we noticed an interesting variability among samples. However, what stood out is the low expression levels in kidney compared to the cancer cell line HEK-293, whose origin is also human kidney. The different expression pattern of these two samples is very different, being the 16D variant the most present in the healthy kidney tissue while HEK-293 mainly expresses the wt isoform. These results suggest a different expression pattern depending on the cell growing conditions instead of being tissue-specific, coinciding with the results shown in figure 32.

15.6 DISCUSSION

For the last few years, alternative splicing has been proved to be one of the most important mechanisms in generating a large number of mRNA and protein isoforms from a low number of genes (Bracco & Kearsey 2003). In addition, it has been demonstrated that alternative splicing is also a mechanism of regulation changing the structure of transcripts and their encoded proteins. These changes determine the binding properties, intracellular localization, enzymatic activity, protein stability and post-translational modifications of a large number of proteins. Consequences of alternative splicing might range from a complete loss of function or acquisition of a new one to very subtle modulations (Stamm *et al*. 2005).

Alternative splicing occurs in a high percentage of transcripts derived from the whole genome and in most cases results in either proteins with a new function, localization or regulatory activity such as producing dominant negatives which block the activity of the wild type protein. New proteins generated by alternative splicing may

have lost a specific domain or residues that determine localization or are responsible for activity (Jang 2002; Vallejo-Illarramendi *et al*. 2005). Dominant negative variants are generated, in most cases, when the proteins affected interact with themselves as monomers. As a consequence, a truncated or non-functional protein might block or inhibit the functionality of the complex (J.-Y. Wu *et al*. 2003; Kitayama *et al*. 1999; Sairam *et al*. 1996; Y. Wang & Miksicek 1991; Watanabe *et al*. 1995). In both cases, there is a high risk of causing disease or dysfunction in the organism.

For nucleoside transporters, very few spliced variants have been described and their roles as novel functional transporters remains unclear. For the SLC28 family, the Concentrative Nucleoside Transporters, one spliced variant has been described for the CNT3 family member (Errasti-Murugarren et al. 2009). In this case, the novel protein does not reach the cytoplasmic membrane but it is retained at the endoplasmic reticulum, except when in a polarized system. This variant seems to be functional although its role inside the cell remains unclear.

In the case of ENTs more variants have been previously described. For mENT1, the first variant was described in 2000, and is a protein which is identical to the wild type isoform but with 2 extra amino-acids in the internal loop. This addition results in the protein acquiring a new putative CK2 phosphorylation site that makes the protein functional but less active than the wild type (Kiss *et al*. 2000). In 2008, a novel variant was found in which exon 11 had been skipped resulting in the protein missing the last three transmembrane domains. This protein reaches the plasma membrane and is active like the wild type but is less sensitive to the inhibitor NBMPR (Robillard *et al*. 2008). Intriguingly, no spliced variants have been described for hENT1 to date. In contrast, many polymorphic variants have been analyzed and it has been determined that there are cases where regulation by CK2 might be altered (Handa *et al*. 2001; Bone *et al*. 2007), or where the functionality as a nucleoside transporter is altered (Osato *et al*. 2003; Fukuchi *et al*. 2010; Kim *et al*. 2011).

ENT2 is the nucleoside transporter with the most spliced variants described so far. In 2005, a rbENT2 protein isoform was described which was missing 41 residues but which was still functional (S. K. Wu *et al*. 2005). Previously, in 2003, a hENT2 spliced variant was found, which possessed a 40 base pair deletion in exon 9 resulting in a 301 amino acid protein named hENT2A (Mangravite *et al*. 2003). This protein never reached the plasma membrane but stayed in an intracellular location within vesicular structures and consequently no transport activity was determined. The most interesting, due to its novel location, ENT2 spliced variant found to date is the HNP36 protein, which is a 36 KDa hydrophobic nucleolar protein described as a mitogenic delayed-early response gene (Williams & Lanahan 1995; Crawford *et al*. 1998).

Among all the spliced variants we cloned for the hENT2 gene we found the one previously defined as hENT2A, which is equivalent to our identified variant 22C, together with another similar isoform which we named as 17G. In both cases, the potential proteins would lack the last 5 transmembrane domains. Unlike the report from 2003 (Mangravite *et al*. 2003), we could not demonstrate protein synthesis of these variants either by immunoblotting or immunocytochemistry. We had the same results with variants P143 and P120, which would have produced proteins of 143 and 120 amino acids respectively. The results of Mangravite *et al*. (2003) are more similar to our results for the constructs 4D-HA and I16D-HA, where the protein is synthesized but retained intracellularly in a vesicular structure. Our interpretation of these results is that these proteins are artefacts which are a consequence of the overexpression of the constructs, resulting in the synthesis of misfolded or nonsense proteins which are retained in vesicles to be degraded instead of being expressed with a functional purpose. Considering that, we decided to continue further studies with the proteins located at the nuclear membrane since they seemed to be potentially more physiologically relevant.

When we compare our results relating to the nuclear variants with what has been published in the literature, the main discrepancy we found is the amino-acidic sequence of the HNP36 protein (Williams & Lanahan 1995; Crawford *et al*. 1998). This protein was predicted from the cDNA sequence X86681 which would result in a

product of 326 amino acids. However, current bioinformatic analysis programs designed to find Open Reading Frames (ORF) in a DNA sequence predict a protein of 336 amino acids for this sequence. Therefore, we predicted that HNP36 is a 336 amino acid protein, although this remains to be confirmed.

Interestingly, we not only cloned the X86681 isoform but another cDNA variant in which exon 4 had been skipped resulting in the same 336 amino acid protein. In addition, three other spliced variants were found, whose predicted ORFs gave an identical 302 amino acid protein, similar to our predicted HNP36 but which lacked the fourth transmembrane domain. The fact that several spliced variants would produce the same or similar proteins suggests a significant role of those proteins.

Immunocytochemical assays confirmed our hypothesis about the localization of these proteins since we observed that they co-localized with the NPC at the nuclear membrane. Our results also show a concentration of protein around the nuclear membrane, probably within the ER, indicating that even though the proteins are being over-expressed in an heterologous system, trafficking to nuclear membrane is finely regulated such that not all the protein is sent to the final location but some is retained in the ER. These data suggest that these proteins might have a specific role inside the cell and that the presence at the membrane is highly regulated.

Furthermore, immunoblotting confirmed the expression of the nuclear variants but not the other variants. The molecular weight, 36 KDa, of the 4A-HA protein coincides with that described for HNP36. Our novel hENT2 isoform of 302 amino acids has a predicted molecular weight of 32 KDa, and was therefore named as HNP32. In addition, we determined that the antibody against the ENT2 intracellular loop also recognizes those variants whether expressed heterologously or endogenously. BeWo cells were previously described to have ENT type proteins at nuclear membranes (Mani *et al*. 1998) and we demonstrated that they express both nuclear hENT2 isoforms HNP36 and HNP32 at readily detected levels. We confirmed that our results obtained by transient expression after transfection are reliable since NMD pathway assays determined those variants are not degraded by the machinery in that pathway but rather, they are translated into proteins.

Functional assays in which we transfected nuclear variants into HeLa cells did provide evidence of functional transporters which supported the proposal that these proteins are sorted to the nuclear membrane. When wild type isoform was transfected, we observed an increase of hENT2 activity at the same time that hENT1 decreased, both of them significantly. That suggests hENT activity is also highly regulated at the plasma membrane so when hENT2 increases, hENT1 decreases to compensate and produce minimal changes in the total hENT activity. Similar results had been previously reported in HUVEC cells, where it appeared that ENT1 and ENT2, despite being co-expressed, had an opposite regulation (Aguayo *et al*. 2005). However, we can not confirm that these variants do play a dominant negative role since HeLa cells do not show hENT2 endogenous activity to be blocked. Although the location of variants was confirmed to be at the nuclear membrane, they could also act as dominant negative proteins. Assuming the wild type protein interacts with any nuclear variant forming a kind of heteromer (figure 61 - appendix I), then the wild type ENT2 might be retained at the nuclear membrane instead of trafficking to the plasma membrane. As a consequence, nuclear variants would act as dominant-negative for the wild type hENT2. One example of this kind of regulation is the ghrelin receptor (GRLN-R), which is located at the plasma membrane as homodimer. This protein has a spliced variant isoform, GHS-R1b, that acts as a dominant-negative in such a way that it changes the localization of the wild type receptor by forming heterodimers GRLN-R/GHS-R1b and retaining the functional receptor at the nuclear membrane (P.-K. Leung *et al*. 2007). Further studies are needed to either confirm or discard this possibility regarding the hENT2 protein.

Interestingly, nuclear variants injected into oocytes seem to be sorted to the cytoplasmic membrane, what facilitated the transport assays. Preliminary results show hypoxanthine uptake when injected hENT2 wild type and also with the three nuclear variants, however nuclear variants rate is minor than the wild type apparently, either because they have less affinity to the substrate or are less expressed than the full-length protein. Interestingly, hENT2 wild type transports chloro-adenosine inside the cell but not the nuclear variants. Based on the structural determinants of ENTs described to date, transmembrane domains (TMD) 5-6 of hENT2 would be responsible

for nucleobase transport (Yao *et al*. 2002) and these are totally or partially conserved in HNP36 and HNP32. In contrast, the first TMD seem to be determinants for the 3'-deoxy-nucleotides transport (Yao *et al*. 2001), which are not conserved in HNP36 or HNP32 but are present in the wild type isoform. As expected, we saw a chloro-adenosine uptake through hENT2 wt but not by the nuclear variants. According to previous work, the first TMD are the ones responsible for the interaction of the transporter with its inhibitors like NMBPR or dilazep and dipyridamole (Visser, Baldwin, *et al*. 2005; Visser, Zhang, *et al*. 2005), however, we could not determine if this was the case for our variants.

Glycosylation of hENT1 affects its activity and binding to the inhibitor NMBPPR. Glycosylation of hENT2 influences its trafficking to the plasma membrane (Vickers *et al*. 1999) and hENT2 is heterogenously glycosylated on the residues Asn48 and Asn57 in the extracellular loop between TM1 and TM2. Loss of both glycosylation sites has been demonstrated to considerably decrease hENT2 sorting to the plasma membrane, although it does not affect its activity (Ward *et al*. 2003). These data support our observations that the nuclear variants lack the first transmembrane domains, including glycosylation sites and might explain, in part why these variants are trafficked to the nuclear membrane instead of the plasma membrane.

The presence of a functional nucleoside transporter at the nuclear membrane may be correlated with the presence of nucleoside metabolism enzymes which are translocated into the nucleus to convert nucleosides into nucleotides required for RNA / DNA synthesis. There is some evidence for the presence of CAD, aspartate carbamoyltransferase, inside the nucleus, where it is translocated to after being phosphorylated. CAD is a multifunctional protein that performs the three first reactions of *de novo* nucleotide synthesis which migrates into the nucleus in a cell cycle-dependent manner (Sigoillot *et al*. 2005). However there are no evidences of enzymes of the salvage pathway inside the nucleus.

hENT2 nuclear variants might be able to transport more than nucleosides into the cell nucleus. It has been demonstrated that hENT2 was responsible for the internalization of an intranuclear delivery vehicle for the transport of therapeutic macromolecules across the plasma and nuclear membrane, the anti-DNA antibody fragment 3E10 Fv (Hansen *et al.* 2007). Although they showed the presence of this peptide inside the nucleus, the only transport across the plasma membrane was proved to be carried out by hENT2, assuming it was also responsible for its nuclear translocation. This way, further studies need to be performed in order to understand the relevance of hENT2 at the nuclear membrane as an active transporter.

Since the role of alternative splicing in cell physiology involves multiple transcript expression and protein modulation at different levels, the regulation of splicing itself is finely controlled by many other factors and pathways. Changing alternative splicing patterns in response to an external stimulus is likely to be a physiological process performed by many cells. This regulation mainly controls the concentration and activity of splicing regulatory factors, either by de novo synthesis of those proteins, regulating their intracellular localization or phosphorylation. Hence, external stimuli like growth factors, cytokines, hormones or depolarization result in a change of splice site selection regulating the alternative splicing pattern as a part of the physiological adaptation of the cell (Stamm 2002).

In the case of hENT2, the role of growth factors in stimulating the expression of the nuclear protein HNP36 has already been described and, based upon our results, we suggest that induction might be conditioned to the regulation of alternative splicing phenomenon triggered by the same factors. We also show here that the splicing profile for hENT2 changes according to the growth conditions of the cells and the nature of either cell line or tissue.The fact that so many different mRNA isoforms produce the same functional protein at the nuclear membrane suggests that the alternative splicing process for hENT2 is highly regulated.

We could not demonstrate the translation or functionality of all hENT2 spliced variants and while they seemed to be widely expressed in different tissues, they do not

have a clear role in the cell (Mangravite *et al*. 2003). To understand the reasons underlying the existence of these non-functional isoforms, we propose that the cell uses the alternative splicing as a mechanism to regulate the expression of wild type hENT2 and its nuclear isoforms. The promoter region of a gene is in charge of the transcript generation, the same pre-mRNA for all the spliced variants. A second level of post-transcriptional regulation might be the checkpoint where the cell can decide to produce more transporter at the plasma or nuclear membrane according to the needs of the situation. Additionally, the situation might require less transporter so the cell might prefer to increase the production of non-translated or non-functional variants just to reduce the rate of wild type or nuclear isoform expressed.

Many recent studies describe a large number of molecules that modify the alternative splicing pattern in different models (Hagiwara 2005; Sumanasekera *et al*. 2008). In many cases, hENT2 plays a crucial role as a nucleoside derived anticancer drugs transporter. Often, the bottle-neck in these treatments is the internalization of the drug into the cell, specially in the case of CLL where hENT2 plays a crucial role for drug uptake (Molina-Arcas *et al*. 2003; Pastor-Anglada *et al*. 2004). Therefore, an understanding of the pharmacological modulation of hENT2 splicing profile in cancer cells, with the aim of optimizing the expression of the transporter at the cytoplasmic membrane, is an important goal. A deeper understanding of this form of regulation of ENT2 may allow us to increase the drug uptake rate and improve the therapy. This is particularly relevant because it has been frequently described that in cancer cells the pattern of alternative splicing undergoes considerable change promoting cell proliferation (Tazi *et al*. 2009; Venables *et al*. 2009; Al-Ayoubi *et al*. 2012; Das *et al*. 2012). Since HNP36 was detected as a mitogenic response gene it seems it might be involved in the cell proliferation process. So, we raise the possibility the hENT2 expression profile varies considerably in cancer cells.

16 STUDY OF PHOSPHORYLATION STATUS OF HENT2 AND THE ROLE OF PHOSPHORYLATION IN TRAFFICKING

16.1 PREVIOUS FINDINGS

Previous experiments of immunocytochemistry performed with the hENT2 wt HA-tagged construct during the study of its splice variants, gave us some evidence that the full-length protein was located just under the plasma membrane rather than being inserted in it. As shown in figure 35, hENT2 wt (green) does not co-localize with the plasma membrane (red) but seems to be present just below it. Interestingly, it does not seem that hENT2 wt is clustered in vesicles or in specific sub-membrane regions but rather, is widely extended close yo the plasma membrane.

To confirm whether hENT2 wt is located at the sub-membrane region we performed biotinylation assays treating intact HeLa cells with biotin, a molecule that attaches covalently to lysine residues on proteins at the plasma membrane. Once we lysed the cells, we separated the intracellular fraction from the membrane fraction using streptavidin beads. Streptavidin recognizes and binds biotin, together with the proteins present at the plasma membrane attached to biotin. Fractions obtained were separated by SDS-PAGE and the presence of hENT2 was determined by immunoblotting using a commercial hENT2 antibody.

In this experiment we used two different batches of HeLa cells, one without endogenous hENT2 activity (lane 1) and another with endogenous hENT2 activity (lane 2), to detect differences in the protein patterns. As shown in figure 36, what a priori we thought was a single band at 54 KDa is in fact a doublet where the smallest band (‡) is present at the plasma membrane while the largest (#) remains in the intracellular fraction. Coinciding with hENT2 activity of the samples, those cells with active hENT2 (2) show higher levels of the protein of 54 KDa present at the membrane (‡) while the levels of protein for the sample with no hENT2 activity (1) are lower. The band at 45 KDa (✱) is present at similar levels in both preparations suggesting it is not correlated with functional hENT2.

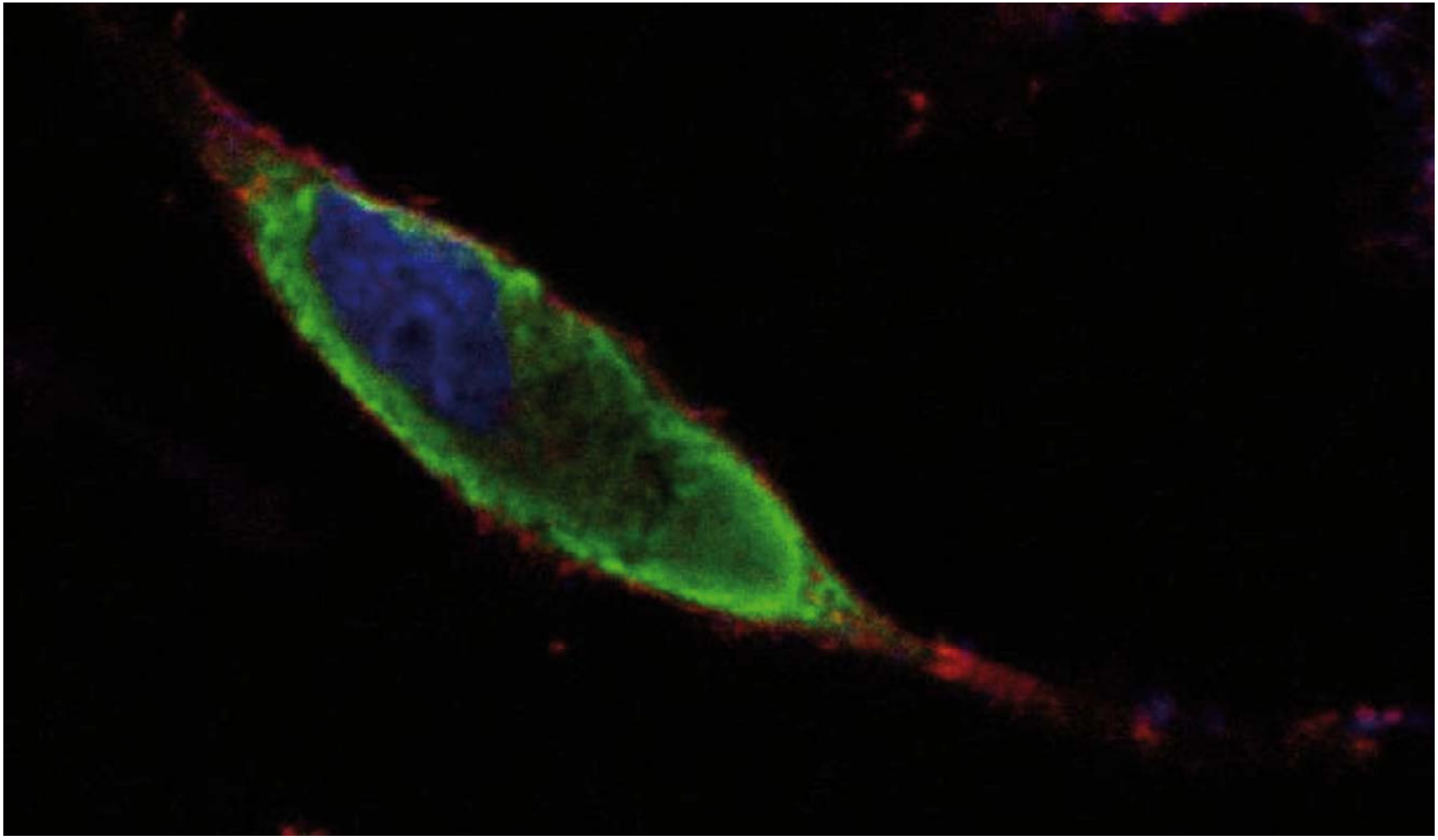

Figure 35. Immunocytochemistry of HeLa cells transiently transfected with hENT2 wt HA-tagged construct. HeLa cells expressing transfected F10C-HA construct, which generates hENT2 full-length protein, is seen in green located below the plasma membrane Plasma membrane is labelled with WGA (red) while the nucleoplasma is stained with DAPI (blue).

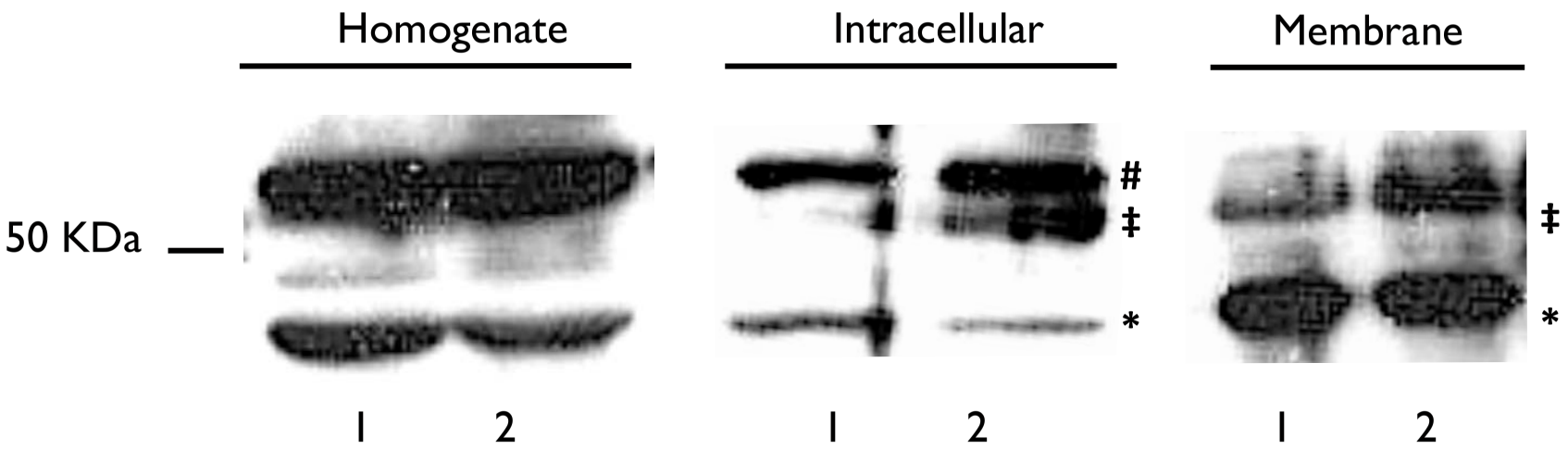

Figure 36. Immunoblotting of different protein fractions obtained from HeLa cells after Biotinylation. Protein fractions obtained after Biotin-Streptavidin extraction from HeLa cells were anaylzed using an anti-hENT2 antibody (Lane 1 = HeLa cells with no endogenous hENT2 activity, lane 2 = HeLa cells with endogenous hENT2 activity).

To date we cannot explain the differences of weight between bands at 54 and 45 KDa. However, since the difference between the doublet at 54 KDa is small, we propose that the doublet may represent hENT2 variants with different phosphorylation profiles with the non-phosphorylated (lower molecular weight - ‡) isoform being present at the plasma membrane.

Based on these antecedents, we decided to study the phosphorylation status of hENT2 in more depth and determine the effects of this kind of regulation on hENT2 localization and/or function.

16.2 BIOINFORMATIC ANALYSIS OF hENT2 PUTATIVE PHOSPHORYLATION SITES

The ENTs intracellular loop between TMD 6 and 7 is the best candidate for a region of regulation and protein-protein interactions since is the largest part of the protein that is accessible to cytoplasmic factors. Therefore, we designed two different constructs containing the mouse and human ENT2-loop sequence preceded by 6 histidines (His) and a ubiquitin (Ubq) sequence (figure 37a). These constructs were over-expressed in bacteria and ENT2-loop peptides produced. The His tag is needed for the peptide purification using nickel-column affinity, and the advantage of fusing our peptide to Ubq is the dramatic increase in yield of protein production. Complete sequences are included in the appendix I - table 22 and table 23. Constructs were ordered generated in pJExpress401-T5-kan expression vector by DNA 2.0[G].

Analysis of mouse and human ENT2 by NetPhosK[H] identified putative phosphosites and directed which kinases we would test in further experiments. Results are shown in figure 37b. Similar constructs were generated for ENT1 (Coe *et al.* unpublished). We compared these sequences with ENT2 since protein similarity between ENT1 and ENT2 is around 50%. For the four peptides, three kinases stood out as potential candidates to phosphorylate ENT1 and ENT2: PKA, PKC and CKII.

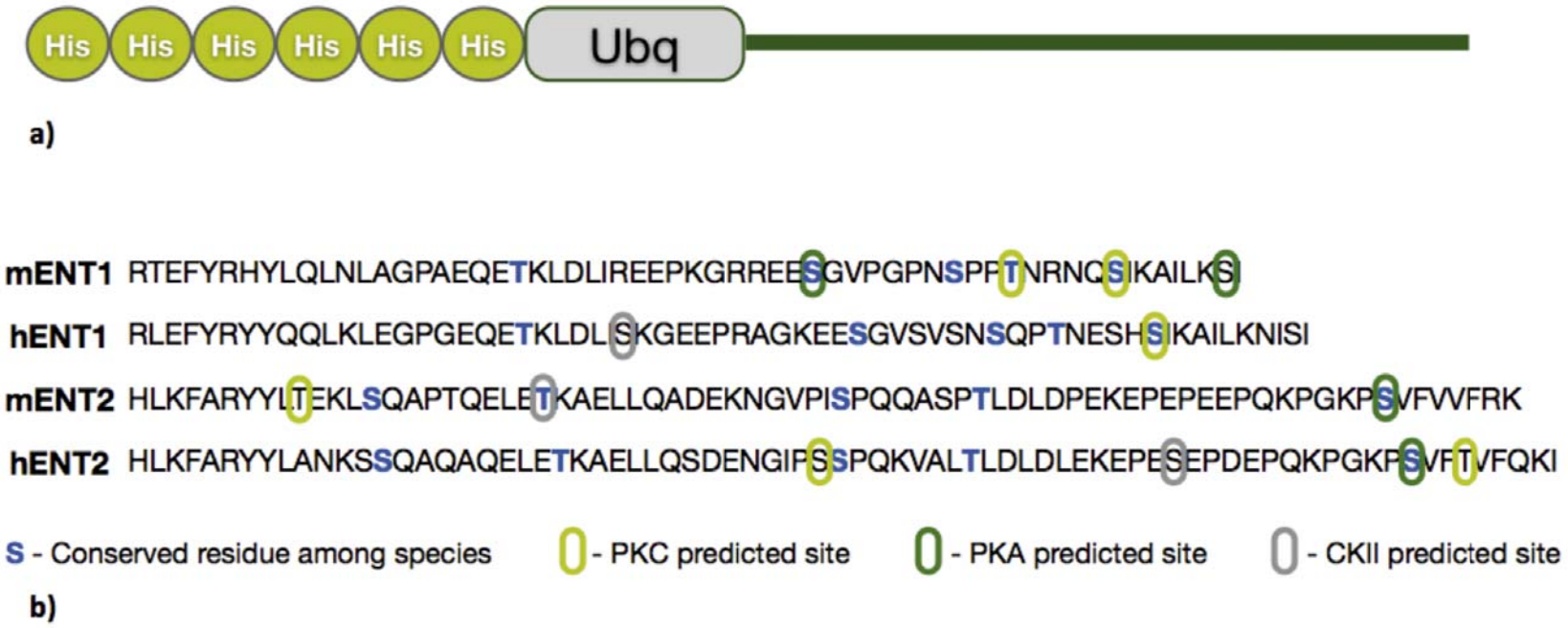

Figure 37. ENT-loop peptide design and NetPhosK 1.0 analysis. (a) Structure of the His/Ubiquitin tagged ENT-loop constructs designed. Six histidine (His) residues followed by ubiquitin (Ubq) and the ENT-loop sequence. (b) Computational analysis of ENT-loop with the predicted consensus targets sites with PKA, PKC and CKII. Those residues conserved among species are highlighted in blue.

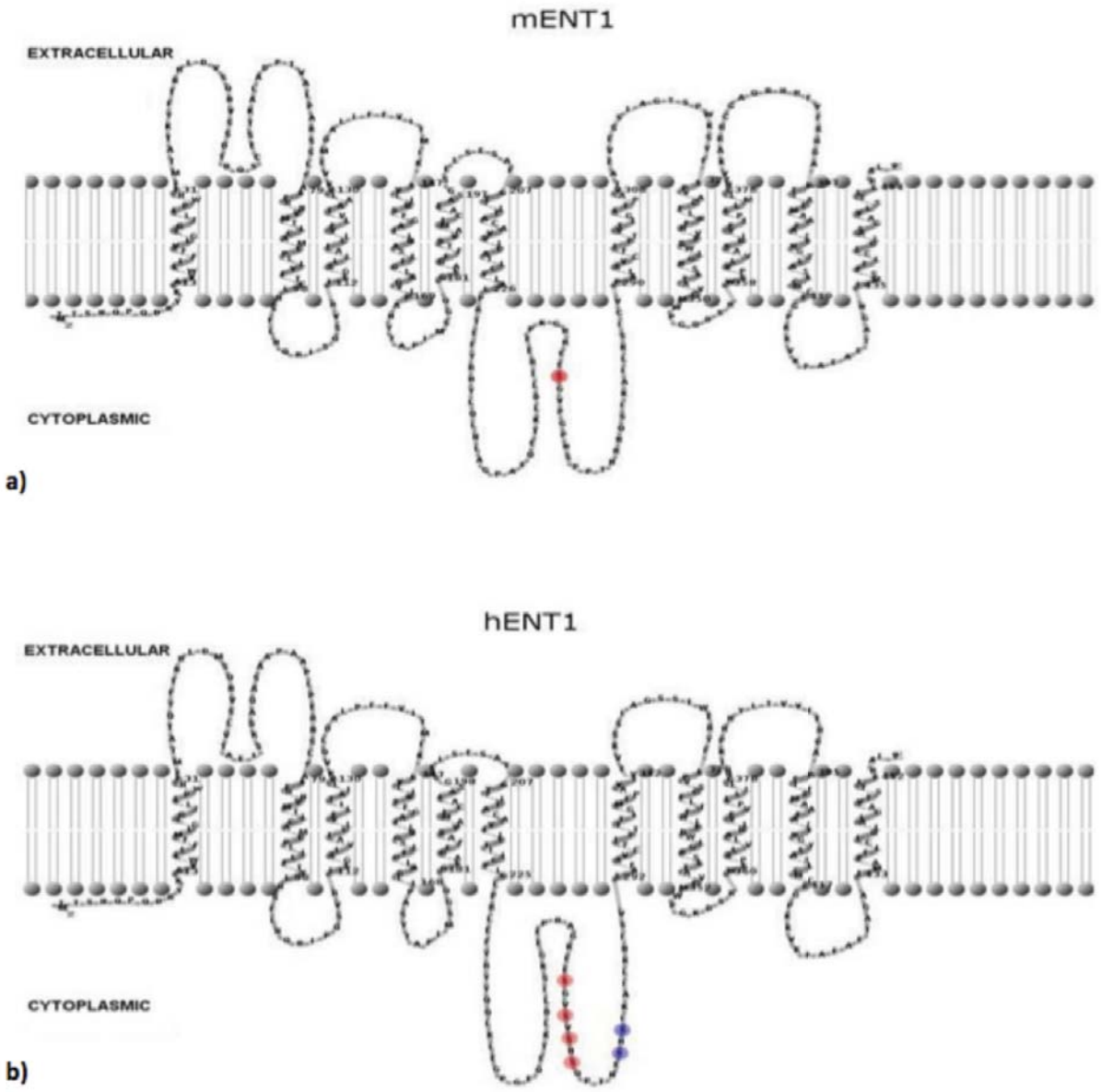

Figure 38. mENT1 and hENT1 phosphosites. Proposed 2D topologies of mENT1 and hENT1 with the confirmed phosphosites shown in red. (a) mENT1: Ser264 was the only serine in the large intracellular loop that was shown to be phosphorylated by PKA *in vitro*. (b) hENT1: Ser266, Ser269, Ser271, Ser273 and Ser279/281 were confirmed as being phosphorylated by PKA *in vitro*. Ser279 and Ser281 are highlighted in blue, since both have been implicated, but not yet confirmed, as being phosphorylated. *Taken from MSc thesis, Pedram Mehrabi 2010, with permission*.

Previous research in Dr. Coe's lab analyzed the phosphorylation status of ENT1 and described the phosphorylation by PKA and PKC (Reyes *et al*. 2011) although specific target residues were not defined. Following studies by mass spectrometry, specific target residues have now been identified as being phosphorylated by PKA *in vitro* and confirmed them in an *ex vivo* model (data not published). Those residues are serine 264 for mENT1, and serines 266, 269, 271, 273 and 279/281 (only one of them is phosphorylated but it remains unclear which one) for the case of hENT1 (figure 38).

16.3 *IN VITRO* PHOSPHORYLATION ASSAYS OF ENT2-LOOPS WITH RADIO-LABELED ATP

We performed *in vitro* phosphorylation assays with radio-labeled ATP to determine which kinases phosphorylate the h/mENT2-loop. The kinases selected for testing were the main three kinases obtained by the computational analysis: PKA, PKC and CKII. We also included Ca^{2+}/Calmodulin-Kinase II (CamKII) in our study since recent work from Dr. Coe's lab has found a clear link between ENT1-loop and calmodulin (data not published). In these experiments we used Histone H1 (H1) of 30 KDa as a positive control for PKA, PKC and CKII. Following the *in vitro* reactions, we separated the samples by SDS-PAGE and detected the signal by auto-radiography. Assays were performed according to the protocol previously described in the materials and methods section.

The in vitro phosphorylation assay (figure 39) showed positive results for CKII in both mouse and human ENT2. Negative controls (i.e. those lacking enzyme - lanes 1, 3 and 5) did not show any signal. The positive control with H1 showed a pattern of three bands, of which we could only identify the band around 30 KDa (‡) as corresponding to the H1 protein, together with CKII which auto-phosphorylates. This pattern was repeated at lower intensity in lanes 4 and 6, confirming it was the auto-phosphorylated CKII kinase. Both human and mouse ENT2-loops showed a radio-labeled signal at approximately 17 KDa (✱) which corresponds to the size of the loop.

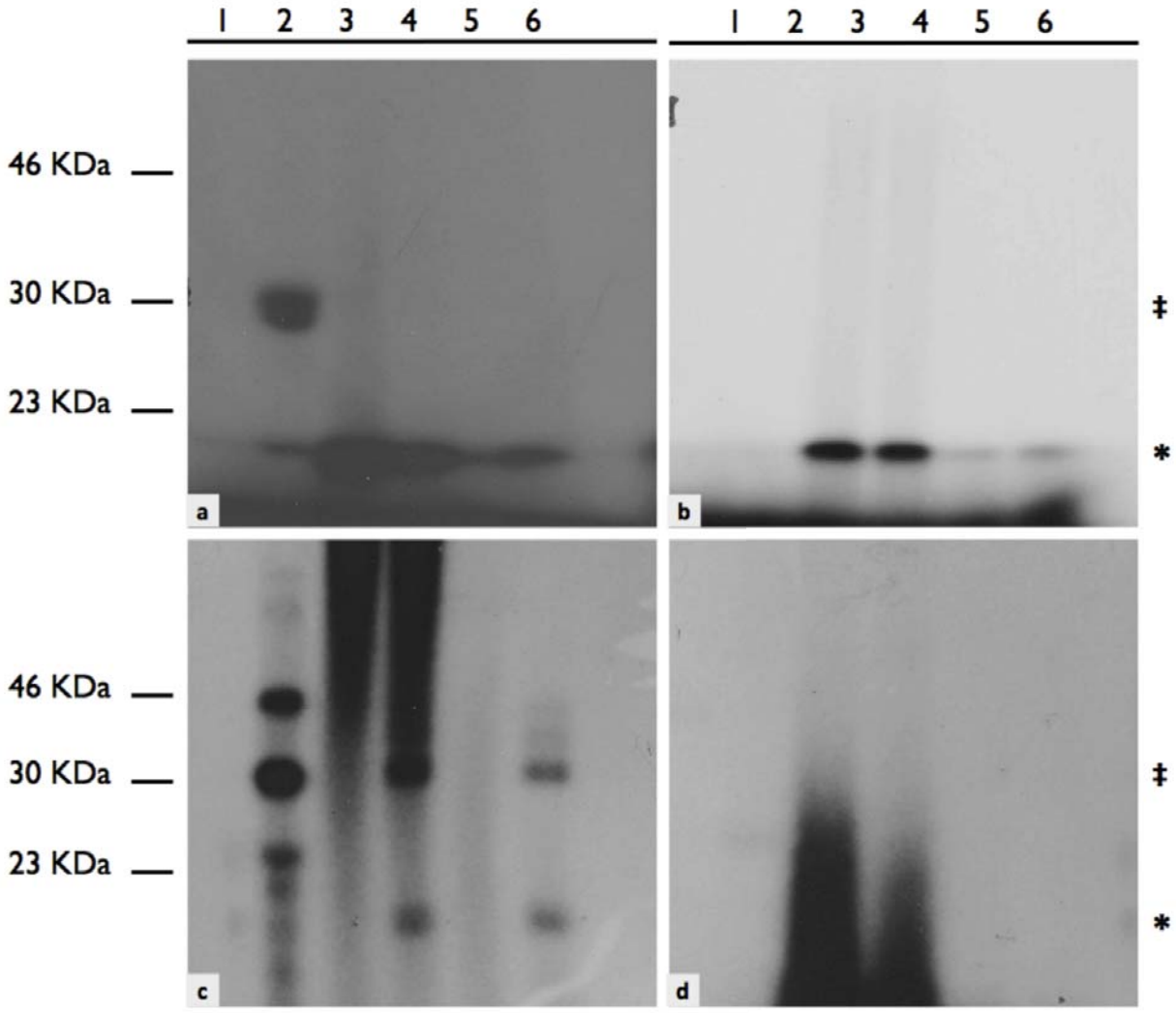

Figure 39. *In vitro* phosphorylation of h/mENT2-loop using radio-labeled ATP. Samples used in these assays: H1 without (1) and with (2) enzyme; hENT2-loop without (3) and with (4) enzyme; mENT2-loop without (5) and with (6) enzyme. Kinases tested: PKA (a), PKC (b), CKII (c) and CamKII (d). Positive results were obtained for CKII were the band shown at 30 KDa corresponds to H1 and CKII auto-phosphorylated (‡). The band around 17 KDa corresponds to the ENT2-loop (✱). PKA results were positive for H1 and mENT2-loop but the negative control of hENT2 shown an intense band, like the case of PKC, invalidating the positive results. Negative results were obtained for CamKII.

Therefore, we concluded CKII does phosphorylate both the hENT2 and the mENT2 loop *in vitro*. PKA also appeared to phosphorylate H1 (30kDa signal - ‡) and mENT2 (17 KDa - ✱) corresponding to the mENT2. There is band in the negative control of mENT2. Negative controls for H1 and the mENT2-loop showed no labelling. However, there was a significant signal for the hENT2-loop negative control. We could not explain the appearance of that band which was repeated in the case of PKC but not for CKII or CamKII. Unfortunately, we cannot rely on the positive bands found for hENT2 with both PKA and PKC since the negative control showed specific labelling. PKC results did not show any other signal even though H1 is a known target for that kinase and we detected PKC-phosphorylated H1 by MS in later analysis. CamKII did not show any positive results, neither for H1, which actually is not a positive control for CamKII.

16.4 MASS SPECTROMETRIC ANALYSIS OF ENT2-LOOP PHOSPHOSITES AFTER *IN VITRO* PHOSPHORYLATION ASSAYS

To determine which phospho-amino sites are present in the ENT2-loop, we performed the same reactions as before using unlabeled ATP and analyzed the samples by MRM/MS. The mass spectrometry analysis has not, to date, been successful in identifying phosphosites in the hENT2-loop. Despite ubiquitin is always detected indicating that the hENT2 peptide is definitively present, it has not been possible to obtain sufficient coverage of the hENT2-loop sequence to identify specific phospho-amino sites. However, the sensitivity of the analysis was sufficient for the mENT2-loop and specific residues targeted by PKA and CKII were identified. No phosphosites were found in mENT2-loop following incubation with PKC and CamK while the H1 protein was clearly phosphorylated suggesting that the enzymes were functional and that the ENT2 loop is not a target of either kinase.

Phospho-amino sites for the mENT2-loop are shown in figure 40 together with the residues previously identified for mENT1 and hENT1 loops. MRM/MS results shown a phosphosite in Thre223 after CKII *in vitro* phosphorylation and also Ser227 phosphorylated by PKA. Thre223 is not conserved in the human peptide so we do not know where CKII would phosphorylate hENT2-loop if it does. However, Ser227 is conserved among species, therefore we propose that hENT2 could also be phosphorylated by PKA at the conserved residue, which would be Ser228.

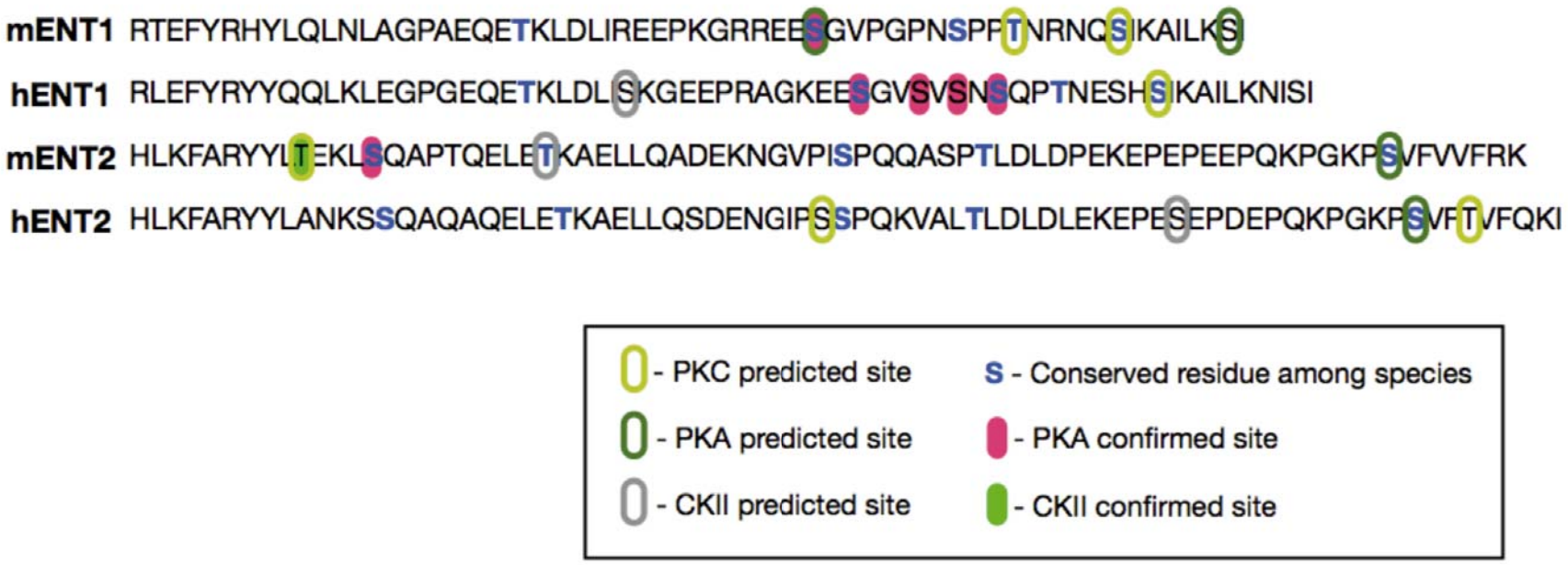

Figure 40. ENT-loops phosphosites confirmed by mass spectrometry. Sequences of the four ENT-loops analyzed by Mass Spectrometry after *in vitro* phosphorylation with different kinases. Confirmed serines phosphorylated by PKA *in vitro* are highlighted in red. Threonine confirmed to be phosphorylated *in vitro* by CKII is highlighted in green.

Since the data obtained by the mass spectrometry analysis are still preliminary, further experiments need to be done in order to improve the detection of specific phosphosites (such as those suspected to be targeted by CKII) in the hENT2-loop.

16.5 EFFECT OF PKC ACTIVATION BY PDD TREATMENT ON hENT2

As previously explained, there is a lot of evidence for regulation of ENTs by kinase-dependent pathways. After we confirmed ENT2 was phosphorylated *in vitro* by CKII, we studied the role of phosphorylation in ENT2 physiology inside the cell. Despite ENT2 phosphorylation by PKC has not been confirmed yet, we cannot discard the possibility of ENT2 being regulated by PKC based on previous work.

PDD (Phorbol 12,13-didecanoate) strongly stimulates the action of PKC and has been previously described to increase transport activity presumably by activating hENT2 in a neuronal model (G. Lu *et al*. 2010). To determine if activation of PKC affects ENT2-dependent uptake in other cell types, we treated HEK-293 cells with PDD (500nM, 10 min) and measured chloro-adenosine uptake via hENT1 and hENT2. Chloro-adenosine uptake via hENT1 was significantly decreased after PKC activation, whereas hENT2-dependent uptake did not seem to be affected by the treatment (figure 41).

To determine if a PKC-dependent pathway regulates hENT2 trafficking to the plasma membrane, we also performed immunocytochemistry (ICC) assays using the hENT2 HA-tagged construct. As a membrane marker we used hENT1-FLAG, since both tags are different we could use different non cross-reactive antibodies to detect them separately. HEK-293 cells were co-transfected with both constructs according to the protocol previously described. After 48 hours of expression, we treated the cells with PDD (500 nM, 10 min) and fixed them with paraformaldehyde followed by the ICC protocol described in the materials and methods section (figure 42).

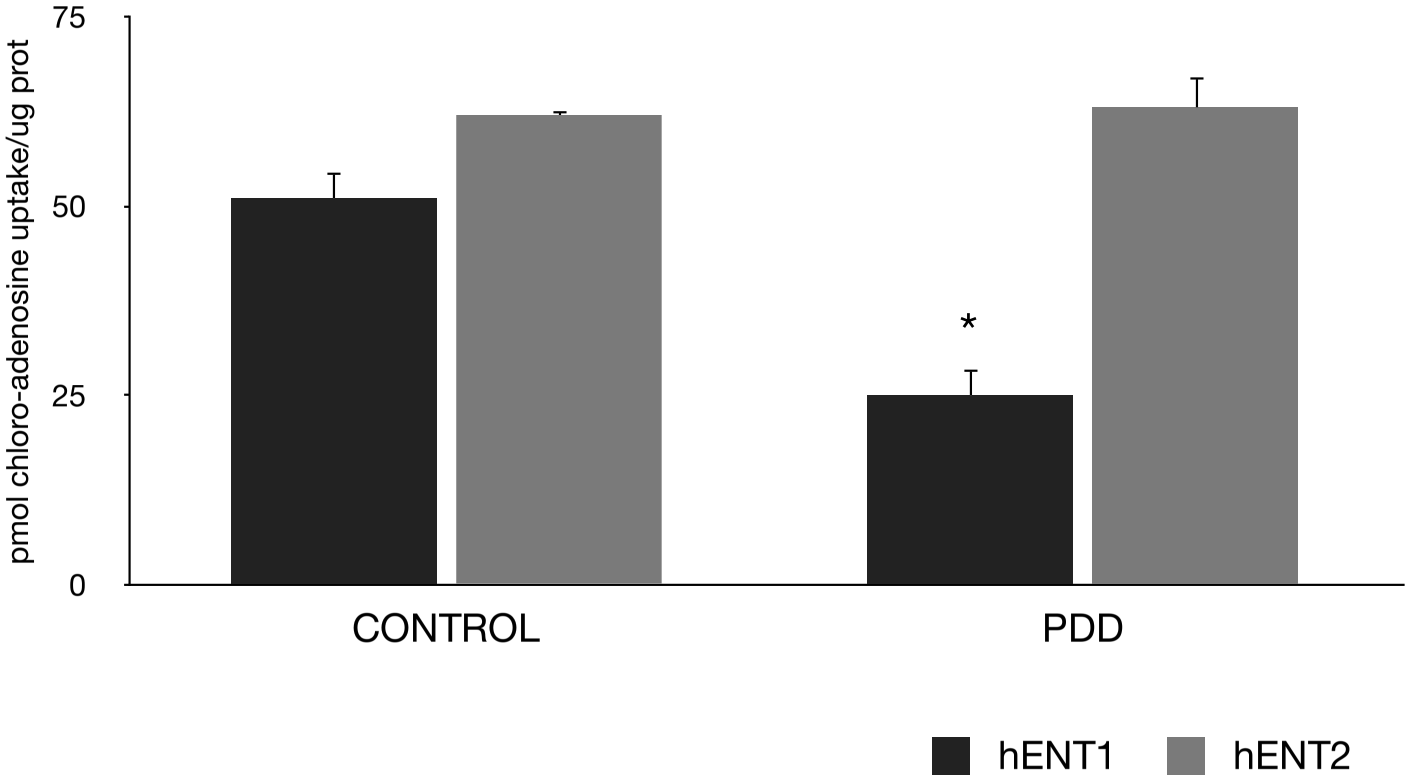

Figure 41. Effect of PKC activation on hENT2 activity. HEK-293 cells treated with PDD (500 nM, 10 min.) to activate PKC and measured chloro-adenosine uptake via hENT1 and hENT2. hENT1-dependent chloro-adenosine uptake is significantly decreased by PKC activation while uptake via hENT2 seems not to be affected by the treatment. Results show the mean of three independent experiments (n=3) with standard deviation represented by bars. Statistics: * = $p<0.05$

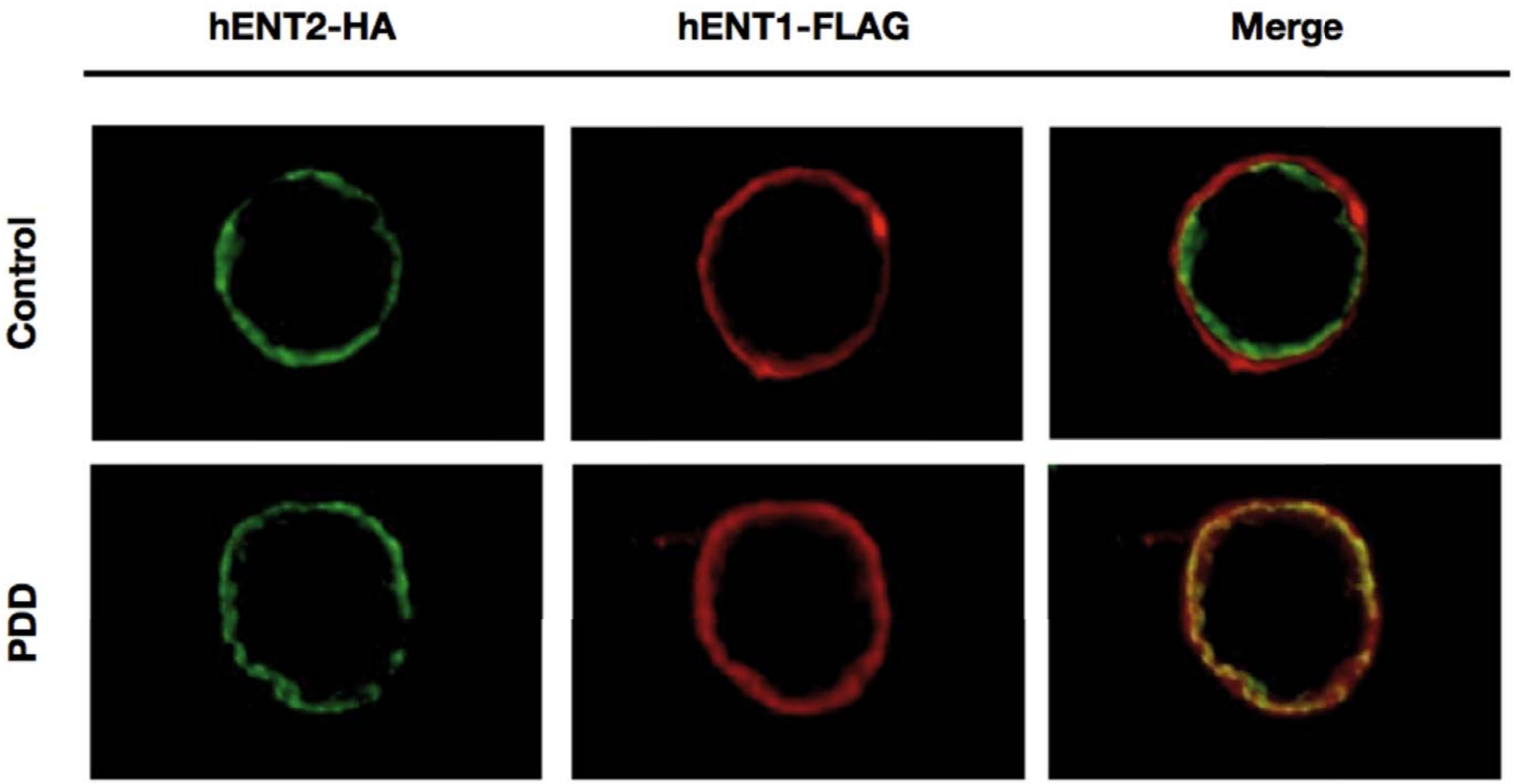

Figure 42. Effect of PKC activation on hENT2 trafficking. HEK-293 cells transfected with hENT2-HA and hENT1-FLAG constructs were treated with PDD to activate PKC. In unstimulated conditions, hENT2 is predominantly present under the membrane (green) while hENT1 is localized at the plasma membrane (red). Following PKC stimulation, hENT2 co-localizes with hENT1 at the membrane (yellow).

Control cells treated with DMSO express hENT1 (red) at the plasma membrane while hENT2 (green) is present just below the plasma membrane, in a sub-membrane region. After PDD treatment and presumably consequent PKC activation, hENT2 is trafficked to the membrane and co-localizes with hENT1 (yellow).

To confirm the results obtained by ICC, we conducted and analyzed if there was any significant change in the hENT2 protein pattern after PDD treatment. As shown in figure 43b, ENT2 (✱) at 46 KDa increases significantly in intensity after PKC activation. The smallest band of the doublet at 54 KDa (‡) also seems to increase after the treatment but not as dramatically as the band at 46 KDa. These bands correlate with those identified to be at the plasma membrane by biotinylation assays (figure 43a) confirming that PDD appears to trigger hENT2 translocation to the plasma membrane.

16.6 DISCUSSION

Phosphorylation is the main mechanism whereby a cell can have rapid and reversible regulation. Many enzymes, receptors and transporters switch their status from active to inactive due to the conformational change in their structure caused by de/phosphorylation. Previous work has studied the involvement of phosphorylation in the regulation of ENTs, however the presence and physiological relevance of this phenomenon still remains unclear. PKA, PKC and CKII are likely candidates in the regulation of ENTs although it has not been determined yet if there is direct phosphorylation of ENTs. Recently, it has been proved that direct phosphorylation of ENT1 by PKA and PKC occurs *in vitro* (Reyes *et al*. 2011) and also *ex vivo* (data not published). However, further studies are needed to fully understand the role of phosphorylation on ENTs.

In this chapter we demonstrated the existence of *in vitro* phosphorylation of both human and mouse ENT2 by CKII, and also by PKA for mouse ENT2 using an *in vitro* kinase assay. These results were later confirmed by MRM/MS analysis for the mouse sample, revealing the specific residues phosphorylated in each case: Thre223 by CKII and Ser227 by PKA. However, more assays need to be performed to have a better coverage of the hENT2-loop and define the specific phospho-sites of the human protein.

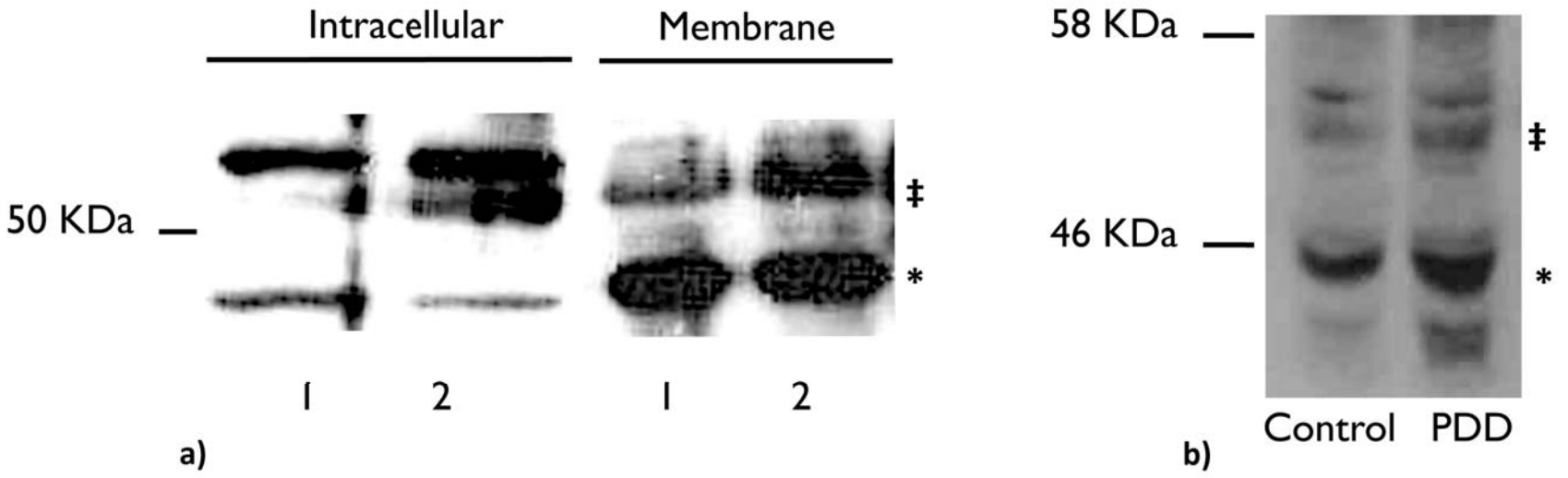

Figure 43. Comparison of HeLa protein fractions obtained after biotinylation versus total protein extracted from HEK-293 cells treated with PDD. (a) Intracellular and plasmatic membrane fractions from endogenous HeLa cells protein after biotin-streptavidin extraction incubated with antibody anti-hENT2 (Lane 1 = HeLa cells with no endogenous hENT2 activity, lane 2 = HeLa cells with endogenous hENT2 activity). The smaller band of the doublet above 50 KDa (‡) appears to be present at the membrane fraction while the largest band remains intracellular. The band around 46 KDa (✱) is also located mostly at the membrane. (b) Total protein extraction of HEK-293 cells treated with PDD (500 nM, 10 min.) to activate PKC. The two bands previously determined to be located at the plasma membrane seem to be increased after treatment, despite the most significant increase is in the 46 KDa band.

CKII is ubiquitously expressed and regulates many substrates involved in all kinds of dynamic cellular functions. Paradoxically, despite the central role of CKII in a large number of cellular signalling pathways, its own activity appears to be unregulated since it is constitutively active. Therefore, it has been suggested that changes in the phosphorylation status of CKII substrates would depend on regulated dephosphorylation (Pinna 1990). In contrast, PKA is a highly regulated kinase which is activated by cAMP and down-regulated via a feedback mechanism through phosphodiesterases.

Although we could not definitively demonstrate direct phosphorylation of ENT2 by PKC, we analyzed the effects of PKC activation on both hENT1 and hENT2 activity and localization. Treatment with PDD, a PKC activator, showed a change in the location of hENT2 from a sub-membrane region to the plasma membrane. Contrary to our expectations, this translocation to the membrane did not lead to any increase in hENT2-dependent uptake but it did lead to a significant decrease in hENT1-dependent uptake. When we analyzed the protein pattern of hENT2 by SDS-PAGE following PDD treatment, we observed higher intensity of banding of those bands supposed to be at the membrane, according to biotinylation assays. Our results differ from previous studies where PKC activation by PMA led to an increased hENT1 activity in a cellular model without hENT2 activity (Coe *et al*. 2002). Another study described how PDD treatment increased hENT2 activity in a neuronal model without hENT1 activity (G. Lu *et al*. 2010) demonstrating how flexible and variable regulation of ENTs can be.

The observed effects of PKC activation does not necessarily mean that hENT2 is a direct substrate of the kinase. In fact, direct phosphorylation of hENT2 by PKC has not yet been proved. However we have obtained evidence that phosphorylation of ENT2 by CKII might exist *in vivo*. The protein pattern obtained after biotinylation suggests that the smaller band of the 54 KDa doublet may be the form of the protein present at the plasma membrane while the largest band would be the form which is retained intracellularly. If the difference in the weight of these two bands is due to phosphorylation, then the non-phosphorylated isoform would be the active form and is located at the plasma membrane. As we previously explained, CKII is constitutively

active so if hENT2 were a CKII substrate, the transporter could probably be constitutively phosphorylated. As a consequence, regulation of hENT2 activity would be particularly sensitive to phosphatases instead of kinases, promoting the active isoform at the membrane depending on the cell necessities. The trafficking and "activation" might be a phosphatase dependent event.

Based on our results, we propose the existence of two different populations of hENT2, one located at the sub-membrane region and the other one at the plasma membrane. Translocation to the plasma membrane is regulated by the PKC signalling pathway. However, translocation to the membrane would not have any specific effect on hENT2 activity since there are two different isoforms at the membrane, one apparently related with active hENT2 (54 KDa), and another one non-correlated with the transport activity (45 KDa). Although we hypothesised the difference between the bands in the doublet might be due to their phosphorylation status, we currently cannot explain the difference between the bands at 54 KDa and 45 KDa. There may be some differences in glycosylation although we think that is quite unlikely since it has been previously described the involvement of glycosylation in the ENTs trafficking to the plasma membrane (Vickers *et al*. 1999; Ward *et al*. 2003). Therefore, ENT2 non-glycosylated (45 KDa) would be less present at the plasma membrane that the protein glycosylated (54 KDa) unlike our results show. Another possibility is that hENT2 activity is regulated by cleavage, as it happens for the case of the GABA transporter (Gomes *et al*. 2011), the ENaC channel (Hamm *et al*. 2010) or the glycine transporter GlyT2, whose cleavage is regulated by phosphatases (Baliova *et al*. 2004). We propose that the isoform which is capable of functioning as a nucleoside transporter is the full-length un-phosphorylated protein of 54 KDa approximately, whereas the band shown at 45 KDa could be an hENT2 isoform inactivated by cleavage. Further experiments need to be done to understand the origin of this 9 KDa weight difference.

A recent study described a disrupted localization of hENT2 at the plasma membrane while protein expression and mRNA levels were not altered, supporting the idea that hENT2 is localised intracellularly. The concept of a hENT2 sub-membrane population is novel for nucleoside transporters although it has been previously

described for other membrane proteins such as ABC transporters in hepatocytes and other transporters or potassium channels in myocytes (Kipp & Arias 2002; Roma 2008; Sathe *et al*. 2011; Balse *et al.* 2009). In all these examples, the researchers describe the presence of a population of vesicles in the sub-membrane space that undergo rapid recycling which is finely regulated. Taken together, our hypothesis is that hENT2 is localised at the plasma membrane or in vesicles below the membrane generating a rapid system to send or remove hENT2 proteins from the membrane according to the cell needs.

17 LARGE-SCALE SCREENING FOR hENT2 INTERACTIONS USING MEMBRANE YEAST TWO-HYBRID TECHNIQUE (MYTH)

17.1 BAIT GENERATION AND VALIDATION BY N_{UB}G/I CONTROL TEST

The Two-Hybrid technique is commonly used to identify putative partners for proteins providing information about their biological function. Membrane proteins are of particular interest because of their role in disease and as pharmaceutical targets. However, due to their hydrophobic nature the classic Two-Hybrid technique could not be applied to full-length membrane proteins (Huber-Ruano *et al*. 2010; Carneiro *et al*. 2002). Recently, a new version of the Two-Hybrid technique has been developed by Dr. Staglar which allows this principle to be applied to membrane proteins. This technique is known as the Membrane Yeast Two-Hybrid (MYTH). A large-scale screen for hENT2 interactions using the MYTH technique identified novel putative partners of hENT2. These candidates will provide us with relevant information about the biology of hENT2.

The first step of the MYTH screening is to clone the gene that encodes our protein of interest, hENT2, into an appropriate vector to generate the bait plasmid. The bait must have its intracellular terminus attached to the ubiquitin C-terminal (C_{ub}) moiety together with the transcription factors for the reporter genes and all the component must be in frame. hENT2 is a transmembrane protein with a cytosolic N-terminus and an extracellular C-terminus. Therefore, we cloned hENT2 full-length cDNA sequence into the pTLB-1 vector so the C_{ub} fraction would be in frame just before the intracellular hENT2 N-terminal (figure 44).

To clone hENT2 into the pTLB-1 vector first we inserted PstI and StuI restriction enzyme sites at both ends of hENT2 open reading frame (ORF), using a PCR technique according to the protocol described in the materials and methods section. We digested both hENT2 and the vector with these enzymes and ligated them in order to incorporate our gene into the vector. The product generated by this cloning process was validated by sequencing to ensure there were no mutations in the hENT2 cDNA. The next step was to validate our generated hENT2-bait plasmid as an appropriate bait for the large-scale screening using the N_{ub}I/N_{ub}G test.

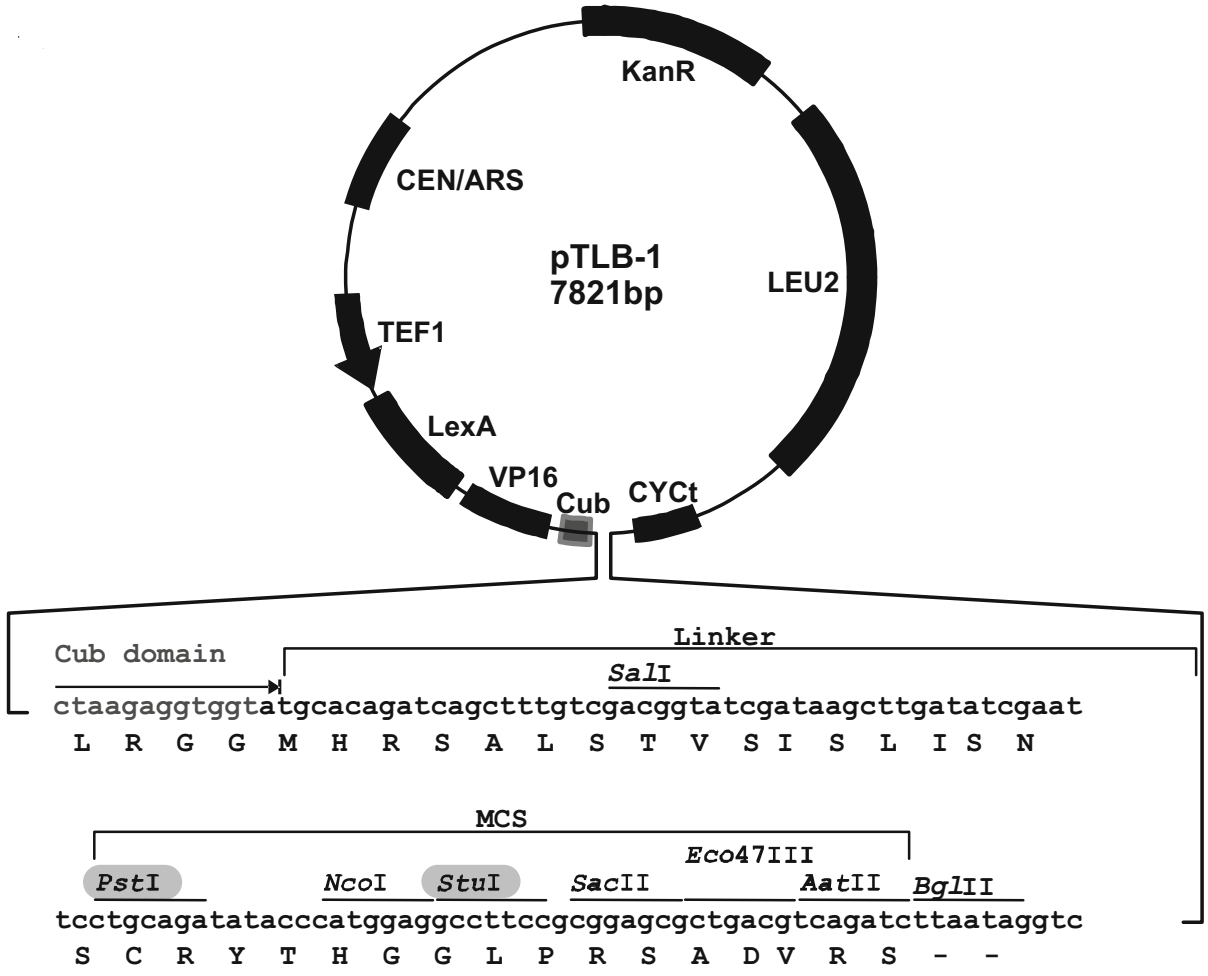

Figure 44. pTLB-1 vector. pTLB-1 vector contains the sequences for LexA and VP16 transcription factors followed by the C_{ub} domain and a multi-cloning site (MCS). We cloned hENT2 into pTBL-1 vector using the PstI and StuI restriction enzymes to ensure that hENT2 would be in frame with the other genes upstream.

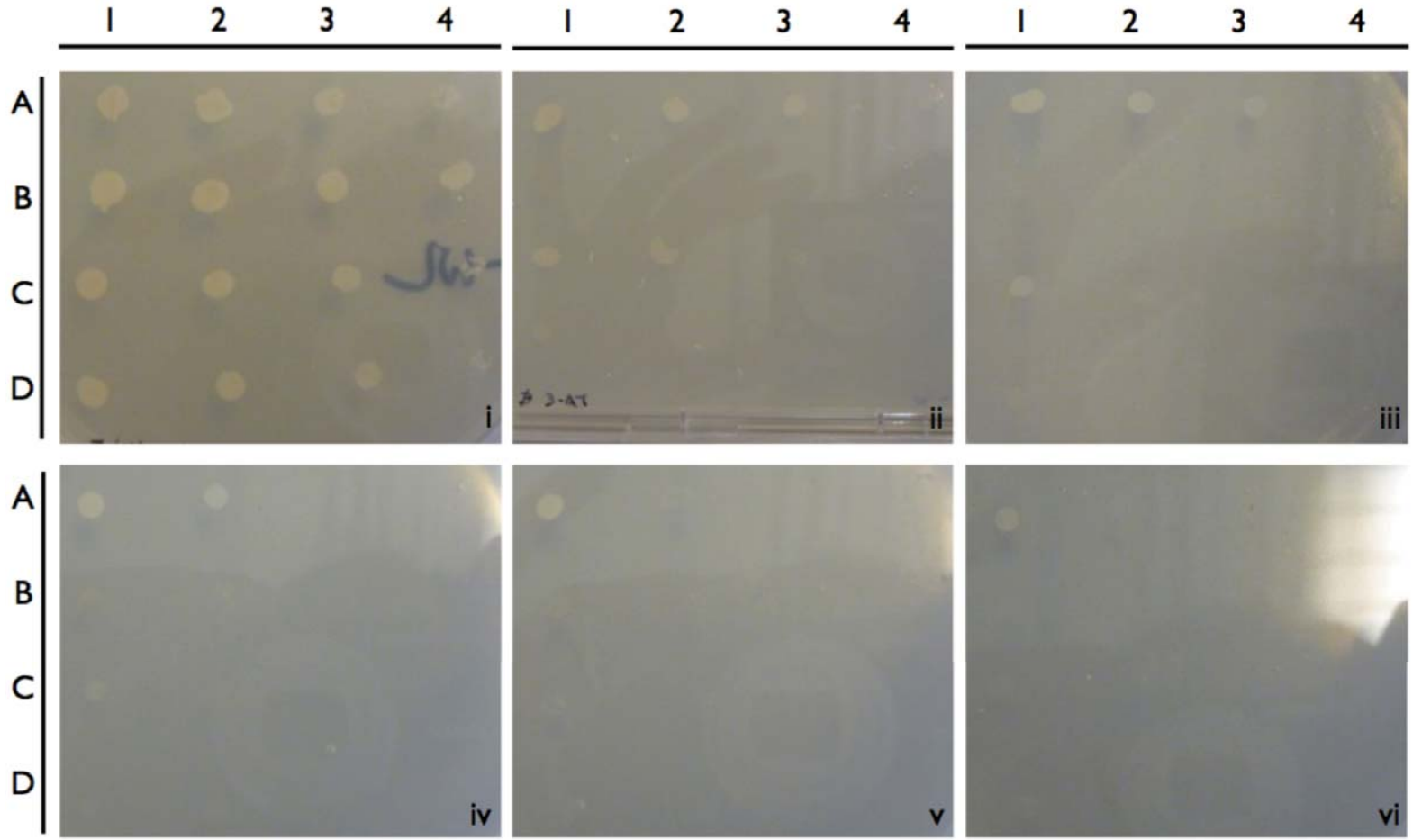

Figure 45. Bait validation using NubI/NubG control test. NMY51 yeast cells expressing hENT2-bait construct plus one prey: OstI-N_{ub}I (A), OstI-N_{ub}G (B), Fur4-N_{ub}I (C) and Fur4-N_{ub}G (D). Colonies were spotted after being diluted several times: 1/1 (1), 1/10 (2), 1/100 (3) and 1/1000 (4). Each sample was grown in different selection media: SD-WL (i), SD-WLAH (ii), SD-WLAH + 10 mM 3'AT (iii), SD-WLAH + 25 mM 3'AT (iv), SD-WLAH + 50 mM 3'AT (v), SD-WLAH + 100 mM 3'AT (vi). Cells containing the four preys grew on the non-interaction selective medium SD-WL but only the N_{ub}I preys grew on the interaction selective media SD-WLAH +/- 3'AT. Results confirmed hENT2-bait construct as a valid plasmid for the MYTH screening.

The prey proteins of the library are fused to the N-terminal moiety of ubiquitin (N_{ub}). Wild type N_{ub} has an isoleucine at position 13 ($N_{ub}I$) which is responsible of the high affinity between $N_{ub}I$ and C_{ub}. Consequently, the pseudo-ubiquitin protein is spontaneously reassembled and activates the reporter genes. By replacing Ile-13 with a glycine ($N_{ub}G$), the affinity between $N_{ub}G$ and C_{ub} is decreased in a way that the pseudo-ubiquitin protein is reconstituted only when bait and prey proteins interact with each other. To validate our hENT2-bait construct, we transformed the plasmid in the yeast strain NMY51 together with the $N_{ub}I$ or $N_{ub}G$ version of two different control preys. In our case, the controls used were Ost1, a component of the oligosaccharyltransferase complex localized to the endoplasmic reticulum membrane, and Fur4, an uracil permease localized to the plasma membrane.

Yeast cells containing hENT2-bait and the four preys were spotted on different selection media. Cells containing both bait and prey plasmids will grow on SD-WL plates but only the cells with a bait-prey interaction will grow on SD-WLAH with or without 3'AT medium. Results (figure 45) confirmed our hENT2-bait construct as a valid plasmid for the MYTH screening. Positive colonies were obtained for the four preys (A-D) when grown on SD-WL plate (i). However, on SD-WLAH (ii) medium $N_{ub}G$ preys did not grow unlike the $N_{ub}I$ (positive control). When increasing the 3'AT concentration (iii-vi) we observed a decrease of the $N_{ub}I$ colonies growth according to the selectivity of the media.

17.2 LIBRARY SCREENING AND BAIT DEPENDENCY TEST

The large-scale screening for hENT2 interactors was performed following the protocol described in the materials and methods section. The library used was a cDNA library from a mouse embryo on day 11 (Dual-systems P02234). Preys were inserted into the pPR3-N vector with the $N_{ub}G$ domain fused to the N-terminal and a total of 1.5x106 independent clones were screened. Library transformation into yeast cells containing hENT2-bait had a coverage of 950,000 total transformants, which is within the optimal range for a full coverage of the library.

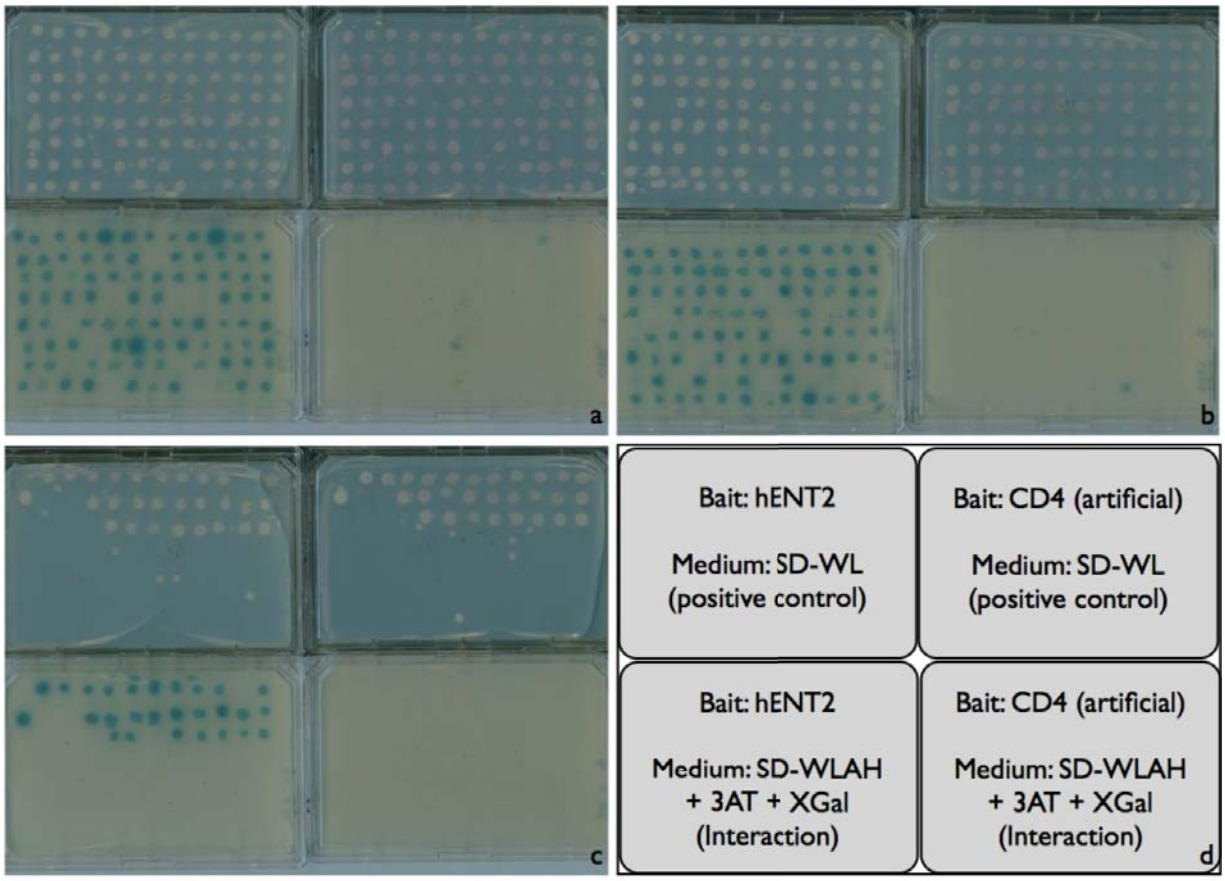

Figure 46. Bait dependency test. Each prey was transformed in different yeast cells containing either hENT2-bait or CD4-artificial bait (negative control). All the samples were grown on a non-interaction medium SD-WL as a control of bait and prey expression but not interacting necessarily. Samples were also plated on SD-WLAH + 10 mM 3'AT + XGal to identify those who were unspecific positives (positives for both hENT2 and CD4 baits) from those interactors specific for hENT2 (negatives for CD4 bait). Each spot of figures a-c represent one single prey grown in different media and baits. Figure d explains the distribution of baits and media of the plates in figures a-c.

We obtained around 400 positive colonies during the screening but after the prey plasmid recovery and propagation in *E. coli*, the number of positives was reduced to approximately 220 colonies. These 220 preys were revalidated by the bait dependency test by transforming them into yeast cells containing either hENT2-bait or CD4-bait, an artificial bait used as a negative control. Those which were positive for the CD4-artificial bait were discarded as a false positive interactors of hENT2 and only those clones which were positive for hENT2 but not CD4 were considered for the bioinformatic analysis (figure 46).

17.3 BIOINFORMATIC ANALYSIS

After we discarded false-positives from the preliminary screen, we sequenced a total of 198 samples using the $N_{ub}G$ forward internal sequencing primer, which gave us 171 good quality sequences. We identified those sequences using BLASTF analysis, being certain to verify that detected sequences are appropriately in frame with the $N_{ub}G$ tag to ensure proper identification of preys and discard potentially spurious interactions with short peptide sequences.

We obtained a final number of 110 genes that are putative hENT2 interacting partners. In order to facilitate the discussion and understanding of all the putative interactors, we sub-classified them into different sets according to their known function, localization or activity. Results are shown in the next 8 tables and discussed below.

Table 12. Nuclear-related hENT2 MYTH partners

Gene	Protein	Function known
Snrpb	Small nuclear ribonucleoprotein B	Spliceosome member; determines site cleavage in pre-mRNA processing promoting exon skipping (Yang *et al*. 2009; Cheng *et al*. 2007)
Snapc2	Small nuclear RNA activating complex	Small nuclear RNA genes transcription activator Factor required for mitotic progression: localizes to centrosomes during mitosis (Shanmugam *et al*. 2008)
SERTAD2	TRIP-Br2	Proto-oncogene exported out of the nucleus through CRM1 (Exportin 1) to the cytosol where it is ubiquitinated and degraded (Cheong *et al*. 2008)
SAP18	Sin3A-associated protein 18 KDa	Component of the Histone Deacetylase Complex (HDAC) together with RbAp46 Nuclear protein involved in RNA splicing mediating assembly of splicing regulatory multiprotein complex (Singh *et al*. 2010)
Rbbp7 / RbAp46	Retinoblastoma binding protein 7	Component of the Histone Deacetylase Complex (HDAC) together with SAP18
Ptma	Prothymosin alpha	Mediates nuclear import of Keap1/Cul3 Rbx1 complex to degrade nuclear Nrf2 (Niture & Jaiswal 2009)
Phax	Phosphorylated adaptor for RNA export	Additional factor required for U snRNA export but not for CRM1-mediated export. PHAX is phosphorylated in the nucleus and then exported with RNA to the cytoplasm (Ohno *et al*. 2000; Boulon *et al*. 2004)
Med30	Mediator complex subunit 30	Mediator of RNA polymerase II transcription
Habp4 / Ki-1/57	Hyaluronic acid binding protein 4	Nuclear unstructured protein with capacity to interact with many different proteins, most of them involved in pre-mRNA splicing control (Bressan *et al*. 2009; Bressan & Kobarg 2010).
H2afz	H2A histone family member Z	Nuclear protein responsible for the nucleosome structure of the chromosomal fibre in eukaryotes
FOXK1	Forkhead box K1	Nuclear protein.
Eif6	Eukaryotic translation initiation factor	Insoluble protein found both in the nucleus and cytoplasm. It functions as a translation initiation factor and catalyzes the association of the 40S and 60S ribosomal subunits. Calcineurin phosphatase regulates its nuclear localization by phosphorylation (Biswas *et al*. 2011)
Pdcd5	Programmed cell death	Protein up-regulated during apoptosis where it translocates rapidly from the cytoplasm to the nucleus
Cd2bp2	CD2 Antigen (cytoplasmic tail) binding protein	Bi-functional protein. In cytoplasm, it binds the cytoplasmic tail of human surface antigen CD2. In the nucleus, it's a component of the U5 small nuclear ribonucleoprotein complex and is involved in RNA splicing
Irf3	Interferon regulatory factor 3	Inactive in the cytoplasm, once phosphorylated forms a complex with CREBBP and translocates into the nucleus as a TF
Hmgb1	High Mobility Group - 1	Intracellular protein that can translocate to the nucleus where it binds DNS and regulates gene expression

Table 13. Mitochondria-related hENT2 MYTH partners

Gene	Protein	Function known
Sucla2	Succinate-CoA ligase	Mitochondrial matrix enzyme that catalyzes the reversible synthesis of succinyl-CoA from succinate and CoA. The reverse reaction occurs in the Krebs cycle, while the forward reaction may produce succinyl-CoA for activation of ketone bodies and heme synthesis
Slc25a3	Mitochondrial phosphate carrier	Catalyzes the transport of phosphate into the mitochondrial matrix, either by proton co-transport or in exchange for hydroxyl ions
Ndufa5	NADH dehydrogenase (ubiquinone) 1 alpha subcomplex, 5	The multisubunit NADH:ubiquinone oxidoreductase (complex I) is the first enzyme complex in the electron transport chain of mitochondria.
Ndufs3	NADH dehydrogenase (ubiquinone) Fe-S protein 3	The multisubunit NADH:ubiquinone oxidoreductase (complex I) is the first enzyme complex in the electron transport chain of mitochondria.
Ndufb9	NADH dehydrogenase (ubiquinone) 1 beta subcomplex, 9	The multisubunit NADH:ubiquinone oxidoreductase (complex I) is the first enzyme complex in the electron transport chain of mitochondria.
Ndufa7	NADH dehydrogenase (ubiquinone) 1 alpha subcomplex, 7	The multisubunit NADH:ubiquinone oxidoreductase (complex I) is the first enzyme complex in the electron transport chain of mitochondria.
Ndufa10	NADH dehydrogenase (ubiquinone) 1 alpha subcomplex 10	The multisubunit NADH:ubiquinone oxidoreductase (complex I) is the first enzyme complex in the electron transport chain of mitochondria.
Cox5a	Cytochrome c oxidase, subunit Va	The terminal component of the mitochondrial respiratory chain, catalyzes the electron transfer from reduced cytochrome c to oxygen
Coq4	Coenzyme Q4 homolog (yeast)	Coenzyme Q (CoQ) is a small lipophilic molecule that transports electrons between mitochondrial respiratory chain complexes and functions as a cofactor for mitochondrial enzymes
Atp5g1	ATP synthase, H+ transporting, mitochondrial F0 complex, subunit c1	Subunit of mitochondrial ATP synthase. Mitochondrial ATP synthase catalyzes ATP synthesis, using an electrochemical gradient of protons across the inner membrane during oxidative phosphorylation.
LOC100046684	ES1 protein homolog, mitochondrial-like	ES1 is serving a basic function in mitochondria, however, no function of the human ES1 protein is known yet.

Table 14. ER-Golgi - Vesicle - Trafficking related hENT2 MYTH partners

Gene	Protein	Function known
Tusc3	Tumor suppressor candidate 3	Subunit of the oligosaccharyltransferase (OST) complex that glycosylates Asn residues in the acceptor proteins in the ER lumen
Krtcap2	Keratinocyte associated protein 2	Subunit of the oligosaccharyltransferase (OST) complex that glycosylates Asn residues in the acceptor proteins in the ER lumen
Tmem59	Transmembrane protein 59	Membrane bound protein that is localized to the Golgi apparatus. Its functions is not know but related to amyloid peptide formation in Alzheimer disease
Tmem111	Transmembrane protein 111	Part of the endoplasmic reticulum-associated secretory pathway
Pdia6	Protein disulfide isomerase 6	Enzyme in the ER in eukaryotes that catalyzes the formation and breakage of disulfide bonds between cysteine residues within proteins as they fold
Arf1	ADP-ribosylation factor 1	Protein localized to the Golgi apparatus with a central role in intra-Golgi transport
Sec 13	SEC13 homolog (S.cerevisiae)	Member of the family of WD-repeat proteins. It has similarity to the yeast SEC13 protein, which is required for vesicle biogenesis from ER during the transport of proteins
Scamp3	Secretory carrier membrane protein 3	Function as carrier to the cell surface in post-Golgi recycling pathways
RAB14	Member Ras oncogene family 14	Protein involved in membrane trafficking between the Golgi complex and endosomes
SGMS1	Sphingomyelin Synthetase 1	Five-pass transmembrane protein that regulates protein trafficking and secretion
Becn1	Beclin 1	Also known as autophagy related gene 6, that protein is requires for the initiation of the formation of the autophagosome in autophagy
Hspe1	Heat shock protein 1	This gene encodes a major heat shock protein which functions as a chaperonin

Table 15. Cytoskeletal-related hENT2 MYTH partners

Gene	Protein	Function known
Tubg1	Tubulin gamma 1	Tubulin, cytoskeleton
Tubb2a	Tubulin beta 2A	Tubulin, cytoskeleton
Tsg101	Tumor susceptibility gene 101	This gene belongs to a group of apparently inactive homologs of ubiquitin-conjugating enzymes. Tsg101 Interacts with Stathmin, a cytosolic phosphoprotein implicated in tumorigenesis.
STMN1	Stathmin 1	Cytosolic phosphoprotein that functions as an important regulatory protein of microtubule (tubulin) dynamics
Tpm3	Tropomyosin 3	Cytoskeleton - Actin related
Tpm1	Tropomyosin 1	Cytoskeleton - Actin related

Table 16. Ribosome related hENT2 MYTH partners

Gene	Protein	Function known
Mrpl53	mitochondrial ribosomal protein L53	Encoded by nuclear genes to help in protein synthesis within the mitochondrion
RPS8	Ribosomal protein S8	40S Ribosomal Protein
RPS25	Ribosomal protein S25	40S Ribosomal Protein
RPS16	Ribosomal protein S16	40S Ribosomal Protein
RPLP0	Ribosomal protein large P0	60S acidic ribosomal protein P0
RPL8	Ribosomal protein L8	60S Ribosomal protein
RPL3	Ribosomal protein L3	60S Ribosomal protein
RPL27	Ribosomal protein L27	60S Ribosomal protein
RPL18	Ribosomal protein L18	60S Ribosomal protein
RPL15	Ribosomal protein L15	60S Ribosomal protein

Table 17. Enzyme-related hENT2 MYTH partners

Gene	Protein	Function known
Ruvbl2	RuvB-like protein	Protein belonging to the AAA+ family, ATPases Associated with diverse cellular Activities
Rnaseh2c	Ribonuclease H2	RNAse H2 complex
Ppp1r7	Protein Phosphatase 1	Ser/Thre Phosphatase. Pp1 has been found to be important in the control of glycogen metabolism, neuronal activities, RNA splicing and regulation of membrane receptors and channels.
Ppp3cc	Calcineurin	Calmodulin-dependent protein phosphatase, calcineurin, is involved in a wide range of biological activities acting as a Ca^{2+}-dependent modifier of phosphorylation status.
NME/NM23	Nucleoside diphosphate Kinase 2	Involved in diverse physiological and pathological processes including proliferation, differentiation and ciliary functions.
Htra1	Htra serine peptidase 1	Member of the trypsin family of Ser proteases. This protein is a secreted enzyme that is proposed to regulate the availability of insulin-like growth factors by cleaving their binding proteins
Hint1	His triad nucleotide binding protein 1	Adenosine 5'-monophosphoramidase or protein Kinase C-interacting protein 1. It exerts its major cellular function as gene transcription regulator.
DDT	DE-Dopachrome tautomerase	Protein belonging to the family of carboxy-lyases that cleave carbon-carbon bonds
Ctsz	Cathepsin Z	Lysosomal cysteine proteinase and member of the peptidase C1 family
BCR	Breakpoint Cluster Region	The BCR gene is one of the two genes in the bcr-abl complex with Tyr kinase activity
Dok2	Docking Protein 2	Protein constitutively Tyr phosphorylated and possibly a critical substrate of the bcr-abl complex
Aarsd1	Alanyl-tRNA synthetase	Enzyme that interprets the RNA code and attaches specific aminoacids (alanine) to the tRNAs

Table 18. hENT2 MYTH partners with unknown or miscellaneous functions

Gene	Protein	Function known
Tmem150a	Transmembrane protein 150A	Function unknown
Tmem 119	Transmembrane protein 119	Induced by parathyroid hormone. Promotes osteoblast differentiation and interacts with the bone morphogenetic protein-Runx2 pathway
TCTE1	T-complex- Associated-Testis-Expressed 1	Function unknown
Sssca1	Sjogren's Syndrome/ scleroderma autoantigen 1	Function unknown
Selh	Selenoproetin H	Protein that includes a Selenocystein aminoacid residue
NTN4	Netrin 4	Class of proteins involved in axon guidance
NEFL	Nasal Embryonic LHRH factor	Protein involved in guidance of olfactory axon projections and migration of luteinizing hormone-releasing hormone neurons
MTRNR2L2	16S RNA / humanin	Mitochondrial 16S ribosomal RNA and also the humanin polypeptide
Morf4l2	Mortality Factor 4 like 2	Transcriptional regulator
Mlf1ip	Myeloid leukemia factor 1 interacting protein	Function unknown
Mettl9	Methyltransferase like 9	Function unknown
Mettl3	Methyltransferase like 3	Function unknown
Lrrc58	Leucine Rich repeat containing 58	Function unknown
Lgals1	Galectin-1	Family of beta-galactoside-binding proteins implicated in modulating cell-cell and cell-matrix interactions. Galectin-1 modulates CaV1.2 calcium channel activity binding to the transporter's loop (Wang *et al*. 2011).
Ifitm2	Interferon induced transmembrane protein	Activated in response to bacterial and viral infections
Id3	Inhibitor of DNA binding 3	Helix-loop-helix (HLH) protein that inhibits DNA binding of any HLH protein that interacts with.
GNAS	Gs alpha subunit	G protein subunit that activates the cAMP-dependent pathway by activating adenylate cyclase. It's coupled to many different receptors, adenosine A_{2a} and A_{2b} receptors among them
Ctla2a	Cytotoxic T lymphocyte-associated protein 2^{A}	Function unknown. Cathepsin L inhibitor
Cthrc1	Collagen Triple Helix repeat containing 1	Protein that may play a role in the cellular response to arterial injury through involvement in vascular remodelling
Creg1	CREG	Protein may contribute to the transcriptional control of cell growth and differentiation
CLU	Clusterin	Protein able to bind and form complexes with numerous partners
Atxn10	Ataxin 10	Protein may function in neuronal survival and differentiation

Table 19. hENT2 MYTH partners described as common false positives*

Gene	Protein	Function known
USP11	Ubiquitin specific peptidase	Ubiquitin related enzyme
Ufc1	Ub-fold modifier conjugating enzyme	Ubiquitin related enzyme
Ubl3	Ubiquitin-like 3	Ubiquitin related
Ube2n	Ub-conjugating enzyme E2	Ubiquitin related enzyme
Ube2j1	Ub-conjugating enzyme E2J 1	Ubiquitin related enzyme
Ubb	Ubiquitin B	Ubiquitin
CYC1	Cytochrome C 1	Heme protein component of the electron transport chain in mitochondria
Cyb5b	Cytochrome B 5b	Component of the respiratory chain complex III
Rabac1	Rab acceptor 1 (prenylated)	Protein involved in vesicles trafficking
RNF41	Ringer finger protein 41	E3 Ubiquitin-protein ligase NRDP1. Function not yet determined
Hbb-y	Hemoglobin gamma	Iron-containing oxygen-transport protein in the red blood cells
Hba-a1/a2	Hemoglobin alpha	Iron-containing oxygen-transport protein in the red blood cells
Gpx1	gluthatione peroxidase1	Detoxification of hydrogen peroxide
Gpx3	gluthatione peroxidase3	Detoxification of hydrogen peroxide
Prdx6	Peroxiredoxin 6	Member of the thiol-specific antioxidant protein family
FTL1	Ferritin light chain	Ubiquitous intracellular protein that stores iron
Ttr*	Transthyretin	Thyroxine and retinol carrier in fluids. Pre-Albumin family member
SCMH1*	Sex comb on midleg homolog 1	Acts as a E3 Ub-ligase for Geminin, a DNA replication inhibitor
LEPREL2*	Leprecan-like 2	Family of collagen prolyl hydroxylases required for proper collagen biosynthesis, folding and assembly
Cd63*	Cd63 antigen	Cell surface glycoprotein that is known to complex with integrins
AldoA*	Aldolase A, fructose bisphosphate	Enzyme that catalyzes a reversible reaction of the glycolysis

* Proteins in this table have been previously described as common false-positives for the Two-Hybrid technique based on data-bases compiling thousands of results obtained during years. Specific false-positive for MYTH technique found by Dr. Staglar are also included. The last five proteins have not been described as false-positives for MYTH but based on results obtained in two other two-hybrid screenings for ENT1 and CNT2, we decided to discard them as such since they also appeared as putative partners of those nucleoside transporters (Huber-Ruano *et al*. 2010; Ratushny & Golemis 2008; Berggård *et al*. 2007; Deane *et al*. 2002; Serebriiskii & Golemis 2001).

17.4 DISCUSSION OF PUTATIVE hENT2 PARTNERS IDENTIFIED BY MYTH

The two-hybrid system if one of the most widely used methods to screen or confirm protein-protein interactions (PPI). However, there are several disadvantages to using this system for screening of PPIs. First, only binary interactions can be identified with this technique, limiting the detection of proteins involved as complexes. Another inconvenience is the large number of false positive identified with this system. However, the Membrane Yeast Two Hybrid (MYTH) provides us with the capacity to detect potential partners for full-length membrane proteins, which has been impossible to do to date.

A major limitation of MYTH is the potential isolation of false positives. It is important to discard those predicted to be false positives. Over the years, several studies have analyzed and described what we call “common false-positives” based on the results of thousands of large-scale two-hybrid screenings. The exact rate of identification of false-positive results is not known, but it has been estimated to be as high as 50% of the identified interactions (Deane *et al*. 2002; Berggård *et al*. 2007).

False positives can be divided into two categories: technical and biological. Technical false-positives are due to the reporter system, wherein reporter activity is induced in the absence of any PPI. In this category are proteins that interact directly with the promoter, or in general with DNA upstream of the reporter genes like transcription factors or histone-related proteins. This class of false-positives was much reduced with widespread adaptation of dual reporter system with minimal sequence overlap in their promoter regions, in our case LexA and VP16. Nevertheless, proteins that appear to be operating at the level of chromatin and transcription still are occasionally isolated with apparently biologically irrelevant baits.

Biological false-positive are genuine interactions that occur in the context of the two-hybrid system but are not representative PPI in a cellular model based on the known physiology of bait and prey. There are some common false-positives obtained with many diverse baits: ribosomal subunits, heat-shock proteins, proteasome subunits and cytoskeletal components. It has been hypothesized that their false positive character is because these proteins are intrinsically “sticky” and their natural biological

function involves binding a large number of different proteins. In addition, many eukaryotic protein interactions depend on post-translational modifications and the yeast model is quite limited in this respect compared with mammalian cells. Of course, even if an interaction does not make immediate sense to the investigator, it may still occur inside living cells and contribute to regulatory pathways yet to be discovered (Ratushny & Golemis 2008; Serebriiskii & Golemis 2001).

Following we discuss about the most relevant PPI found for hENT2 and their possible meaning in cell physiology. We discarded those partners found belonging to ER-Golgi and vesicular trafficking system, as well as cytoskeletal and ribosomal proteins as common false-positives proteins.

17.4.1 Nuclear-related hENT2 MYTH putative partners:

Within the group of potential nuclear partners for hENT2, we found two different kinds of proteins: those connected with alternative splicing regulation, and some other proteins related with the transport across the nuclear membrane, either as a substrates or cofactors.

As outlined in the introduction, the pre-mRNA splicing process is carried out within the nuclei by a complex machinery called the spliceosome. Each spliceosome is composed of five small nuclear RNA (snRNA) and a range of associated protein factors comprising a dynamic PPI network (Hegele *et al.* 2012). Combined, they make an RNA-protein complex called snRNP, which catalyzes the removal of introns and the ligation of the flanking exons (Ritchie *et al*. 2009). Alternative splicing is a process by which the exons of a molecule of RNA are reconnected in multiple ways during the pre-mRNA splicing. The production of alternatively spliced mRNAs is regulated by a variety of proteins acting either as activators promoting the usage of a particular splice site, or repressors reducing the usage of it. Mechanisms of alternative splicing are highly variable but mainly they are regulated by changing the concentration and activity of these splicing regulatory factors. This is achieved by de novo protein synthesis, regulation of the intracellular localization and phosphorylation.

In our MYTH screening for hENT2, we found putative interactions with 5 different proteins involved in alternative splicing regulation:

- Snrpb: Spliceosome member that determines site cleavage promoting exon skipping (Yang *et al*. 2009; Cheng *et al*. 2007).

- SAP18 and RbAp46: two members of the Histone Deacetylase complex (HDAC). Nuclear proteins involved in RNA splicing mediating assembly of splicing regulatory multiprotein complex (Singh *et al*. 2010) and chromatin modifications (Hnilicová *et al*. 2011).

- Habp4: Nuclear unstructured protein with capacity to interact with many different proteins, most of them involved in pre-mRNA splicing control (Bressan *et al*. 2009; Bressan & Kobarg 2010).

- Cd2bp2: Component of the U5 small nuclear ribonucleoprotein complex involved in RNA splicing (Kofler 2004; Laggerbauer 2005).

Considering the hENT2 wild type isoform as a possible partner of interaction of these proteins, our results might not have any sense as that isoform is mainly located at the plasma membrane and is thus inaccessible to the splicing regulation factors. However, in this thesis we describe two novel hENT2 functional variants located at the nuclear membrane, which share around 70% of their structure with the wild type and, most importantly, the internal loop between transmembrane domains 6 and 7. Based on hENT2 2D structure, we consider this loop as the principal region of regulation and interaction with other proteins, since it has 76 amino acids which are accessible for interaction while the rest of the protein is inserted into the membrane. MYTH screening was carried out using the full-length isoform, therefore partners of the nuclear variants might also be isolated if interaction takes place at the conserved intracellular loop. Thus, nuclear proteins found to be possible hENT2 partners make sense in terms of plausible cell physiology but also help us to figure out new roles of the nuclear variants of this transporter.

Our interpretation of these data suggest that nuclear variants of hENT2 might be linked to the regulation process of pre-mRNA splicing. This hypothesis is strengthened by the fact that the isoforms are generated by an alternative splicing phenomenon. There are some examples of self-regulation of alternative splicing by specific proteins. For instance, SF2/ASF is a serine/arginine-rich (SR) protein involved in regulating and selecting splice sites and therefore crucial for the alternative splicing. It has been found that SF2/ASF negatively autoregulates its expression to maintain homeostatic levels. This autoregulation involves a post-transcriptional control that generates alternative spliced RNA isoforms that would either be retained in the nucleus or degraded by NMD (Sun *et al*. 2010). Another similar case is the one of SC35, another SR protein that regulates alternative splicing in a concentration-dependent manner. This protein also regulates its own wild type expression levels by promoting alternative splicing non-functional isoforms to keep homeostatic expression levels (Sureau *et al*. 2001). A more interesting example of self-regulation is the case of AHNAK, a 700 KDa protein involved in cytoarchitecture and calcium signalling. A common AHNAK transcript encodes two different proteins, a large one of 700 KDa and a smaller one of 17 KDa. During muscle differentiation the small 17 KDa isoform shows strongly increased trafficking into the nucleus where it establishes a positive feedback loop to regulate mRNA splicing of its own locus (de Morree *et al*. 2012). Considering these examples, we propose the hypothesis that nuclear isoforms of hENT2 play a role in the regulation of the alternative splicing process thereby modulating their own expression and the expression of the wild type isoform. That way, hENT2 could adapt the levels of expression of it's own isoforms levels or even generate nonsense spliced variants, as a response and adaptation to cell growth conditions and demands.

Another interesting set of proteins found in our MYTH results are nucleus-related proteins involved in cytoplasm-nuclear transport:

- SERTAD2: Proto-oncogene exported out of the nucleus through Exportin 1 to the cytosol where is ubiquitinated and degraded (Cheong *et al*. 2008).

• Ptma: Mediates nuclear import of Keap1/Cul3 Rbx1 complex to degrade nuclear Nrf2 (Niture & Jaiswal 2009).

• Phax: Aditional factor required for U snRNA export but not for CRM1-mediated export. PHAX is phosphorylated in the nucleus and then exported together with RNA to the cytoplasm. The transporter that mediates the exportation is still undetermined (Ohno *et al*. 2000; Boulon *et al*. 2004).

• Eif6: Insoluble protein found both in the nucleus and cytoplasm where it functions as a translation initiation factor. Calcineurin phosphatase regulates its nuclear localization by phosphorylation(Biswas *et al*. 2011)

• Pdcd5: Protein upregulated during apoptosis where it translocates rapidly from the cytoplasm to the nucleus.

• Irf3: Inactive in the cytoplasm, once phosphorylated forms a complex with CREBBP and translocates into the nucleus as a transcription factor.

• HMG-1: Intracellular protein that can translocate to the nucleus where it regulates gene expression interacting with DNA / Chromatin (Stros 2010)

The underlying commonality for all these proteins is the fact that all are translocated through the nuclear membrane at some specific moment and all of them need a transporter to mediate their translocation. All of them could be potential substrates for the novel hENT2 nuclear variants except that hENT2 has been characterized as a nucleoside / nucleobase transporter and is highly unlikely to translocate small proteins. However, a previous study demonstrated for the first time a protein transport through ENT2. In that study, the substrate was an intranuclear delivery vehicle and pathway for the transport of therapeutic macromolecules across plasma and nuclear membranes, the anti-DNA antibody fragment 3E10 Fv. These researchers showed that 3E10 Fv is unable to penetrate into cells deficient in ENT2 and reconstitution of the transporter restores its transport into cell nuclei (Hansen *et al*.

2007). 3E10 Fv is a 30 KDa protein with the property of binding nucleic acids, similar to Phax, one of the proteins found to interact with hENT2. Phax is a 394 amino acid protein, similar in size to 3E10 Fv, with the similar capability to bind nucleic acids, specifically RNA. Therefore, we should consider the possibility that hENT2 plays a major role in the nuclear membrane in addition to being a nucleoside transporter but also as a transporter involved in translocating bigger molecules with a protein nature such as transcriptional factors or specific carriers like Phax.

Furthermore, this is not the first time that a nuclear isoform of hENT2 has been associated with HMG-1, one of the proteins found with the MYTH screening. In 1995, when HNP36 was cloned for the first time, HMG-1 was identified as a delayed-early response gene (Williams & Lanahan 1995). These researchers could not relate ENT2 and HMG-1 in a functional way but our results suggest there may be a role for these proteins in a mitogenic response.

Four more nuclear proteins were identified in the MYTH screening (Snapc2, Med30, H2afz and Foxk1). These proteins could be considered as false-positives since are proteins that either bind a large number of different proteins, as they are considered “sticky” proteins, or they are involved in gene transcription and activation of the promoter which could activate the reporter genes without physiologically relevant real PPI.

As a summary, from the first set of results obtained by the MYTH technique, we pose the hypothesis that nuclear hENT2 variants might play a dual role at the nuclear membrane as alternative splicing regulators binding to splicing factors and interfering with their availability to promote/inhibit some alternative sites, and as a nuclear translocator of small proteins or carriers. In addition, it is described how mRNA export is coupled to pre-mRNA splicing in an even more complex multiprotein machinery (Reed & Hurt 2002), where hENT2 might have its own role.

17.4.2 Mitochondria-related hENT2 MYTH partners:

We found a total of 11 different proteins in the mitochondria that could be interacting with hENT2 at some specific point. Curiously, 8 over 11 are elements of the respiratory chain found in the mitochondrial membrane. We have to consider these results cautiously although there are a number of studies that confirm the presence of ENTs at the mitochondrial membrane. ENT1 was shown to be present at the mitochondrial membrane (Lai *et al*. 2004) and the use of autofluorescent nucleosides confirmed functionality of the protein at the mitochondria (Zhang, Sun, *et al*. 2006a). More recently, hENT3 was also described to be located at the mitochondrial membrane (Govindarajan *et al*. 2009). Despite lack of evidence, the presence of ENT2 in the mitochondria can be indirectly inferred from experimental data since ENT1 and ENT3 cannot be responsible for the internalization of all the drugs tested in the previous studies (Leung & Tse 2007).

Furthermore, recent work describes a link between mitochondrial DNA (mtDNA) depletion and molecular mechanisms involving ENTs to compensate the mitochondrial respiratory chain and ensure respiratory activity despite profound depletion in mtDNA levels (Villarroya *et al*. 2011). In this case, a decrease in thymidine kinase 2 (TK2) levels with consequent severe mtDNA depletion, showed increased cytochrome c oxidase activity together with higher transcript and protein levels. No alterations of the deoxynucleotide pools were found, whereas a reduction in the expression of genes involved in the nucleoside/nucleotide homeostasis (hENT1 among others) was observed, indicating a connection between the respiratory chain activity and the role of ENTs at the mitochondrial membrane. In addition, it has been published recently that Fun26, a yeast ENT homolog, is responsible of the intracellular pool of NmR, one of the substrates for NAD^+ synthesis, though the salvage pathway (S. P. Lu & Lin 2011), since NAD^+/NADH is a crucial element of the respiratory chain.

Mitochondrial proteins are also common false-positives of MYTH, especially cytochrome C oxidase and NADH dehydrogenase, which means we must be cautious about our results. Therefore, the possible connection between hENT2, NAD^+

metabolism and respiratory chain remains to be confirmed by other techniques. However, the presence of functional ENTs at the mitochondria seems to be certain and their role in mitochondrial physiology remains to be clarified. Two other protein interactors have been found: Slc25a3, a phosphate carrier and the enzyme Sucla2, what supports a presence of hENT2 at the mitochondrial membrane but does not give us any information about the role of ENTs at the mitochondria.

17.4.3 hENT2 MYTH partners with enzymatic activity and other proteins:

A total of 12 potential protein interactors with an enzymatic activity have been identified. Among them, some are particularly noted:

PHOSPHATASES:

• Ppp1r7: Ser/Thre phosphatase. Interesting for its important role in RNA splicing and regulation of membrane receptors and channels.

• Calcineurin: Calmodulin-dependent protein phosphatase. Involved in a wide range of biological activities acting as a Ca^{2+}-dependent modifier of phosphorylation status.

KINASES:

• NME/NM23: Nucleoside Kinase. Involved in diverse physiological roles like proliferation, differentiation and ciliary functions.

• BCR: Element of the bcr-abl complex with Tyr kinase activity.

• Dok2: Constitutively Tyr phosphorylated, it may be a critical substrate of the bcr-abl complex.

LYASES:

• Ruvbl2: ATPase associated with diverse cellular activities.

• Htra1: Member of the trypsin family of Ser proteases.

• Hint1: Adenosine 5'-monophosphoramidase or protein Kinase C-interacting protein 1. It exerts its major cellular function as gene transcription regulator.

• DDT: A member of the family of carboxy-lyases that cleave carbon-carbon bonds.

• Cathepsin Z: Lysosomal cysteine proteinase and member of the peptidase C1 family.

Phosphatases and kinases are especially interesting given our interest in phosphorylation-dependent regulation of hENT2. Protein phosphatase 1 has been described to play a very important role in alternative splicing regulation. PP1 binds directly to some specific splicing factors via a phylogenetically conserved RVDF sequence and dephosphorylates them, promoting recognition of alternative RNA splice sites (Novoyatleva *et al*. 2008; Stamm 2008). We have previously discussed the possible role of hENT2 in its own splicing regulation since we found that it might interact with some splicing factors. If those PPI were confirmed, we could propose a plausible scenario where, through PP1-dependent pathway, which is regulated upstream by second messengers like cAMP and ceramide, the phosphorylation status of hENT2 would be altered to affect or regulate its own splicing pattern to adapt it to the cell conditions and needs.

Another interesting finding in our screen is calcineurin, a Ca^{2+}/calmodulin dependent phosphatase. A previous MYTH study performed with mENT1 as a bait found calmodulin as an interacting protein of ENT1, and this interaction has been confirmed in further studies (data not published). ENT1 and ENT2 seem to have a fine cross-regulated activity where overexpression of one transporter seems to be compensated by a decrease of the other (Aguayo *et al*. 2005). Therefore, the possibility of a dual regulation of ENT1 and ENT2 via Ca^{2+}/Calmodulin opens a new and important line of research.

The other enzymes found in the screen do not seem to have a clear connection with hENT2's role as a transporter at the plasma membrane or at the nuclear membrane. DDT is the only gene with a previous connection to ENT2, since it is described as a DER gene together with HNP36, although any functional link with ENT2 was not established (Lanahan *et al*. 1992; Williams & Lanahan 1995).

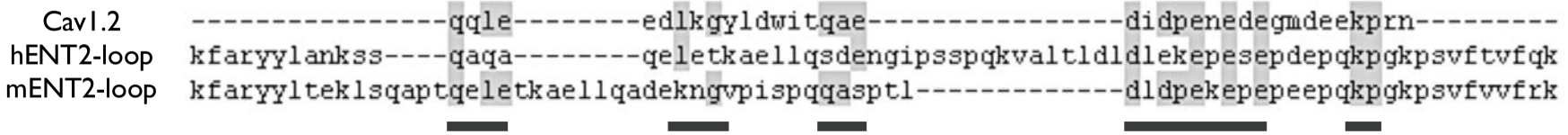

Figure 47. Alignment of Gal-1 binding domain in Cav1.2 and m/hENT2-loop sequences. The region determined to bind Gal-1 in Cav1.2 channel shows a high homology with both human and mouse ENT2-loop sequences. The amino acid sequence DXDPEXEXEXXXXXKP at the C-term of ENT2-loops could be responsible of the interaction between the nucleoside transporter and Gal-1, in case that interaction were further confirmed.

Among the other putative hENT2 PPI partners, we want to highlight the identification of Galectin-1 and the Gs_{α} subunit. Galectin-1 is a family member of beta-galactoside-binding proteins implicated in modulating cell-cell and cell-matrix interactions. It is interesting to note that there is a demonstrated interaction between Gal-1 and the Cav1.2 calcium channel. Gal-1 binds to the internal loop of Cav1.2 for a specific splice variant of the channel decreasing its functional surface expression (J. Wang *et al*. 2011). Since hENT2 coincides having a large intracellular loop, we pose the possibility that Gal-1 binds hENT2 intracellular loop regulating its activity or localisation. When comparing the amino acid sequence of the calcium channel determined to bind Gal-1 and the sequences of the mouse and human ENT2-loop, we notice a highly coincident region critical for Gal-1 recognition and binding (figure 47). The amino acid sequence DXDPEXEXEXXXXXKP might be responsible for the interaction between Gal-1 and Cav1.2, and also between Gal-1 and ENT2 in case that interaction were confirmed by other techniques. In addition, recent work from our laboratory (Fernández-Calotti and Pastor-Anglada - data not published) demonstrated the interaction between CNT3 and Gal-4, which has been previously described to be involved in trafficking of glycosylated proteins to the apical membrane.

Gs_{α} subunit triggers the cAMP-dependent pathway by activating adenylate cyclase. Gs_{α} it is coupled to many receptors, including adenosine A_{2a} and A_{2b} receptors among them. Previous work has described the regulation by P_1 adenosine receptors on nucleoside transporters at the plasma membrane. In the case of CNT2, ATP-sensitive potassium channels have been shown to regulate CNT2 through A_1 adenosine receptors (Duflot *et al*. 2004). For ENT2, there is some evidence that shows a regulation of ENT2 at the plasma membrane via activation of A_1 adenosine receptors (G. Lu *et al*. 2010; Knight *et al*. 2010). A_1 receptors are not typically linked to Gs_{α} specifically but those studies show an existing linkage between the pathways triggered by adenosine receptors and nucleoside transporters. In addition, during this chapter we have been developing a hypothesis where PP1 is activated via cAMP, triggered by Gs_{α} leading to the dephosphorylation of a hENT2 variant at the nuclear membrane thereby altering its splicing pattern in response to the physiological needs of the cell. This novel hypothesis is shown in figure 48.

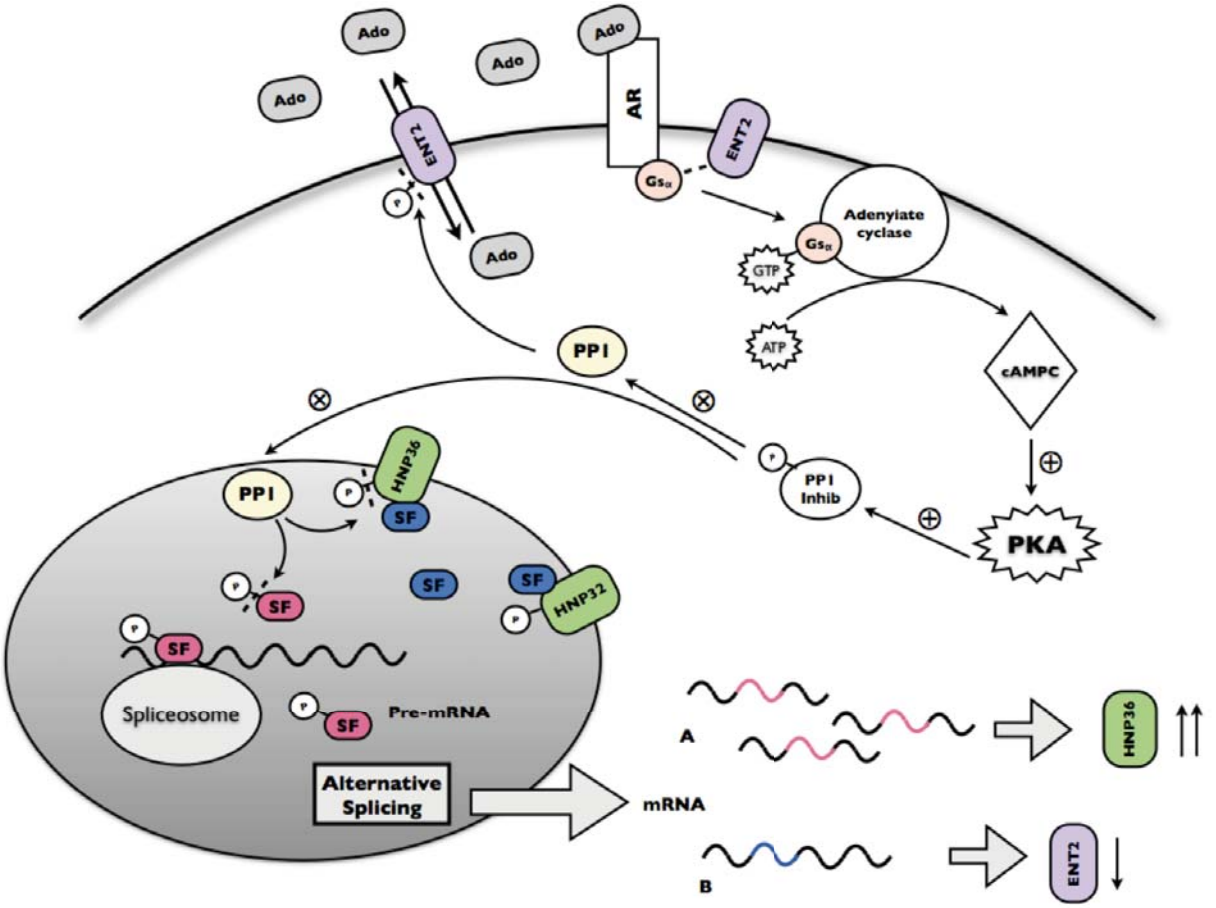

Figure 48. Cartoon showing possible regulation of hENT2 splicing pattern by phosphorylation. ENT2 transports adenosine (Ado) into the cell thereby modulating its extracellular levels. Extracellular adenosine binds to adenosine receptors (AR), activating Gs protein which may also interact with ENT2 directly according to our MYTH results. Gs also activates adenylate cyclase which synthesizes cAMP from ATP. cAMP activates PKA which phosphorylates the PP1 inhibitor proteins (DARP-32 and I-1). These inhibitors interact allosterically with PP1, inhibiting phosphatase activity (Aggen *et al*. 2000). PP1 may interact directly with hENT2 and also HNP32 and HNP36 regulating their phosphorylation status. PP1 is also involved in alternative splicing regulation since it dephosphorylates splicing factors (SF). Phosphorylation status of the SF would determine its affinity to some specific splice sites but also could be involved in the interaction between SF and HNP32/36. If HNP32/36 binds to SF, this would compromise their availability to determine the sites recognised by the spliceosome during the pre-mRNA processing. Therefore, depending on the phosphorylation status of HNP32/36 and SF, the cell would produce a different pattern of alternative splicing, thereby modulating the expression of the hENT2 isoforms. In our example, phosphorylated SF (red) would determine some specific splice sites producing a mRNA variant "A" that codifies for HNP36 protein. Non-phosphoryated SF (blue) would be interacting with HNP32/36 proteins and would be retained at the nuclear membrane and thus would not be available for the splicing process. As a consequence, less mRNA "B" product would be generated and so hENT2 protein expression would be decreased.

18 PHARMACOGENOMIC ANALYSIS OF THE RESPONSIVENESS OF SOLID TUMORS TO DRUG THERAPY: A TRANSPORTOME APPROACH

18.1 THE TRANSPORTOME PROJECT

Drug transport across the plasma membrane is mediated by a wide range of membrane proteins, which are crucial for their cytotoxic action. To establish the role these proteins might play in anticancer therapy we performed a “transportome” transcriptomic approach on cell lines derived from gastrointestinal tumors. The aim of this study was to identify a discrete set of genes whose expression levels in tumor cells may allow prediction of sensitivity/resistance to chemotherapy, and also to identify putative novel networks of biological relevance.

We selected a total of 15 cell lines from three different kind of tumors representative of three gastro-hepatic cancers: pancreas, stomach and biliary tract (figure 49a). Those samples were treated with 6 drugs commonly administrated as a treatment for these kinds of tumors. Three of these drugs are nucleoside-derived: 5-Fluorouracil, its pro-drug 5’-DFUR and gemcitabine. The other three treatments have a different chemical nature: cisplatin, doxorubicin and paclitaxel (figure 49b).

For the transcriptomic study we chose, based upon existing knowledge, a total of 96 genes to be analyzed by real-time PCR. These genes encompass the main membrane proteins involved in anticancer drugs import and export, like OATP, OCT, OAT, NT, AQPs and ABC families. We also included enzymes related to drug metabolism and detoxification, and genes with a highlighted role in apoptosis/survival balance and DNA repairing (figure 49c).

PANCREAS	STOMACH	BILIARY TRACT
PanC-1	AGS	Mz-ChA-1
BxPC3	SNU-1	Mz-ChA-2
NP9	SNU-5	SK-ChA-1
NP29	MKN-45	TFK-1
NP31	KATO III	EGI-1

a)

DRUG TREATMENTS	
5'-DFUR	Cisplatin
5-FU	Doxorubicin
Gemcitabine	Paclitaxel

b)

UPTAKE CARRIERS		EFFLUX PUMPS	METABOLISM	APOPTOSIS-SURVIVAL-PROLIFERATION-INVASION		NORMALIZERS
OATP1B1	ENT1	ABCA2	Dihydropyrimidine dehydrogenase - DPYD	ERCC1	Bax	18S
OATP1B3	ENT2	ABCA3	Thymidine phosphorylase - TYMP	XPA	p21	GAPDH
OATP2B1	ENT3	ABCB1	Uridine phosphorylase 1 - UPP1	XPC	Fas	GUSB
OATP4A1	ENT4	ABCB4	Uridine phosphorylase 2 - UPP2	Uracil-DNA glycosylase - UDG	Bcl-2	
OCT1	CNT1	ABCB11	Epoxide hydrolase 1 - EPHX1	hMLH1	Smac/DIABLO	
OCT2	CNT2	ABCC1	Deoxycytidine kinase - DCK	hPMS2	c-IAP-1 - BIRC2	
OCT3	CNT3	ABCC11	Ribonucleoside-diphosphate reductase - RRM1	hMSH2	XIAP	
OCTN1		ABCC2	Thymidilate synthetase - TYMS	GTBP/hMSH6	survivin - BIRC5	
OCTN2	AQP1	ABCC3	Thymidine kinase 1 - TK1	GADD45	Livin - BIRC7	
OAT1	AQP3	ABCC4	5'-Nucleotidase, cytosolic IA - NT5C1A	Topoisomerase I - TOP1	c-FLIP - CFLAR	
OAT2	AQP4	ABCC5	5'-Nucleotidase, cytosolic IB - NT5C1B	Topoisomerase II-alpha - TOP2A	EGFR	
OAT3	AQP5	ABCG2	Orotate phosphoribosyl transferase o UMPS	KIT	PI3K	
OAT4	AQP7		Uridine-cytidine kinase 2 - UCK2	PDGFRA	c-myc	
CTR1	AQP8	LRP o MVP	Folylpolyglutamate synthase - FPGS	Matrix Metalloproteinase 1 - MMP1	tigar/C12orf5	
	AQP9	ATP7A	γ-Glutamyl cistein synthetase - GCLC	Matrix Metalloproteinase 2 - MMP2	NRF2	
		ATP7B	Metallothionein 4 - MT4	Matrix Metalloproteinase 3 - MMP3	KEAP1	
			UGT1A1/UGT1A8/UGT1A10 - UGTX	α-Fetoprotein - AFP		

c)

Figure 49. Transportome design. (a) Cell lines selected for this study, 15 in total. These samples come from three different kinds of tumor: pancreas, stomach and biliary tract. (b) Treatments chosen for the cytotoxicity assays. Three of them are nucleoside derived drugs (5'-DFUR, 5-FU and gemcitabine) while the rest has a different chemical nature (cisplatin, doxorrubicin and paclitaxel). (c) Genes selected for the transcriptomic study. These genes encompass uptake carriers and efflux pumps, metabolism enzymes, and genes related to apoptosis/survival. We also included three housekeeping genes as normalizers.

18.2 CYTOTOXICITY ASSAYS

In the cytotoxic assays, we treated the 15 cell lines with each drug at 5 different doses inside the normal range of usage. Determining IC_{50} for 6 drugs and 15 cell lines turned out to be very complex and laborious, so we defined the profile of each cell lines for each drug inside the dose framework of the treatments. After 48 hours of treatments we analyzed cell survival using the MTT technique. Assays were performed as described in the materials and methods section.

Results obtained (figure 50) show the differences in the responsiveness profiles to a specific treatment inside a same kind of tumor and among the three different types. When we compared results obtained with the three nucleoside-derived drugs (figure 50a), we observed cases where the response inside the same kind of tumor is quite similar for the 5 cell lines, like 5-FU in stomach samples, where the profiles are almost identical. On the contrary, we also found profiles completely different among samples with the same origin, like the case of gemcitabine in pancreas cell lines, where we have cells 100% resistant to the treatment (PanC-1) or cell that almost reach 25% survival with the lowest dose (NP31).

When comparing results obtained for the three non nucleoside-derived drugs, we also found different varieties of patterns inside the same kind of samples. For instance, in pancreas cell lines, the responsiveness profile in doxorubicin treatment is quite similar for the 5 cell lines. On the contrary, cisplatin and paclitaxel show profiles completely different inside the same kind of tumor. Considering this variety of response we assume that in these cases we cannot consider responsiveness to a treatment dependent to the kind of tumor of the sample but to a specific cell line. Therefore, in further analyzes, we do not consider samples divided in three different groups (pancreas, stomach and biliary tract) but as a pool of 15 different cell lines, since responsiveness is not tumor-dependent.

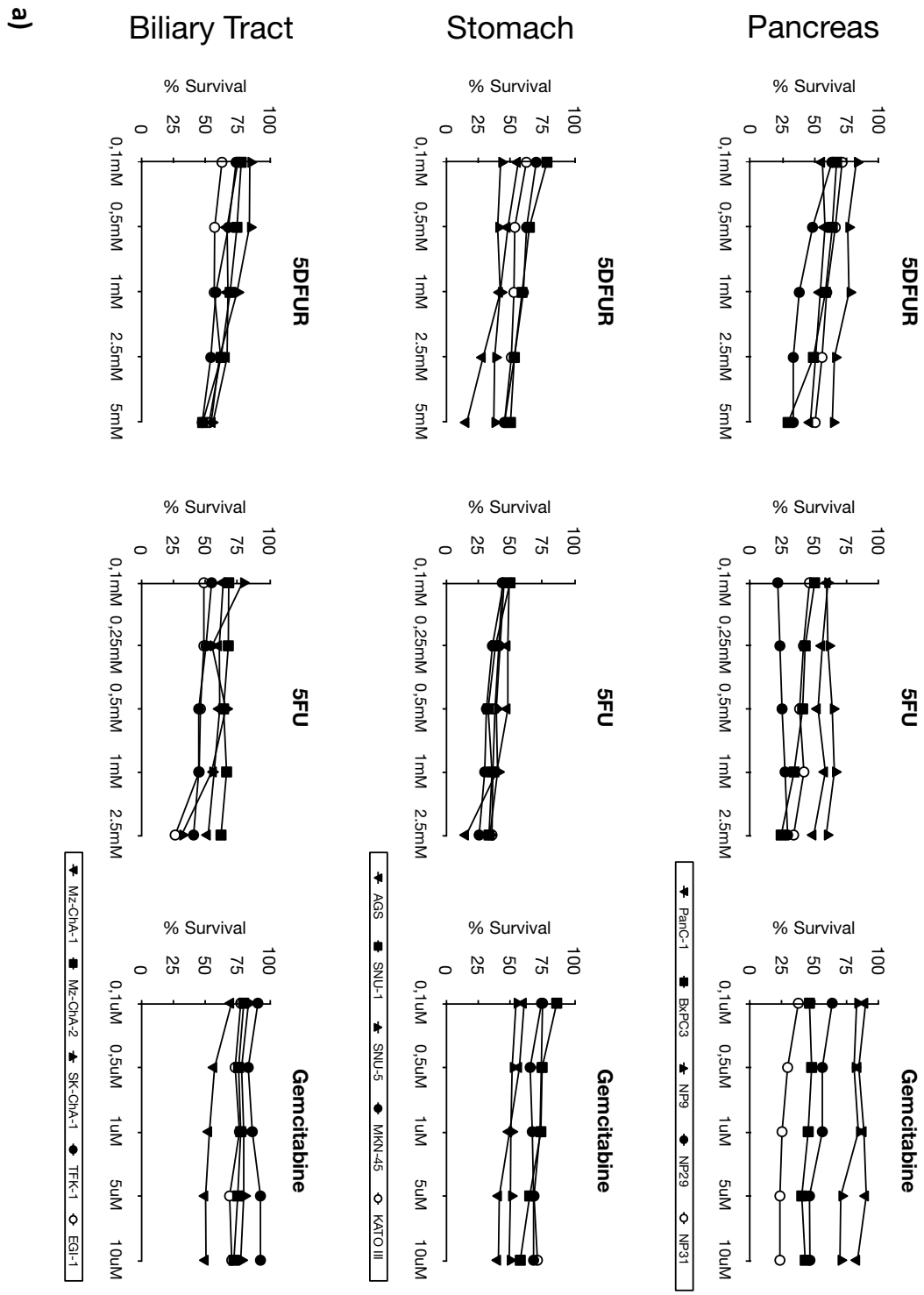

Figure 50. Responsiveness to cytotoxicity assays. Each graph represents the results obtained of cytotoxicity assays for one drug and five cell lines from the same kind of tumor. Y axis represents the percentage of survival compared to control cells no treated. X axis represents the 5 concrete doses applied for each treatment.

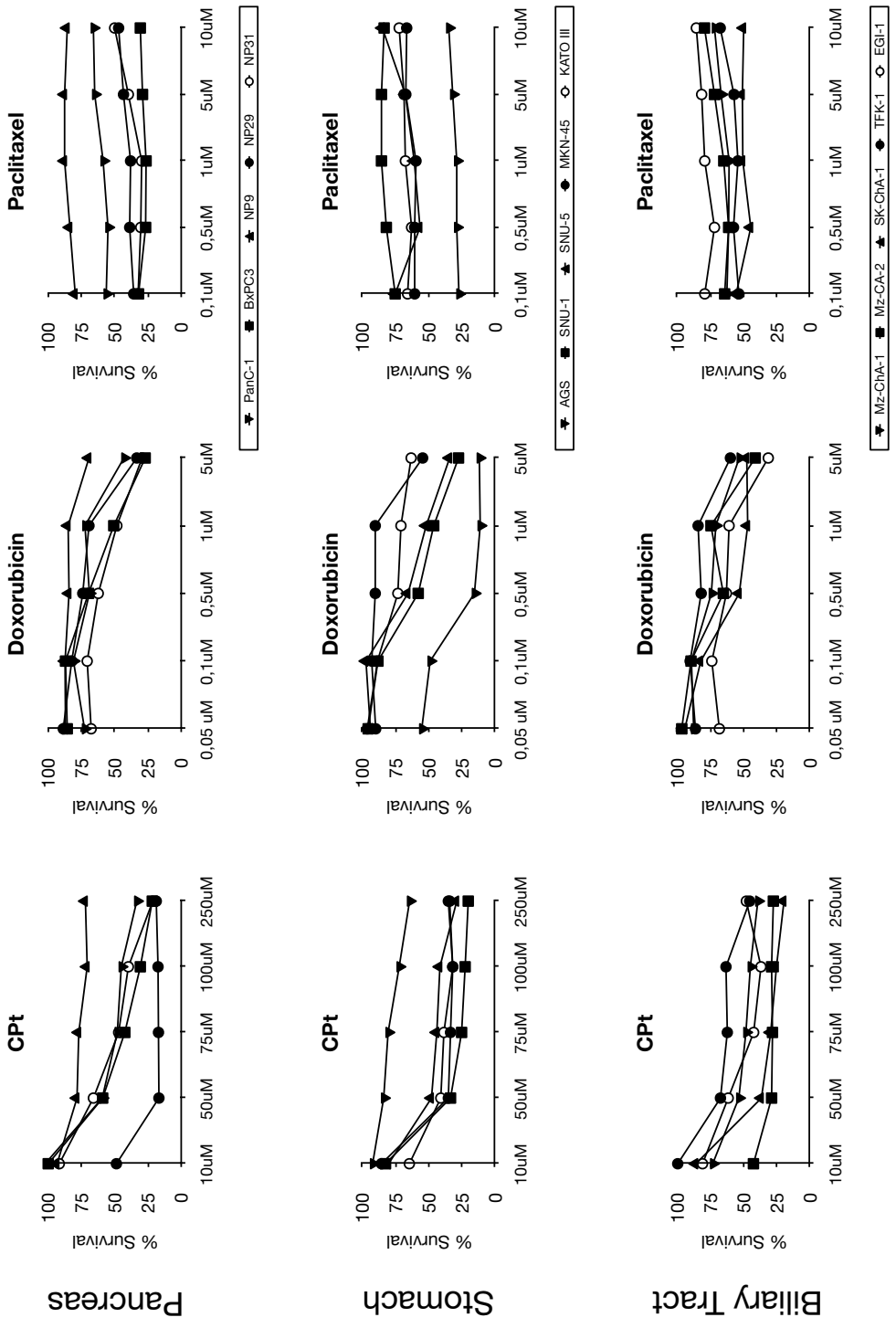

(a) Results obtained after treatment with three nucleoside-derived drugs : 5-FU, 5'-DFUR and gemcitabine. (b) Results obtained after treatment with three non nucleoside-derived drugs: cisplatine (CPt), doxorubicin and paclitaxel.

18.3 GENE EXPRESSION ANALYSIS

To perform the transcriptomic analysis we used microfluidic cards, also know as TaqMan® Low Density Arrays (TLDA). This tool allows us to run 384 real-time PCR at once with predetermined TaqMan® probes already tested and validated. We analyzed as explained in materials and methods section, a total of 96 genes in 30 different cDNA samples, obtained from two independent RNA extractions of the 15 different cells lines. Each sample was analyzed twice to discard errors due to the technique.

Nineteen of these genes (highlighted in grey in figure 51) could not be used in later studies as their expression levels were too low to be detected by the TLDA system, like CNT1 and CNT2 for instance, or because the number of samples that expressed them did not reach the minimum to be analyzed statistically (supplementary data in appendix I - tables 24-26). As our group experience focuses mostly on nucleoside transporters, we decided to determine CNT1 and CNT2 expression levels by using individual TaqMan® probes in a relative real time PCR. We re-analyzed ENT1, ENT2, CNT1, CNT2 and CNT3 expression levels and compared them with previous values obtained by TLDA. As results obtained for ENT1, ENT2 and CNT3 were the same in both techniques, we decided to include the new values for CNT1 and CNT2 to the global correlation analysis in order to keep them in the study.

Once we got gene expression levels, we studied correlations among cell lines based on their expression values to determine whether data should be treated separately depending upon the origin of the samples or as a global set (figure 52). As the heatmap did not define any cluster grouping samples, we considered them disparate enough to be analyzed as a whole instead of 3 different kinds of tumors separately. All computation were done by CIBERehd bioinformatics platform[J] using R v2.12.o software[I].

UPTAKE CARRIERS		EFFLUX PUMPS	METABOLISM	APOPTOSIS-SURVIVAL-PROLIFERATION-INVASION		NORMALIZERS
OATP1B1	ENT1	ABCA2	Dihydropyrimidine dehydrogenase - DPYD	ERCC1	Bax	18S
OATP1B3	ENT2	ABCA3	Thymidine phosphorylase - TYMP	XPA	p21	GAPDH
OATP2B1	ENT3	ABCB1	Uridine phosphorylase 1 - UPP1	XPC	Fas	GUSB
OATP4A1	ENT4	ABCB4	Uridine phosphorylase 2 - UPP2	Uracil-DNA glycosylase - UDG	Bcl-2	
OCT1	CNT1	ABCB11	Epoxide hydrolase 1 - EPHX1	hMLH1	Smac/DIABLO	
OCT2	CNT2	ABCC1	Deoxycytidine kinase - DCK	hPMS2	c-IAP-1 - BIRC2	
OCT3	CNT3	ABCC11	Ribonucleoside-diphosphate reductase - RRM1	hMSH2	XIAP	
OCTN1		ABCC2	Thymidilate synthetase - TYMS	GTBP/hMSH6	survivin - BIRC5	
OCTN2	AQP1	ABCC3	Thymidine kinase 1 - TK1	GADD45	Livin - BIRC7	
OAT1	AQP3	ABCC4	5'-Nucleotidase, cytosolic IA - NT5C1A	Topoisomerase I - TOP1	c-FLIP - CFLAR	
OAT2	AQP4	ABCC5	5'-Nucleotidase, cytosolic IB - NT5C1B	Topoisomerase II-alpha - TOP2A	EGFR	
OAT3	AQP5	ABCG2	Orotate phosphoribosyl transferase o UMPS	KIT	PI3K	
OAT4	AQP7		Uridine-cytidine kinase 2 - UCK2	PDGFRA	c-myc	
CTR1	AQP8	LRP o MVP	Folylpolyglutamate synthase - FPGS	Matrix Metalloproteinase 1 - MMP1	tigar/C12orf5	
	AQP9	ATP7A	γ-Glutamyl cistein synthetase - GCLC	Matrix Metalloproteinase 2 - MMP2	NRF2	
		ATP7B	Metallothionein 4 - MT4	Matrix Metalloproteinase 3 - MMP3	KEAP1	
			UGT1A1/UGT1A8/UGT1A10 - UGTX	α-Fetoprotein - AFP		

Figure 51. Genes analyzed by TLDA. A total of 93 genes, besides 3 normalizers (18S, GAPDH and GUSB), were analyzed by TLDA system and classified according to their main physiological role. Nineteen of these genes (highlighted in grey) were not included in later studies as they were not detected in most of the 15 cell lines, therefore a total of 74 genes would be considered in further analysis.

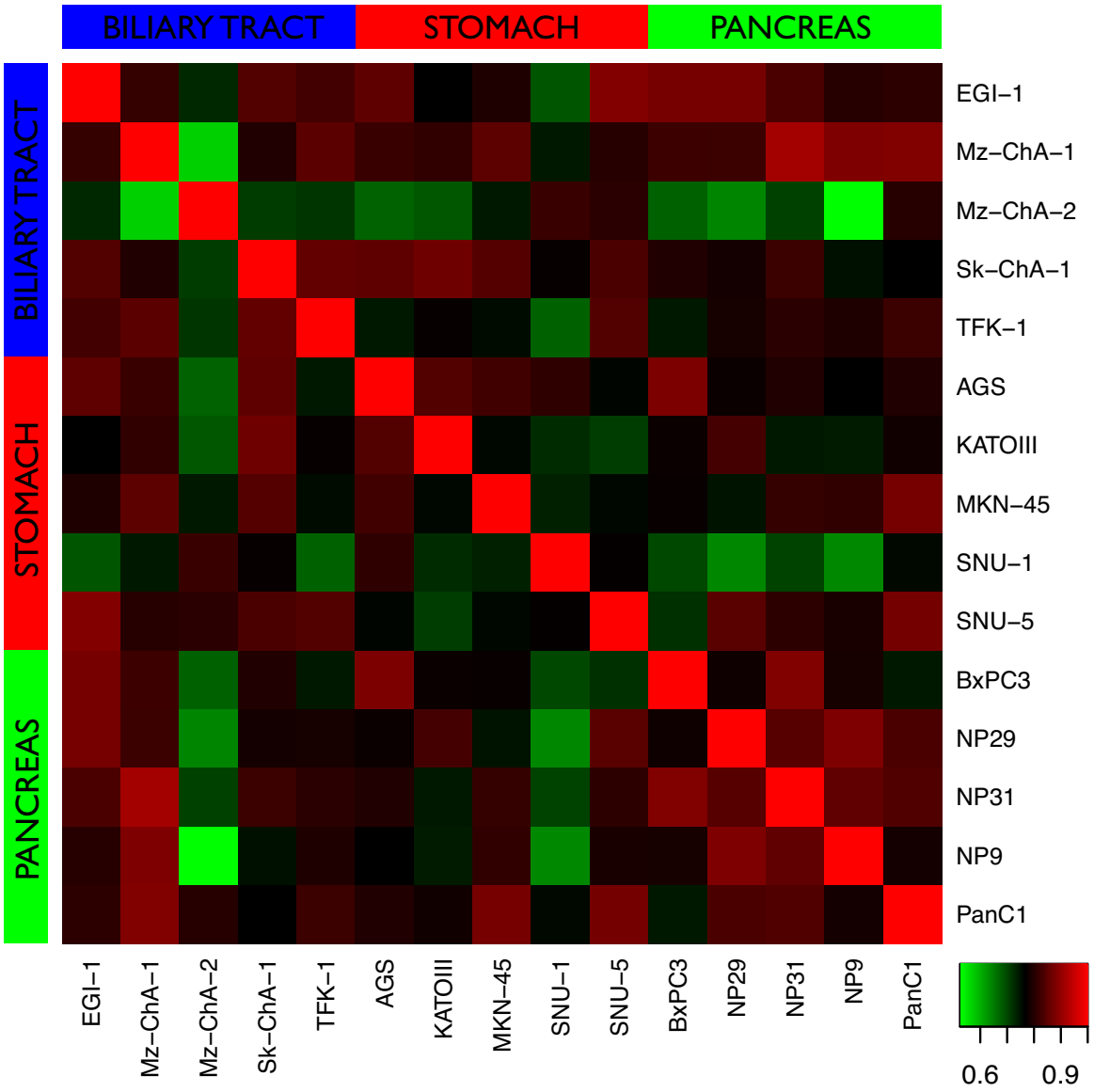

Figure 52. Correlations between samples based on genes expression profiles. Heatmap depicting Pearson correlations among samples based on their genes expression profiles. Data do not generate any specific cluster matching with the different tissues origin. Red pixels correspond to positive correlations, whereas green pixels indicate negative correlations.

Next step was to evaluate correlations among genes to determine possible clusters or linking networks (figure 53). In this case, we could clearly notice two clusters well-defined with forceful statistics, and how they might be related by some other genes in common. When we extracted correlation values from these clusters (figure 54a) we appreciated how consistent these clusters are with all genes strongly connected among themselves supported by statistics values most of them with a p value under 0,01 (figure 54b). When we analyzed these genes in detail focusing in their physiological role, we classified them in 4 main groups: membrane proteins (including NT transporters, OATPs and OCTs transporters, and Growth Factor Receptors), enzymes of nucleotide metabolism and genes belonging to IAP family and the DNA mismatch repair system (figure 55).

Regarding membrane proteins, we exclusively found hENT1 and hCNT3 as nucleoside transporters, both of them showing broad substrate selectivity and being major players in providing nucleosides for growth purposes (promoting salvage pathways). Several works describe ENT1 as an essential gene involved in proliferation. When proliferation of murine bone marrow-derived macrophages is induced by M-CSF, mENT1 is up-regulated becoming indispensable, whereas its expression level decreases when proliferation is blocked by macrophage activation through IFN-y. Also in rat intestinal epithelia cells, rENT1 is up-regulated when cell proliferation is induced by EGF, as well as in rat liver (del Santo *et al*. 1998) or human proximal tubular cells (Guillén-Gómez *et al*. 2011). In all those cases, CNT1 and CNT2 have been negatively associated with proliferation, acquiring a key role, especially CNT2, in differentiation, modulation of purinergic signaling and energy metabolism in both intestinal and liver parenchymal cells (Duflot *et al*. 2004; Aymerich *et al*. 2006; Huber-Ruano *et al*. 2010). Interestingly, those more specialized transporters, hCNT1 and hCNT2, do not define any particular cluster in our study, like hENT3, which has been described as an intracellular transporter protein (Baldwin *et al*. 2005).

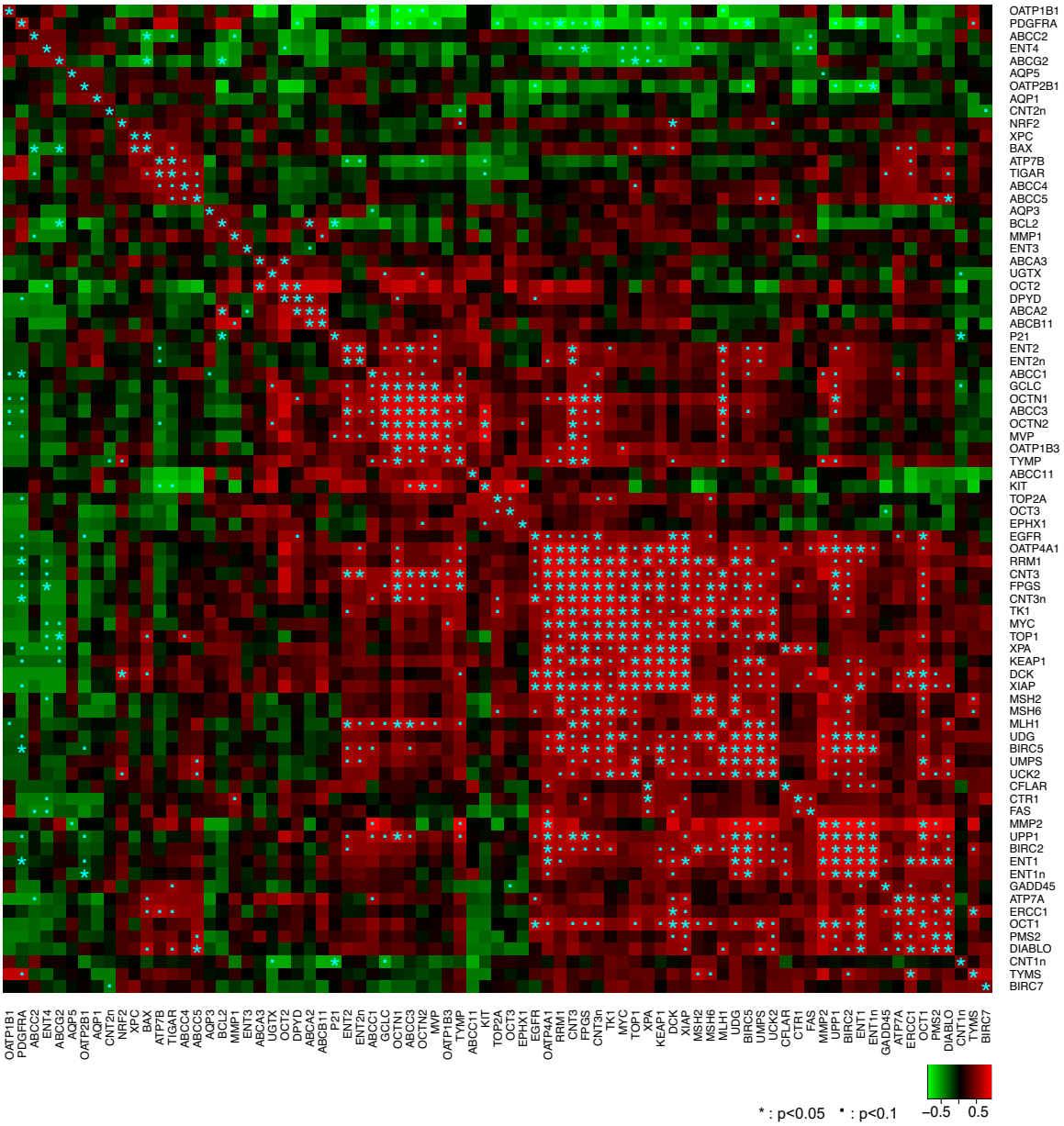

Figure 53. Correlations between genes. Pearson correlation coefficient-based heatmap between genes. ENTs and CNTs expression data obtained by individual Taqman® probes are included and indicated as ENTXn or CNTXn. Associated P-values were also calculated for each gene (* : p<0,01; · : p< 0,05). Red pixels correspond to positive correlations, whereas green pixels indicate negative correlations. All computation were done using R v2.12.o software[l].

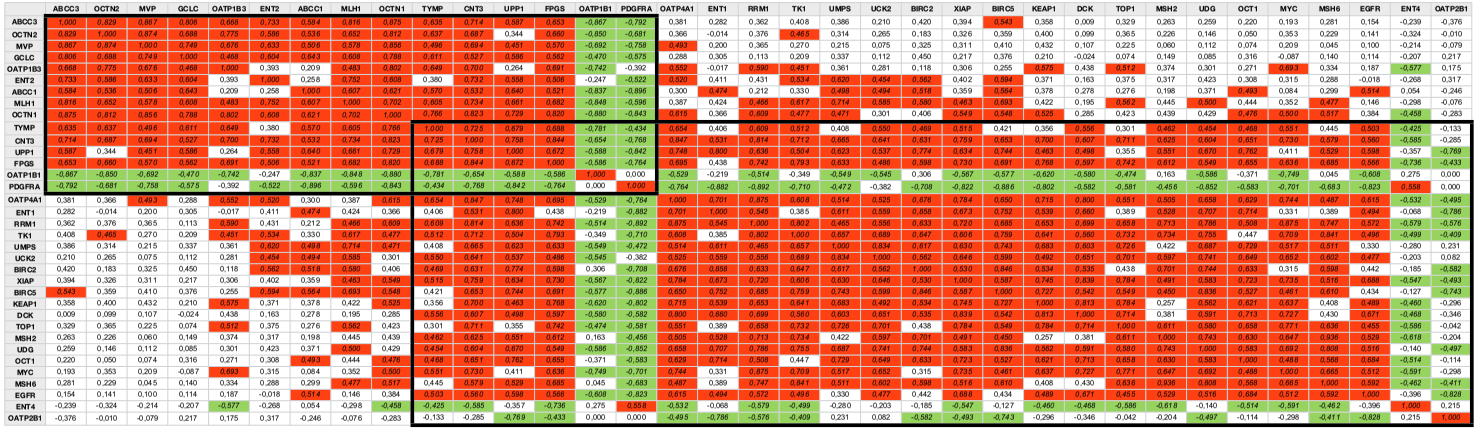

a)

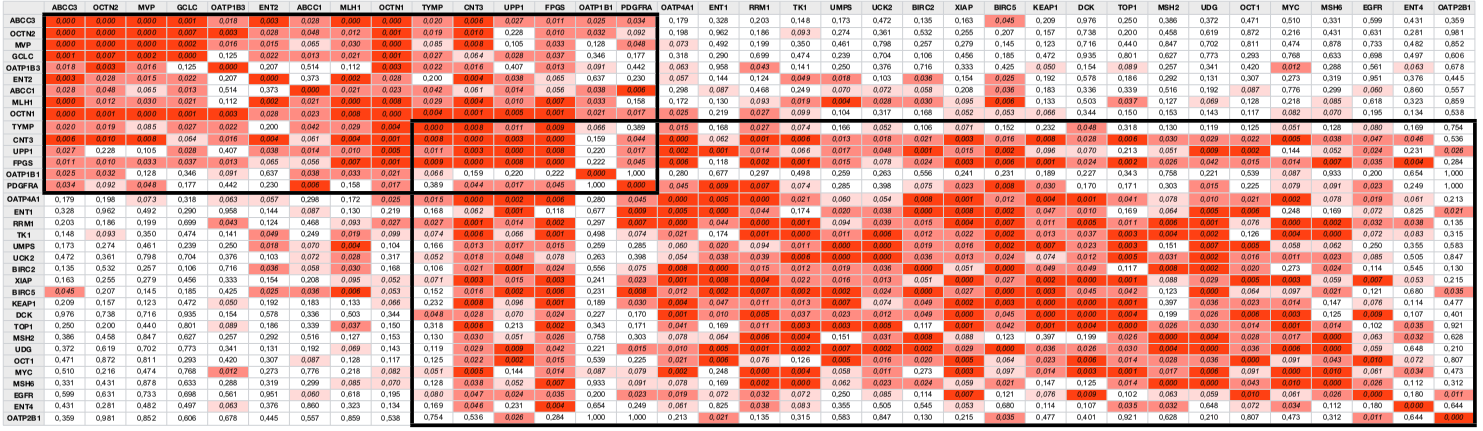

b)

Figure 54. Expression values of the clusters obtained from heatmap of gene correlations. (a) Correlation values among 35 genes defining a possible network. Positive correlations (>0,45) are highlighted in red and negative correlations (< -0,45) in green. (b) P values of correlations describe above. Red: p<0,01; Pink: p<0,05 and Light Pink: p<0,1. Two possible networks are framed in black according to forceful correlations of those genes.

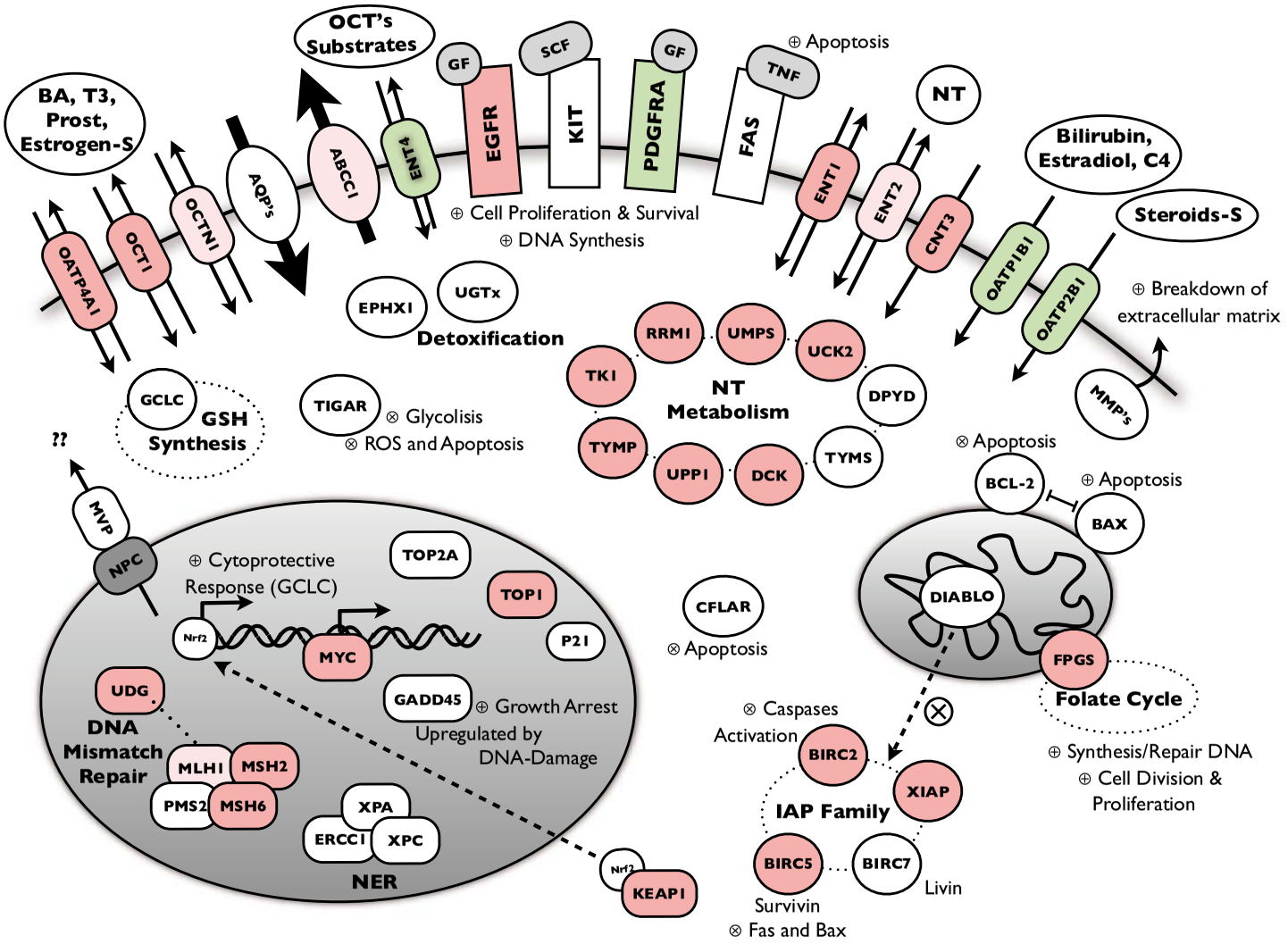

Figure 55. Cartoon representing genes of a putative novel gene network. Diagram depicting physiological roles of genes selected for this study and relations among them stablished from TLDA analysis. In red, genes with a highly positive correlation; in light pink, genes whose positive correlation is not so forceful in the context of the global set of genes; in green, genes correlating negatively.

Gene clusters defined by broad selectivity transporter proteins also incorporate almost all genes (7 out of 9) included in the card and related to nucleotide metabolism, highlighting the probable link between membrane processes implicated in nucleoside salvage and nucleos(t)ide metabolism. Furthermore, some of these enzymes have been demonstrated to be important for cell proliferation and crucial for dTTP supply in DNA repairing, in the case of TK1 (Y. L. Chen *et al*. 2010), and also to induce metastasis, angiogenesis and to protect cancer cells against apoptosis, in the case of TYMP (Bronckaers *et al*. 2009).

hENT2 also shows some positive correlation with different genes of interest, being relevant as it is the main known transporter protein so far implicated in nucleobase salvage. hENT2 has been described as a putative cancer gene in human hepatocellular carcinoma, where its aberrant up-regulation was significantly associated with advanced stages, vascular invasion and poor patient survival. At the same time, when hENT2 was down-regulated, cell proliferation and tumor formation decreased considerably (C.-F. Chen *et al*. 2010). Curiously, hENT1 and hENT2 are both involved in cellular proliferation but not at the same time, as they're differently regulated in a cell cycle-dependent way (del Santo *et al*. 1998). On the other hand, hCNT3 is the only member of the SLC28 family with a broad selectivity, highly conserved in species including procaryotes, in contrast with equilibrative transporters. In addition, hCNT3 appears to be highly expressed in human endothelial stem cells, together with hENT1 (Guzmán-Gutiérrez *et al*. 2010).

Surprisingly, hENT4 shows a strong negative correlation with genes defining hENT1 and hCNT3 related clusters. Despite it was assigned to the equilibrative nucleoside transporter family, hENT4 (also known as PMAT) mainly functions as a polyspecific organic cations transporter (M. Zhou *et al*. 2007). It has been demonstrated that PMAT-mediated adenosine transport is saturable, pH-dependent, and membrane-potential sensitive (M. Zhou *et al*. 2010). These functional differences between hENT1-2 and hENT4 coincide with their no-correlated expression. Besides the possibility of being an adenosine transporter, hENT4 might be contributing to translocate substrates also recognized by SLC22 members, such as selected hOCTs. A previous study about non-neuronal monoamine transporters reported a negative correlation between hENT4 and OCT1 expression, coinciding with our results (Bottalico *et al*. 2007).

Interestingly, hOATP1B1 and hOAT2B1 show significant negative correlations with these gene clusters and also their transport activity is pH gradient influenced, as it happens with hENT4 (Svoboda *et al*. 2011). Some studies reported that tissue-specific distribution of OATPs is not maintained in cancer cells and, according with our results, hOATP4A1 shows increased mRNA levels in tumors, while hOATP1B1/2B1 are downregulated comparing cancerous versus non-cancerous samples (Wlcek *et al*. 2011). Genes in the defined clusters also showing positive correlations include those of the IAP family implicated in cell survival blocking caspase activity and also regulating canonical NF-kB activation (Plati *et al*. 2011). Therefore, an enhanced expression of IAPs has been seen to contribute to colon carcinogenesis and its poor prognosis, acquiring a potential role as prognostic markers (Miura *et al*. 2011).

Growth factor receptors, EGFR and PDGFRA, also show significant correlations with those clusters although they maintain an inverse relationship, being EGFR positively and PDGFRA negatively correlated with this novel gene network. Despite these two receptors trigger similar pathways involved in proliferation, it has been reported in different cases that their gene amplification are mutually exclusive (Fleming *et al*. 1992; Perrone *et al*. 2010). However, it still remains unclear the reason of their mutual exclusion although probably it would be related to the distinct signalling cascades triggered by their different ligands (Besson & Yong 2001). Anyway, this discrimination between genes apparently contributing to similar cellular events also occurs with genes encoding some of the proteins implicated in DNA repair. Genes of the DNA mismatch repair (MMR) system positively correlate whereas the NER system is not included in the cluster. Once again, there is no evidence to explain this phenomenon, beyond the reported connection between mRNA expression among members of MMR (D. Chang *et al*. 2000) and also the fact proliferating cells have higher expression levels of MMR genes than resting cells (Jascur & Boland 2006).

18.4 CORRELATION BETWEEN GENE EXPRESSION AND TREATMENT RESPONSE

To determine if there is any set of genes whose expression would predict responsiveness to those specific treatments, we analyzed correlations between the percentage of survival for each sample and treatment condition, and the basal expression of each gene, based on the Pearson coefficient. Results are shown in figure 56.

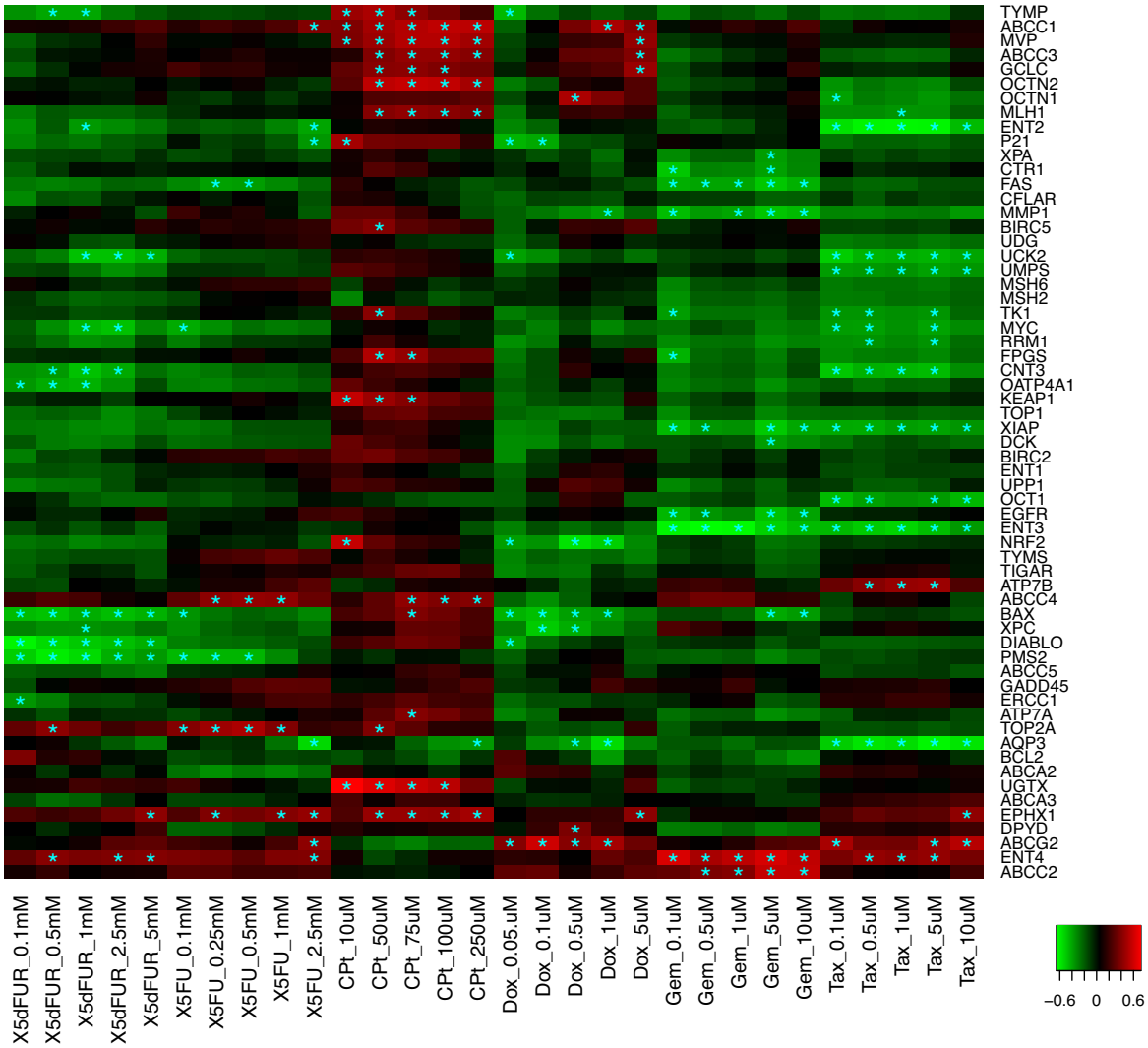

Figure 56. Heatmap representing correlations between genes expression and responsiveness to treatments. Pearson correlation coefficient-based heatmap between genes and percentage of survival in each treatment condition. Positive values are highlighted in red while negative correlations in green. Statistics: * = p<0,05

As results show, for each treatment there is a discrete set of genes that significantly correlates with the responsiveness to the drug. Since we represent percentage of survival versus gene expression, a positive value means that the expression of the gene is correlated with resistance to the treatment. On the contrary, a negative value means the expression of the gene is correlated with sensitivity to the treatment.

In the case of paclitaxel, there are 11 genes (OCT1, ENT2, CNT3, TKI, RRMI, UMPS, UCK2, XIAP, AQP3, ENT3 and MYC) whose expression would be associated to sensitivity of the cell to the treatment. Interestingly, 9 of these genes (all except AQP3 and ENT3) belong to the previous network described in figure 55. There are also 4 genes (ABCG2, ENT4, EPHX1 and ATP7B) that correlate with resistance to the treatment. There is no apparent reason to justify why these genes would determine the cell response to this drug since most of they are nucleoside-related genes, like enzymes from the nucleot(s)ide metabolism and also some transporters, and paclitaxel is not a nucleoside-derived drug. However, based on our previous speculations about the existence of a putative global network, these genes would be linked to the expression of other genes, not identified in this study, which might be directly responsible of the cell response to that specific treatment. Therefore, if these correlations were confirmed in further studies, we could define a set of genes as markers/predictors for treatment responsiveness.

Another example illustrated here is the case of cisplatin, where 4 genes are correlated with sensitivity to the treatment (AQPs, ABCG2, ENT4 and CNT1) and 9 other genes correlate with resistance to that drug (MVP. GCLC, OCTN2, ABCC1, EPHX1, UGTx, TYMP, KEAP1 and MLH1). Also in that case we cannot find a plausible reason to justify the correlation between the expression of these genes and the cell response to cisplatin. Interestingly, the genes found for cisplatin are totally different than the ones obtained for the response to paclitaxel treatment.

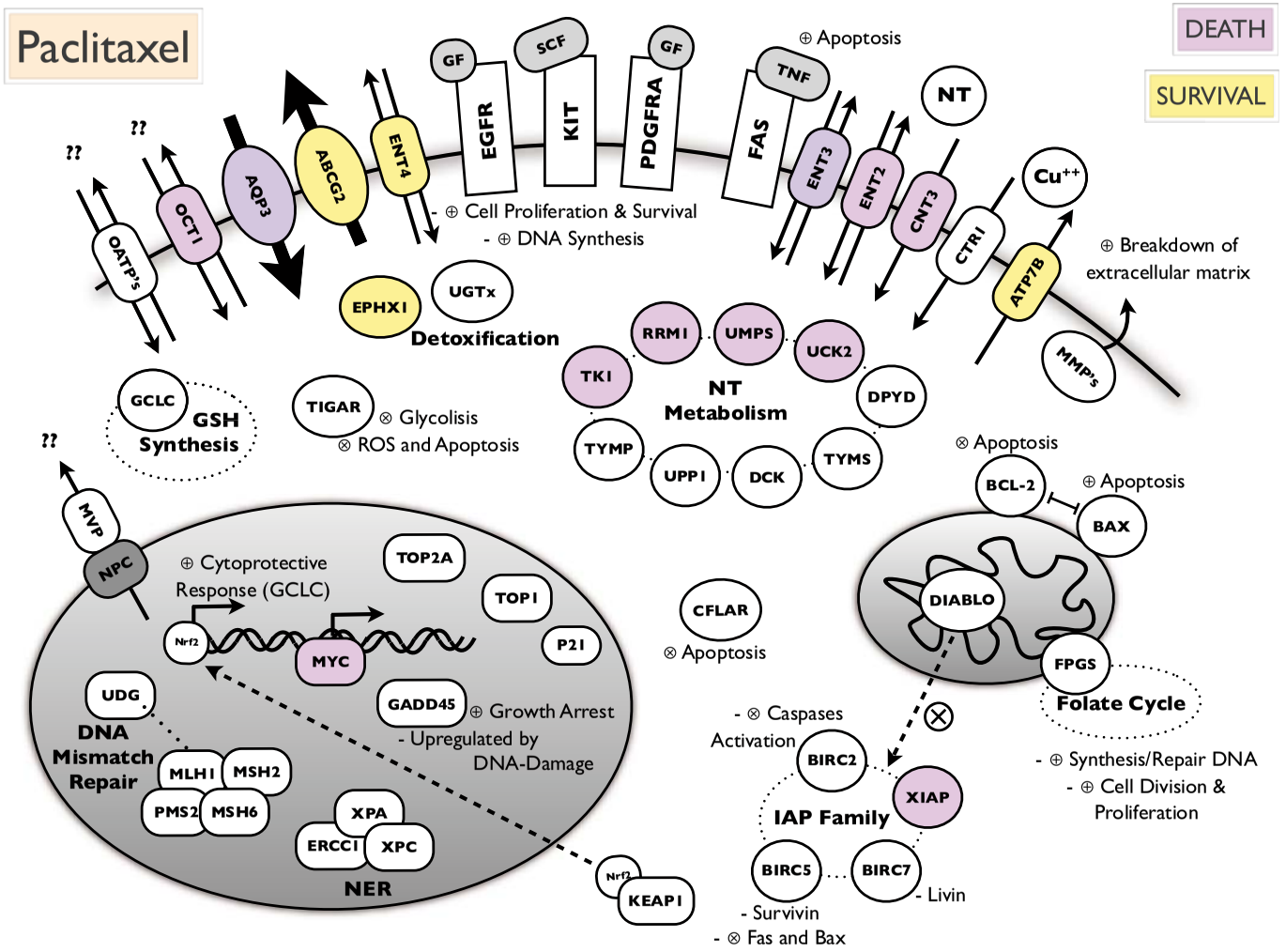

Figure 57. Cartoon representing genes with a significant correlation to cell responsiveness to paclitaxel treatment. Genes highlighted in purple positively correlate with cell sensitivity to the treatment. Genes highlighted in yellow positively correlate with cell resistance to the treatment.

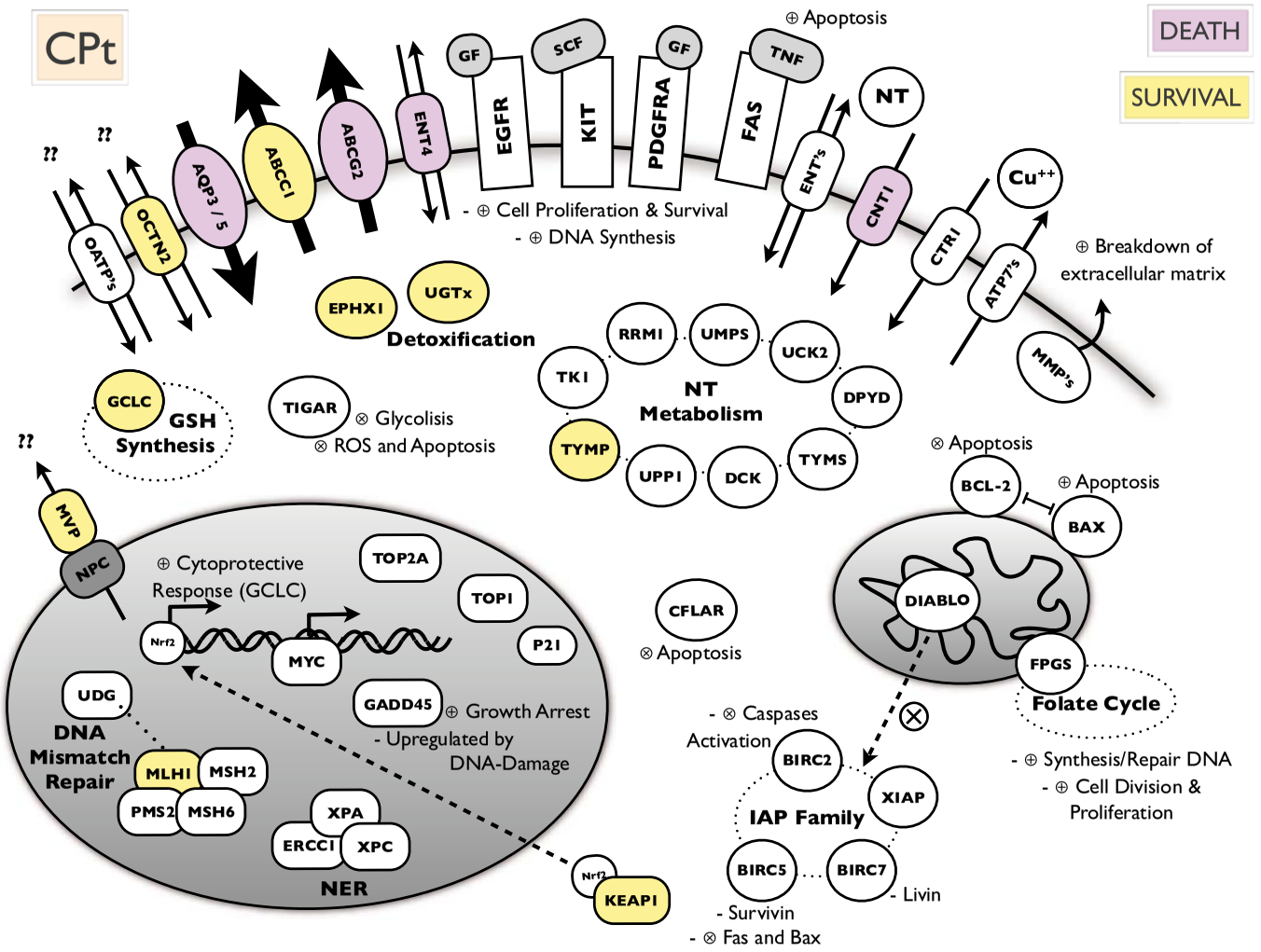

Figure 58. Cartoon representing genes with a significant correlation to cell responsiveness to cisplatin treatment. Genes highlighted in purple positively correlate with cell sensitivity to the treatment. Genes highlighted in yellow positively correlate with cell resistance to the treatment.

18.5 DISCUSSION

There is wide variability in the response of individuals to standard doses of drug therapy. This is an important problem in clinical practice, where it can lead to therapeutic failures or adverse drug events. Polymorphisms and different expression levels in genes coding for metabolising enzymes and drug transporters can affect drug efficacy and toxicity. Pharmacogenetics aims to identify individuals predisposed to high risk of toxicity and low response from standard doses of anticancer drugs. Therefore, measurement of transporter and drug metabolising enzyme genes may prove useful in predicting anticancer drug response (Y. Huang *et al*. 2004; Bosch 2008)

Drug metabolising enzymes are proteins that catalyse the biochemical modifications of xenobiotics (e.g. drugs) and endogenous chemicals (e.g. hormones, neurotransmitters). Broadly, drug metabolising enzymes are divided into two categories: Phase I (functionalising) enzymes that introduce or remove functional groups in a substrate through oxidation, reduction, or hydrolysis; and Phase II (conjugating) enzymes that transfer moieties from a cofactor to a substrate. Essentially all of the major human metabolising enzymes exhibit genetic polymorphisms at the genomic level or variable expression levels, and many of these enzymes have clinically relevant genetic polymorphisms. A gene is considered to be polymorphic when the frequency of a variant allele in a specific population is at least 1%. (Evans & Relling 1999; Bluth & J. Li 2011).

Membrane transporters play a critical role in drug response as they provide the targets for many commonly used drugs and are major determinants of drug absorption, distribution, and elimination. Most of them belong to one of the two major super-families of membrane transport proteins, the ATP-binding cassette (ABC) transporters, and the solute carrier (SLC) transporters. They are subject to both genotypic and phenotypic polymorphisms, and variation in drug transporters may be the reason for inter-individual variability in pharmacokinetic disposition, efficacy, and toxicity of drug transporter substrates (Benjeddou 2010; Y. Huang *et al*. 2004; V. H. Lee *et al*. 2001).

The solute carrier (SLC) superfamily of transporters consists of more than 300 members subdivided into 47 families. They are expressed in most tissues, but primarily in the liver, lung, kidney, and intestine. Most solute carrier transporters are localised at either the basolateral or apical plasma membrane of polarised cells, but some are expressed in mitochondria and other organelles (Wojtal *et al*. 2009). Typical SLC transporters consist of several trans-membranes α-helices connected by intra- and extracellular loops and function as either monomers or hetero- or homodimers (Wojtal *et al*. 2009). SLC transporters are membrane-associated transporters that facilitate the passage of solutes, including peptides, bile acids, amino acids, ions, xenobiotics, drugs, and other biologically active compounds, across cell membranes in epithelial tissues, such as intestine and liver (Hediger *et al*. 2004; Koepsell *et al*. 2007). In the intestine, SLCs are critically involved in drug absorption, thus determining distribution and pharmacokinetic characteristics of many drugs (Meier *et al*. 2007).

The new era of personalised medicine, which integrates the uniqueness of an individual with respect to the pharmacokinetics and pharmacodynamics of a drug, holds promise as a means to provide greater safety and efficacy in drug design and development. Personalised medicine is particularly important in oncology, whereby most clinically used anticancer drugs have a narrow therapeutic window and exhibit a large interindividual pharmacokinetic and pharmacodynamic variability. This variability can be explained, at least in part, by genetic variations in the genes encoding drug metabolising enzymes, transporters, or drug targets. Understanding of how genetic variations influence drug disposition and action could help in tailoring cancer therapy based on individual's genetic makeup. The growing number of publications reporting genetic population data for the solute carrier transporters in particular shows their importance, as well as the increased interest in investigating them in most recent pharmacogenetics/genomics research projects (Bluth & J. Li 2011; Benjeddou 2010).

An overview picture of the gene clusters here identified would suggest that genes encoding broad selectivity NT transporters positively correlate with nucleos(t)ide metabolism related genes, selected growth factor receptors, DNA MMR system and IAP family members, together with some other genes (FPGS, KEAP1, MYC and

TOP1), they all providing a general framework for cell survival and proliferation. Some other transporter proteins belonging to the SLC22 and SLCO families show very consistent correlations, either positive or negative thus suggesting they might play roles in these events, however the rationale for that will require further analysis. Correlations within clusters are statistically very consistent and it is highly likely that they define particular cell phenotypes, probably implicated in cell survival and proliferation, as discussed above.

In fact, the concept of a global network connecting different pathways has been previously developed, specially in yeast, where a global network governing DNA integrity was identified including 16 functional modules like DNA replication, oxidative stress response or DNA repair, all of them being essential for efficient repair of the endogenous DNA damage and cell survival (Pan *et al.* 2006). Subsequent studies compiled extensive experimental data in yeast and human models and performed an even wider gene association, where genes involved in regulation of nucleotide metabolism and DNA repair stood out as the most solid related pathways by both natural and synthetic connections (Hannum *et al*. 2009; Conde-Pueyo *et al*. 2009).

Going one step further, we analyzed possible master genes that could regulate or connect somehow all these different modules or mini-pathways among them, closing this global network as a whole. One potential candidate was Protein Kinase C (PKC), at least as a meeting point for most of them.

PKC is a family of phospholipid-dependent serine/threonine kinases that regulate a wide variety of cellular functions. The PKC family consists of at least eleven members that have been categorised into three groups based on their structure and biochemical properties. Conventional or cPKCs (α, βI, βII and γ) require Ca^{2+} and diacylglycerol (DAG) for their activation. Novel or nPKCs(δ, ε, η and θ) are dependent on DAG but not Ca^{2+} whereas atypical or aPKCs (ζ and λ/ι) are independent of both Ca^{2+} and DAG (Basu & Sivaprasad 2007). Various PKC isozymes are present in the same cell and mediate specific functions, some of them being capable to phosphorylate the same protein substrate (Totoń *et al*. 2011). However, PKCε is the

only PKC isozyme that has been associated with oncogenesis, behaving as an oncoprotein and is believed to function as an antiapoptotic protein. Such a way that PKCε contribution to oncogenesis is not only by inducing disordered cell growth but also by inhibiting cell death (Basu & Sivaprasad 2007).

Numerous cellular activities are modulated by PKCε interaction with cytoskeletal structures, including migration and adhesion, proliferation and differentiation. Gene expression, transport mechanisms, inflammation and immunity and secretory functions are also affected by PKCε-mediated mechanisms (Figure 59) (Totoń *et al*. 2011). One of those mechanisms to regulate cell proliferation is via activation of Ras/Raf-1 pathway acting downstream of Ras but upstream of Raf-1, remaining unclear if it exists a direct phosphorylation, and also at some other points of this cascade. On the other hand, PKCε involvement in NF-kB activation develops a key role in differentiation and regulation of apoptosis, together with the ERKs/MAPKs cascade activation.

Growth factor tyrosine kinase receptors, including EGFR and PDGFR, once bounded to their ligands, trigger a signalling cascade that leads to activation of transcription and translation of genes involved in proliferation, increasing growth activity. Precisely, signalling pathways activated by RTK stimulation include the Ras/Raf/MAPK pathway, the PLCγ /PKC pathway, PI3K/Akt, and Src family tyrosine kinases (Besson & Yong 2001). In fact, it has been reported that PKCε could activate both indirectly and directly phosphorylating Akt, promoting cell survival. Even more, the PKCε-Akt complex could crosstalk with a third pathway to mediate antiapoptotic effects (Basu & Sivaprasad 2007).

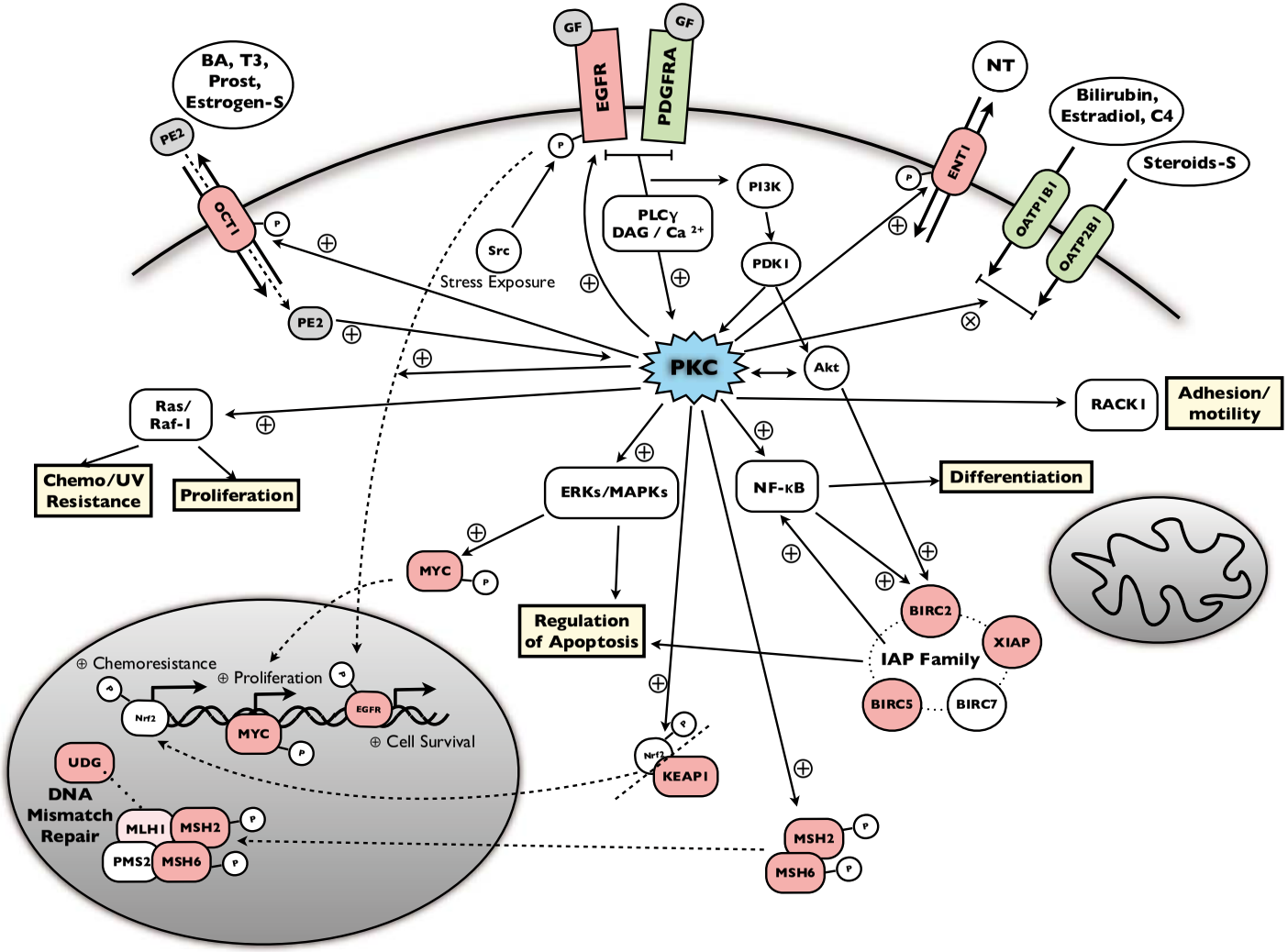

Figure 59. Cartoon representing a novel network connected to PKC. Representation of the global network involved in cell survival and proliferation and the role of PKC regulating and connecting the different mini-pathways that compose it. Colored genes were found to be correlated in our transcriptomic study. Genes in red have a positive correlation among them. Genes in green have negative correlations respect to the genes colored in red. PKC seems to be a common element that might establish a global connection inside the network.

Being EGFR and PDGFRA members of the same family and activating, in principle, the same kind of pathways, might not be easy to understand the rationale for the inverse correlation of those RTK with PKC shown in our results. A possible explanation could be, on one hand, EGFR PKC-mediated phosphorylation stabilises ligand-receptor interactions and results in intensification of EGFR signalling (Gulliford *et al*. 1999). Furthermore, it has been recently described that this phosphorylation is also a key step in Src-mediated translocation of EGFR to the nucleus, where it induces the transcription of genes essential for cell survival after stress exposure (Dittmann *et al*. 2009). On the other hand, different biochemical events are initiated by PDGF depending on the cell stage (Jones & Kazlauskas 2001). PDGF activates PKC at two different times and these two intervals of PKC activity make unequal contributions to the mitogenic response (Balciunaite *et al*. 2000) in a way that progression into phase S can be promoted or inhibited depending on the time when PKC is activated (W. Zhou *et al*. 1993). Ambiguous role of PDGF-mediated PKC activation and the multiple implications of EGFR in survival and cell proliferation might explain why the first one is negatively correlated with those gene clusters, whereas the second one is positively correlated with the global network apparently focused on proliferation and cell survival.

Inhibitors of apoptosis protein (IAP) family members can bind and potently inhibit the proteolytic activities of some caspases and block their activation, and thus prevent apoptosis induced by TNF. In addition, IAPs have diverse functions in signal transduction, independently of caspase inhibition, like playing a complex role in modulating the signalling pathways that activate NF-kB transcription factors promoting cell survival (Plati *et al*. 2011; Altieri 2010). In turn, it has been shown that c-IAP2 expression is upregulated by PKC in PMA-mediated induction (Q. Wang *et al*. 2003) and also by activating Akt via PI3K-dependent signalling (Sade & Sarin 2003), thus completing a complex system of reciprocal regulation.

Members of the DNA MMR system are also closely regulated by PKC. It has been reported a correlation between PKC activity and MMR protein expression and activity (Humbert *et al*. 2002), consistent with our results of mRNA expression levels. Furthermore, it has been demonstrated a direct interaction between PKC and hMSH2

and hMSH6 and their consequent phosphorylation (Hernandez-Pigeon *et al*. 2005), in such a manner that hMutSα, a protein complex formed by hMSH2 and hMSH6, increases its stability and is translocated into the nucleus (Christmann *et al*. 2002)

Genes like KEAP1 or c-Myc, that appeared to be positively correlated with gene clusters of our study, have their own connection with PKC. In the case of KEAP1, PKC directly phosphorylates the transcription factor Nrf2 while bound to KEAP1, promoting their dissociation and Nrf2 translocation into the nucleus in response to oxidative stress (H. C. Huang 2002; Niture *et al*. 2010). Regarding c-Myc, an oncogenic transcription factor, a recent study demonstrated how Prostaglandin E2 (an OCT1 substrate), increased the mRNA and protein expression of c-Myc and its nuclear accumulation via phosphorylation in a ERK-dependent manner, post PKC activation (L. Yu *et al*. 2009).

Concerning transporter membrane proteins, several studies described how they are generally regulated by different kinases, including PKC, but probably never being linked to a global network of proliferation and cell survival. In the particular case of ENT1, it was proved that an acute stimulation of PKC causes a rapid increase in hENT1 nucleoside uptake in a manner which is PKC δ or ε-dependent (Coe *et al*. 2002). Most recently, this group also demonstrated, for the same time, a directly phosphorylation of ENT1 by PKC (Reyes *et al*. 2011). Similarly, OCT1 is stimulated by PKC-dependent phosphorylation (Ciarimboli 2005; Mehrens *et al*. 2000), despite a direct interaction between the transporter and the kinase has not been proved yet. In contrast, OATP1B1/2B1 transporter activity is downregulated by PKC but not by direct phosphorylation, but in a PKC-mediated clathrin-dependent internalization and followed by lysosomal degradation (Köck *et al*. 2010; Guo & Klaassen 2001).

In conclusion, in this study we present a potential global network, which encompasses genes from several modules some of them have not been related before, with the general purpose of promoting cell survival and proliferation. This network would probably be connected/modulated through PKC and its different mechanisms of regulation (figure 59). In addition, this is the first time such idea is

raised in a human model with the particularity to include key membrane transporters, considering their role far beyond than mere substrate transporters. Finally, further analysis should be performed in order to understand more in depth how this system is regulated and, over all, how it could be applied in future strategies against cancer.

Regarding the correlation between gene expression and cell response to a specific treatment, results obtained to date anticipate the existence of sets of genes whose expression correlate with chemosensitivity, in a manner which appears to be independent of the origin of the cell line, thus proving to be probable common predictors of digestive cancer chemotherapy. However, further studies need to be done to validate these results and define a reliable set of chemotherapy responsiveness predictors.

V. General Discussion

As previously explained, hENT2 is the human nucleoside transporter for which most splice variants have been described to date, in contrast to hENT1 for which no variants have been reported yet. In this dissertation, we have identified 3 novel splice variants of hENT2 which encode 2 novel nuclear isoforms of this transporter protein. As we demonstrated, these variants appear to be functional and ubiquitously expressed among cell lines and tissues, although the pattern of expression levels may vary depending on the growth conditions and the cellular needs.

The physiological role of these novel nuclear variants of hENT2 still remains unclear, since there is no evidence of the presence of the nucleoside salvage pathway inside the nucleus. If that would be eventually the case, the presence of nucleoside transporters at the nuclear membrane might not have any relevant meaning. Nonetheless, based on the protein-protein interactions obtained from the screening with MYTH technique, other functional implications might be coming up.

On one hand, nuclear variants of hENT2 could be involved in alternative splicing regulation, since they appeared to interact with several splicing factors. As we proved, hENT2 splicing patterns vary depending upon growth conditions, suggesting the existence of a regulation (or even a self-regulation) mechanism of the splicing phenomenon. Several proteins have been previously described as self-regulators of alternative splicing (Sureau *et al*. 2001; Sun *et al*. 2010; de Morree *et al*. 2012). In this dissertation we propose the hypothesis of HNP32 and HNP36 proteins, localised at the nuclear membrane, interacting with splice regulation factors and modulating their availability to bind pre-mRNA, thus determining the splice sites recognised by the spliceosome. In such a way, hENT2 itself would regulate the ratio between the wt isoform and the nuclear variants to adapt itself to the cellular situation.

On the other hand, there is the possibility that HNP32 and HNP36 would function as nuclear translocators of small peptides or carriers. In fact, the nuclear internalization of a drug vehicle used in therapy via hENT2 has been reported (Hansen *et al*. 2007). In our results, we found several putative interactions between hENT2 and proteins involved in mRNA export to the cytosol. Although this hypothesis comes from

our speculations of the results obtained by MYTH, we consider the necessity of a deeper study on the transport capacity of the hENT2 nuclear variants and their potential role in alternative splicing regulation.

Among the PPI obtained from the MYTH screening, several proteins were kinases and phosphatases, outstanding the case of protein phosphatase 1 (PP1). This protein is well known to regulate alternative splicing phenomena by phosphorylation (Novoyatleva *et al*. 2008; Stamm 2008), coinciding with our proposal of HNP32 and HNP36 as alternative splicing self-regulators. In addition, PP1 could also participate in the hENT2 wt regulation by phosphorylation.

According to our *in vitro* phosphorylation assays, hENT2 could be phosphorylated by CKII inside the cell. CKII is a kinase that appears to be unregulated because it is constitutively active. Therefore, it has been suggested that changes in the phosphorylation status of CKII substrates would depend on regulated dephosphorylation (Pinna 1990). Considering the putative interaction between hENT2 and PP1, we propose a possible regulation of hENT2 by phosphorylation, where the transporter would be phosphorylated by default and regulation would come by dephosphorylation via PP1. Actually, considering our biotinylation results where we found a double band at 54 KDa, the supposed phosphorylated protein would remain intracellular while the supposed non-phosphorylated protein would be active at the plasma membrane.

Although we could not demonstrate a direct *in vitro* phosphorylation of hENT2 by PKC, this kinase appears to be involved in hENT2 trafficking regulation. Activation of PKC promotes hENT2 trafficking to the plasma membrane although it does not necessarily entails an increase of hENT2-related transport activity. Actually, the clear consequence of the hENT2 translocation to the plasma membrane is a significant decrease on hENT1 activity. These observations coincide with the fact that hENT1 and hENT2 appear to have a fine opposite regulated transport activity (Aguayo *et al*. 2005). As a consequence, an increase of hENT2 presence at the plasma membrane supposes a downregulation on hENT1 activity.

GLUT-4 has been described to have a dual population at the plasma membrane, where some of the proteins are active while the others are not functional (Funaki *et al*. 2004). Considering all the results obtained from the phosphorylation and biotinylation assays we performed, we propose the theory of a dual population of hENT2 proteins at the plasma membrane. One non-phosphorylated hENT2 isoform of 54 KDa could be related with transport activity, while another isoform of 45 KDa would not be active as a transporter, despite being present at the plasma membrane. Similarly, two different kinds of regulation by phosphorylation would affect hENT2 function, either regulating its trafficking to the plasma membrane via PKC, or activating its function as a nucleoside transporter via PP1. These two putative pathways of regulation would not necessarily be independent of each other.

Finally, our transcriptomic analysis of gastro-hepatic cell lines allowed us to place hENT2 within a global gene network involved in cell proliferation and survival. PKC appeared to be a possible central point of regulation of that network, coordinating a global response of the cell to the growth and environmental conditions. In addition, part of that novel network, including hENT2, could be involved in response to paclitaxel treatment. As we understand, a positive response to the therapy would not be determined by the hENT2 role as a transporter, but by the context of this network connecting several genes involved in proliferation and cell survival. Further studies need to be developed in order to validate those genes as potential response predictors.

VI. Conclusions

1. We have identified 3 novel splice variants of hENT2 which encode 2 novel nuclear isoforms of the transporter. These variants appear to be functional and ubiquitously expressed among cell lines and tissues.

2. hENT2 is *in vitro* phosphorylated by CKII. Since CKII is constitutively active, hENT2 could be regulated by dephosphorylation via PP1.

3. Activation of PKC by PDD treatment promotes hENT2 trafficking to the plasma membrane in HEK-293 cells, at the same time that it decreases hENT1 transport activity.

4. hENT2 could have a dual population at the plasma membrane. One non-phosphorylated hENT2 isoform of 54 KDa could be related with transport activity, while another isoform of 45 KDa would not be active as a transporter, despite being present at the plasma membrane.

5. We defined a novel global gene network apparently involved in cell proliferation and survival. ENT1, ENT2 and CNT3 are part of this network, where PKC could play a central role as a regulator.

6. ENT2, together with some other genes involved in cell proliferation and survival, negatively correlate to cell survival as a response to paclitaxel treatment in gastro-hepatic cell lines.

VII. Bibliography

A

Abdulla, P. & Coe, I.R., 2007. Characterization and functional analysis of the promoter for the human equilibrative nucleoside transporter gene, hENT1. *Nucleosides, Nucleotides and Nucleic Acids*, 26(1), pp.99–110.

Acimovic, Y. & Coe, I.R., 2002. Molecular evolution of the equilibrative nucleoside transporter family: identification of novel family members in prokaryotes and eukaryotes. *Molecular biology and evolution*, 19(12), pp.2199–2210.

Aggen, J.B., Nairn, A.C. & Chamberlin, R., 2000. Regulation of protein phosphatase-1. *Chemistry & biology*, 7(1), pp.R13–23.

Aguayo, C. et al., 2005. Equilibrative nucleoside transporter 2 is expressed in human umbilical vein endothelium, but is not involved in the inhibition of adenosine transport induced by hyperglycaemia. *Placenta*, 26(8-9), pp.641–653.

Al-Ayoubi, A.M. et al., 2012. Mitogen-Activated Protein Kinase Phosphorylation of Splicing Factor 45 (SPF45) Regulates SPF45 Alternative Splicing Site Utilization, Proliferation, and Cell Adhesion. *Molecular and cellular biology*, 32 (14), pp.2880–2893.

Altieri, D.C., 2010. Survivin and IAP proteins in cell-death mechanisms. *The Biochemical journal*, 430(2), pp.199–205.

Aly, A.S.I. et al., 2010. Subpatent infection with nucleoside transporter 1-deficient Plasmodium blood stage parasites confers sterile protection against lethal malaria in mice. *Cellular microbiology*, 12(7), pp.930–938.

Amanchy, R. et al., 2007. A curated compendium of phosphorylation motifs. *Nature biotechnology*, 25(3), pp.285–286.

Angelakos, E.T. & Glassman, P.M., 1961. Cardiovascular action of adenosine and other nucleosides. *Proceedings of the Society for Experimental Biology and Medicine. Society for Experimental Biology and Medicine (New York, N.Y.)*, 106, pp.762–763.

Arastu-Kapur, S. et al., 2005. Second-site suppression of a nonfunctional mutation within the Leishmania donovani inosine-guanosine transporter. *The Journal of biological chemistry*, 280(3), pp.2213–2219.

Aridor, M. & Traub, L.M., 2002. Cargo selection in vesicular transport: the making and breaking of a coat. *Traffic (Copenhagen, Denmark)*, 3(8), pp.537–546.

Aymerich, I. et al., 2006. Extracellular adenosine activates AMP-dependent protein kinase (AMPK). *Journal of cell science*, 119(Pt 8), pp.1612–1621.

Aymerich, I. et al., 2005. The concentrative nucleoside transporter family (SLC28): new roles beyond salvage? *Biochemical Society transactions*, 33(Pt 1), pp.216–219.

B

Balciunaite, E. et al., 2000. PDGF initiates two distinct phases of protein kinase C activity that make unequal contributions to the G0 to S transition. *Current biology : CB*, 10(5), pp.261–267.

Baldwin, S.A. et al., 2005. Functional characterization of novel human and mouse equilibrative nucleoside transporters (hENT3 and mENT3) located in intracellular membranes. *The Journal of biological chemistry*, 280(16), pp.15880–15887.

Baldwin, S.A. et al., 1999. Nucleoside transporters: molecular biology and implications for therapeutic development. *Molecular medicine today*, 5(5), pp.216–224.

Baliova, M., Betz, H. & Jursky, F., 2004. Calpain-mediated proteolytic cleavage of the neuronal glycine transporter, GlyT2. *Journal of neurochemistry*, 88(1), pp.227–232.

Balnave, K. et al., 1981. Observation on the efficacy and pharmacokinetics of betaxolol (SL 75212), a cardioselective beta-adrenoceptor blocking drug. *British journal of clinical pharmacology*, 11(2), pp.171–180.

Balse, E. et al., 2009. Cholesterol modulates the recruitment of Kv1.5 channels from Rab11-associated recycling endosome in native atrial myocytes. *Proceedings of the National Academy of Sciences of the United States of America*, 106(34), pp. 14681–14686.

Bardenheuer, W. et al., 2005. Resistance to cytarabine and gemcitabine and in vitro selection of transduced cells after retroviral expression of cytidine deaminase in human hematopoietic progenitor cells. *Leukemia : official journal of the Leukemia Society of America, Leukemia Research Fund, UK*, 19(12), pp.2281–2288.

Barlowe, C., 1998. COPII and selective export from the endoplasmic reticulum. *Biochimica et biophysica acta*, 1404(1-2), pp.67–76.

Barnes, K. et al., 2006. Distribution and functional characterization of equilibrative nucleoside transporter-4, a novel cardiac adenosine transporter activated at acidic pH. *Circulation Research*, 99(5), pp.510–519.

Basu, A. & Sivaprasad, U., 2007. Protein kinase Cepsilon makes the life and death decision. *Cellular signalling*, 19(8), pp.1633–1642.

Bauer, P.M. et al., 2003. Compensatory phosphorylation and protein-protein interactions revealed by loss of function and gain of function mutants of multiple serine phosphorylation sites in endothelial nitric-oxide synthase. *The Journal of biological chemistry*, 278(17), pp.14841–14849.

Beal, P.R. et al., 2004. The equilibrative nucleoside transporter family, SLC29. *Pfl gers Archiv European Journal of Physiology*, 447(5), pp.735–743.

Benjeddou, M., 2010. Solute carrier transporters: Pharmacogenomics research opportunities in Africa. *African Journal of Biotechnology*, 9(54), pp.9191–9195.

Bennett, E.R. & Kanner, B.I., 1997. The membrane topology of GAT-1, a (Na+ + Cl-)-coupled gamma-aminobutyric acid transporter from rat brain. *The Journal of biological chemistry*, 272(2), pp.1203–1210.

Berggård, T., Linse, S. & James, P., 2007. Methods for the detection and analysis of protein-protein interactions. *Proteomics*, 7(16), pp.2833–2842.

Besson, A. & Yong, V.W., 2001. Mitogenic signaling and the relationship to cell cycle regulation in astrocytomas. *Journal of neuro-oncology*, 51(3), pp.245–264.

Bi, X., Corpina, R.A. & Goldberg, J., 2002. Structure of the Sec23/24-Sar1 pre-budding complex of the COPII vesicle coat. *Nature*, 419(6904), pp.271–277.

Bielli, A. et al., 2005. Regulation of Sar1 NH2 terminus by GTP binding and hydrolysis promotes membrane deformation to control COPII vesicle fission. *The Journal of cell biology*, 171(6), pp.919–924.

Biswas, A. et al., 2011. Opposing Action of Casein Kinase 1 and Calcineurin in Nucleo-cytoplasmic Shuttling of Mammalian Translation Initiation Factor eIF6. *Journal of Biological Chemistry*, 286(4), pp.3129–3138.

Black, D.L., 2003. Mechanisms of alternative pre-messenger RNA splicing. *Annual review of biochemistry*, 72, pp.291–336.

Bluth, M. & Li, J., 2011. Pharmacogenomics of drug metabolizing enzymes and transporters: implications for cancer therapy. *Pharmacogenomics and Personalized Medicine*, p.11.

Boleti, H. et al., 1997. Molecular identification of the equilibrative NBMPR-sensitive (es) nucleoside transporter and demonstration of an equilibrative NBMPR-insensitive (ei) transport activity in human erythroleukemia (K562) cells. *Neuropharmacology*, 36(9), pp.1167–1179.

Bone, D.B.J. et al., 2007. Differential regulation of mouse equilibrative nucleoside transporter 1 (mENT1) splice variants by protein kinase CK2. *Molecular Membrane Biology*, 24(4), pp.294–303.

Bonifacino, J.S. & Glick, B.S., 2004. The mechanisms of vesicle budding and fusion. *Cell*, 116(2), pp.153–166.

Bosch, T.M., 2008. *Methods in Molecular Biology™* J. M. Walker & Q. Yan, eds., Totowa, NJ: Humana Press.

Bottalico, B. et al., 2007. The organic cation transporters (OCT1, OCT2, EMT) and the plasma membrane monoamine transporter (PMAT) show differential distribution and cyclic expression pattern in human endometrium and early pregnancy decidua. *Molecular Reproduction and Development*, 74(10), pp.1303–1311.

Boulon, S. et al., 2004. PHAX and CRM1 Are Required Sequentially to Transport U3 snoRNA to Nucleoli. *Molecular Cell*, 16(5), pp.777–787.

Boutz, P.L. et al., 2007. A post-transcriptional regulatory switch in polypyrimidine tract-binding proteins reprograms alternative splicing in developing neurons. *Genes & development*, 21(13), pp.1636–1652.

Bracco, L. & Kearsey, J., 2003. The relevance of alternative RNA splicing to pharmacogenomics. *Trends in biotechnology*, 21(8), pp.346–353.

Bressan, G.C. & Kobarg, J., 2010. From protein interaction profile to functional assignment: the human protein Ki-1/57 is associated with pre-mRNA splicing events. *RNA biology*, 7(3), pp.268–271.

Bressan, G.C. et al., 2009. Functional association of human Ki-1/57 with pre-mRNA splicing events. *FEBS Journal*, 276(14), pp.3770–3783.

Bronckaers, A. et al., 2009. The dual role of thymidine phosphorylase in cancer development and chemotherapy. *Medicinal research reviews*, 29(6), pp.903–953.

Buck, T.M., Eledge, J. & Skach, W.R., 2004. Evidence for stabilization of aquaporin-2 folding mutants by N-linked glycosylation in endoplasmic reticulum. *American journal of physiology. Cell physiology*, 287(5), pp.C1292–9.

Butt, S.J.B. & Pitman, R.M., 2005. Indirect phosphorylation-dependent modulation of postsynaptic nicotinic acetylcholine responses by 5-hydroxytryptamine. *The European journal of neuroscience*, 21(5), pp.1181–1188.

C

Cabrita, M.A. et al., 2002. Molecular biology and regulation of nucleoside and nucleobase transporter proteins in eukaryotes and prokaryotes. *Biochemistry and cell biology = Biochimie et biologie cellulaire*, 80(5), pp.623–638.

Cai, G. et al., 2005. The role of N-glycosylation in the stability, trafficking and GABA-uptake of GABA-transporter 1. Terminal N-glycans facilitate efficient GABA-uptake activity of the GABA transporter. *The FEBS journal*, 272(7), pp.1625–1638.

Cao, W., Jamison, S.F. & Garcia-Blanco, M.A., 1997. Both phosphorylation and dephosphorylation of ASF/SF2 are required for pre-mRNA splicing in vitro. *RNA (New York, NY)*, 3(12), pp.1456–1467.

Carneiro, A.M. et al., 2002. The multiple LIM domain-containing adaptor protein Hic-5 synaptically colocalizes and interacts with the dopamine transporter. *Journal of Neuroscience*, 22(16), pp.7045–7054.

Castro-Fernández, C., Maya-Núñez, G. & Conn, P.M., 2005. Beyond the signal sequence: protein routing in health and disease. *Endocrine reviews*, 26(4), pp. 479–503.

Cerecedo, L.R., 1927. Studies on the Physiology of Pyrimidines. *The Journal of biological chemistry*, 75, pp.661–670.

Chakrabarti, S. & Freedman, J.E., 2008. Dipyridamole, cerebrovascular disease, and the vasculature. *Vascular pharmacology*, 48(4-6), pp.143–149.

Chang, C. et al., 2004. Molecular requirements of the human nucleoside transporters hCNT1, hCNT2, and hENT1. *Molecular pharmacology*, 65(3), pp.558–570.

Chang, D. et al., 2000. Steady-state regulation of the human DNA mismatch repair system. *Journal of Biological Chemistry*, 275(37), p.29178.

Chanrion, B. et al., 2007. Physical interaction between the serotonin transporter and neuronal nitric oxide synthase underlies reciprocal modulation of their activity. *Proceedings of the National Academy of Sciences of the United States of America*, 104(19), pp.8119–8124.

Chaudary, N. et al., 2004. The adenosine transporter, mENT1, is a target for adenosine receptor signaling and protein kinase Cepsilon in hypoxic and pharmacological preconditioning in the mouse cardiomyocyte cell line, HL-1. *The Journal of pharmacology and experimental therapeutics*, 310(3), pp.1190–1198.

Che, M., Ortiz, D.F. & Arias, I.M., 1995. Primary structure and functional expression of a cDNA encoding the bile canalicular, purine-specific Na(+)-nucleoside cotransporter. *The Journal of biological chemistry*, 270(23), pp.13596–13599.

Chen, C.-F. et al., 2010a. Overlapping high-resolution copy number alterations in cancer genomes identified putative cancer genes in hepatocellular carcinoma. *Hepatology (Baltimore, Md)*, 52(5), pp.1690–1701.

Chen, G. et al., 2006. Loss of N-linked glycosylation reduces urea transporter UT-A1 response to vasopressin. *The Journal of biological chemistry*, 281(37), pp. 27436–27442.

Chen, Y.L., Eriksson, S. & Chang, Z.F., 2010b. Regulation and Functional Contribution of Thymidine Kinase 1 in Repair of DNA Damage. *Journal of Biological Chemistry*, 285(35), pp.27327–27335.

Cheng, D. et al., 2007. The Arginine Methyltransferase CARM1 Regulates the Coupling of Transcription and mRNA Processing. *Molecular Cell*, 25(1), pp.71–83.

Cheong, J.K., Gunaratnam, L. & Hsu, S.I.-H., 2008. CRM1-mediated nuclear export is required for 26 S proteasome-dependent degradation of the TRIP-Br2 proto-oncoprotein. *The Journal of biological chemistry*, 283(17), pp.11661–11676.

Cherry, C.L. & Wesselingh, S.L., 2003. Nucleoside analogues and HIV: the combined cost to mitochondria. *The Journal of antimicrobial chemotherapy*, 51(5), pp. 1091–1093.

Cheung, J.C. & Reithmeier, R.A.F., 2007. Scanning N-glycosylation mutagenesis of membrane proteins. *Methods (San Diego, Calif.)*, 41(4), pp.451–459.

Choi, D.-S.S. et al., 2004. The type 1 equilibrative nucleoside transporter regulates ethanol intoxication and preference. *Nature neuroscience*, 7(8), pp.855–861.

Chow, L. et al., 2005. Analysis of human equilibrative nucleoside transporter 1 (hENT1) protein in non-Hodgkin's lymphoma by immunohistochemistry. *Modern pathology : an official journal of the United States and Canadian Academy of Pathology, Inc*, 18(4), pp.558–564.

Christmann, M., Tomicic, M.T. & Kaina, B., 2002. Phosphorylation of mismatch repair proteins MSH2 and MSH6 affecting MutSalpha mismatch-binding activity. *Nucleic acids research*, 30(9), pp.1959–1966.

Chu, S. et al., 2012. Regulation of adenosine levels during cerebral ischemia. *Nature Publishing Group*, pp.1–7.

Ciarimboli, G., 2005. Individual PKC-Phosphorylation Sites in Organic Cation Transporter 1 Determine Substrate Selectivity and Transport Regulation. *Journal of the American Society of Nephrology*, 16(6), pp.1562–1570.

Clarke, M.L. et al., 2002. The role of membrane transporters in cellular resistance to anticancer nucleoside drugs. *Cancer treatment and research*, 112, pp.27–47.

Coe, I.R. et al., 2002. PKC regulation of the human equilibrative nucleoside transporter, hENT1. *FEBS letters*, 517(1-3), pp.201–205.

Conde-Pueyo, N. et al., 2009. Human synthetic lethal inference as potential anti-cancer target gene detection. *BMC Systems Biology*, 3(1), p.116.

Crawford, C.R. et al., 1998. Cloning of the human equilibrative, nitrobenzylmercaptopurine riboside (NBMPR)-insensitive nucleoside transporter ei by functional expression in a transport-deficient cell line. *The Journal of biological chemistry*, 273(9), pp.5288–5293.

Cui, L., Rajasekariah, G.R. & Martin, S.K., 2001. A nonspecific nucleoside hydrolase from Leishmania donovani: implications for purine salvage by the parasite. *Gene*, 280(1-2), pp.153–162.

D

Damaraju, V.L. et al., 2003. Nucleoside anticancer drugs: the role of nucleoside transporters in resistance to cancer chemotherapy. *Oncogene*, 22(47), pp.7524–7536.

Das, S. et al., 2012. ONCOGENIC SPLICING FACTOR SRSF1 IS A CRITICAL TRANSCRIPTIONAL TARGET OF MYC. *Cell reports*, 1(2), pp.110–117.

de Morree, A. et al., 2012. Self-regulated alternative splicing at the AHNAK locus. *The FASEB journal : official publication of the Federation of American Societies for Experimental Biology*, 26(1), pp.93–103.

De Koning, H.P. et al., 2003. Identification and characterisation of high affinity nucleoside and nucleobase transporters in Toxoplasma gondii. *International Journal for Parasitology*, 33(8), pp.821–831.

Deane, C.M. et al., 2002. Protein interactions: two methods for assessment of the reliability of high throughput observations. *Molecular & cellular proteomics : MCP*, 1(5), pp.349–356.

del Santo, B. et al., 1998. Differential expression and regulation of nucleoside transport systems in rat liver parenchymal and hepatoma cells. *Hepatology (Baltimore, Md)*, 28(6), pp.1504–1511.

Diaz-Font, A. & Beales, P.L., 2008. How to shape cells and influence polarized protein trafficking. *Developmental cell*, 15(6), pp.799–800.

Dittmann, K., Mayer, C. & Rodemann, H.P., 2009. Nuclear EGFR as Novel Therapeutic Target. *Strahlentherapie und Onkologie*, 186(1), pp.1–6.

Doyle, T.H., Mornex, F. & McKenna, W.G., 2001. The clinical implications of gemcitabine radiosensitization. *Clinical cancer research : an official journal of the American Association for Cancer Research*, 7(2), pp.226–228.

Draheim, V. et al., 2010. N-glycosylation of ABC transporters is associated with functional activity in sandwich-cultured rat hepatocytes. *European journal of*

pharmaceutical sciences : official journal of the European Federation for Pharmaceutical Sciences, 41(2), pp.201–209.

Duflot, S. et al., 2004. ATP-sensitive K(+) channels regulate the concentrative adenosine transporter CNT2 following activation by A(1) adenosine receptors. *Molecular and cellular biology*, 24(7), pp.2710–2719.

Dunwiddie, T.V. & Diao, L., 2000. Regulation of extracellular adenosine in rat hippocampal slices is temperature dependent: role of adenosine transporters. *Neuroscience*, 95(1), pp.81–88.

E

Eckford, P.D.W. & Sharom, F.J., 2009. ABC efflux pump-based resistance to chemotherapy drugs. *Chemical reviews*, 109(7), pp.2989–3011.

Edwards, A.S. et al., 1999. Carboxyl-terminal phosphorylation regulates the function and subcellular localization of protein kinase C betaII. *The Journal of biological chemistry*, 274(10), pp.6461–6468.

Eltzschig, H.K. et al., 2005. HIF-1-dependent repression of equilibrative nucleoside transporter (ENT) in hypoxia. *The Journal of experimental medicine*, 202(11), pp. 1493–1505.

Elwi, A.N. et al., 2006. Renal nucleoside transporters: physiological and clinical implications. *Biochemistry and cell biology = Biochimie et biologie cellulaire*, 84 (6), pp.844–858.

Endres, C.J. & Unadkat, J.D., 2005. Residues Met89 and Ser160 in the human equilibrative nucleoside transporter 1 affect its affinity for adenosine, guanosine, S6-(4-nitrobenzyl)-mercaptopurine riboside, and dipyridamole. *Molecular pharmacology*, 67(3), pp.837–844.

Endres, C.J. et al., 2009. The role of the equilibrative nucleoside transporter 1 (ENT1) in transport and metabolism of ribavirin by human and wild-type or Ent1-/- mouse erythrocytes. *Journal of Pharmacology and Experimental Therapeutics*, 329(1), pp.387–398.

Endres, C.J., Sengupta, D.J. & Unadkat, J.D., 2004. Mutation of leucine-92 selectively reduces the apparent affinity of inosine, guanosine, NBMPR [S6-(4-nitrobenzyl)-mercaptopurine riboside] and dilazep for the human equilibrative nucleoside transporter, hENT1. *The Biochemical journal*, 380(Pt 1), pp.131–137.

Engel, A. & Gaub, H.E., 2008. Structure and Mechanics of Membrane Proteins. *Annual review of biochemistry*, 77(1), pp.127–148.

Engel, K., Zhou, M. & Wang, J., 2004. Identification and characterization of a novel monoamine transporter in the human brain. *The Journal of biological chemistry*, 279(48), pp.50042–50049.

Errasti-Murugarren, E. et al., 2012. Role of the Transporter Regulator Protein (RS1) in the Modulation of Concentrative Nucleoside Transporters (CNTs) in Epithelia. *Molecular pharmacology*, 82(1), pp.59–67.

Errasti-Murugarren, E. et al., 2009. A splice variant of the SLC28A3 gene encodes a novel human concentrative nucleoside transporter-3 (hCNT3) protein localized in the endoplasmic reticulum. *The FASEB journal : official publication of the Federation of American Societies for Experimental Biology*, 23(1), pp.172–182.

Errasti-Murugarren, E. et al., 2008. Functional characterization of a nucleoside-derived drug transporter variant (hCNT3C602R) showing altered sodium-binding capacity. *Molecular pharmacology*, 73(2), pp.379–386.

Evans, W.E. & Relling, M.V., 1999. Pharmacogenomics: translating functional genomics into rational therapeutics. *Science*, 286(5439), pp.487–491.

F

Farhan, H. et al., 2007. Concentrative export from the endoplasmic reticulum of the gamma-aminobutyric acid transporter 1 requires binding to SEC24D. *The Journal of biological chemistry*, 282(10), pp.7679–7689.

Farias, M. et al., 2010. Nitric oxide reduces SLC29A1 promoter activity and adenosine transport involving transcription factor complex hCHOP-C/EBP in human umbilical vein endothelial cells from gestational diabetes. *Cardiovascular research*, 86(1), pp.45–54.

Farrell, J.J. et al., 2009. Human equilibrative nucleoside transporter 1 levels predict response to gemcitabine in patients with pancreatic cancer. *Gastroenterology*, 136(1), pp.187–195.

Fleming, T.P. et al., 1992. Amplification and/or overexpression of platelet-derived growth factor receptors and epidermal growth factor receptor in human glial tumors. *Cancer Research*, 52(16), pp.4550–4553.

Fletcher, L.M. et al., 2000. Role for the microtubule cytoskeleton in GLUT4 vesicle trafficking and in the regulation of insulin-stimulated glucose uptake. *The Biochemical journal*, 352 Pt 2, pp.267–276.

Fowler, J.D. et al., 2008. Kinetic investigation of the inhibitory effect of gemcitabine on DNA polymerization catalyzed by human mitochondrial DNA polymerase. *The Journal of biological chemistry*, 283(22), pp.15339–15348.

Freeze, H.H. & Aebi, M., 2005. Altered glycan structures: the molecular basis of congenital disorders of glycosylation. *Current opinion in structural biology*, 15(5), pp.490–498.

Fukuchi, Y. et al., 2010. Characterization of ribavirin uptake systems in human hepatocytes. *Journal of Hepatology*, 52(4), pp.486–492.

Funaki, M., Randhawa, P. & Janmey, P.A., 2004. Separation of insulin signaling into distinct GLUT4 translocation and activation steps. *Molecular and cellular biology*, 24(17), pp.7567–7577.

Futai, E. et al., 2004. GTP/GDP exchange by Sec12p enables COPII vesicle bud formation on synthetic liposomes. *The EMBO journal*, 23(21), pp.4146–4155.

G

Galmarini, C.M. et al., 2002. Expression of a non-functional p53 affects the sensitivity of cancer cells to gemcitabine. *International journal of cancer Journal international du cancer*, 97(4), pp.439–445.

Galmarini, C.M. et al., 2003. Influence of p53 and p21(WAF1) expression on sensitivity of cancer cells to cladribine. *Biochemical pharmacology*, 65(1), pp.121–129.

Garcia-Blanco, M.A., Baraniak, A.P. & Lasda, E.L., 2004. Alternative splicing in disease and therapy. *Nature biotechnology*, 22(5), pp.535–546.

Geiger, J.D., LaBella, F.S. & Nagy, J.I., 1985. Characterization of nitrobenzylthioinosine binding to nucleoside transport sites selective for adenosine in rat brain. *The Journal of neuroscience : the official journal of the Society for Neuroscience*, 5 (3), pp.735–740.

Gerstin, K.M., Dresser, M.J. & Giacomini, K.M., 2002. Specificity of human and rat orthologs of the concentrative nucleoside transporter, SPNT. *American journal of physiology Renal physiology*, 283(2), pp.F344–9.

Gilbert, J.A. et al., 2006. Gemcitabine pharmacogenomics: cytidine deaminase and deoxycytidylate deaminase gene resequencing and functional genomics. *Clinical cancer research : an official journal of the American Association for Cancer Research*, 12(6), pp.1794–1803.

Gill, R.K. et al., 2008. Function, expression, and characterization of the serotonin transporter in the native human intestine. *American journal of physiology. Gastrointestinal and liver physiology*, 294(1), pp.G254–62.

Giovannetti, E. et al., 2008. Correlation between cytidine deaminase genotype and gemcitabine deamination in blood samples. *Nucleosides, Nucleotides and Nucleic Acids*, 27(6), pp.720–725.

Gomes, J.R. et al., 2011. Cleavage of the Vesicular GABA Transporter under Excitotoxic Conditions Is Followed by Accumulation of the Truncated Transporter in Nonsynaptic Sites. *Journal of Neuroscience*, 31(12), pp.4622–4635.

Govindarajan, R. et al., 2009. Facilitated mitochondrial import of antiviral and anticancer nucleoside drugs by human equilibrative nucleoside transporter-3. *AJP: Gastrointestinal and Liver Physiology*, 296(4), pp.G910–G922.

Gray, J.H., Owen, R.P. & Giacomini, K.M., 2004. The concentrative nucleoside transporter family, SLC28. *Pfl gers Archiv European Journal of Physiology*, 447 (5), pp.728–734.

Grden, M. et al., 2008. High glucose suppresses expression of equilibrative nucleoside transporter 1 (ENT1) in rat cardiac fibroblasts through a mechanism dependent on PKC-zeta and MAP kinases. *Journal of Cellular Physiology*, 215(1), pp.151–160.

Griffith, D.A. & Jarvis, S.M., 1996. Nucleoside and nucleobase transport systems of mammalian cells. *Biochimica et biophysica acta*, 1286(3), pp.153–181.

Griffiths, M., Beaumont, N., et al., 1997a. Cloning of a human nucleoside transporter implicated in the cellular uptake of adenosine and chemotherapeutic drugs. *Nature medicine*, 3(1), pp.89–93.

Griffiths, M., Yao, S.Y.M., et al., 1997b. Molecular cloning and characterization of a nitrobenzylthioinosine-insensitive (ei) equilibrative nucleoside transporter from human placenta. *The Biochemical journal*, 328 (Pt 3), pp.739–743.

Guillén-Gómez, E. et al., 2011. New role of the human equilibrative nucleoside transporter 1 (hENT1) in epithelial-to-mesenchymal transition in renal tubular cells. *Journal of Cellular Physiology*, pp.n/a–n/a.

Gulliford, T., Ouyang, X. & Epstein, R.J., 1999. Intensification of growth factor receptor signalling by phorbol treatment of ligand-primed cells implies a dimer-stabilizing effect of protein kinase C-dependent juxtamembrane domain phosphorylation. *Cellular signalling*, 11(4), pp.245–252.

Guo, G.L. & Klaassen, C.D., 2001. Protein kinase C suppresses rat organic anion transporting polypeptide 1- and 2-mediated uptake. *The Journal of pharmacology and experimental therapeutics*, 299(2), pp.551–557.

Guzmán-Gutiérrez, E. et al., 2010. Differential expression of functional nucleoside transporters in non-differentiated and differentiated human endothelial progenitor cells. *Placenta*, 31(10), pp.928–936.

H

Hagiwara, M., 2005. Alternative splicing: a new drug target of the post-genome era. *Biochimica et biophysica acta*, 1754(1-2), pp.324–331.

Hamilton, S.R. et al., 2001. Subcellular distribution and membrane topology of the mammalian concentrative Na+-nucleoside cotransporter rCNT1. *The Journal of biological chemistry*, 276(30), pp.27981–27988.

Hamm, L.L., Feng, Z. & Hering-Smith, K.S., 2010. Regulation of sodium transport by ENaC in the kidney. *Current opinion in nephrology and hypertension*, 19(1), pp. 98–105.

Hammond, J.R., 2000. Interaction of a series of draflazine analogues with equilibrative nucleoside transporters: species differences and transporter subtype selectivity. *Naunyn-Schmiedeberg's archives of pharmacology*, 361(4), pp.373–382.

Handa, M. et al., 2001. Cloning of a novel isoform of the mouse NBMPR-sensitive equilibrative nucleoside transporter (ENT1) lacking a putative phosphorylation site. *Gene*, 262(1-2), pp.301–307.

Hannum, G. et al., 2009. Genome-Wide Association Data Reveal a Global Map of Genetic Interactions among Protein Complexes. *PLoS Genetics*, 5(12), p.e1000782.

Hansen, J.E. et al., 2007. Intranuclear protein transduction through a nucleoside salvage pathway. *The Journal of biological chemistry*, 282(29), pp.20790–20793.

Hanton, S.L. et al., 2005. Diacidic motifs influence the export of transmembrane proteins from the endoplasmic reticulum in plant cells. *The Plant cell*, 17(11), pp. 3081–3093.

Hartmann, E. et al., 2008. Five-gene model to predict survival in mantle-cell lymphoma using frozen or formalin-fixed, paraffin-embedded tissue. *Journal of Clinical Oncology*, 26(30), pp.4966–4972.

Hediger, M.A. et al., 2004. The ABCs of solute carriers: physiological, pathological and therapeutic implications of human membrane transport proteins. *Pfl gers Archiv European Journal of Physiology*, 447(5), pp.465–468.

Hegele, A. et al., 2012. Dynamic Protein-Protein Interaction Wiring of the Human Spliceosome. *Molecular Cell*, 45(4), pp.567–580.

Helenius, A. & Aebi, M., 2001. Intracellular functions of N-linked glycans. *Science*, 291 (5512), pp.2364–2369.

Hendriks, G. et al., 2004. Glycosylation is important for cell surface expression of the water channel aquaporin-2 but is not essential for tetramerization in the endoplasmic reticulum. *The Journal of biological chemistry*, 279(4), pp.2975–2983.

Hernandez-Pigeon, H. et al., 2005. hMutS alpha is protected from ubiquitin-proteasome-dependent degradation by atypical protein kinase C zeta phosphorylation. *Journal of molecular biology*, 348(1), pp.63–74.

Hnilicová, J. et al., 2011. Histone Deacetylase Activity Modulates Alternative Splicing J. Valcarcel, ed. *PLoS ONE*, 6(2), p.e16727.

Hu, H. et al., 2006. Electrophysiological characterization and modeling of the structure activity relationship of the human concentrative nucleoside transporter 3 (hCNT3). *Molecular pharmacology*, 69(5), pp.1542–1553.

Huang, H.C., 2002. Phosphorylation of Nrf2 at Ser-40 by Protein Kinase C Regulates Antioxidant Response Element-mediated Transcription. *Journal of Biological Chemistry*, 277(45), pp.42769–42774.

Huang, Q.Q. et al., 1994. Cloning and functional expression of a complementary DNA encoding a mammalian nucleoside transport protein. *The Journal of biological chemistry*, 269(27), pp.17757–17760.

Huang, Y. et al., 2004. Membrane transporters and channels: role of the transportome in cancer chemosensitivity and chemoresistance. *Cancer Research*, 64(12), pp. 4294–4301.

Hubeek, I. et al., 2005. The human equilibrative nucleoside transporter 1 mediates in vitro cytarabine sensitivity in childhood acute myeloid leukaemia. *British journal of cancer*, 93(12), pp.1388–1394.

Huber-Ruano, I. et al., 2010. Link between high-affinity adenosine concentrative nucleoside transporter-2 (CNT2) and energy metabolism in intestinal and liver parenchymal cells. *Journal of Cellular Physiology*, 225(2), pp.620–630.

Huber-Ruano, I. et al., 2012. Functional outcome of a novel SLC29A3 mutation identified in a patient with H syndrome. *Biochemical and biophysical research communications*, pp.1–6.

Humbert, O. et al., 2002. Implication of protein kinase C in the regulation of DNA mismatch repair protein expression and function. *The Journal of biological chemistry*, 277(20), pp.18061–18068.

Hyde, R.J. et al., 2001. The ENT family of eukaryote nucleoside and nucleobase transporters: recent advances in the investigation of structure/function relationships and the identification of novel isoforms. *Molecular Membrane Biology*, 18(1), pp.53–63.

I

Iyer, K. et al., 2005. Utilizing the split-ubiquitin membrane yeast two-hybrid system to identify protein-protein interactions of integral membrane proteins. *Science's STKE : signal transduction knowledge environment*, 2005(275), p.pl3.

J

Jang, J.-H., 2002. Identification and characterization of soluble isoform of fibroblast growth factor receptor 3 in human SaOS-2 osteosarcoma cells. *Biochemical and biophysical research communications*, 292(2), pp.378–382.

Jascur, T. & Boland, C.R., 2006. Structure and function of the components of the human DNA mismatch repair system. *International journal of cancer Journal international du cancer*, 119(9), pp.2030–2035.

Jayanthi, L.D. et al., 2005. Evidence for biphasic effects of protein kinase C on serotonin transporter function, endocytosis, and phosphorylation. *Molecular pharmacology*, 67(6), pp.2077–2087.

Jennings, L.L. et al., 2001. Distinct regional distribution of human equilibrative nucleoside transporter proteins 1 and 2 (hENT1 and hENT2) in the central nervous system. *Neuropharmacology*, 40(5), pp.722–731.

Johnson, Z.L., Cheong, C.-G. & Lee, S.-Y., 2012. Crystal structure of a concentrative nucleoside transporter from Vibrio cholerae at 2.4 Å. *Nature*, pp.1–6.

Johnsson, N. & Varshavsky, A., 1994. Split ubiquitin as a sensor of protein interactions in vivo. *Proceedings of the National Academy of Sciences of the United States of America*, 91(22), pp.10340–10344.

Jones, S.M. & Kazlauskas, A., 2001. Growth-factor-dependent mitogenesis requires two distinct phases of signalling. *Nature cell biology*, 3(2), pp.165–172.

K

Kaji, H. et al., 2007. Proteomics reveals N-linked glycoprotein diversity in Caenorhabditis elegans and suggests an atypical translocation mechanism for integral membrane proteins. *Molecular & cellular proteomics : MCP*, 6(12), pp. 2100–2109.

Kalckar, H.M., 1950. The biological incorporation of purines and pyrimidines into nucleosides and nucleic acid. *Biochimica et biophysica acta*, 4(1-3), pp.232–237.

Kang, N. et al., 2010. Human equilibrative nucleoside transporter-3 (hENT3) spectrum disorder mutations impair nucleoside transport, protein localization, and stability. *Journal of Biological Chemistry*, 285(36), pp.28343–28352.

Keller, P. & Simons, K., 1997. Post-Golgi biosynthetic trafficking. *Journal of cell science*, 110 (Pt 24), pp.3001–3009.

Keskanokwong, T. et al., 2007. Interaction of integrin-linked kinase with the kidney chloride/bicarbonate exchanger, kAE1. *The Journal of biological chemistry*, 282 (32), pp.23205–23218.

Kim, J.-H. et al., 2011. Functional role of the polymorphic 647 T/C variant of ENT1 (SLC29A1) and its association with alcohol withdrawal seizures. *PLoS ONE*, 6 (1), p.e16331.

King, A.E. et al., 2006. Nucleoside transporters: from scavengers to novel therapeutic targets. *Trends in pharmacological sciences*, 27(8), pp.416–425.

Kipp, H. & Arias, I.M., 2002. Trafficking of Canalicular ABC Transporters in Hepatocytes. *Annual Review of Physiology*, 64(1), pp.595–608.

Kiss, A. et al., 2000. Molecular cloning and functional characterization of inhibitor-sensitive (mENT1) and inhibitor-resistant (mENT2) equilibrative nucleoside transporters from mouse brain. *The Biochemical journal*, 352 Pt 2, pp.363–372.

Kitayama, S. et al., 1999. Dominant negative isoform of rat norepinephrine transporter produced by alternative RNA splicing. *The Journal of biological chemistry*, 274 (16), pp.10731–10736.

Kittanakom, S. et al., 2009. Analysis of membrane protein complexes using the split-ubiquitin membrane yeast two-hybrid (MYTH) system. *Methods in molecular biology (Clifton, N.J.)*, 548, pp.247–271.

Klein, K. et al., 2009. Hepatocyte nuclear factor-4 and bile acids regulate human concentrative nucleoside transporter-1 gene expression. *AJP: Gastrointestinal and Liver Physiology*, 296(4), pp.G936–G947.

Knight, D. et al., 2010. Equilibrative nucleoside transporter 2 regulates associative learning and synaptic function in Drosophila. *Journal of Neuroscience*, 30(14), pp.5047–5057.

Koepsell, H., Lips, K. & Volk, C., 2007. Polyspecific organic cation transporters: structure, function, physiological roles, and biopharmaceutical implications. *Pharmaceutical research*, 24(7), pp.1227–1251.

Kofler, M., 2004. Recognition Sequences for the GYF Domain Reveal a Possible Spliceosomal Function of CD2BP2. *Journal of Biological Chemistry*, 279(27), pp. 28292–28297.

Kong, W., Engel, K. & Wang, J., 2004. Mammalian nucleoside transporters. *Current drug metabolism*, 5(1), pp.63–84.

Korn, T., 2001. The Plasma Membrane-associated Protein RS1 Decreases Transcription of the Transporter SGLT1 in Confluent LLC-PK1 Cells. *Journal of Biological Chemistry*, 276(48), pp.45330–45340.

Köck, K. et al., 2010. Rapid modulation of the organic anion transporting polypeptide 2B1 (OATP2B1, SLCO2B1) function by protein kinase C-mediated internalization. *Journal of Biological Chemistry*, 285(15), pp.11336–11347.

Kroep, J.R. et al., 2002. Pretreatment deoxycytidine kinase levels predict in vivo gemcitabine sensitivity. *Molecular cancer therapeutics*, 1(6), pp.371–376.

L

Laggerbauer, B., 2005. The human U5 snRNP 52K protein (CD2BP2) interacts with U5-102K (hPrp6), a U4/U6.U5 tri-snRNP bridging protein, but dissociates upon tri-snRNP formation. *RNA (New York, NY)*, 11(5), pp.598–608.

Lai, Y., Bakken, A.H. & Unadkat, J.D., 2002. Simultaneous expression of hCNT1-CFP and hENT1-YFP in Madin-Darby canine kidney cells. Localization and vectorial transport studies. *The Journal of biological chemistry*, 277(40), pp.37711–37717.

Lai, Y., Tse, C.-M. & Unadkat, J.D., 2004. Mitochondrial expression of the human equilibrative nucleoside transporter 1 (hENT1) results in enhanced mitochondrial toxicity of antiviral drugs. *The Journal of biological chemistry*, 279(6), pp.4490–4497.

Lamba, J.K., 2009. Genetic factors influencing cytarabine therapy. *Pharmacogenomics*, 10(10), pp.1657–1674.

Lanahan, A. et al., 1992. Growth factor-induced delayed early response genes. *Molecular and cellular biology*, 12(9), pp.3919–3929.

Landfear, S.M., 2010. Transporters for drug delivery and as drug targets in parasitic protozoa. *Clinical pharmacology and therapeutics*, 87(1), pp.122–125.

Larráyoz, I.M. et al., 2004. Electrophysiological characterization of the human Na(+)/nucleoside cotransporter 1 (hCNT1) and role of adenosine on hCNT1 function. *The Journal of biological chemistry*, 279(10), pp.8999–9007.

Law, R.M., Stafford, A. & Quick, M.W., 2000. Functional regulation of gamma-aminobutyric acid transporters by direct tyrosine phosphorylation. *The Journal of biological chemistry*, 275(31), pp.23986–23991.

Leabu, M., 2006. Membrane fusion in cells: molecular machinery and mechanisms. *Journal of cellular and molecular medicine*, 10(2), pp.423–427.

Lee, E.-W. et al., 2006. Identification of the mitochondrial targeting signal of the human equilibrative nucleoside transporter 1 (hENT1): implications for interspecies differences in mitochondrial toxicity of fialuridine. *The Journal of biological chemistry*, 281(24), pp.16700–16706.

Lee, M.C.S. & Miller, E.A., 2007. Molecular mechanisms of COPII vesicle formation. *Seminars in cell & developmental biology*, 18(4), pp.424–434.

Lee, V.H., Sporty, J.L. & Fandy, T.E., 2001. Pharmacogenomics of drug transporters: the next drug delivery challenge. *Advanced drug delivery reviews*, 50 Suppl 1, pp.S33–40.

Leisewitz, A.V. et al., 2011. Regulation of ENT1 expression and ENT1-dependent nucleoside transport by c-Jun N-terminal kinase. *Biochemical and biophysical research communications*, 404(1), pp.370–375. Leung, G.P. et al., 2001. Characterization of nucleoside transport systems in cultured rat epididymal epithelium. *American journal of physiology. Cell physiology*, 280(5), pp.C1076–82.

Leung, G.P.H. & Tse, C.-M., 2007. The role of mitochondrial and plasma membrane nucleoside transporters in drug toxicity. *Expert Opinion on Drug Metabolism & Toxicology*, 3(5), pp.705–718.

Leung, P.-K. et al., 2007. The truncated ghrelin receptor polypeptide (GHS-R1b) acts as a dominant-negative mutant of the ghrelin receptor. *Cellular signalling*, 19 (5), pp.1011–1022.

Levy, E.D., Landry, C.R. & Michnick, S.W., 2010. Cell signaling. Signaling through cooperation. *Science*, 328(5981), pp.983–984.

Li, H. et al., 2008. Adenosine Transporter ENT4 Is a Direct Target of EWS/WT1 Translocation Product and Is Highly Expressed in Desmoplastic Small Round Cell Tumor. *PLoS ONE*, 3(6), p.e2353.

Lodish, H. et al., 2007. *Molecular Cell Biology*, W. H. Freeman.

Lotfi, K. et al., 2001. Pharmacological basis for cladribine resistance in a human acute T lymphoblastic leukaemia cell line selected for resistance to etoposide. *British journal of haematology*, 113(2), pp.339–346.

Löffler, M. et al., 2007. Physiological roles of vascular nucleoside transporters. *Arteriosclerosis, thrombosis, and vascular biology*, 27(5), pp.1004–1013.

Lu, G. et al., 2010. Chronic morphine treatment impaired hippocampal long-term potentiation and spatial memory via accumulation of extracellular adenosine acting on adenosine A1 receptors. *Journal of Neuroscience*, 30(14), pp.5058–5070.

Lu, S.P. & Lin, S.J., 2011. Phosphate-responsive Signaling Pathway Is a Novel Component of NAD+ Metabolism in Saccharomyces cerevisiae. *Journal of Biological Chemistry*, 286(16), pp.14271–14281.

M

Maase, von der, H., 2001. Gemcitabine-containing regimens in bladder cancer: A new standard of care. *Seminars in oncology*, 28(3 Suppl 10), pp.1–3.

Mackey, J.R. et al., 2005. Quantitative analysis of nucleoside transporter and metabolism gene expression in chronic lymphocytic leukemia (CLL): identification of fludarabine-sensitive and -insensitive populations. *Blood*, 105(2), pp.767–774.

Malakooti, J. et al., 2006. Transcriptional stimulation of the human NHE3 promoter activity by PMA: PKC independence and involvement of the transcription factor EGR-1. *The Biochemical journal*, 396(2), pp.327–336.

Mangravite, L.M., Xiao, G. & Giacomini, K.M., 2003. Localization of human equilibrative nucleoside transporters, hENT1 and hENT2, in renal epithelial cells. *American journal of physiology Renal physiology*, 284(5), pp.F902–10.

Mani, R.S. et al., 1998. Demonstration of equilibrative nucleoside transporters (hENT1 and hENT2) in nuclear envelopes of cultured human choriocarcinoma (BeWo) cells by functional reconstitution in proteoliposomes. *The Journal of biological chemistry*, 273(46), pp.30818–30825.

Maniatis, T. & Tasic, B., 2002. Alternative pre-mRNA splicing and proteome expansion in metazoans. *Nature*, 418(6894), pp.236–243.

Martínez-Maza, R. et al., 2001. The role of N-glycosylation in transport to the plasma membrane and sorting of the neuronal glycine transporter GLYT2. *The Journal of biological chemistry*, 276(3), pp.2168–2173.

Matlin, A.J., Clark, F. & Smith, C.W.J., 2005. Understanding alternative splicing: towards a cellular code. *Nature reviews. Molecular cell biology*, 6(5), pp.386–398.

Matsumoto, H. et al., 2005. Congenital muscular dystrophy with glycosylation defects of alpha-dystroglycan in Japan. *Neuromuscular disorders : NMD*, 15(5), pp.342–348.

McGee, S.L. et al., 2008. AMP-activated protein kinase regulates GLUT4 transcription by phosphorylating histone deacetylase 5. *Diabetes*, 57(4), pp.860–867.

Mehrens, T. et al., 2000. The affinity of the organic cation transporter rOCT1 is increased by protein kinase C-dependent phosphorylation. *Journal of the American Society of Nephrology : JASN*, 11(7), pp.1216–1224.

Meier, Y. et al., 2007. Regional distribution of solute carrier mRNA expression along the human intestinal tract. *Drug Metabolism and Disposition*, 35(4), pp.590–594.

Menéndez-Arias, L., 2008. Mechanisms of resistance to nucleoside analogue inhibitors of HIV-1 reverse transcriptase. *Virus research*, 134(1-2), pp.124–146.

Mikosch, M. et al., 2006. Diacidic motif is required for efficient transport of the K+ channel KAT1 to the plasma membrane. *Plant physiology*, 142(3), pp.923–930.

Miura, K. et al., 2011. Inhibitor of apoptosis protein family as diagnostic markers and therapeutic targets of colorectal cancer. *Surgery Today*, 41(2), pp.175–182.

Molina-Arcas, M. et al., 2005. Equilibrative nucleoside transporter-2 (hENT2) protein expression correlates with ex vivo sensitivity to fludarabine in chronic lymphocytic leukemia (CLL) cells. *Leukemia : official journal of the Leukemia Society of America, Leukemia Research Fund, UK*, 19(1), pp.64–68.

Molina-Arcas, M. et al., 2003. Fludarabine uptake mechanisms in B-cell chronic lymphocytic leukemia. *Blood*, 101(6), pp.2328–2334.

Molina-Arcas, M., Casado, F.J. & Pastor-Anglada, M., 2009. Nucleoside transporter proteins. *Current vascular pharmacology*, 7(4), pp.426–434.

Molinari, M., 2007. N-glycan structure dictates extension of protein folding or onset of disposal. *Nature chemical biology*, 3(6), pp.313–320.

Montero, T.D. et al., 2012. PPARa and PPARg regulate the nucleoside transporter hENT1. *Biochemical and biophysical research communications*, 419(2), pp.405–411.

Mornex, F. & Girard, N., 2006. Gemcitabine and radiation therapy in non-small cell lung cancer: state of the art. *Annals of oncology : official journal of the European Society for Medical Oncology / ESMO*, 17(12), pp.1743–1747.

Murray, A.W., 1971. The biological significance of purine salvage. *Annual review of biochemistry*, 40, pp.811–826.

Musa, H. et al., 2002. Immunocytochemical demonstration of the equilibrative nucleoside transporter rENT1 in rat sinoatrial node. *The journal of histochemistry and cytochemistry : official journal of the Histochemistry Society*, 50(3), pp.305–309.

N

Naydenova, Z., Rose, J.B. & Coe, I.R., 2008. Inosine and equilibrative nucleoside transporter 2 contribute to hypoxic preconditioning in the murine cardiomyocyte HL-1 cell line. *American journal of physiology Heart and circulatory physiology*, 294(6), pp.H2687–92.

Nelson, R.D. et al., 1998. Expression of an AQP2 Cre recombinase transgene in kidney and male reproductive system of transgenic mice. *The American journal of physiology*, 275(1 Pt 1), pp.C216–26.

Newton, A.C., 2003. Regulation of the ABC kinases by phosphorylation: protein kinase C as a paradigm. *The Biochemical journal*, 370(Pt 2), pp.361–371.

Nguyen, T.T. & Amara, S.G., 1996. N-linked oligosaccharides are required for cell surface expression of the norepinephrine transporter but do not influence substrate or inhibitor recognition. *Journal of neurochemistry*, 67(2), pp.645–655.

Niture, S.K. & Jaiswal, A.K., 2009. Prothymosin- Mediates Nuclear Import of the INrf2/Cul3{middle dot}Rbx1 Complex to Degrade Nuclear Nrf2. *Journal of Biological Chemistry*, 284(20), pp.13856–13868.

Niture, S.K., Jain, A.K. & Jaiswal, A.K., 2010. Antioxidant-induced modification of INrf2 cysteine 151 and PKC- -mediated phosphorylation of Nrf2 serine 40 are both required for stabilization and nuclear translocation of Nrf2 and increased drug resistance. *Journal of cell science*, 123(11), pp.1969–1969.

Nivillac, N.M.I., Bacani, J. & Coe, I.R., 2011. The life cycle of human equilibrative nucleoside transporter 1: From ER export to degradation. *Experimental cell research*, 317(11), pp.1567–1579.

Noji, T., Karasawa, A. & Kusaka, H., 2004. Adenosine uptake inhibitors. *European journal of pharmacology*, 495(1), pp.1–16.

Novoyatleva, T. et al., 2008. Protein phosphatase 1 binds to the RNA recognition motif of several splicing factors and regulates alternative pre-mRNA processing. *Human molecular genetics*, 17(1), pp.52–70.

O

O'Reilly, E.M., 2009. Pancreatic adenocarcinoma: new strategies for success. *Gastrointestinal cancer research : GCR*, 3(2 Suppl), pp.S11–5.

Oguri, T. et al., 2007. The absence of human equilibrative nucleoside transporter 1 expression predicts nonresponse to gemcitabine-containing chemotherapy in non-small cell lung cancer. *Cancer letters*, 256(1), pp.112–119.

Ohno, M. et al., 2000. PHAX, a Mediator of U snRNA Nuclear Export Whose Activity Is Regulated by Phosphorylation. *Cell*, 101(2), pp.187–198.

Okazaki, T. et al., 2010. Single nucleotide polymorphisms of gemcitabine metabolic genes and pancreatic cancer survival and drug toxicity. *Clinical cancer research : an official journal of the American Association for Cancer Research*, 16(1), pp.320–329.

Olsen, J.V. et al., 2006. Global, in vivo, and site-specific phosphorylation dynamics in signaling networks. *Cell*, 127(3), pp.635–648.

Osato, D.H. et al., 2003. Functional characterization in yeast of genetic variants in the human equilibrative nucleoside transporter, ENT1. *Pharmacogenetics*, 13(5), pp. 297–301.

Otterbein, L.R. et al., 2002. Crystal structures of the vitamin D-binding protein and its complex with actin: structural basis of the actin-scavenger system. *Proceedings of the National Academy of Sciences of the United States of America*, 99(12), pp.8003–8008.

P

Pan, X. et al., 2006. A DNA integrity network in the yeast Saccharomyces cerevisiae. *Cell*, 124(5), pp.1069–1081.

Paproski, R.J. et al., 2008. Mutation of Trp29 of human equilibrative nucleoside transporter 1 alters affinity for coronary vasodilator drugs and nucleoside selectivity. *The Biochemical journal*, 414(2), pp.291–300.

Pastor-Anglada, M. et al., 2005. Cell entry and export of nucleoside analogues. *Virus research*, 107(2), pp.151–164.

Pastor-Anglada, M. et al., 2004. Nucleoside transporters in chronic lymphocytic leukaemia. *Leukemia : official journal of the Leukemia Society of America, Leukemia Research Fund, UK*, 18(3), pp.385–393.

Pastor-Anglada, M. et al., 2008. SLC28 genes and concentrative nucleoside transporter (CNT) proteins. *Xenobiotica; the fate of foreign compounds in biological systems*, 38(7-8), pp.972–994.

Pastor-Anglada, M., Felipe, A. & Casado, F.J., 1998. Transport and mode of action of nucleoside derivatives used in chemical and antiviral therapies. *Trends in pharmacological sciences*, 19(10), pp.424–430.

Pennycooke, M. et al., 2001. Differential expression of human nucleoside transporters in normal and tumor tissue. *Biochemical and biophysical research communications*, 280(3), pp.951–959.

Perez-Bercoff, D. et al., 2007. Human immunodeficiency virus type 1: resistance to nucleoside analogues and replicative capacity in primary human macrophages. *Journal of virology*, 81(9), pp.4540–4550.

Perrone, F. et al., 2010. Receptor tyrosine kinase and downstream signalling analysis in diffuse malignant peritoneal mesothelioma. *European Journal of Cancer*, 46 (15), pp.2837–2848.

Pérez-Torras, S. et al., 2008. Adenoviral-mediated overexpression of human equilibrative nucleoside transporter 1 (hENT1) enhances gemcitabine response in human pancreatic cancer. *Biochemical pharmacology*, 76(3), pp.322–329.

Pinilla-Macua, I., Casado, F.J. & Pastor-Anglada, M., 2012. Structural determinants for rCNT2 sorting to the plasma membrane of polarized and non-polarized cells. *The Biochemical journal*, 442(3), pp.517–525.

Pinna, L.A., 1990. Casein kinase 2: an “eminence grise” in cellular regulation? *Biochimica et biophysica acta*, 1054(3), pp.267–284.

Plati, J., Bucur, O. & Khosravi-Far, R., 2011. Apoptotic cell signaling in cancer progression and therapy. *Integrative Biology*, 3(4), pp.279–296.

Pocard, T. et al., 2007. Distinct v-SNAREs regulate direct and indirect apical delivery in polarized epithelial cells. *Journal of cell science*, 120(Pt 18), pp.3309–3320.

Prakasha Gowda, A.S. et al., 2010. Incorporation of Gemcitabine and Cytarabine into DNA by DNA Polymerase β and Ligase III/XRCC1. *Biochemistry*, 49(23), pp. 4833–4840.

Procino, G. et al., 2003. Ser-256 phosphorylation dynamics of Aquaporin 2 during maturation from the ER to the vesicular compartment in renal cells. *The FASEB journal : official publication of the Federation of American Societies for Experimental Biology*, 17(13), pp.1886–1888.

Puebla, C. et al., 2008. High D-glucose reduces SLC29A1 promoter activity and adenosine transport involving specific protein 1 in human umbilical vein endothelium. *Journal of Cellular Physiology*, 215(3), pp.645–656.

Q

Quashie, N.B. et al., 2008. A comprehensive model of purine uptake by the malaria parasite Plasmodium falciparum: identification of four purine transport activities in intraerythrocytic parasites. *The Biochemical journal*, 411(2), p.287.

R

Racine, V. et al., 2007. Visualization and quantification of vesicle trafficking on a three-dimensional cytoskeleton network in living cells. *Journal of microscopy*, 225(Pt 3), pp.214–228.

Ratushny, V. & Golemis, E.A., 2008. Resolving the network of cell signaling pathways using the evolving yeast two-hybrid system. *BioTechniques*, 44 Supplement(4), pp.655–662.

Reed, R. & Hurt, E., 2002. A conserved mRNA export machinery coupled to pre-mRNA splicing. *Cell*, 108(4), pp.523–531.

Reid, G. et al., 2003. Characterization of the transport of nucleoside analog drugs by the human multidrug resistance proteins MRP4 and MRP5. *Molecular pharmacology*, 63(5), pp.1094–1103.

Reyes, G. & Coe, I.R., 2005. Genomics and proteomics of nucleoside transporters. *Current Pharmacogenomics*.

Reyes, G. et al., 2011. The Equilibrative Nucleoside Transporter (ENT1) can be phosphorylated at multiple sites by PKC and PKA. *Molecular Membrane Biology*, 28(6), pp.412–426.

Riegelhaupt, P.M., Frame, I.J. & Akabas, M.H., 2010. Transmembrane segment 11 appears to line the purine permeation pathway of the Plasmodium falciparum equilibrative nucleoside transporter 1 (PfENT1). *Journal of Biological Chemistry*, 285(22), pp.17001–17010.

Ritchie, D.B., Schellenberg, M.J. & MacMillan, A.M., 2009. Spliceosome structure: Piece by piece. *BBA - Gene Regulatory Mechanisms*, 1789(9-10), pp.624–633.

Ritzel, M.W. et al., 1997. Molecular cloning and functional expression of cDNAs encoding a human Na+-nucleoside cotransporter (hCNT1). *The American journal of physiology*, 272(2 Pt 1), pp.C707–14.

Ritzel, M.W. et al., 2001. Molecular identification and characterization of novel human and mouse concentrative Na+-nucleoside cotransporter proteins (hCNT3 and mCNT3) broadly selective for purine and pyrimidine nucleosides (system cib). *The Journal of biological chemistry*, 276(4), pp.2914–2927.

Rius, M. et al., 2010. Vectorial transport of nucleoside analogs from the apical to the basolateral membrane in double-transfected cells expressing the human concentrative nucleoside transporter hCNT3 and the export pump ABCC4. *Drug metabolism and disposition: the biological fate of chemicals*, 38(7), pp.1054–1063.

Robak, T., Korycka, A. & Robak, E., 2006. Older and new formulations of cladribine. Pharmacology and clinical efficacy in hematological malignancies. *Recent patents on anti-cancer drug discovery*, 1(1), pp.23–38.

Robertson, A.S., Smythe, E. & Ayscough, K.R., 2009. Functions of actin in endocytosis. *Cellular and molecular life sciences : CMLS*, 66(13), pp.2049–2065.

Robillard, K.R. et al., 2008. Characterization of mENT1 11, a Novel Alternative Splice Variant of the Mouse Equilibrative Nucleoside Transporter 1. *Molecular pharmacology*, 74(1), pp.264–273.

Rodriguez, O.C. et al., 2003. Conserved microtubule-actin interactions in cell movement and morphogenesis. *Nature cell biology*, 5(7), pp.599–609.

Roffers-Agarwal, J., Xanthos, J.B. & Miller, J.R., 2005. Regulation of actin cytoskeleton architecture by Eps8 and Abi1. *BMC cell biology*, 6, p.36.

Roma, M.-G., 2008. Dynamic localization of hepatocellular transporters in health and disease. *World journal of gastroenterology : WJG*, 14(44), p.6786.

Rose, J.B. et al., 2010. Equilibrative nucleoside transporter 1 plays an essential role in cardioprotection. *American journal of physiology Heart and circulatory physiology*, 298(3), pp.H771–7.

Ross, S.R., McTavish, D. & Faulds, D., 1993. Fludarabine. A review of its pharmacological properties and therapeutic potential in malignancy. *Drugs*, 45 (5), pp.737–759.

S

Saarikangas, J., Zhao, H. & Lappalainen, P., 2010. Regulation of the actin cytoskeleton-plasma membrane interplay by phosphoinositides. *Physiological reviews*, 90(1), pp.259–289.

Sabolić, I. et al., 2002. NHE3 and NHERF are targeted to the basolateral membrane in proximal tubules of colchicine-treated rats. *Kidney international*, 61(4), pp.1351–1364.

Sade, H. & Sarin, A., 2003. IL-7 inhibits dexamethasone-induced apoptosis via Akt/PKB in mature, peripheral T cells. *European journal of immunology*, 33(4), pp. 913–919.

Safarjalani, Al, O.N., Naguib, F.N.M. & Kouni, El, M.H., 2003. Uptake of nitrobenzylthioinosine and purine beta-L-nucleosides by intracellular Toxoplasma gondii. *Antimicrobial agents and chemotherapy*, 47(10), pp.3247–3251.

Sairam, M.R. et al., 1996. Follitropin signal transduction: alternative splicing of the FSH receptor gene produces a dominant negative form of receptor which inhibits hormone action. *Biochemical and biophysical research communications*, 226(3), pp.717–722.

Salazar, C. & Höfer, T., 2009. Multisite protein phosphorylation--from molecular mechanisms to kinetic models. *The FEBS journal*, 276(12), pp.3177–3198.

Salmon, W.C., Adams, M.C. & Waterman-Storer, C.M., 2002. Dual-wavelength fluorescent speckle microscopy reveals coupling of microtubule and actin movements in migrating cells. *The Journal of cell biology*, 158(1), pp.31–37.

Santini, D. et al., 2011. Human equilibrative nucleoside transporter 1 (hENT1) levels predict response to gemcitabine in patients with biliary tract cancer (BTC). *Current cancer drug targets*, 11(1), pp.123–129.

Sathe, M.N. et al., 2011. Regulation of Purinergic Signaling in Biliary Epithelial Cells by Exocytosis of SLC17A9-dependent ATP-enriched Vesicles. *Journal of Biological Chemistry*, 286(28), pp.25363–25376.

Sechi, A.S. & Wehland, J., 2000. The actin cytoskeleton and plasma membrane connection: PtdIns(4,5)P(2) influences cytoskeletal protein activity at the plasma membrane. *Journal of cell science*, 113 Pt 21, pp.3685–3695.

Sengupta, D.J. & Unadkat, J.D., 2004. Glycine 154 of the equilibrative nucleoside transporter, hENT1, is important for nucleoside transport and for conferring sensitivity to the inhibitors nitrobenzylthioinosine, dipyridamole, and dilazep. *Biochemical pharmacology*, 67(3), pp.453–458.

Sengupta, D.J. et al., 2002. A single glycine mutation in the equilibrative nucleoside transporter gene, hENT1, alters nucleoside transport activity and sensitivity to nitrobenzylthioinosine. *Biochemistry*, 41(5), pp.1512–1519.

Serebriiskii, I.G. & Golemis, E.A., 2001. Two-hybrid system and false positives. Approaches to detection and elimination. *Methods in molecular biology (Clifton, N.J.)*, 177, pp.123–134.

Sevier, C.S. et al., 2000. Efficient export of the vesicular stomatitis virus G protein from the endoplasmic reticulum requires a signal in the cytoplasmic tail that includes both tyrosine-based and di-acidic motifs. *Molecular biology of the cell*, 11(1), pp. 13–22.

Shanmugam, M. & Hernandez, N., 2008. Mitotic Functions for SNAP45, a Subunit of the Small Nuclear RNA-activating Protein Complex SNAPc. *Journal of Biological Chemistry*, 283(21), pp.14845–14856.

Sigoillot, F.D. et al., 2005. Nuclear localization and mitogen-activated protein kinase phosphorylation of the multifunctional protein CAD. *The Journal of biological chemistry*, 280(27), pp.25611–25620.

Singh, K.K. et al., 2010. Human SAP18 mediates assembly of a splicing regulatory multiprotein complex via its ubiquitin-like fold. *RNA (New York, NY)*, 16(12), pp. 2442–2454.

Smith, C.W. & Valcárcel, J., 2000. Alternative pre-mRNA splicing: the logic of combinatorial control. *Trends in biochemical sciences*, 25(8), pp.381–388.

Snider, J. et al., 2010. Detecting interactions with membrane proteins using a membrane two-hybrid assay in yeast. *Nature Protocols*, 5(7), pp.1281–1293.

Stamm, S., 2008. Regulation of alternative splicing by reversible protein phosphorylation. *The Journal of biological chemistry*, 283(3), pp.1223–1227.

Stamm, S., 2002. Signals and their transduction pathways regulating alternative splicing: a new dimension of the human genome. *Human molecular genetics*, 11 (20), pp.2409–2416.

Stamm, S. et al., 2005. Function of alternative splicing. *Gene*, 344, pp.1–20.

Stamnes, M., 2002. Regulating the actin cytoskeleton during vesicular transport. *Current Opinion in Cell Biology*, 14(4), pp.428–433.

Stewart, M., 2007. Molecular mechanism of the nuclear protein import cycle. *Nature reviews. Molecular cell biology*, 8(3), pp.195–208.

Stolk, M. et al., 2005. Subtype-specific regulation of equilibrative nucleoside transporters by protein kinase CK2. *The Biochemical journal*, 386(Pt 2), pp.281–289.

Stros, M., 2010. HMGB proteins: interactions with DNA and chromatin. *Biochimica et biophysica acta*, 1799(1-2), pp.101–113.

Sturiale, L. et al., 2005. Hypoglycosylation with increased fucosylation and branching of serum transferrin N-glycans in untreated galactosemia. *Glycobiology*, 15(12), pp.1268–1276.

Sumanasekera, C., Watt, D.S. & Stamm, S., 2008. Substances that can change alternative splice-site selection. *Biochemical Society transactions*, 36(Pt 3), pp. 483–490.

Sun, S. et al., 2010. SF2/ASF autoregulation involves multiple layers of post-transcriptional and translational control. *Nature structural & molecular biology*, 17(3), pp.306–312.

Sundaram, M. et al., 1998. Chimeric constructs between human and rat equilibrative nucleoside transporters (hENT1 and rENT1) reveal hENT1 structural domains interacting with coronary vasoactive drugs. *The Journal of biological chemistry*, 273(34), pp.21519–21525.

Sundaram, M. et al., 2001. Topology of a human equilibrative, nitrobenzylthioinosine (NBMPR)-sensitive nucleoside transporter (hENT1) implicated in the cellular uptake of adenosine and anti-cancer drugs. *The Journal of biological chemistry*, 276(48), pp.45270–45275.

Sureau, A. et al., 2001. SC35 autoregulates its expression by promoting splicing events that destabilize its mRNAs. *The EMBO journal*, 20(7), pp.1785–1796.

Suzuki, T. & Lennarz, W.J., 2002. Glycopeptide export from the endoplasmic reticulum into cytosol is mediated by a mechanism distinct from that for export of misfolded glycoprotein. *Glycobiology*, 12(12), pp.803–811.

Svoboda, M. et al., 2011. Organic anion transporting polypeptides (OATPs): regulation of expression and function. *Current drug metabolism*, 12(2), pp.139–153.

T

Takahashi, T. et al., 2010. Adenosine and inosine release during hypoxia in the isolated spinal cord of neonatal rats. *British Journal of Pharmacology*, 161(8), pp.1806–1816.

Tazi, J., Bakkour, N. & Stamm, S., 2009. Alternative splicing and disease. *Biochimica et biophysica acta*, 1792(1), pp.14–26.

Tietz, P.S. et al., 2006. Cytoskeletal and motor proteins facilitate trafficking of AQP1-containing vesicles in cholangiocytes. *Biology of the cell / under the auspices of the European Cell Biology Organization*, 98(1), pp.43–52.

Tilgner, H. et al., 2012. Deep sequencing of subcellular RNA fractions shows splicing to be predominantly co-transcriptional in the human genome but inefficient for lncRNAs. *Genome research*, 22(9), pp.1616–1625.

Tortorella, L.L. & Pilch, P.F., 2002. C2C12 myocytes lack an insulin-responsive vesicular compartment despite dexamethasone-induced GLUT4 expression. *American journal of physiology Endocrinology and metabolism*, 283(3), pp.E514–24.

Totoń, E. et al., 2011. Protein kinase Cε as a cancer marker and target for anticancer therapy. *Pharmacological reports : PR*, 63(1), pp.19–29.

Tsang, R.Y. et al., 2008. Immunohistochemistry for human concentrative nucleoside transporter 3 protein predicts fludarabine sensitivity in chronic lymphocytic leukemia. *Modern pathology : an official journal of the United States and Canadian Academy of Pathology, Inc*, 21(11), pp.1387–1393.

Tseng, Y. et al., 2005. How actin crosslinking and bundling proteins cooperate to generate an enhanced cell mechanical response. *Biochemical and biophysical research communications*, 334(1), pp.183–192.

U

Ukairo, O.T. et al., 2005. Recognition of benztropine by the dopamine transporter (DAT) differs from that of the classical dopamine uptake inhibitors cocaine, methylphenidate, and mazindol as a function of a DAT transmembrane 1 aspartic acid residue. *The Journal of pharmacology and experimental therapeutics*, 314(2), pp.575–583.

V

Valdés, R. et al., 2006. TGF-β transcriptionally activates the gene encoding the high-affinity adenosine transporter CNT2 in rat liver parenchymal cells. *Cellular and molecular life sciences : CMLS*, 63(21), pp.2527–2537.

Valdés, R. et al., 2009. An ab Initio structural model of a nucleoside permease predicts functionally important residues. *The Journal of biological chemistry*, 284(28), pp.19067–19076.

Valdés, R., Shinde, U. & Landfear, S.M., 2012. Cysteine Crosslinking Defines the Extracellular Gate for the Leishmania donovani Nucleoside Transporter 1.1. (LdNT1.1). *Journal of Biological Chemistry*.

Vallejo-Illarramendi, A., Domercq, M. & Matute, C., 2005. A novel alternative splicing form of excitatory amino acid transporter 1 is a negative regulator of glutamate uptake. *Journal of neurochemistry*, 95(2), pp.341–348.

van Balkom, B.W.M. et al., 2002. The role of putative phosphorylation sites in the targeting and shuttling of the aquaporin-2 water channel. *The Journal of biological chemistry*, 277(44), pp.41473–41479.

Van Belle, H., 1993. Nucleoside transport inhibition: a therapeutic approach to cardioprotection via adenosine? *Cardiovascular research*, 27(1), pp.68–76.

van den Ent, F., Amos, L.A. & Löwe, J., 2001. Prokaryotic origin of the actin cytoskeleton. *Nature*, 413(6851), pp.39–44.

Venables, J.P., 2006. Unbalanced alternative splicing and its significance in cancer. *BioEssays : news and reviews in molecular, cellular and developmental biology*, 28(4), pp.378–386.

Venables, J.P. et al., 2009. Cancer-associated regulation of alternative splicing. *Nature structural & molecular biology*, 16(6), pp.670–676.

Vickers, M.F. et al., 1999. Functional production and reconstitution of the human equilibrative nucleoside transporter (hENT1) in Saccharomyces cerevisiae. Interaction of inhibitors of nucleoside transport with recombinant hENT1 and a glycosylation-defective derivative (hENT1/N48Q). *The Biochemical journal*, 339 (Pt 1), pp.21–32.

Villarroya, J. et al., 2011. Targeted impairment of thymidine kinase 2 expression in cells induces mitochondrial DNA depletion and reveals molecular mechanisms of compensation of mitochondrial respiratory activity. *Biochemical and biophysical research communications*, 407(2), pp.333–338.

Visser, F. et al., 2002. Mutation of residue 33 of human equilibrative nucleoside transporters 1 and 2 alters sensitivity to inhibition of transport by dilazep and dipyridamole. *The Journal of biological chemistry*, 277(1), pp.395–401.

Visser, F., Baldwin, S.A., et al., 2005a. Identification and mutational analysis of amino acid residues involved in dipyridamole interactions with human and Caenorhabditis elegans equilibrative nucleoside transporters. *The Journal of biological chemistry*, 280(12), pp.11025–11034.

Visser, F., Zhang, J., et al., 2005b. Residue 33 of human equilibrative nucleoside transporter 2 is a functionally important component of both the dipyridamole and nucleoside binding sites. *Molecular pharmacology*, 67(4), pp.1291–1298.

Vivet-Boudou, V. et al., 2006. Nucleoside and nucleotide inhibitors of HIV-1 replication. *Cellular and molecular life sciences : CMLS*, 63(2), pp.163–186.

W

Wang, J. et al., 1997. Functional and molecular characteristics of Na(+)-dependent nucleoside transporters. *Pharmaceutical research*, 14(11), pp.1524–1532.

Wang, J. et al., 2011. Splice Variant Specific Modulation of CaV1.2 Calcium Channel by Galectin-1 Regulates Arterial Constriction. *Circulation Research*, 109(11), pp. 1250–1258.

Wang, Q., Wang, X. & Evers, B.M., 2003. Induction of cIAP-2 in human colon cancer cells through PKC delta/NF-kappa B. *The Journal of biological chemistry*, 278 (51), pp.51091–51099.

Wang, X. et al., 2004. COPII-dependent export of cystic fibrosis transmembrane conductance regulator from the ER uses a di-acidic exit code. *The Journal of cell biology*, 167(1), pp.65–74.

Wang, Y. & Miksicek, R.J., 1991. Identification of a dominant negative form of the human estrogen receptor. *Molecular endocrinology (Baltimore, Md.)*, 5(11), pp. 1707–1715.

Wang, Y.-N. et al., 2010. Nuclear trafficking of the epidermal growth factor receptor family membrane proteins. *Oncogene*, 29(28), pp.3997–4006.

Ward, J.L. et al., 2003. Functional analysis of site-directed glycosylation mutants of the human equilibrative nucleoside transporter-2. *Archives of Biochemistry and Biophysics*, 411(1), pp.19–26.

Ward, J.L. et al., 2000. Kinetic and pharmacological properties of cloned human equilibrative nucleoside transporters, ENT1 and ENT2, stably expressed in nucleoside transporter-deficient PK15 cells. Ent2 exhibits a low affinity for guanosine and cytidine but a high affinity for inosine. *The Journal of biological chemistry*, 275(12), pp.8375–8381.

Watanabe, K. et al., 1995. Splicing isoforms of rat Ash/Grb2. Isolation and characterization of the cDNA and genomic DNA clones and implications for the physiological roles of the isoforms. *The Journal of biological chemistry*, 270(23), pp.13733–13739.

Watson, P. & Stephens, D.J., 2005. ER-to-Golgi transport: form and formation of vesicular and tubular carriers. *Biochimica et biophysica acta*, 1744(3), pp.304–315.

Wendeler, M.W., Paccaud, J.-P. & Hauri, H.-P., 2007. Role of Sec24 isoforms in selective export of membrane proteins from the endoplasmic reticulum. *EMBO reports*, 8(3), pp.258–264.

Wiley, J.S. et al., 1982. Cytosine arabinoside influx and nucleoside transport sites in acute leukemia. *The Journal of clinical investigation*, 69(2), pp.479–489.

Williams, J.B. & Lanahan, A.A., 1995. A mammalian delayed-early response gene encodes HNP36, a novel, conserved nucleolar protein. *Biochemical and biophysical research communications*, 213(1), pp.325–333.

Wlcek, K. et al., 2011. The analysis of organic anion transporting polypeptide (OATP) mRNA and protein patterns in primary and metastatic liver cancer. *Cancer biology & therapy*, 11(9), pp.801–811.

Wojtal, K.A. et al., 2009. Changes in mRNA Expression Levels of Solute Carrier Transporters in Inflammatory Bowel Disease Patients. *Drug Metabolism and Disposition*, 37(9), pp.1871–1877.

Wu, J.-C., Liang, Z.-Q. & Qin, Z.-H., 2006. Quality control system of the endoplasmic reticulum and related diseases. *Acta biochimica et biophysica Sinica*, 38(4), pp. 219–226.

Wu, J.-Y., Tang, H. & Havlioglu, N., 2003. Alternative pre-mRNA splicing and regulation of programmed cell death. *Progress in molecular and subcellular biology*, 31, pp. 153–185.

Wu, S.K. et al., 2005. Fine tuning of rabbit equilibrative nucleoside transporter activity by an alternatively spliced variant. *Journal of drug targeting*, 13(8-9), pp.521–533.

X

Xia, L., Zhou, M. & Wang, J., 2007. *Drug Transporters* G. You & M. E. Morris, eds., Hoboken, NJ, USA: John Wiley & Sons, Inc.

Y

Yang, X.C. et al., 2009. Three Proteins of the U7-Specific Sm Ring Function as the Molecular Ruler To Determine the Site of 3'-End Processing in Mammalian Histone Pre-mRNA. *Molecular and cellular biology*, 29(15), pp.4045–4056.

Yao, S.Y.M. et al., 2002. Functional and molecular characterization of nucleobase transport by recombinant human and rat equilibrative nucleoside transporters 1 and 2. Chimeric constructs reveal a role for the ENT2 helix 5-6 region in nucleobase translocation. *The Journal of biological chemistry*, 277(28), pp. 24938–24948.

Yao, S.Y.M. et al., 2011. Nucleobase Transport by Human Equilibrative Nucleoside Transporter 1 (hENT1). *Journal of Biological Chemistry*, 286(37), pp.32552–32562.

Yao, S.Y.M. et al., 2001. Transport of antiviral 3'-deoxy-nucleoside drugs by recombinant human and rat equilibrative, nitrobenzylthioinosine (NBMPR)-insensitive (ENT2) nucleoside transporter proteins produced in Xenopus oocytes. *Molecular Membrane Biology*, 18(2), pp.161–167.

Yegutkin, G.G., 2008. Nucleotide- and nucleoside-converting ectoenzymes: Important modulators of purinergic signalling cascade. *Biochimica et biophysica acta*, 1783 (5), pp.673–694.

Young, J.D. et al., 2008. Human equilibrative nucleoside transporter (ENT) family of nucleoside and nucleobase transporter proteins. *Xenobiotica; the fate of foreign compounds in biological systems*, 38(7-8), pp.995–1021.

Yu, L. et al., 2009a. Prostaglandin E 2promotes cell proliferation viaprotein kinase C/ extracellular signal regulated kinase pathway-dependent induction of c-Myc expression in human esophageal squamous cell carcinoma cells. *International journal of cancer Journal international du cancer*, 125(11), pp.2540–2546.

Yu, M.-J. et al., 2009b. Systems-level analysis of cell-specific AQP2 gene expression in renal collecting duct. *Proceedings of the National Academy of Sciences of the United States of America*, 106(7), pp.2441–2446.

Z

Zhang, J. et al., 2007. The role of nucleoside transporters in cancer chemotherapy with nucleoside drugs. *Cancer and Metastasis Reviews*, 26(1), pp.85–110.

Zhang, J., Sun, X., et al., 2006a. Studies of nucleoside transporters using novel autofluorescent nucleoside probes. *Biochemistry*, 45(4), pp.1087–1098.

Zhang, J., Tackaberry, T., et al., 2006b. Cysteine-accessibility analysis of transmembrane domains 11-13 of human concentrative nucleoside transporter 3. *The Biochemical journal*, 394(Pt 2), pp.389–398.

Zhou, F. et al., 2005. The role of N-linked glycosylation in protein folding, membrane targeting, and substrate binding of human organic anion transporter hOAT4. *Molecular pharmacology*, 67(3), pp.868–876.

Zhou, M. et al., 2010. Adenosine Transport by Plasma Membrane Monoamine Transporter: Reinvestigation and Comparison with Organic Cations. *Drug metabolism and disposition: the biological fate of chemicals*, 38(10), pp.1798–1805.

Zhou, M. et al., 2007. Molecular determinants of substrate selectivity of a novel organic cation transporter (PMAT) in the SLC29 family. *The Journal of biological chemistry*, 282(5), pp.3188–3195.

Zhou, W. et al., 1993. Protein kinase C-mediated bidirectional regulation of DNA synthesis, RB protein phosphorylation, and cyclin-dependent kinases in human vascular endothelial cells. *The Journal of biological chemistry*, 268(31), pp. 23041–23048.

Zoulim, F., 2005. Combination of nucleoside analogues in the treatment of chronic hepatitis B virus infection: lesson from experimental models. *The Journal of antimicrobial chemotherapy*, 55(5), pp.608–611.

Zuleger, N., Korfali, N. & Schirmer, E.C., 2008. Inner nuclear membrane protein transport is mediated by multiple mechanisms. *Biochemical Society transactions*, 36(Pt 6), pp.1373–1377.

Zuzarte, M. et al., 2007. A di-acidic sequence motif enhances the surface expression of the potassium channel TASK-3. *Traffic (Copenhagen, Denmark)*, 8(8), pp.1093–1100.

VIII. Resumen en Castellano

19 ANTECEDENTES

La bioasequibilidad y la acción de los fármacos derivados de nucleósidos utilizados en la terapia antitumoral dependen en gran medida de la capacidad de las células diana para internalizarlos y activarlos metabólicamente. Estos fármacos interfieren en los procesos de captación y metabolización de los nucleósidos naturales, incidiendo así en una de las rutas metabólicas probablemente mejor conservadas evolutivamente, la vía de recuperación, finamente regulada y de notable eficacia energética si se tiene en cuenta el coste asociado a la síntesis de novo de nucleósidos (Molina-Arcas *et al*. 2006).

Dado su carácter hidrofílico, tanto los nucleósidos como sus derivados requieren de transportadores de membrana para poder ser internalizados. Existen dos grupos de transportadores de nucleósidos (NTs) según su dependencia energética: los transportadores de tipo equilibrativo (ENTs) independientes de sodio, los cuales transportan sustratos por difusión facilitada a favor de gradiente, y los transportadores de tipo concentrativo (CNTs), que transportan en contra de gradiente con un gasto energético asociado (Molina-Arcas *et al*. 2006; Pastor-Anglada *et al*. 2004). De todos ellos, sólo uno, hENT2 (human Equilibrative Nucleoside Transporter 2) tiene además la capacidad de poder transportar nucleobases, lo cual le confiere un papel crucial en la captación de estas unidades elementales susceptibles también de ser incorporadas a ácidos nucleicos mediante las vías de recuperación de las nucleobases.

Por otro lado, el fenómeno de splicing alternativo es una de las mayores fuentes de diversidad proteómica en humanos, destacando su efecto tanto en enfermedades como en terapéutica (Garcia-Blanco *et al*. 2004). La actividad fisiológica de los distintos productos obtenidos mediante este proceso, en comparación con la proteína original, pueden ser totalmente distintos. Por ejemplo, se han descrito variantes que actúan como dominantes negativos, bloqueando la actividad de la proteína original (Wu *et al*. 2003), mientras que otros pueden alterar su localización subcelular, transformando así proteínas integrales de membrana en proteínas solubles

(Jang 2002) o asociadas a otros orgánulos como el retículo endoplasmático o el núcleo (Vallejo-Illarramendi *et al*. 2005; Errasti-Murugarren *et al*. 2009).

Tal y como se ha comentado, los transportadores de nucleósidos, además de transportar sus sustratos naturales, los nucleósidos, tienen también la capacidad de transportar fármacos antivirales y antitumorales derivados de nucleósidos. En estas terapias se suelen dar casos de resistencia a dichos tratamientos, lo cual podría ser debido, entre otros factores, a deficiencias en el transporte y entrada de los fármacos al interior celular. En el caso concreto de hENT2, éste juega un importante papel en el tratamiento de leucemia linfática crónica (LLC) (Pastor-Anglada *et al*. 2004), dado que es el mediador de la respuesta transcriptómica derivada del tratamiento con fludarabina, el fármaco más utilizado en el tratamiento de LLC, por lo que hENT2 se erige claramente como diana farmacológica en ésta y quizá otras enfermedades linfoproliferativas. Por otro lado, hENT2 también fue identificado, independientemente, como uno de los cinco genes que permiten anticipar progresión y/o mejoría de la enfermedad en pacientes diagnosticados de linfoma de células de manto (LCM) (Hartmann *et al*. 2008). De esta manera, la existencia de formas de splicing alternativo de hENT2 las cuales no fuesen funcionales o, incluso, actuasen como dominantes negativos de la proteína natural, podrían estar relacionados con mecanismos de resistencia a tratamientos con fármacos derivados de nucleósidos.

El gen SLC29A2 codifica para una proteína de 456 aminoácidos, hENT2, de amplia expresión tisular y poco caracterizada hasta la fecha en cuanto a su regulación y a su papel biológico. No obstante, existen evidencias descritas sobre dos posibles variantes fruto del splicing alternativo de este transportador. Una de ellas es una variante con una deleción de 40 pares de bases en el exón 9 del ARNm. Dicha alteración produce un codón de parada prematuro, el cual se traduce en una proteína de tan solo 6 dominios transmembrana, mientras que la proteína original tiene 11. Se apunta que esta proteína no sería funcional en cuanto a transporte de nucleósidos y derivados, y que probablemente vaya dirigida al retículo endoplasmático en lugar de la membrana plasmática (Mangravite *et al.* 2003). La otra variante descrita fue identificada antes de la clonación de hENT2. Se identificó como un gen de respuesta

tardía a estímulos mitogénicos (HNP36), a pesar de que su papel funcional no se determinó entonces. Esta variante es fruto de una deleción de 65 pares de bases en el exón 4, hecho que genera una proteína que contiene los últimos 8 dominios transmembrana de la proteína natural. A pesar de no saber su funcionalidad sí que se observó su localización en la periferia del núcleo celular (Williams & Lanahan 1995).

En nuestro laboratorio se generaron evidencias de la posible existencia de una nueva variante de splicing del transportador de hENT2, a pesar de que en su momento no se profundizó ni en su caracterización ni en su papel funcional. Aún así, nos sirvió como punto de partida para iniciar una nueva vía de investigación sobre las variantes de splicing alternativo del transportador de nucleósidos y fármacos antitumorales hENT2.

Recientemente, se ha sugerido que el análisis transcriptómico de genes que codifiquen para proteínas transportadoras de membrana, determinantes para la internalización de fármacos y su acción citotóxica, en tumores podría suponer una herramienta de predicción de respuesta terapéutica, introduciendo así el concepto de Transportoma (Huang *et al*. 2004). En base a esto, surge la idea de poder desarrollar un test reproducible que, mediante la caracterización de la expresión de una batería de genes, incluyendo transportadores de nucleósidos y sus correspondientes variantes de splicing, permita predecir la sensibilidad/resistencia a la quimioterapia en tumores digestivos.

20 OBJETIVOS GENERALES

- Identificación y clonación de posibles nuevas variantes de *splicing* del transportador hENT2.

- Caracterización y análisis de la localización y función de dichas variantes en su posible papel como transportadores de nucleósidos y fármacos derivados de éstos.

- Análisis de la presencia de estas variantes de *splicing* en distintas líneas y tejidos, tanto tumorales como muestras sanas.

- Identificación de los aminoácidos fosforilados por determinadas kinasas en el *loop* intracelular de h/mENT2.

- Efecto de la regulación de hENT2 por fosforilación.

- Identificación de posibles proteínas de interacción del transportador de nucleósidos hENT2 mediante la técnica del doble-híbrido en membrana de levaduras (MYTH).

- Identificación de genes relacionados con transportadores de membrana cuya expresión basal permita predecir la respuesta a distintos tratamientos antineoplásicos.

21 RESUMEN DE LOS RESULTADOS OBTENIDOS EN EL PROYECTO DE TESIS

21.1 IDENTIFICACIÓN Y CARACTERIZACIÓN DE 3 NUEVAS VARIANTES NUCLEARES DE SPLICING ALTERNATIVO DEL TRANSPORTADOR DE NUCLEÓSIDOS EQUILIBRATIVO HUMANO 2 (hENT2)

El principal objetivo en la fase inicial de este proyecto ha sido la identificación y clonación de nuevas variantes de splicing del gen SLC29A2, el cual codifica para la proteína hENT2, a partir del ADNc de la línea celular de cáncer de mama MCF7. De todas las posibles variantes de este gen generadas por el proceso de splicing alternativo, decidimos seguir con el estudio de 6 de ellas: 3 con deleciones al inicio del tránscrito (exones 2 y 4), 2 con deleciones al final del tránscrito (exón 8 y 40 pbs del exón 9) y otra variante con deleciones tanto al inicio como al final de la secuencia (exón 2 y 40 pbs del exón 9).

Para analizar la expresión proteica de dichas variantes y su localización subcelular, se le añadió un epítopo “HA” de nueve aminoácidos a cada una de las isoformas de hENT2. De esta manera, con un anticuerpo específico contra el epítopo distinguimos la banda proteica que se corresponde a cada una de las variantes mediante la técnica de Western-Blott (WB) y así determinamos su peso molecular alrededor de 32 - 36KDa. Estas mismas bandas fueron identificadas en el extracto de proteína total de células pertenecientes a la línea celular de placenta BeWo, de la cual ya se había descrito previamente la presencia de transportadores ENTs en la membrana nuclear (Mani *et al*. 1998). Dado que dichas variantes conservan el loop intracelular entre los dominios transmembrana 6 y 7, el uso de un anticuerpo comercial diseñado para reconocer esta región como epítopo nos permitió detectar las nuevas variantes nucleares de hENT2 endógenamente.

Una vez confirmada la síntesis proteica de estas variantes de splicing, realizamos experimentos de inmunocitoquímica (ICQ) en células HeLa y también HEK-293, transfectadas con los distintos constructos con el epítopo HA para poder determinar la localización subcelular de las distintas variantes. Los resultados obtenidos a partir de estos experimentos nos muestran claramente como las tres variantes con deleciones en los exones 2 y/o 4 sintetizan proteínas localizadas en la membrana nuclear en lugar de la membrana plasmática. En cuanto a las otras tres posibles variantes que probamos, no las llegamos a identificar ni por WB ni por ICQ.

A pesar de tener evidencias de la síntesis proteica de las isoformas nucleares de hENT2 tanto por WB como por ICQ, queríamos descartar la posibilidad de que fuese un hecho artefactual debido a la sobreexpresión de estas variantes. Realizamos experimentos de bloqueo de la vía de NMD para ver si realmente el ARNm de estas variantes de splicing es estable y no se degrada, permitiendo sintetizar las proteínas resultantes de manera endógena, sin que sea por efecto de la sobreexpresión (Boutz *et al*. 2007).

La vía de NMD (Non-sense Mediated Decay) es un mecanismo celular que permite degradar todos aquellos ARNm generados durante su proceso de maduración y cuyos productos no tengan ninguna viabilidad, de manera que no se llegue a sintetizar tal proteína aberrante. Al bloquear esta vía tratando las muestras con cicloheximida (CHX), impedimos que este mecanismo tenga lugar. De esta manera, si los niveles de expresión de un determinado transcrito aumentan después del tratamiento con CHX significa que éste es degradado por dicha vía y por tanto no expresado endógenamente. Por lo contrario, si los niveles no se ven alterados tras el tratamiento significa que ese mensajero se traduce a proteína regularmente.

En nuestro caso hicimos estos ensayos con células HEK-293. Para analizar los niveles de expresión de las distintas variantes usamos la técnica de PCR a tiempo real utilizando el reactivo SYBRGreen® y un conjunto de oligos diseñados específicamente para reconocer cada una de las isoformas individualmente. Los resultados muestran que, coincidiendo con los resultados observados por WB e ICQ, las variantes nucleares de hENT2 se llegan a sintetizar de manera natural al no degradar su ARNm, mientras que las demás variantes serían degradadas a través de la vía de NMD.

Seguidamente, determinamos la capacidad transportadora de dichas isoformas transfectadas en células HeLa. En aquellas muestras que sobreexpresaban hENT2 wt sí que se observó un aumento de la capacidad de transportar el sustrato uridina marcado radioactivamente. En cambio, no se apreciaron cambios en el transporte basal cuando se transfectaron las variantes de splicing de hENT2, coincidiendo así con su localización celular alrededor del núcleo en vez de la membrana plasmática. Con tal de determinar si dichas variantes de hENT2 son funcionales en la membrana nuclear, inyectamos oocitos de Xenopus laevis con las distintas isoformas de hENT2 para poder sustraer los núcleos y determinar su capacidad transportadora. Sorprendentemente, las variantes nucleares de hENT2 parecen ir dirigidas a la membrana plasmática en lugar de la nuclear tal y como sucedió con células humanas. Así pues, pudimos realizar ensayos de transporte con oocitos para determinar que las variantes nucleares de hENT2 son ciertamente

funcionales, capaces de internalizar la nucleobase hipoxantina pero no el nucleósido cloro-adenosina.

Finalmente, analizamos la expresión de las variantes de hENT2 por PCR cualitativa en una batería de líneas tumorales con distintas condiciones de crecimiento. Los resultados observados mostraban cambios en los perfiles de expresión según las condiciones de crecimiento y entre las líneas de distintos orígenes tumorales. De esta manera se abre una posible vía de estudio sobre las distintas condiciones y mecanismos de regulación del fenómeno de splicing alternativo que afecta al gen de hENT2.

21.2 ESTUDIO DE LA REGULACIÓN DE hENT2 POR FOSFORILACIÓN Y SU EFECTO EN EL TRÁFICO A MEMBRANA PLASMÁTICA

Cuando realizamos los experimentos de inmunocitoquímica en células HeLa transfectadas con las distintas isoformas de hENT2-HA, observamos que la proteína wt no solamente se encontraba en la membrana plasmática sino que además podía hallarse justo por debajo de ésta. Con tal de verificar la presencia de esta proteína tanto en membrana plasmática como en el interior celular, hicimos ensayos de biotinilización en células HeLa, esta vez sin transfectar.

En el proceso de biotinilización lo que se hace es incubar células intactas con una solución rica en biotina, una molécula capaz de unirse a residuos NHS de otras proteínas, de manera que se formen enlaces entre las proteínas presentes en la membrana plasmática y la biotina. A continuación, se obtiene un homogenado proteico total de estas células, el cual se incubará con Streptavidina unida a unas bolitas de resina. La Streptavidina tiene la capacidad de unirse a la biotina, y al estar unida a una resina nos permite separar la biotina unida a las proteínas de membrana del extracto proteico total. De esta manera, mediante la técnica de WB aplicada a las proteínas de membrana obtenidas por biotinilización, observamos que la banda perteneciente a hENT2 wt realmente era un doblete, cuya banda de menor peso molecular se encuentra en la membrana plasmática, mientras que la otra es intracelular,

probablemente justo por debajo de la membrana según mostraba la ICQ. Nuestra hipótesis, basada en parte en trabajos previos sobre hENT1 (Stolk *et al*. 2005; Bone *et al*. 2007), fue que la pequeña diferencia de peso entre las dos bandas podría deberse a la presencia de residuos fosforilados. De modo que según el estado de fosforilación de hENT2, éste podría estar localizado en la membrana plasmática o bien en vesículas cercanas a esta región, listas para ser enviadas a la membrana en caso de ser necesario.

Basados en estas suposiciones, decidimos estudiar en detalle el estado de fosforilación de la proteína hENT2 y los efectos de este tipo de regulación en el transportador. Para ello, decidimos centrarnos en la región del loop intracelular entre los dominios transmembrana 6 y 7 dado que es la región con más probabilidades de interaccionar con otras proteínas tales como kinasas. Así pues, analizamos bioinformáticamente los posibles residuos susceptibles de ser fosforilados por determinadas kinasas en tal secuencia de aminoácidos, tanto para la proteína humana hENT2 como su ortólogo en ratón, mENT2. Tales resultados apuntan como los principales candidatos para fosforilar ENT2 las kinasas PKA, PKC y CKII.

Con tal de llevar a cabo estudios de fosforilación in vitro y análisis por espectrometria de masas (MS), obtuvimos grandes cantidades de péptido artificial con la secuencia del loop de ENT2 incorporada, sobreexpresándolo y purificándolo a partir de cultivo bacteriano. Ambos péptidos, hENT2-loop y mENT2-loop, fueron tratados in vitro con las distintas kinasas predichas, utilizando ATP marcado radioactivamente para detectar los casos en los que se añadieron grupos fosfatos en el péptido. Los resultados mostraron claramente como tanto hENT2 y mENT2 son fosforilados por CKII. La misma reacción fue repetida con ATP frío solamente y se procesaron las muestras por MS/MRM con tal de hallar aquellos residuos los cuales son fosforilados por CKII. Desafortunadamente, hasta la fecha solo hemos identificado un residuo fosforilado por CKII en el caso de mENT2, Thre223, mientras que los protocolos seguidos hasta la fecha no han conseguido una buena cobertura de la secuencia total de la muestra humana.

A pesar de que nuestros resultados de fosforilación in vitro con PKC no fueron concluyentes, se publicó anteriormente cómo la activación de PKC a través del tratamiento con PDD (10 minutos, 500 nM) incrementa la actividad del transportador (Lu *et al*. 2010). Decidimos analizar el efecto de la activación de PKC en la actividad y localización subcelular de hENT2. Cuando realizamos ensayos de transporte en células HEK-293 tratadas con PDD, no observamos ningún cambio aparente en la actividad del transportador. Sin embargo, hubo una significativa disminución de la actividad de hENT1 debido a la activación de PKC. Por otro lado, realizamos ensayos de ICQ con células HEK-293 transfectadas con los constructos hENT2-HA y hENT1-FLAG, con tal de detectar selectivamente cada uno de los transportadores según su epítopo específico. Después de tratar las células con PDD lo que observamos fue como en células no estimuladas, hENT2 se encuentra mayoritariamente por debajo de la membrana, dónde se encuentra hENT1. Sin embargo, después de la activación de PKC hENT2 es translocado a la membrana plasmática donde colocaliza con hENT1 (figura 1 - figure 42).

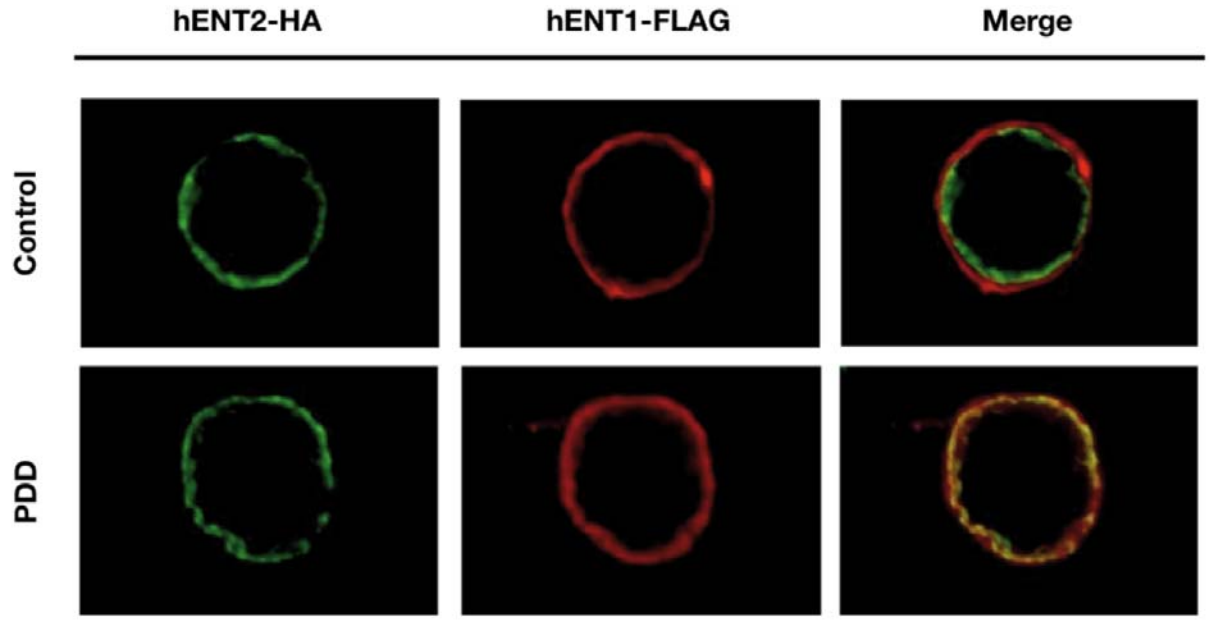

Figura 1 (figure 42). **Efecto de la activación de PKC por PDD en el tráfico de hENT2 a la membrana plasmática.** Células HEK-293 transfectadas con los constructos de hENT2-HA y hENT1-FLAG y tratadas con PDD para activar PKC. En condiciones control, hENT2 es predominantemente presente por debajo de la membrana plasmática (verde) mientras que hENT1 está localizado en la membrana plasmática (rojo). Después del tratamiento con PDD, hENT2 colocaliza con hENT1 en la membrana plasmática (amarillo).

Estos resultados nos muestran claramente como existe una cierta regulación de hENT2 por fosforilación, a pesar de que aún no se haya resuelto qué kinasa es responsable de ello en un sistema ex vivo. No obstante, la activación de PKC, ya sea por fosforilación directa o indirecta, promueve la translocación de hENT2 a la membrana plasmática, inhibiendo aparentemente la actividad del transportador de la misma familia , hENT1.

21.3 DETECCIÓN A GRAN ESCALA DE PROTEÍNAS DE INTERACCIÓN DE hENT2 MEDIANTE LA TÉCNICA DE DOBLE-HÍBRIDO EN MEMBRANA DE LEVADURAS (MYTH)

La técnica del doble-híbrido es comúnmente utilizada para identificar posibles proteínas de interacción aportando información sobre la función biológica de tales proteínas. Debido a su carácter hidrófobo, la clásica técnica del doble-híbrido difícilmente proporciona resultados positivos fiables en el caso de las proteínas de membrana tales como nuestro transportador hENT2. Recientemente, una nueva versión del doble-híbrido desarrollada por el laboratorio del Dr. Staglar nos permite aplicar el principio de esta técnica a proteínas de membrana, el MYTH (Snider *et al*. 2010).

Esta técnica se basa en los estudios previos de 1994 (Johnsson & Varshavsky 1994) en los que se describía como la ubiquitina, dividida en dos mitades podía re-asociarse debido a la alta afinidad de dichas mitades entre sí. Estás dos fracciones fueron nombradas Nub para el N-terminal de la proteína, y Cub para el C-terminal de la ubiquitina. De esta manera, al fusionar Cub con nuestra proteína de interés, llamada cebo, y analizarla frente a una librería de cDNAs con el Nub fusionado en cada tránscrito, llamado presas, podemos detectar aquellas proteínas que interactuen con nuestro cebo re-estableciendo la molécula de ubiquitina. Una vez se completa la unión de Nub y Cub completando la ubiquitina, ésta es reconocida por proteasas específicas que cortarán la proteína Cub, liberando los genes reporteros unidos a ella. Dado que esta técnica tiene lugar en el citosol en lugar del interior nuclear, se puede aplicar a

proteínas de membrana las cuales tienen un lado intracellular con el que interactuar con otras proteínas y restaurar la molécula de ubiquitina.

Los resultados obtenidos para hENT2 mediante esta técnica han dado un número muy elevado de posibles proteínas de interacción, faltando ser validadas mediante otras técnicas. Un total de 110 proteínas fueron identificadas, buena parte de ellas pudiendo ser consideradas como falsos positivos de la técnica en sí. Sorprendentemente, los resultados mostraron un buen número de proteínas localizadas en el interior nuclear, la mayoría relacionadas con el proceso de splicing o bien con el transporte de moléculas a través de la membrana nuclear. A priori, estos resultados no tendrían sentido de solo considerar ENT2 como proteína cebo. No obstante, en apartados anteriores hemos descrito 3 nuevas variantes de splicing de hENT2 que codifican dos nuevas isoformas nucleares del transportador. Estas variantes conservan el gran loop intracelular de hENT2, la única región a través de la cual esta proteína podría interactuar con otras. De manera que los resultados obtenidos referentes a proteínas nucleares reflejen posibles interacciones con las variantes nucleares del transportador.

Otras proteínas interesantes halladas a partir del MYTH son ciertas kinasas y fosfatasas, junto la proteína Gs vinculada a la activación de PKA por AMP cíclico (cAMP). A pesar de que tales interacciones aún no has sido validadas, proponemos un plausible escenario en el que ENT2 regularía su propia expresión modulando su propio patrón de splicing a través de su estado de fosforilación (figura 2 - figure 48).

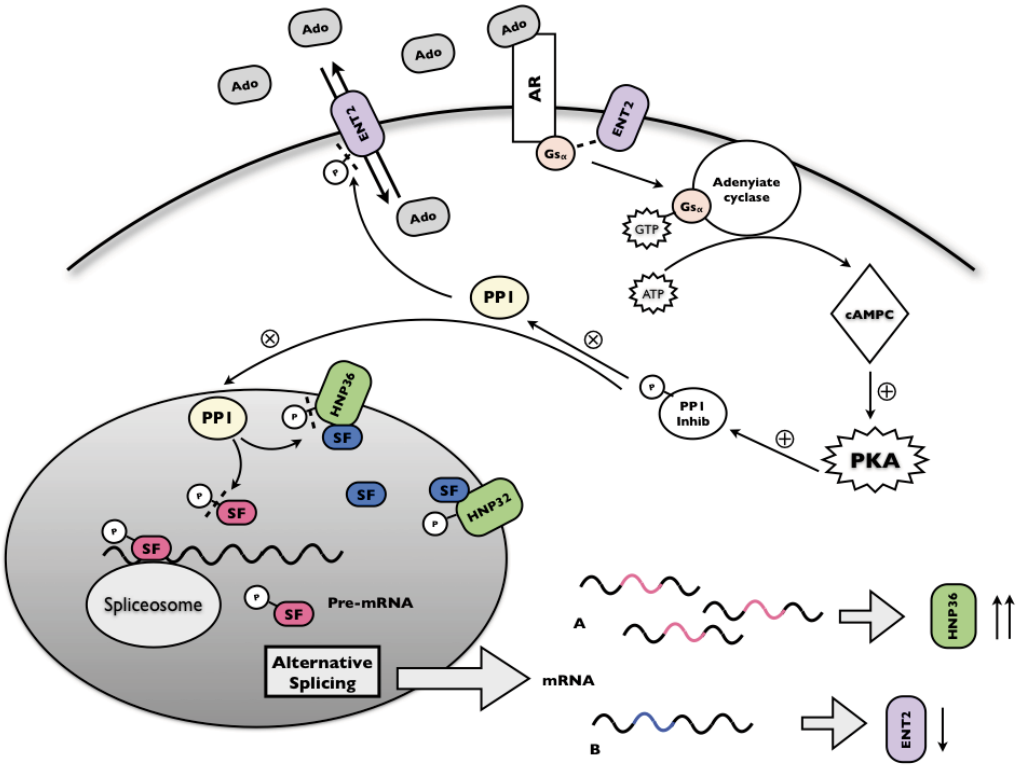

Figura 2 (figure 48). Especulación de una plausible regulación del patrón de *splicing* de hENT2 mediante fosforilación. ENT2 internaliza adenosina (Ado) modulando sus niveles extracelulares. La adenosina extracelular se une a los receptores de adenosina (AR) dependiendo de su concentración, activando así la proteína Gs, la cual a su vez podría estar interactuando con ENT2 según nuestros resultados obtenidos con la técnica del MYTH. Gs activa la adenilato ciclasa la cual sintetiza cAMP a partir de ATP. cAMP activa PKA quien fosforila los inhibidores de la proteína fosfatasa 1 (PP1) (DARP-32 i I-1). Estos inhibidores una vez fosforilados interactúan alostéricamente con PP1 inhibiendo su actividad fosfatasa. Tal y como muestran nuestros resultados, PP1 podría interactuar con hENT2 al igual que HNP32 y HNP36, sus variantes nucleares de 32 y 36 KDa respectivamente, regulando su estado de fosforilación. Se ha descrito que PP1 está también involucrada en en la regulación del *splicing* alternativo dado que desfosforila un buen número de factores de *splicing* (SF). El estado de fosforilación de dichos factores puede condicionar su afinidad por determinados sitios de corte en el pre-mRNA, aunque a su vez también podría determinar la interacción entre SF y HNP32/36. Si HNP32/36 se unieses a determinados SF, esto comprometería la disponibilidad de éstos para definir los sitios de corte del pre-mRNA por el spliceosoma. De esta manera, dependiendo del estado de fosforilación de tanto HNP32/36 como de los SF, la célula produciría un patrón distinto de *splicing* alternativo modulando la expresión de las isoformas de HENT2. En nuestro ejemplo, el SF fosforilado (rojo) determinaría unos sitios concretos de corte del pre-mRNA que producirían la variante de *splicing* "A", la cual codifica la proteína HNP36. En cambio, los SF no fosforilados (azul), permanecerían unidos a HNP32/36 siendo retenidos en la membrana nuclear y no estando disponibles durante el proceso de *splicing*. Como consecuencia, se producirían menores cantidades del producto "b" y por lo tanto la expresión de ENT2 disminuiría.

21.4 ANÁLISIS FARMACOGENÓMICO DE LA RESPUESTA A TRATAMIENTOS DE TUMORES SÓLIDOS: PROYECTO TRANSPORTOMA

Paralelamente, se empezó otro proyecto basado en el concepto de "Transportoma". Durante el primer período de la tesis se llevó a cabo toda la parte experimental, que incluía los tratamientos de las 15 lineas tumorales con los 6 fármacos antineoplásicos, además del análisis de expresión de 96 genes.

El objetivo inicial de este proyecto, tal y como se ha explicado anteriormente, era el de poder correlacionar niveles expresión basal de genes que codifican para distintas proteínas transportadoras con respuesta a tratamientos antitumorales. Una vez realizada toda la parte experimental, tanto los tratamientos con fármacos como el análisis de los niveles de ARNm de los 96 genes, restaba procesar todos los datos obtenidos para ver si existía tales correlaciones que nos permitiesen obtener una herramienta de carácter predictivo.

Una vez realizado el análisis bioinformático, obtuvimos correlaciones entre niveles de expresión entre determinados genes y respuesta a los tratamientos con cisplatino y paclitaxel, principalmente. No obstante, resta por hacer algunos experimentos adicionales que nos permitan acabar de confirmar estas correlaciones ampliando el número de muestras.

Por otro lado, solamente el análisis de expresión de todos estos genes en 15 muestras distintas nos ha permitido definir redes de genes correlacionados entre sí, independientemente de las respuestas a los tratamientos. Este análisis nos ha reportado resultados inesperados en los que se vincula, a nivel de expresión de ARNm, transportadores de membrana (entre ellos hENT2) con genes clave para el metabolismo de nucleótidos, reparación del ADN, proliferación y supervivencia celular (figura 3 - figure 55). Dichas correlaciones no han sido descritas en humanos hasta la fecha. No obstante, en el campo de las levaduras sí que existen trabajos de análisis masivo del genoma en que se establecen vínculos entre genes del metabolismo de nucleótidos con sistemas de reparación del ADN, proliferación y supervivencia, donde

describen la vital importancia de estas redes génicas a nivel celular (Hannum et al. 2009; Pan et al. 2006; Conde-Pueyo et al. 2009).

Después de un intensivo trabajo bibliográfica, encontramos evidencias de la regulación y/o interacción de muchos de los genes encontrados en nuestra red génica con la kinasa PKC, ya sea directa o indirectamente (figura 4 - figure 59). Estas interacciones se corresponden además con el tipo de correlaciones halladas en las expresiones génicas, de manera que PKC regularía de manera similar a genes con una correlación positiva entre sí. Estos hallazgos nos indican que dicha red de genes correlacionados entre sí no sería algo azaroso sino finamente regulado por otros elementos no identificados en nuestro análisis inicial.

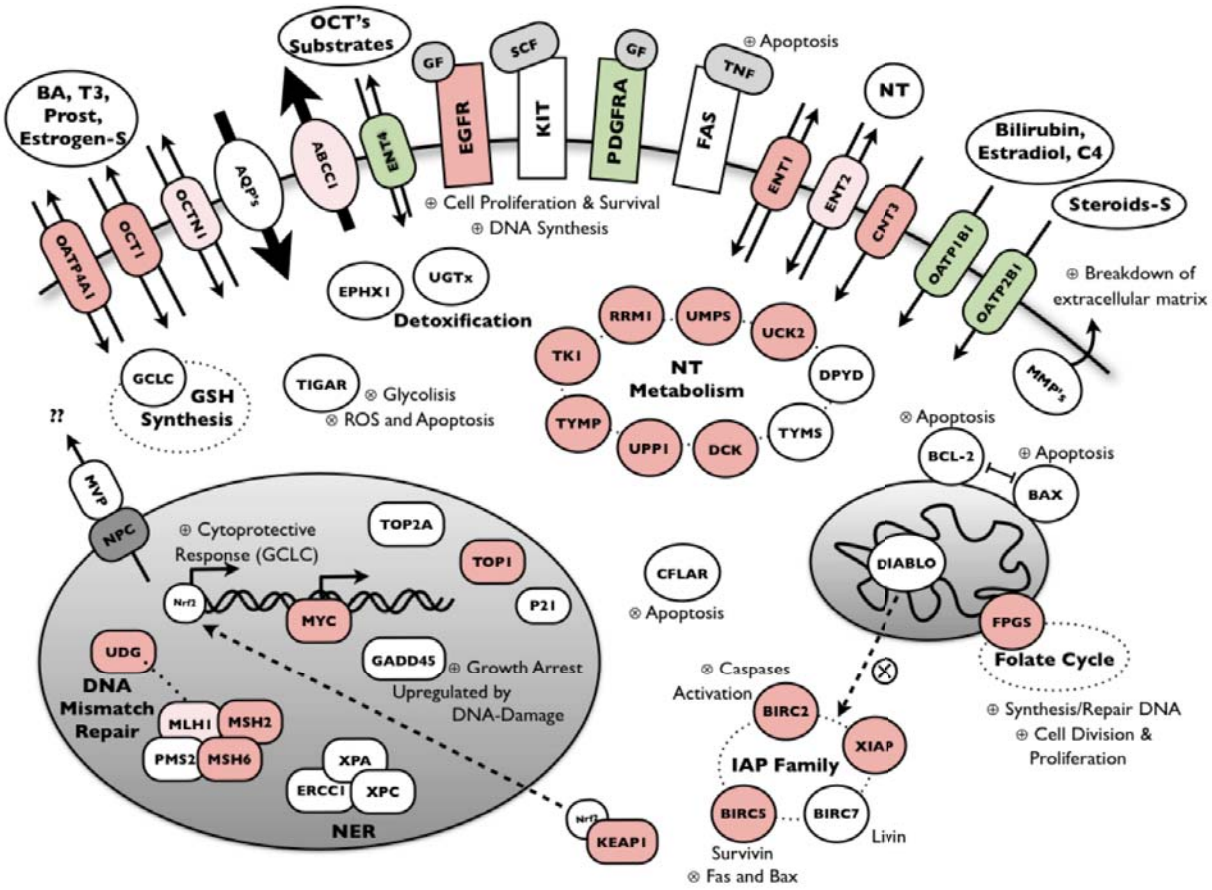

Figura 3 (figure 55). Esquema de los genes correlacionados entre sí, todos ellos involucrados en vías de metabolismo de nuceótidos, reparación del ADN, supervivencia y proliferación. En rojo están representados genes que correlacionan significativamente entre ellos y en verde aquellos con correlaciones negativas.

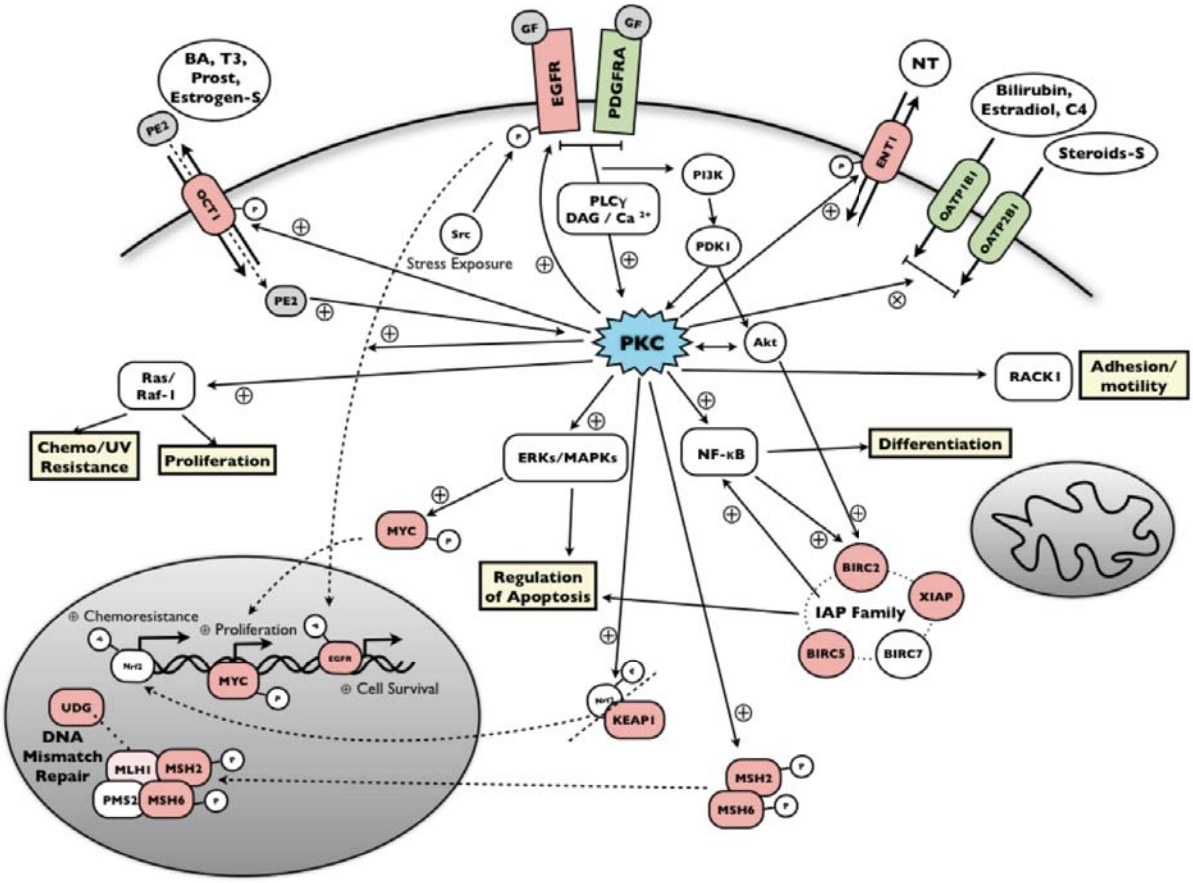

Figura 4 (figure 59). Representación de aquellos genes presentes en nuestra red génica, de los cuales hay evidencias de su relación/interacción con PKC, directa o indirectamente.

22 CONCLUSIONES

1. Hemos identificado 3 nuevas variantes de *splicing* del transportador de nucleósidos equilibrativo 2 (hENT2), las cuales codifican dos nuevas isoformas nucleares de la proteína. Dichas variantes parecen ser funcionales i estar ubicuamente expresadas en líneas celulares y tejidos sanos.

2. hENT2 es fosforilado *in vitro* por la kinasa CKII. Dado que CKII se encuentra constitutivamente activa, hENT2 podría estar regulado por desfosforilación a través de PP1.

3. La activación de PKC mediante el tratamiento con PDD promueve la translocación de de hENT2 hacia la membrana plasmática en células HEK-293, a la vez que disminuye la actividad transportadora de hENT1.

4. hENT2 podría tener una población dual en la membrana plasmática. De manera que una isoforma no fosforilada de hENT2, de unos 54 KDa, podría estar relacionada con la actividad transportadora, mientras que otra isoforma de 45 KDa no sería activa como transportador, a pesar de estar situada en la membrana plasmática.

5. Hemos definido una red global de genes aparentemente invueltos en proliferación celular y proliferación. ENT1, ENT2 y CNT3 forman parte de esta red génica, en la cual PKC podría tener un papel central regulador.

6. ENT2, junto con otros genes implicados en la proliferación celular y supervivencia, correlacionan negativamente con la supervivencia celular en respuesta al tratamiento con paclitaxel en lineas celulares gastro-hepáticas.

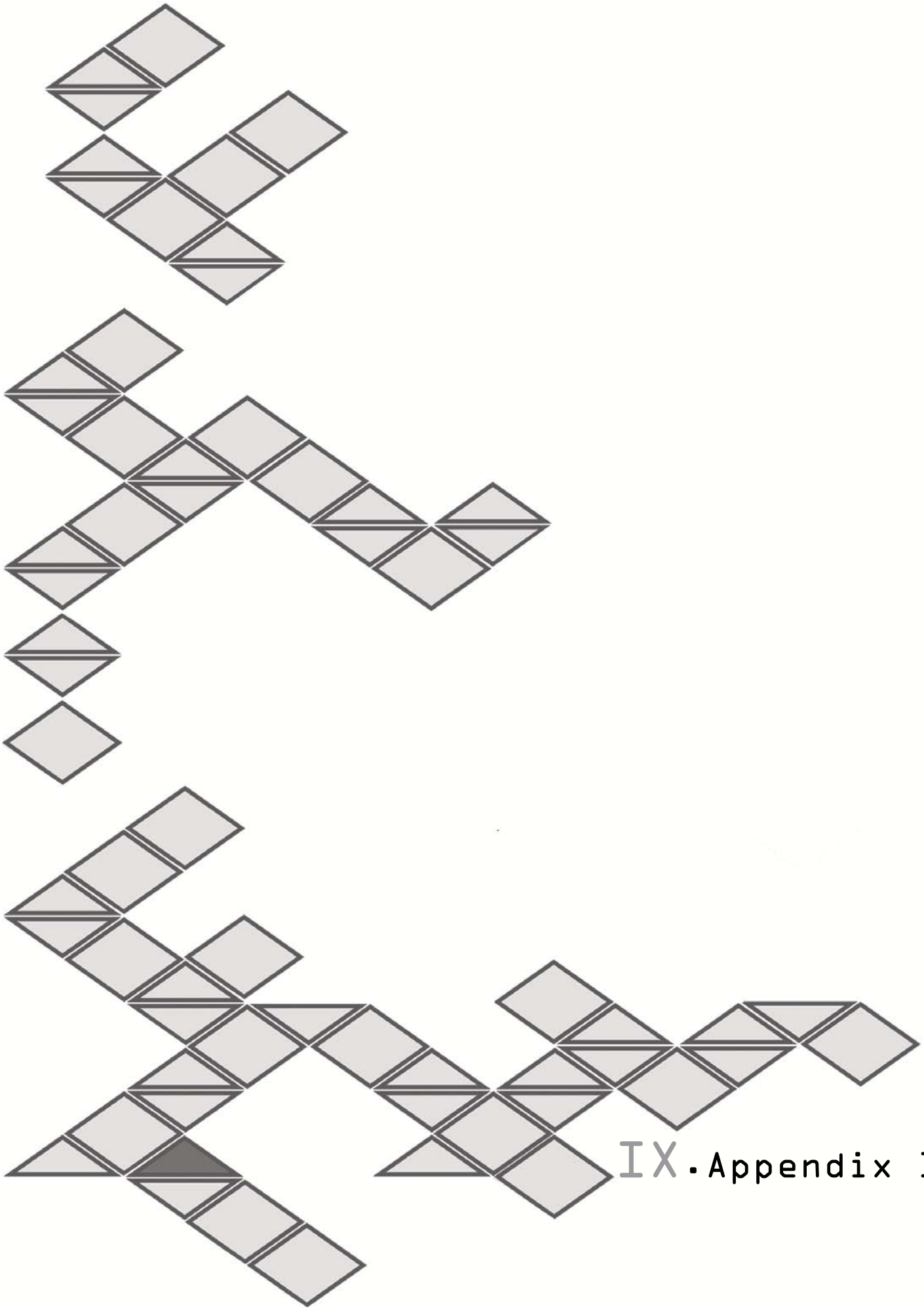

IX. Appendix I

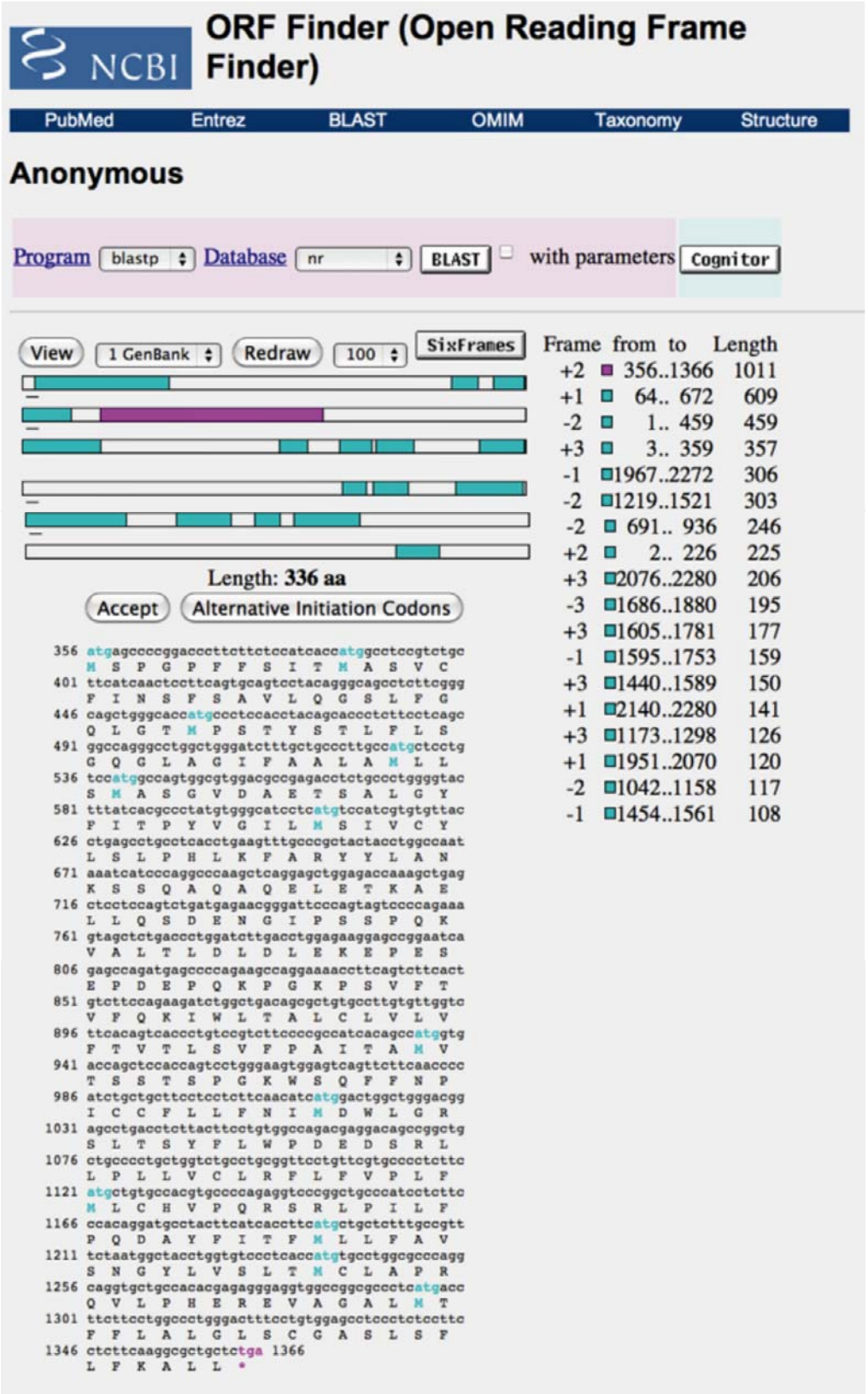

Figure 60. Predicted ORF for the transcript X86681. Unlike it has been described in 1995, results obtained from ORF Finder software and "Clone Manager" program we used, the main ORF predicted for the transcript X86681 is a 336 aa protein, instead of 326 aa they assumed for the HNP36 protein, which would start at the second methionine highlighted.

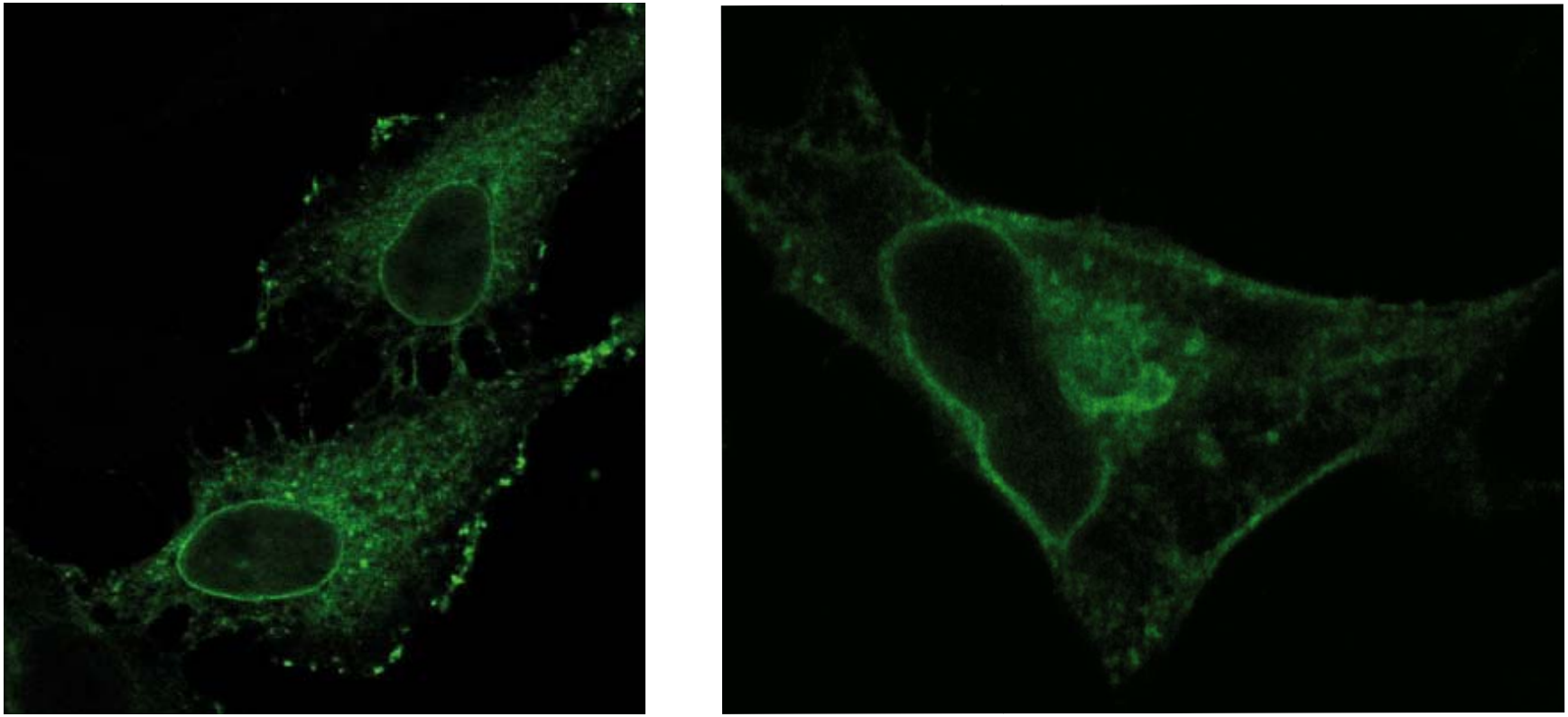

Figure 61. Immunocytochemistry of hENT2-HA wt constructs in HeLa cells. Unlike our data from HEK-293 cells, the wt hENT2-HA construct was sorted to the nuclear membrane (or related structures). However, these results are preliminary and hENT2-HA wt is usually located to the plasma membrane. We propose that the wt may form heteromers with the nuclear variants, and thus act as a dominant negative. HeLa splicing patterns suggest that these cells express more nuclear variant 45F than wt as shown in figure 32. Further assays need to be performed to confirm or discard that hypothesis.

Table 20. Primers used for this dissertation

hENT2 CLONING :

FL4F: 5'-CCTGTAGGACTGCACTGAAG-3'

FL5R: 5'-GGATCTCAGCTCCGGAAGG-3'

E4R: 5'-CCTGTAGGACTGCACTGAAC-3'

SYBR GREEN REAL-RIME PCR:

F1: 5'-CGCGGGACAGTACTTCCAGG-3'

F2: 5'-CCGCCATCCCGTACTTCCAGG-3'

R1: 5'-CCGGGACGCACTGGTACAGG-3'

R2: 5'-GCACTGAAGGCACTGGTACAGG-3'

nPTB exon 8 Fwd: 5'-GCATTTGCCAAGGAGACATCC-3'

nPTB exon 9-11 Rv: 5'-CCATAAACACCTCTTCATTT-3'

GAPDH Fwd: 5'-GACCTTGGCCAGGGGTGCTAA-3'

GAPDH Rv: 5'-GGAGAAGGCTGGGGCTCATTTG-3'

Combination : Wt =F2 + R1; 4A = F1 + R1; 16D = F2 + R2; 45F = F1 + R2

CLONING INTO pBSxG VECTOR:

SmaI - FL4F: 5'-TCCCCCGGGGGACCCCAGGCGCATCCG-3'

FL5R - SmaI: 5'-TCCCCCGGGGGATGGATCTCAGCTCCG-3'

CLONING INTO pTLB1 VECTOR:

PstI - FL4F: 5'-AACTGCAGTTTCACCCCAGGCGCATCCG-3'

FL5R - StuI: 5'-AAGGCCTGGATCTCAGCTCCGGAAGG-3'

Table 21. Primers used for the HA-hENT2 constructs cloning

Initial HA - Samples: 22C, 17G and 16D

Initial F1: 5'-CCAGGCGCATCCGCCGCGGCGGCCGACTACGCGATGGCGCGAGGAGACGCCCGC-3'
Initial F2 : 5'-CCAGGCGCATCCGCCGCGGCGGCCGACGTCCCAGACTACGCGATGGCGCGAGGAGACG-3'
Initial F3: 5'-CCAGGCGCATCCGCCGCGGCGGCCCCGTATGACGTCCCAGACTACGCGATGGCGCGAGG-3'
Initial F4: 5'-CCAGGCGCATCCGCCGCGGCGGCCATGTACCCGTATGACGTCCCAGACTACGCGATGG-3'

Initial R1: 5'-GCGGGCGTCTCCTCGCGCCATCGCGTAGTCGGCCGCCGCGGCGGATGCGCCTGG-3'
Initial R2: 5'-CGTCTCCTCGCGCCATCGCGTAGTCTGGGACGTCGGCCGCCGCGGCGGATGCGCCTGG-3'
Initial R3: 5'-CCTCGCGCCATCGCGTAGTCTGGGACGTCATACGGGGCCGCCGCGGCGGATGCGCCTGG-3'
Initial R4: 5'-CCATCGCGTAGTCTGGGACGTCATACGGGTACATGGCCGCCGCGGCGGATGCGCCTGG-3'

Final HA - Samples: 10C, 22C, 17G, 4A, 16D, 45F and 4D

Final F1: 5'- CTTCCTCTTCAAGGCGCTGCTCGACTACGCGTGAAGTGGCCCCTCCAGGCTC -3'
Final F2: 5'-CCTTCCTCTTCAAGGCGCTGCTCGACGTCCCAGACTACGCGTGAAGTGGCCCCTCC-3'
Final F3: 5'-CCTTCCTCTTCAAGGCGCTGCTCTACCCGTATGACGTCCCAGACTACGCGTGAAGTG-3'

Final R1: 5'-GAGCCTGGAGGGGCCACTTCACGCGTAGTCGAGCAGCGCCTTGAAGAGGAAG-3'
Final R2: 5'-GGAGGGGCCACTTCACGCGTAGTCTGGGACGTCGAGCAGCGCCTTGAAGAGGAAG-3'
Final R3: 5'-CACTTCACGCGTAGTCTGGGACGTCATACGGGTAGAGCAGCGCCTTGAAGAGGAAG-3'

4D HA - Samples: 4D

4D F1: 5'-CTTCCCCGCCATCACAGCCATGGTACCCGTATTGACCAGCTCCACCAGTCCTGGG-3'
4D F2: 5'-GCCATCACAGCCATGGTACCCGTATGACGTCCCATGACCAGCTCCACCAGTCCTGGG-3'
4D F3: 5'-GCCATGGTACCCGTATGACGTCCCAGACTACGCGTGACCAGCTCCACCAGTCCTGGG-3'

4D R1: 5'-CCCAGGACTGGTGGAGCTGGTCAATACGGGTACCATGGCTGTGATGGCGGGGAAG-3'
4D R2: 5'-CCCAGGACTGGTGGAGCTGGTCATGGGACGTCATACGGGTACCATGGCTGTGATGGC-3'
4D R3: 5'-CCCAGGACTGGTGGAGCTGGTCACGCGTAGTCTGGGACGTCATACGGGTACCATGGC-3'

P120 HA - 22C and 4D

P120 F1: 5'-CCTTCATGCTGCTCTTTGCCGTTTCGACTACGCGTAATGGCTACCTGGTGTCCCTCACC-3'
P120 F2: 5'-CCTTCATGCTGCTCTTTGCCGTTTCGACGTCCCAGACTACGCGTAATGGCTACCTGG-3'
P120 F3: 5'-CCTTCATGCTGCTCTTTGCCGTTTCTACCCGTATGACGTCCCAGACTACGCGTAATGG-3'

P120 R1: 5'-GGTGAGGGACACCAGGTAGCCATTACGCGTAGTCGAAACGGCAAAGAGCAGCATGAAGG-3'
P120 R2: 5'-CCAGGTAGCCATTACGCGTAGTCTGGGACGTCGAAACGGCAAAGAGCAGCATGAAGG-3'
P120 R3: 5'-CCATTACGCGTAGTCTGGGACGTCATACGGGTAGAAACGGCAAAGAGCAGCATGAAGG-3'

Table 22. Ubq-hENT2-loop construct sequences

518 pb:

AGGAGGTAAAACATATGCACCACCACCATCATCACATGCAAATCTTCGTGAAAACGTTGACCGGCAAG
ACCATTACCCTGGAGGTCGAGCCAAGCGACACGATCGAGAATGTTAAAGCAAAGATCCAGGATAAAGA
AGGCATTCCGCCGGATCAGCAGCGTCTGATTTTTGCGGGTAAGCAACTGGAAGATGGCCGCACCCTG
AGCGACTACAACATTCAGAAAGAGTCCACCCTGCATCTGGTTCTGCGTTTGCGCGGTGGTCTGGTGC
CGCGTGGATCCCACCTGAAGTTTGCCCGCTACTACCTGGCCAATAAATCATCCCAGGCCCAAGCTCAG
GAGCTGGAGACCAAAGCTGAGCTCCTCCAGTCTGATGAGAACGGGATTCCCAGTAGTCCCCAGAAAG
TAGCTCTGACCCTGGATCTTGACCTGGAGAAGGAGCCGGAATCAGAGCCAGATGAGCCCCAGAAGCC
AGGAAAACCTTCAGTCTTCACTGTCTTCCAGAAGATCTAACTCGAG

Protein - 165 aa:

MHHHHHHMQIFVKTLTGKTITLEVEPSDTIENVKAKIQDKEGIPPDQQRLIFAGKQLEDGRTLSDYNIQKEST
LHLVLRLRGGLVPRGSHLKFARYYLANKSSQAQAQELETKAELLQSDENGIPSSPQKVALTLDLDLEKEPES
EPDEPQKPGKPSVFTVFQKI

Table 23. Ubq-mENT2-loop construct sequences

518 pb:

AGGAGGTAAAACATATGCACCACCACCATCATCACATGCAAATCTTCGTGAAAACGTTGACCGGCAAG
ACCATTACCCTGGAGGTCGAGCCAAGCGACACGATCGAGAATGTTAAAGCAAAGATCCAGGATAAAGA
AGGCATTCCGCCGGATCAGCAGCGTCTGATTTTTGCGGGTAAGCAACTGGAAGATGGCCGCACCCTG
AGCGACTACAACATTCAGAAAGAGTCCACCCTGCATCTGGTTCTGCGTTTGCGCGGTGGTCTGGTGC
CGCGTGGATCCCATCTGAAGTTTGCCCGTTACTACCTGACCGAGAAGCTGTCTCAGGCTCCAACTCAG
GAGCTGGAGACTAAAGCTGAGCTCCTCCAAGCTGATGAGAAGAATGGGGTTCCCATCAGCCCCCAAC
AGGCCAGCCCAACTCTGGATCTTGACCCTGAGAAGGAGCCAGAGCCGGAGGAGCCACAGAAGCCAG
GAAAACCTTCAGTCTTTGTTGTCTTCCGGAAGTAACTCGAG

Protein - 163 aa:

MHHHHHHMQIFVKTLTGKTITLEVEPSDTIENVKAKIQDKEGIPPDQQRLIFAGKQLEDGRTLSDYNIQKEST
LHLVLRLRGGLVPRGSHLKFARYYLTEKLSQAPTQELETKAELLQADEKNGVPISPQQASPTLDLDPEKEPE
PEEPQKPGKPSVFVVFRK

Cell/Gen	OATP1B1	OATP1B3	OATP2B1	OATP4A1	OCT1	OCT2	OCT3	OCTN1	OCTN2	OAT1	OAT2	OAT3	OAT4	CTR1
AGS	NA	-4,20971	-5,435465	-3,665235	-11,76831	NA	NA	-11,18556	-5,034325	NA	NA	NA	NA	-4,429015
BxPC3	-10,69173	-4,956665	NA	-2,994855	-9,23744	NA	-7,13413	-8,595715	-6,61803	NA	NA	NA	NA	-3,462865
EGI-1	-10,05249	-3,556385	NA	-2,60149	-11,42369	NA	-9,728725	-10,01162	-6,00497	NA	NA	NA	NA	-4,36339
MKN-45	NA	-11,52148	-7,797	-5,1114	-12,05624	NA	-9,94456	NA	-6,752815	NA	NA	NA	-12,3437	-4,79635
Mz-ChA-1	NA	NA	NA	-4,92122	-11,42547	-10,17476	-6,24082	-8,692235	-5,46582	NA	NA	NA	NA	-4,71838
Mz-ChA-2	-9,6066	-15,72675	-8,36523	-7,16294	-11,76959	-15,44028	-8,3963	-15,15602	-8,9475	NA	NA	-13,68473	-9,23388	-4,443935
NP29	-11,09852	-3,81181	NA	-0,941765	-9,278685	NA	-7,247705	-8,004215	-5,61443	NA	NA	NA	NA	-4,818325
NP31	NA	-10,80012	-13,39471	-2,29445	-11,79997	-10,75569	-5,4065	-10,36194	-5,74578	NA	NA	NA	NA	-3,633275
NP9	-11,17343	-3,31581	-10,7776	-3,286005	NA	NA	-7,98885	-7,961525	-5,246475	NA	NA	NA	NA	-3,971235
PanC1	NA	-9,16901	NA	-1,682615	-9,62681	NA	NA	-9,57969	-7,194345	NA	NA	NA	NA	-4,430015
Sk-ChA-1	NA	-7,711915	-7,512015	-4,444155	-12,95942	-12,65529	-6,603785	-11,07523	-6,35938	NA	NA	NA	-11,02004	-4,750225
SNU-1	NA	NA	NA	-4,8176	-12,17037	NA	NA	-15,67475	-9,32421	NA	NA	NA	NA	-4,788885
SNU-5	NA	-7,65809	-9,12831	-3,933715	-12,86918	-12,07471	-7,621695	-10,55413	-6,777625	NA	NA	NA	NA	-4,30338
TFK-1	-11,12423	-4,87962	-7,93727	-5,139255	-12,2882	-13,96125	-6,711245	-9,08694	-4,36496	NA	NA	NA	NA	-5,371035

Cell/Gen	ENT1	ENT2	ENT3	ENT4	CNT1	CNT2	CNT3	AQP1	AQP3	AQP4	AQP5	AQP7	AQP8	AQP9
AGS	-4,48816	-5,108655	-6,040615	-10,3049	NA	NA	-8,621785	-9,74808	-3,3001	NA	-8,815705	NA	NA	NA
BxPC3	-3,55663	-5,66195	-6,83732	-13,29748	NA	NA	-8,855135	-13,68616	-1,75554	NA	-11,16697	NA	NA	NA
EGI-1	-4,11311	-4,856205	-7,358815	-10,41705	NA	NA	-8,522945	NA	-3,558975	NA	-11,23419	NA	-14,70913	NA
MKN-45	-4,477365	-5,755195	-7,417955	-6,713935	NA	-10,88145	-11,11477	-7,709175	-8,0008	NA	-11,38667	NA	NA	NA
Mz-ChA-1	-4,828465	-8,21024	-5,51053	-9,28921	NA	NA	-10,05569	-14,936	-9,18969	NA	-9,50263	NA	NA	NA
Mz-ChA-2	-4,51722	-8,28933	-5,609685	-5,6049	-12,63622	-15,20588	-12,7799	-13,03119	-7,02197	-14,94784	NA	-14,48962	NA	NA
NP29	-3,32804	-4,16842	-5,790305	-11,14844	NA	NA	-5,531055	-9,19134	-6,130935	NA	-5,60757	NA	NA	NA
NP31	-3,61151	-5,758665	-4,788785	-9,689315	NA	NA	-8,662195	-13,70469	-4,382915	NA	-12,68652	NA	NA	NA
NP9	-3,912125	-8,428165	-9,151665	NA	NA	NA	-8,9394	NA	-9,831825	NA	-11,59395	NA	NA	NA
PanC1	-1,12045	-5,23147	-7,26113	-5,52936	NA	NA	-8,536215	NA	-9,22808	NA	NA	-12,06724	-13,1866	NA
Sk-ChA-1	-4,598565	-5,58829	-7,100105	-5,64634	NA	NA	-11,14247	-6,78028	-0,748245	NA	-7,765215	NA	NA	NA
SNU-1	-5,110555	-12,08074	-8,540745	-7,36897	NA	NA	-13,41086	-12,03358	NA	NA	NA	NA	NA	NA
SNU-5	-4,458995	-5,963585	-7,863375	-8,37507	-14,23356	NA	NA	NA	-6,72121	NA	-10,72669	-14,92393	NA	NA
TFK-1	-5,06459	-5,582785	-6,37544	-5,81507	NA	NA	-9,595065	-10,3983	-6,68229	NA	-11,49227	NA	NA	-11,062

Cell/Gen	ABCA2	ABCA3	ABCB1	ABCB4	ABCB11	ABCC1	ABCC2	ABCC3	ABCC4	ABCC5	ABCC11	ABCG2	MVP	ATP7A
AGS	-5,41722	-7,085075	NA	NA	NA	-3,98453	-11,48586	-4,385635	-3,52155	-6,188875	NA	-13,55328	-3,040235	-4,75924
BxPC3	-3,89874	-13,65283	NA	NA	-8,7893	-3,818015	-10,5806	-4,492505	-5,212655	-5,75565	NA	-10,40449	-4,80388	-5,17156
EGI-1	-5,697745	-14,46329	NA	NA	-12,26137	-3,948185	-9,49191	-3,4013	-5,90329	-8,199575	NA	-7,87334	-2,54769	-6,87543
MKN-45	-4,64829	-9,264445	NA	NA	NA	-3,754625	-12,19454	-3,643625	-5,616965	-6,257425	-12,23887	NA	-2,929135	-5,508155
Mz-ChA-1	-4,93282	-6,126265	NA	NA	-9,86442	-2,67724	-10,66025	-1,87665	-5,22998	-7,244495	NA	-5,24591	-2,76473	-4,51397
Mz-ChA-2	-6,902985	-12,97593	NA	-11,24568	-12,65375	-4,290905	-6,95164	-8,108415	-4,071185	-5,710435	-13,2543	-6,889	-6,93537	-6,27479
NP29	-4,807005	-5,20956	NA	NA	-10,62884	-3,240725	-10,26468	-2,27473	-4,75562	-6,24291	-12,66776	-9,610475	-2,894275	-5,324655
NP31	-4,90704	-5,735895	-9,296155	NA	-10,65084	-3,353325	-10,70574	-2,757485	-5,65783	-7,260135	-11,82627	-8,274495	-3,383585	-5,04453
NP9	-3,402425	-5,71973	NA	NA	NA	-2,56444	-10,63572	-1,76093	-3,500135	-6,145955	NA	-11,4493	-2,24129	-4,36951
PanC1	-5,89955	-3,693405	NA	NA	NA	-1,825585	-8,23494	-3,891615	-3,875345	-5,406305	NA	-5,377025	-3,44152	-4,479565
Sk-ChA-1	-4,616145	-7,74906	-6,95206	NA	-10,19418	-5,00557	-6,014445	-4,854745	-4,81766	-7,748145	-11,27209	-8,65869	-3,48108	-7,022115
SNU-1	-4,07565	-4,69544	NA	NA	NA	-5,231355	-11,28198	-16,26229	-5,26948	-7,47478	-12,61088	NA	-7,070585	-5,908625
SNU-5	-4,348695	-7,673805	-9,67136	NA	NA	-5,40117	-5,89557	-4,068065	-6,87289	-6,869305	NA	-5,988395	-3,734565	-6,33067
TFK-1	-5,595585	NA	NA	NA	-12,95264	-1,987495	-2,14282	-2,27818	-5,07186	-6,322225	-12,2226	-6,54682	-3,025015	-6,492285

Cell/Gen	ATP7B	DPYD	TYMP	UPP1	UPP2	EPHX1	DCK	RRM1	TYMS	TK1	NT5C1A	NT5C1B	UMPS	UCK2
AGS	-5,2312	-9,55241	-5,03248	-4,81043	NA	-3,312615	-3,94119	-2,20443	-1,967005	-1,01614	NA	NA	-3,782425	-2,740605
BxPC3	-7,655925	-6,64923	-4,79445	-1,69193	NA	-4,28779	-3,81116	-1,86295	-2,268095	-0,751955	NA	NA	-2,90513	-2,948895
EGI-1	-8,76941	-6,546565	-6,34925	-2,777885	NA	-2,470405	-4,618635	-1,535325	-1,84546	-0,65284	NA	NA	-4,23781	-3,77673
MKN-45	-6,315025	-6,48279	-9,385135	-3,84305	NA	-5,43189	-5,132985	-3,93188	-3,70968	-3,26001	NA	NA	-4,370795	-4,194575
Mz-ChA-1	-6,429625	-4,174035	-5,122935	-3,21162	NA	-0,299175	-5,288545	-3,067245	-2,373485	-2,475675	NA	NA	-5,29534	-4,19783
Mz-ChA-2	-4,50392	-10,93061	-10,97152	-5,02388	NA	-3,8264	-5,34487	-3,347995	-2,14418	-1,763025	NA	NA	-4,27379	-3,37312
NP29	-7,55245	-5,028225	-5,425465	-1,62119	NA	-2,43024	-3,505315	-1,063265	-2,54269	-0,65654	NA	NA	-3,1979	-2,20119
NP31	-7,975065	-5,22744	-5,48285	-2,40618	NA	-1,95234	-3,91126	-1,3618	-2,710565	-0,206065	NA	NA	-4,25396	-3,169075
NP9	-5,356765	-3,229125	-6,5662	-3,274425	NA	-0,8261	-3,89873	-1,67711	-2,506805	-1,375045	NA	NA	-4,0643	-3,566115
PanC1	-5,139875	-7,363455	-3,869365	-0,482755	NA	-3,48613	-3,531935	-1,77187	-1,6029	-1,414395	NA	NA	-3,216435	-2,446915
Sk-ChA-1	-8,66074	-9,320865	-8,471835	-5,091665	NA	-3,0345	-4,89407	-2,78724	-3,26232	-1,84193	-12,77128	NA	-4,403795	-3,96438
SNU-1	-4,74977	-6,472475	NA	-5,713025	NA	-2,89532	-4,165195	-2,94331	-2,36634	-2,7432	NA	NA	-5,27619	-3,838375
SNU-5	-7,56741	-5,611825	-6,65077	-3,417005	NA	-3,444625	-5,289615	-1,92674	-2,499755	-2,24703	-12,00014	NA	-5,07836	-3,935285
TFK-1	-9,39455	-8,229725	-4,402055	-3,224915	NA	-0,02381	-5,153975	-2,667355	-3,318605	-1,073245	NA	NA	-3,60683	-2,668715

Cell/Gen	FPGS	GCLC	MT4	UGTX	TOP1	TOP2A	KIT	PDGFRA	ERCC1	XPA	XPC	UDG	MLH1	PMS2
AGS	-2,83425	-3,09693	NA	-3,744045	-1,93892	-0,80761	NA	-4,54685	-2,95385	-4,518545	-3,809865	-4,488545	-4,329915	-4,100245
BxPC3	-1,94934	-2,684275	NA	-1,233145	-2,165455	-0,750075	-12,19914	-9,22018	-3,176485	-4,03085	-6,438705	-3,670535	-4,10751	-4,059545
EGI-1	-2,56791	-2,682565	NA	-9,74681	-2,957845	-0,92547	NA	NA	-3,71978	-4,045945	-5,793415	-3,786175	-4,57863	-5,10102
MKN-45	-4,1679	-2,8151	NA	-3,01843	-3,78872	-2,76173	NA	NA	-4,237545	-5,395835	-5,015945	-5,35719	-5,121545	-3,84644
Mz-ChA-1	-3,08278	-1,71934	NA	-1,798195	-3,664065	-0,94129	NA	NA	-4,00461	-5,544315	-6,047305	-4,94315	-5,489885	-4,301985
Mz-ChA-2	-4,23683	-4,505625	NA	-12,18246	-2,869695	-1,121205	-13,7148	-4,40695	-3,711855	-5,400275	-5,7583	-4,09597	-5,07167	-4,59143
NP29	-2,483215	-3,41416	NA	-10,15364	-1,62344	-0,92748	NA	-14,29259	-3,410115	-4,11076	-4,998695	-3,210885	-4,17463	-3,231165
NP31	-2,525425	-3,40312	NA	-2,029025	-2,78366	-0,116265	-9,76655	-13,76424	-4,19674	-3,935955	-5,48546	-3,75522	-4,731805	-4,03652
NP9	-2,28207	-3,4213	NA	-3,001175	-1,974945	-0,11038	NA	-14,04978	-2,28218	-3,989205	-4,606745	-3,834125	-4,37435	-4,552975
PanC1	-3,05818	-2,385335	NA	NA	-2,902915	-1,1054	-11,74103	NA	-1,82376	-4,755265	-5,209425	-2,987445	-4,268455	-2,79553
Sk-ChA-1	-3,680795	-3,27236	NA	-4,4128	-3,228395	0,702535	-9,71743	NA	-4,96376	-4,585485	-5,589145	-4,08331	-6,203325	-5,611255
SNU-1	-4,669465	-5,506225	NA	NA	-3,72961	-1,971265	NA	-2,68858	-3,666895	-5,072695	-4,652205	-4,64091	-8,15654	-4,44663
SNU-5	-3,98417	-3,8363	NA	-10,82671	-3,633195	-1,59533	NA	NA	-3,883085	-4,832885	-5,14812	-4,152435	-4,86563	-4,176445
TFK-1	-3,26699	-2,65895	NA	-0,862465	-3,243055	-0,81168	-8,83685	NA	-5,47927	-6,02476	-5,73341	-3,804205	-3,768235	-4,737925

Cell/Gen	MSH2	MSH6	GADD45	BAX	P21	FAS	BCL2	DIABLO	BIRC2	XIAP	BIRC5	BIRC7	CFLAR	EGFR
AGS	-3,459645	-4,247045	-3,84307	0,488515	-1,24083	-4,762275	NA	-2,236875	-4,441605	-4,282845	-3,255655	-8,380915	-5,30825	-3,450015
BxPC3	-3,167525	-3,31743	-4,507185	-1,455085	-4,69617	-3,541885	-6,6567	-2,70301	-4,062575	-3,967425	-2,60949	NA	-5,4731	-1,762135
EGI-1	-3,10419	-3,48713	-3,51895	-1,675695	-2,16363	-3,935825	-9,35913	-3,41603	-2,873845	-5,537715	-2,48763	NA	-4,70796	-2,706125
MKN-45	-4,698175	-5,81438	-3,133125	-1,211575	-2,37337	-4,28363	-10,81212	-2,8193	-5,43695	-5,45988	-3,43222	-13,80426	-5,57455	-3,751195
Mz-ChA-1	-3,371035	-4,086815	-4,41253	-2,323115	-3,8269	-5,86882	-9,66895	-4,15395	-5,026565	-5,14086	-3,76406	-12,96066	-6,5353	-1,48603
Mz-ChA-2	-3,33151	-3,7091	-3,028615	-2,511515	-8,08444	NA	NA	-3,487355	-4,60777	-5,54674	-3,172805	-10,38	-6,699595	-3,040785
NP29	-2,747765	-3,176625	-3,20866	-0,80986	-4,546285	-4,15081	-8,14708	-2,88111	-3,850535	-3,456385	-2,669715	-11,61153	-5,858845	-0,140285
NP31	-3,44189	-3,59144	-4,56694	-2,0975	-4,29661	-3,328465	-8,072075	-3,50348	-3,64403	-3,866945	-2,324725	NA	-5,20667	-0,435
NP9	-3,69125	-3,90251	-2,80108	-1,05884	-5,49351	-5,01614	-7,005225	-3,074095	-4,567035	-4,18329	-2,46183	NA	-5,792455	-1,61083
PanC1	NA	-3,79927	-2,75506	-1,716555	-2,160485	-4,464	-13,27072	-1,894005	-1,753005	-4,028315	-1,963575	-9,188175	-4,68466	-1,368455
Sk-ChA-1	-3,90591	-4,32886	-4,429765	-3,03571	-3,78881	-6,126575	-9,156065	-4,691465	-5,12595	-5,12644	-3,02137	-11,9623	-5,19976	-3,53287
SNU-1	-3,983925	-4,69763	-5,522745	-1,502165	-4,521185	-4,773355	-6,00932	-4,191125	-6,156315	-5,619	-4,032565	NA	-6,368255	-2,05668
SNU-5	-3,54879	-4,29558	-4,807325	-2,569065	-4,867085	-5,200455	-9,973355	-3,2266	-5,229685	-5,22723	-3,37898	-7,613685	-5,23483	-4,06814
TFK-1	-3,626835	-3,88848	-5,90541	-2,74736	-4,11514	-5,883515	-10,09025	-3,60978	-4,94117	-5,64547	-2,74347	-11,22107	-7,56556	-2,81749

Cell/Gen	PI3K	MYC	MMP1	MMP2	MMP3	AFP	TIGAR	NRF2	KEAP1	ENT1n	ENT2n	CNT1n	CNT2n	CNT3n
AGS	NA	-1,743085	-2,22808	-11,91178	NA	NA	-3,271425	-3,312215	-3,61227	-3,700049	-8,668126	-16,54985	-18,2536	-9,609247
BxPC3	-7,199105	-1,41507	-0,668855	NA	NA	NA	-4,80616	-3,51612	-3,310605	-2,071276	-8,768869	-16,71301	-16,0193	-9,62803
EGI-1	-7,862385	-2,67423	-8,232075	-10,57992	NA	NA	-5,20692	-4,14742	-3,66429	-2,457211	-7,360897	-16,12107	-16,82166	-9,977932
MKN-45	NA	-5,216055	-6,07865	NA	NA	NA	-3,83117	-4,57965	-4,350795	-3,066386	-7,971486	-18,06109	-12,39992	-13,14338
Mz-ChA-1	NA	-4,1619	-5,793285	NA	NA	-15,11438	-5,448265	-4,681545	-5,06276	-3,873138	-12,01284	-18,19187	-16,98654	-9,917473
Mz-ChA-2	NA	-4,17769	NA	NA	NA	-0,580935	-3,560275	-4,366645	-4,96801	-3,299921	-11,26149	-12,3137	-14,21486	-11,65455
NP29	-11,57008	0,271045	-8,63939	NA	NA	NA	-5,385585	-3,821965	-3,23286	-2,861931	-5,600281	-13,77298	-16,13238	-6,368245
NP31	NA	-1,879395	-2,60261	-10,50093	NA	NA	-4,92335	-3,71385	-3,518305	-2,025837	-8,521285	-14,00645	-15,80163	-8,148745
NP9	-13,01374	-1,45755	-8,29967	-10,91249	NA	NA	-4,67876	-4,2399	-2,62472	-2,970685	-11,16807	-15,60731	-14,13019	-8,033955
PanC1	NA	-2,637895	-6,76227	-5,55476	NA	NA	-3,911425	-3,22109	-3,48964	0,0084813	-8,161475	-16,80808	-15,48811	-10,062
Sk-ChA-1	NA	-2,877845	-5,659205	-14,91166	NA	-11,40031	-6,55251	-3,953105	-3,831825	-2,806299	-8,133876	-16,88235	-14,28706	-11,61002
SNU-1	NA	-2,799495	NA	NA	NA	NA	-4,662585	-3,078135	-4,65431	-3,231682	-13,48696	-15,89879	-17,02107	-13,67259
SNU-5	NA	-2,131115	-11,83926	NA	NA	NA	-6,43421	-4,711915	-5,195785	-2,834947	-8,504425	-13,97103	-18,9253	-13,39149
TFK-1	NA	-2,6331	-11,1846	NA	NA	NA	-5,93218	-3,74637	-4,435795	-3,576006	-8,991659	-14,70727	-16,30568	-10,12759

Table 24. Values of normalized expression of the Transportome genes in the 15 cell lines.

Correlat.	OATP1B1	OATP1B3	OATP2B1	OATP4A1	OCT1	OCT2	OCT3	OCTN1	OCTN2	CTR1	ENT1	ENT2	ENT3	ENT4	CNT3
OATP1B1	1,000	-0,742	0,000	-0,529	-0,371	0,000	-0,684	-0,880	-0,850	0,167	-0,219	-0,247	0,351	0,275	-0,654
OATP1B3	-0,742	1,000	0,175	0,552	0,271	0,342	0,065	0,802	0,775	-0,015	-0,017	0,393	-0,355	-0,577	0,700
OATP2B1	0,000	0,175	1,000	-0,495	-0,114	-0,702	-0,520	-0,283	-0,010	-0,697	-0,786	0,317	-0,078	0,215	-0,285
OATP4A1	-0,529	0,552	-0,495	1,000	0,629	0,754	0,184	0,615	0,366	0,360	0,701	0,520	0,001	-0,532	0,847
OCT1	-0,371	0,271	-0,114	0,629	1,000	0,193	0,030	0,476	0,050	0,341	0,714	0,308	0,195	-0,514	0,651
OCT2	0,000	0,342	-0,702	0,754	0,193	1,000	0,764	0,708	0,503	0,394	0,347	0,102	0,181	-0,877	0,704
OCT3	-0,684	0,065	-0,520	0,184	0,030	0,764	1,000	0,227	0,376	0,134	0,064	-0,050	0,523	-0,113	0,199
OCTN1	-0,880	0,802	-0,283	0,615	0,476	0,708	0,227	1,000	0,812	0,161	0,366	0,608	0,058	-0,458	0,823
OCTN2	-0,850	0,775	-0,010	0,366	0,050	0,503	0,376	0,812	1,000	-0,051	-0,014	0,586	0,239	-0,324	0,687
CTR1	0,167	-0,015	-0,697	0,360	0,341	0,394	0,134	0,161	-0,051	1,000	0,369	0,065	0,009	-0,587	0,219
ENT1	-0,219	-0,017	-0,786	0,701	0,714	0,347	0,064	0,366	-0,014	0,369	1,000	0,411	0,020	-0,068	0,531
ENT2	-0,247	0,393	0,317	0,520	0,308	0,102	-0,050	0,608	0,586	0,065	0,411	1,000	0,372	-0,268	0,732
ENT3	0,351	-0,355	-0,078	0,001	0,195	0,181	0,523	0,058	0,239	0,009	0,020	0,372	1,000	-0,224	0,253
ENT4	0,275	-0,577	0,215	-0,532	-0,514	-0,877	-0,113	-0,458	-0,324	-0,587	-0,068	-0,268	-0,224	1,000	-0,585
CNT3	-0,654	0,700	-0,285	0,847	0,651	0,704	0,199	0,823	0,687	0,219	0,531	0,732	0,253	-0,585	1,000
AQP1	0,000	0,230	0,631	0,072	-0,294	-0,345	-0,422	0,044	0,167	-0,500	-0,085	0,427	-0,396	0,373	0,075
AQP3	0,278	0,206	0,274	0,121	-0,085	-0,060	0,184	-0,186	0,047	0,243	-0,191	0,507	0,215	-0,401	0,042
AQP5	-0,268	0,320	0,735	0,285	0,291	-0,066	0,131	0,043	0,042	-0,413	0,104	0,355	0,217	-0,073	0,393
ABCA2	-0,733	0,484	-0,331	0,257	0,003	0,766	0,168	0,319	0,140	0,308	-0,134	-0,243	-0,549	-0,429	0,088
ABCA3	-0,791	0,096	-0,392	0,314	-0,009	0,970	0,553	0,116	0,140	-0,283	0,249	-0,197	-0,080	0,266	0,149
ABCB11	-0,323	0,229	0,000	0,404	0,471	0,850	0,473	0,472	0,064	0,531	0,452	0,056	0,013	-0,611	0,256
ABCC1	-0,837	0,209	-0,246	0,300	0,493	0,128	0,220	0,621	0,536	-0,085	0,474	0,258	0,212	0,054	0,532
ABCC2	-0,002	-0,073	0,154	-0,292	-0,346	-0,683	0,217	-0,017	0,118	-0,419	-0,136	0,189	0,048	0,533	-0,119
ABCC3	-0,867	0,668	-0,376	0,381	0,220	0,737	0,263	0,875	0,829	0,128	0,282	0,733	0,304	-0,239	0,714
ABCC4	-0,164	0,065	0,286	0,012	0,336	-0,557	0,042	-0,000	0,074	-0,006	0,297	-0,082	0,006	0,192	0,094
ABCC5	-0,207	-0,201	0,275	0,010	0,527	-0,775	-0,080	0,154	-0,042	0,124	0,467	0,147	0,064	0,073	0,174
ABCC11	0,000	0,339	-0,139	0,300	-0,469	0,000	0,472	0,422	0,513	0,110	0,020	0,394	-0,068	0,065	0,146
ABCG2	0,505	-0,514	-0,261	-0,242	-0,164	0,120	0,115	-0,129	-0,341	-0,343	0,098	-0,167	0,139	0,558	-0,319
MVP	-0,692	0,676	-0,079	0,493	0,074	0,741	0,011	0,856	0,874	-0,040	0,200	0,633	0,033	-0,214	0,694
ATP7A	-0,580	0,117	-0,299	0,362	0,562	0,707	0,265	0,389	0,222	0,372	0,465	-0,075	0,085	-0,327	0,368
ATP7B	0,340	-0,383	0,165	-0,248	0,119	-0,245	-0,283	-0,477	-0,547	0,089	0,151	-0,575	-0,206	0,216	-0,379
DPYD	-0,710	0,419	-0,684	0,473	0,261	0,918	0,137	0,564	0,300	0,266	0,135	-0,124	-0,257	-0,472	0,404
TYMP	-0,781	0,649	-0,133	0,654	0,468	0,628	0,527	0,766	0,637	0,106	0,406	0,380	0,093	-0,425	0,725
UPP1	-0,588	0,264	-0,769	0,748	0,762	0,647	0,201	0,729	0,344	0,328	0,800	0,558	0,164	-0,357	0,758
EPHX1	-0,628	0,481	-0,355	0,053	-0,128	0,378	0,519	0,423	0,559	-0,230	-0,212	-0,158	0,124	0,009	0,222
DCK	-0,580	0,438	-0,346	0,800	0,713	0,431	0,221	0,285	0,099	0,438	0,660	0,163	-0,064	-0,468	0,607
RRM1	-0,514	0,590	-0,576	0,875	0,508	0,503	0,282	0,609	0,376	0,482	0,545	0,431	0,041	-0,579	0,814
TYMS	0,703	0,146	0,004	0,336	0,468	0,038	-0,055	-0,125	-0,225	0,386	0,477	-0,065	0,015	-0,311	0,216
TK1	-0,349	0,451	-0,409	0,608	0,447	-0,016	0,360	0,477	0,465	0,431	0,385	0,534	0,401	-0,499	0,712
UMPS	-0,549	0,361	0,231	0,514	0,729	-0,603	0,015	0,471	0,314	0,215	0,611	0,620	0,181	-0,280	0,665
UCK2	-0,545	0,281	0,082	0,525	0,649	-0,479	0,318	0,301	0,265	0,039	0,559	0,454	0,343	-0,203	0,641
FPGS	-0,586	0,691	-0,433	0,695	0,655	0,697	0,291	0,820	0,660	0,537	0,438	0,506	0,208	-0,736	0,844
GCLC	-0,470	0,468	0,217	0,288	0,316	0,619	0,121	0,788	0,688	0,009	0,305	0,604	0,290	-0,207	0,527
UGTX	-0,666	0,231	-0,119	0,012	0,005	0,517	0,422	0,491	0,583	0,092	-0,130	-0,082	0,038	-0,091	-0,012
TOP1	-0,474	0,512	-0,042	0,551	0,658	-0,397	0,121	0,423	0,365	0,404	0,389	0,375	0,162	-0,586	0,711
TOP2A	-0,625	0,296	-0,252	0,251	0,006	0,157	0,621	0,391	0,428	0,281	0,112	0,230	0,214	-0,103	0,299
KIT	0,000	0,578	0,000	0,250	-0,526	0,000	0,792	0,551	0,921	-0,393	-0,294	0,667	0,018	0,123	0,391
PDGFRA	0,000	-0,392	0,000	-0,764	-0,583	0,000	-0,515	-0,843	-0,681	-0,398	-0,882	-0,522	-0,105	0,558	-0,768
ERCC1	-0,025	0,157	-0,096	0,470	0,667	0,166	-0,260	0,138	-0,163	0,478	0,686	-0,059	-0,305	-0,273	0,309
XPA	-0,135	0,429	-0,511	0,747	0,433	0,441	0,049	0,329	0,153	0,730	0,438	0,299	-0,100	-0,674	0,562
XPC	-0,459	0,210	0,338	0,133	-0,200	0,003	-0,260	-0,189	0,037	-0,153	-0,019	-0,122	-0,312	0,100	0,058
UDG	-0,586	0,301	-0,497	0,658	0,583	-0,435	0,303	0,429	0,146	0,265	0,707	0,423	0,078	-0,140	0,604
MLH1	-0,848	0,483	-0,076	0,387	0,444	-0,252	-0,042	0,702	0,652	0,226	0,424	0,752	0,304	-0,298	0,734
PMS2	-0,429	-0,087	-0,193	0,513	0,678	0,390	0,043	0,263	-0,044	0,132	0,706	0,229	0,162	-0,174	0,461
MSH2	0,163	0,374	-0,204	0,505	0,630	0,063	0,301	0,439	0,226	0,273	0,528	0,317	0,438	-0,618	0,625
MSH6	0,045	0,334	-0,411	0,487	0,568	-0,193	0,402	0,517	0,229	0,377	0,389	0,288	0,363	-0,462	0,579
GADD45	0,315	-0,185	0,007	0,253	0,452	-0,256	-0,607	0,186	-0,062	0,227	0,558	0,251	-0,060	0,006	0,292
BAX	-0,424	0,415	0,290	0,392	0,408	0,485	-0,399	0,134	0,179	0,183	0,184	0,118	-0,089	-0,509	0,410
P21	-0,303	0,390	0,406	0,418	0,061	0,717	-0,202	0,320	0,402	-0,155	0,221	0,449	-0,049	-0,144	0,339
FAS	0,595	-0,143	-0,561	0,635	0,551	0,446	-0,206	0,063	-0,190	0,648	0,465	0,243	0,170	-0,596	0,388
BCL2	-0,198	0,497	-0,710	-0,028	0,020	0,482	0,309	-0,258	-0,155	0,357	-0,431	-0,499	-0,155	-0,580	-0,138
DIABLO	-0,390	0,129	0,201	0,470	0,597	-0,210	-0,433	0,328	0,145	0,300	0,671	0,463	-0,014	-0,254	0,526
BIRC2	0,306	0,118	-0,582	0,676	0,633	0,173	-0,051	0,406	0,183	0,350	0,858	0,562	0,215	-0,185	0,631
XIAP	-0,567	0,306	-0,493	0,784	0,723	0,655	0,435	0,549	0,326	0,539	0,673	0,402	0,233	-0,547	0,759
BIRC5	-0,577	0,255	-0,743	0,650	0,527	-0,127	0,116	0,548	0,359	0,405	0,752	0,594	0,093	-0,127	0,653
BIRC7	0,000	0,187	0,057	0,232	-0,017	-0,258	0,139	-0,289	-0,122	0,598	0,278	0,193	-0,233	-0,108	0,234
CFLAR	0,182	0,111	-0,151	0,621	0,202	0,472	-0,232	0,189	-0,007	0,526	0,572	0,448	-0,179	-0,278	0,365
EGFR	-0,608	0,187	-0,828	0,615	0,684	0,562	0,497	0,384	0,141	0,291	0,494	-0,018	0,301	-0,396	0,560
MYC	-0,749	0,693	-0,298	0,744	0,488	0,260	0,363	0,500	0,353	0,316	0,331	0,315	-0,000	-0,591	0,730
MMP1	0,271	-0,170	-0,015	0,126	0,307	0,649	0,268	-0,176	-0,129	0,579	0,152	0,036	0,408	-0,464	-0,106
MMP2	0,000	-0,260	0,000	0,920	0,986	0,000	0,000	0,425	-0,496	0,241	0,926	0,094	-0,055	0,147	0,712
TIGAR	0,685	-0,332	0,197	-0,100	0,294	-0,379	-0,475	-0,326	-0,294	0,197	0,268	-0,136	0,086	0,009	-0,141
NRF2	-0,530	0,306	0,156	0,374	0,363	-0,157	0,414	-0,194	-0,123	0,075	0,345	-0,047	-0,016	-0,100	0,112
KEAP1	-0,620	0,575	-0,296	0,715	0,621	0,187	0,031	0,525	0,400	0,449	0,539	0,371	-0,142	-0,460	0,700
ENT1n	0,083	-0,124	-0,842	0,603	0,519	0,220	0,035	0,196	-0,180	0,410	0,915	0,321	-0,106	0,044	0,302
ENT2n	-0,252	0,335	0,192	0,609	0,332	0,031	-0,159	0,524	0,437	0,019	0,425	0,943	0,247	-0,267	0,724
CNT1n	0,340	-0,271	-0,414	-0,048	-0,055	-0,627	0,143	-0,304	-0,183	0,081	-0,030	-0,005	0,249	0,067	0,063
CNT2n	0,144	-0,454	-0,132	-0,223	0,039	-0,473	-0,343	0,001	-0,153	-0,027	0,125	-0,023	-0,098	0,429	-0,278
CNT3n	-0,735	0,507	-0,460	0,651	0,639	0,405	0,395	0,705	0,620	0,281	0,417	0,426	0,395	-0,533	0,892

P Values	OATP1B1	OATP1B3	OATP2B1	OATP4A1	OCT1	OCT2	OCT3	OCTN1	OCTN2	CTR1	ENT1	ENT2	ENT3	ENT4	CNT3
OATP1B1	0,000	0,091	1,000	0,280	0,539	1,000	0,134	0,021	0,032	0,752	0,677	0,637	0,495	0,654	0,159
OATP1B3	0,091	0,000	0,678	0,063	0,420	0,573	0,858	0,003	0,003	0,964	0,958	0,207	0,258	0,063	0,016
OATP2B1	1,000	0,678	0,000	0,213	0,807	0,186	0,232	0,538	0,981	0,055	0,021	0,445	0,854	0,644	0,536
OATP4A1	0,280	0,063	0,213	0,000	0,021	0,084	0,589	0,025	0,198	0,206	0,005	0,057	0,996	0,061	0,000
OCT1	0,539	0,420	0,807	0,021	0,000	0,714	0,933	0,117	0,872	0,254	0,006	0,307	0,523	0,072	0,022
OCT2	1,000	0,573	0,186	0,084	0,714	0,000	0,077	0,116	0,310	0,440	0,501	0,848	0,732	0,022	0,185
OCT3	0,134	0,858	0,232	0,589	0,933	0,077	0,000	0,528	0,255	0,694	0,851	0,883	0,099	0,756	0,581
OCTN1	0,021	0,003	0,538	0,025	0,117	0,116	0,528	0,000	0,001	0,599	0,219	0,028	0,850	0,134	0,001
OCTN2	0,032	0,003	0,981	0,198	0,872	0,310	0,255	0,001	0,000	0,862	0,962	0,028	0,411	0,281	0,010
CTR1	0,752	0,964	0,055	0,206	0,254	0,440	0,694	0,599	0,862	0,000	0,194	0,824	0,975	0,035	0,473
ENT1	0,677	0,958	0,021	0,005	0,006	0,501	0,851	0,219	0,962	0,194	0,000	0,144	0,946	0,825	0,062
ENT2	0,637	0,207	0,445	0,057	0,307	0,848	0,883	0,028	0,028	0,824	0,144	0,000	0,190	0,376	0,004
ENT3	0,495	0,258	0,854	0,996	0,523	0,732	0,099	0,850	0,411	0,975	0,946	0,190	0,000	0,462	0,404
ENT4	0,654	0,063	0,644	0,061	0,072	0,022	0,756	0,134	0,281	0,035	0,825	0,376	0,462	0,000	0,046
CNT3	0,159	0,016	0,536	0,000	0,022	0,185	0,581	0,001	0,010	0,473	0,062	0,004	0,404	0,046	0,000
AQP1	1,000	0,584	0,179	0,843	0,409	0,570	0,298	0,911	0,644	0,141	0,815	0,219	0,257	0,289	0,836
AQP3	0,593	0,520	0,512	0,695	0,792	0,911	0,589	0,563	0,879	0,423	0,533	0,077	0,481	0,197	0,896
AQP5	0,663	0,367	0,060	0,396	0,415	0,916	0,718	0,907	0,902	0,207	0,761	0,284	0,522	0,842	0,261
ABCA2	0,098	0,111	0,423	0,375	0,993	0,075	0,622	0,288	0,633	0,283	0,649	0,403	0,042	0,143	0,776
ABCA3	0,111	0,778	0,384	0,296	0,978	0,006	0,098	0,720	0,649	0,350	0,412	0,519	0,794	0,404	0,643
ABCB11	0,596	0,621	1,000	0,321	0,239	0,068	0,237	0,237	0,881	0,176	0,261	0,894	0,975	0,108	0,540
ABCC1	0,038	0,514	0,557	0,298	0,087	0,809	0,516	0,023	0,048	0,773	0,087	0,373	0,466	0,860	0,061
ABCC2	0,997	0,822	0,716	0,311	0,247	0,135	0,522	0,955	0,687	0,136	0,644	0,517	0,870	0,061	0,700
ABCC3	0,025	0,018	0,359	0,179	0,471	0,094	0,435	0,000	0,000	0,663	0,328	0,003	0,291	0,431	0,006
ABCC4	0,756	0,841	0,492	0,968	0,262	0,251	0,903	1,000	0,801	0,985	0,303	0,780	0,982	0,529	0,760
ABCC5	0,694	0,531	0,511	0,972	0,064	0,070	0,815	0,616	0,887	0,673	0,092	0,615	0,827	0,814	0,570
ABCC11	1,000	0,511	0,823	0,514	0,288	1,000	0,344	0,405	0,239	0,814	0,966	0,382	0,885	0,891	0,755
ABCG2	0,306	0,106	0,572	0,448	0,629	0,821	0,751	0,690	0,278	0,274	0,762	0,604	0,668	0,075	0,340
MVP	0,128	0,016	0,852	0,073	0,811	0,092	0,975	0,000	0,000	0,891	0,492	0,015	0,912	0,482	0,008
ATP7A	0,227	0,718	0,472	0,203	0,046	0,116	0,431	0,189	0,446	0,190	0,094	0,800	0,773	0,275	0,217
ATP7B	0,509	0,220	0,695	0,393	0,698	0,639	0,399	0,099	0,043	0,762	0,607	0,031	0,480	0,478	0,201
DPYD	0,114	0,175	0,061	0,087	0,390	0,010	0,687	0,045	0,298	0,358	0,645	0,672	0,376	0,103	0,171
TYMP	0,066	0,022	0,754	0,015	0,125	0,182	0,096	0,004	0,019	0,729	0,168	0,200	0,763	0,169	0,008
UPP1	0,220	0,407	0,026	0,002	0,002	0,165	0,554	0,005	0,228	0,252	0,001	0,038	0,575	0,231	0,003
EPHX1	0,182	0,113	0,388	0,857	0,678	0,460	0,102	0,150	0,038	0,430	0,468	0,589	0,672	0,977	0,465
DCK	0,227	0,154	0,401	0,001	0,006	0,394	0,513	0,344	0,738	0,117	0,010	0,578	0,827	0,107	0,028
RRM1	0,297	0,043	0,135	0,000	0,076	0,309	0,401	0,027	0,186	0,081	0,044	0,124	0,890	0,038	0,001
TYMS	0,119	0,652	0,992	0,240	0,107	0,942	0,871	0,684	0,439	0,173	0,084	0,825	0,958	0,301	0,478
TK1	0,498	0,141	0,315	0,021	0,126	0,976	0,277	0,099	0,093	0,124	0,174	0,049	0,155	0,083	0,006
UMPS	0,259	0,250	0,583	0,060	0,005	0,205	0,964	0,104	0,274	0,460	0,020	0,018	0,535	0,355	0,013
UCK2	0,263	0,376	0,847	0,054	0,016	0,336	0,341	0,317	0,361	0,896	0,038	0,103	0,231	0,505	0,018
FPGS	0,222	0,013	0,284	0,006	0,015	0,124	0,386	0,001	0,010	0,048	0,118	0,065	0,475	0,004	0,000
GCLC	0,346	0,125	0,606	0,318	0,293	0,190	0,724	0,001	0,007	0,976	0,290	0,022	0,314	0,497	0,064
UGTX	0,149	0,495	0,780	0,971	0,989	0,294	0,196	0,125	0,047	0,777	0,687	0,800	0,907	0,790	0,972
TOP1	0,343	0,089	0,921	0,041	0,014	0,436	0,723	0,150	0,200	0,152	0,169	0,186	0,581	0,035	0,006
TOP2A	0,185	0,351	0,547	0,386	0,984	0,767	0,042	0,186	0,127	0,331	0,704	0,429	0,463	0,737	0,320
KIT	1,000	0,230	1,000	0,632	0,284	1,000	0,110	0,257	0,009	0,441	0,572	0,148	0,973	0,817	0,444
PDGFRA	1,000	0,442	1,000	0,045	0,225	1,000	0,375	0,017	0,092	0,377	0,009	0,230	0,823	0,249	0,044
ERCC1	0,963	0,625	0,821	0,090	0,013	0,753	0,439	0,653	0,579	0,084	0,007	0,841	0,289	0,367	0,305
XPA	0,799	0,164	0,195	0,002	0,139	0,381	0,887	0,273	0,601	0,003	0,117	0,299	0,733	0,012	0,046
XPC	0,360	0,512	0,414	0,649	0,512	0,996	0,441	0,537	0,900	0,601	0,950	0,678	0,277	0,746	0,851
UDG	0,221	0,341	0,210	0,010	0,036	0,389	0,365	0,143	0,619	0,360	0,005	0,131	0,790	0,648	0,029
MLH1	0,033	0,112	0,859	0,172	0,128	0,630	0,902	0,008	0,012	0,438	0,130	0,002	0,291	0,323	0,004
PMS2	0,396	0,787	0,647	0,061	0,011	0,445	0,900	0,385	0,882	0,653	0,005	0,431	0,581	0,569	0,113
MSH2	0,758	0,257	0,628	0,078	0,028	0,906	0,368	0,153	0,458	0,367	0,064	0,292	0,135	0,032	0,030
MSH6	0,933	0,288	0,312	0,078	0,043	0,714	0,221	0,070	0,431	0,184	0,169	0,319	0,202	0,112	0,038
GADD45	0,543	0,565	0,987	0,383	0,121	0,624	0,048	0,543	0,832	0,435	0,038	0,386	0,838	0,983	0,333
BAX	0,402	0,180	0,486	0,165	0,166	0,330	0,224	0,661	0,540	0,531	0,528	0,688	0,763	0,076	0,164
P21	0,559	0,210	0,319	0,136	0,843	0,109	0,551	0,287	0,155	0,596	0,448	0,108	0,869	0,638	0,257
FAS	0,290	0,674	0,190	0,020	0,063	0,451	0,568	0,847	0,533	0,017	0,110	0,424	0,579	0,041	0,213
BCL2	0,749	0,144	0,114	0,931	0,954	0,411	0,386	0,443	0,630	0,255	0,162	0,099	0,631	0,061	0,687
DIABLO	0,444	0,689	0,633	0,090	0,031	0,690	0,183	0,273	0,620	0,298	0,009	0,095	0,963	0,402	0,065
BIRC2	0,556	0,716	0,130	0,008	0,020	0,743	0,882	0,168	0,532	0,221	0,000	0,036	0,460	0,545	0,021
XIAP	0,241	0,333	0,215	0,001	0,005	0,158	0,181	0,052	0,255	0,046	0,008	0,154	0,423	0,053	0,003
BIRC5	0,231	0,425	0,035	0,012	0,064	0,810	0,735	0,053	0,207	0,150	0,002	0,025	0,752	0,680	0,016
BIRC7	1,000	0,658	0,914	0,547	0,966	0,675	0,767	0,488	0,754	0,089	0,469	0,618	0,546	0,782	0,577
CFLAR	0,730	0,732	0,721	0,018	0,507	0,344	0,492	0,536	0,980	0,053	0,033	0,108	0,541	0,357	0,220
EGFR	0,200	0,561	0,011	0,019	0,010	0,246	0,120	0,195	0,631	0,312	0,072	0,951	0,296	0,180	0,047
MYC	0,087	0,012	0,473	0,002	0,091	0,619	0,272	0,082	0,216	0,270	0,248	0,273	1,000	0,034	0,005
MMP1	0,659	0,616	0,974	0,696	0,359	0,236	0,453	0,604	0,689	0,048	0,637	0,910	0,188	0,151	0,757
MMP2	1,000	0,619	1,000	0,009	0,002	1,000	1,000	0,401	0,317	0,645	0,008	0,859	0,917	0,814	0,113
TIGAR	0,133	0,292	0,639	0,733	0,329	0,459	0,140	0,277	0,308	0,499	0,355	0,643	0,770	0,977	0,645
NRF2	0,280	0,333	0,713	0,188	0,223	0,767	0,206	0,525	0,675	0,800	0,227	0,874	0,958	0,744	0,715
KEAP1	0,189	0,050	0,477	0,004	0,023	0,723	0,928	0,066	0,157	0,108	0,047	0,192	0,628	0,114	0,008
ENT1n	0,876	0,702	0,009	0,023	0,069	0,675	0,920	0,522	0,539	0,146	0,000	0,263	0,718	0,887	0,316
ENT2n	0,630	0,288	0,648	0,021	0,268	0,953	0,642	0,066	0,118	0,948	0,129	0,000	0,395	0,378	0,005
CNT1n	0,510	0,394	0,307	0,869	0,859	0,182	0,676	0,313	0,531	0,783	0,919	0,985	0,390	0,828	0,837
CNT2n	0,786	0,139	0,755	0,444	0,900	0,344	0,302	0,997	0,601	0,926	0,670	0,939	0,740	0,144	0,357
CNT3n	0,096	0,093	0,251	0,012	0,019	0,425	0,230	0,007	0,018	0,331	0,138	0,129	0,163	0,061	0,000

Correlat.	AQP1	AQP3	AQP5	ABCA2	ABCA3	ABCB11	ABCC1	ABCC2	ABCC3	ABCC4	ABCC5	ABCC11	ABCG2	MVP	ATP7A
OATP1B1	0,000	0,278	-0,268	-0,733	-0,791	-0,323	-0,837	-0,002	-0,867	-0,164	-0,207	0,000	0,505	-0,692	-0,580
OATP1B3	0,230	0,206	0,320	0,484	0,096	0,229	0,209	-0,073	0,668	0,065	-0,201	0,339	-0,514	0,676	0,117
OATP2B1	0,631	0,274	0,735	-0,331	-0,392	0,000	-0,246	0,154	-0,376	0,286	0,275	-0,139	-0,261	-0,079	-0,299
OATP4A1	0,072	0,121	0,285	0,257	0,314	0,404	0,300	-0,292	0,381	0,012	0,010	0,300	-0,242	0,493	0,362
OCT1	-0,294	-0,085	0,291	0,003	-0,009	0,471	0,493	-0,346	0,220	0,336	0,527	-0,469	-0,164	0,074	0,562
OCT2	-0,345	-0,060	-0,066	0,766	0,970	0,850	0,128	-0,683	0,737	-0,557	-0,775	0,000	0,120	0,741	0,707
OCT3	-0,422	0,184	0,131	0,168	0,553	0,473	0,220	0,217	0,263	0,042	-0,080	0,472	0,115	0,011	0,265
OCTN1	0,044	-0,186	0,043	0,319	0,116	0,472	0,621	-0,017	0,875	-0,000	0,154	0,422	-0,129	0,856	0,389
OCTN2	0,167	0,047	0,042	0,140	0,140	0,064	0,536	0,118	0,829	0,074	-0,042	0,513	-0,341	0,874	0,222
CTR1	-0,500	0,243	-0,413	0,308	-0,283	0,531	-0,085	-0,419	0,128	-0,006	0,124	0,110	-0,343	-0,040	0,372
ENT1	-0,085	-0,191	0,104	-0,134	0,249	0,452	0,474	-0,136	0,282	0,297	0,467	0,020	0,098	0,200	0,465
ENT2	0,427	0,507	0,355	-0,243	-0,197	0,056	0,258	0,189	0,733	-0,082	0,147	0,394	-0,167	0,633	-0,075
ENT3	-0,396	0,215	0,217	-0,549	-0,080	0,013	0,212	0,048	0,304	0,006	0,064	-0,068	0,139	0,033	0,085
ENT4	0,373	-0,401	-0,073	-0,429	0,266	-0,611	0,054	0,533	-0,239	0,192	0,073	0,065	0,558	-0,214	-0,327
CNT3	0,075	0,042	0,393	0,088	0,149	0,256	0,532	-0,119	0,714	0,094	0,174	0,146	-0,319	0,694	0,368
AQP1	1,000	0,258	0,435	0,080	0,148	-0,160	-0,247	0,178	0,098	0,163	-0,069	0,482	-0,388	0,342	-0,495
AQP3	0,258	1,000	0,193	0,054	-0,446	0,355	-0,567	0,047	-0,307	-0,181	-0,393	0,769	-0,417	-0,163	-0,480
AQP5	0,435	0,193	1,000	-0,108	0,334	0,228	-0,195	-0,020	-0,101	0,294	0,014	-0,170	-0,180	0,068	-0,053
ABCA2	0,080	0,054	-0,108	1,000	0,276	0,876	-0,188	-0,363	-0,023	-0,198	-0,166	0,531	-0,394	0,171	0,248
ABCA3	0,148	-0,446	0,334	0,276	1,000	0,327	0,302	-0,145	-0,031	0,238	0,061	0,363	0,052	0,189	0,514
ABCB11	-0,160	0,355	0,228	0,876	0,327	1,000	-0,196	-0,634	0,206	-0,168	0,012	0,612	-0,475	0,118	0,597
ABCC1	-0,247	-0,567	-0,195	-0,188	0,302	-0,196	1,000	0,067	0,584	0,426	0,443	-0,041	0,153	0,506	0,553
ABCC2	0,178	0,047	-0,020	-0,363	-0,145	-0,634	0,067	1,000	0,125	-0,129	0,022	0,131	0,520	-0,036	-0,596
ABCC3	0,098	-0,307	-0,101	-0,023	-0,031	0,206	0,584	0,125	1,000	0,023	0,159	0,360	-0,034	0,867	0,262
ABCC4	0,163	-0,181	0,294	-0,198	0,238	-0,168	0,426	-0,129	0,023	1,000	0,545	-0,501	-0,467	-0,004	0,478
ABCC5	-0,069	-0,393	0,014	-0,166	0,061	0,012	0,443	0,022	0,159	0,545	1,000	-0,736	-0,142	-0,109	0,500
ABCC11	0,482	0,769	-0,170	0,531	0,363	0,612	-0,041	0,131	0,360	-0,501	-0,736	1,000	-0,301	0,596	-0,232
ABCG2	-0,388	-0,417	-0,180	-0,394	0,052	-0,475	0,153	0,520	-0,034	-0,467	-0,142	-0,301	1,000	-0,174	-0,259
MVP	0,342	-0,163	0,068	0,171	0,189	0,118	0,506	-0,036	0,867	-0,004	-0,109	0,596	-0,174	1,000	0,253
ATP7A	-0,495	-0,480	-0,053	0,248	0,514	0,597	0,553	-0,596	0,262	0,478	0,500	-0,232	-0,259	0,253	1,000
ATP7B	-0,241	-0,516	0,054	-0,083	0,301	0,006	-0,030	-0,459	-0,471	0,561	0,450	-0,718	-0,160	-0,453	0,521
DPYD	-0,329	-0,428	-0,204	0,664	0,374	0,492	0,268	-0,415	0,311	-0,281	-0,179	0,150	0,037	0,442	0,475
TYMP	-0,295	-0,015	-0,012	0,196	0,426	0,329	0,570	-0,026	0,635	0,043	0,076	0,289	-0,048	0,496	0,453
UPP1	-0,265	-0,227	-0,107	0,002	0,091	0,377	0,640	-0,040	0,587	-0,040	0,350	0,058	0,228	0,451	0,421
EPHX1	-0,332	-0,278	-0,052	0,062	0,391	-0,277	0,502	0,295	0,309	0,106	-0,267	0,171	0,177	0,361	0,124
DCK	-0,035	0,121	0,211	0,273	0,376	0,494	0,278	-0,468	0,009	0,428	0,278	0,044	-0,541	0,107	0,552
RRM1	-0,155	0,180	0,106	0,182	0,153	0,222	0,212	-0,068	0,362	0,018	-0,017	0,143	-0,322	0,365	0,220
TYMS	-0,608	-0,044	0,078	-0,293	-0,065	0,026	0,072	-0,218	-0,150	0,302	0,141	-0,631	-0,039	-0,188	0,308
TK1	-0,192	0,433	-0,003	-0,164	-0,154	-0,055	0,330	0,088	0,408	0,193	0,067	0,123	-0,468	0,270	0,080
UMPS	0,183	0,221	0,170	-0,140	-0,148	0,104	0,498	0,062	0,386	0,435	0,625	-0,065	-0,395	0,215	0,228
UCK2	0,013	0,062	0,308	-0,280	0,201	-0,119	0,494	0,144	0,210	0,460	0,584	-0,287	-0,268	0,075	0,286
FPGS	-0,256	0,207	-0,034	0,199	-0,087	0,530	0,521	-0,224	0,653	0,228	0,143	0,290	-0,533	0,570	0,449
GCLC	-0,028	-0,122	-0,090	-0,101	-0,080	0,365	0,643	0,019	0,806	0,020	0,098	0,503	0,203	0,749	0,312
UGTX	-0,131	0,033	-0,409	0,432	0,280	0,446	0,550	-0,164	0,481	0,158	0,067	0,719	-0,223	0,383	0,457
TOP1	0,026	0,208	0,342	0,069	-0,016	0,254	0,276	-0,240	0,329	0,583	0,421	-0,216	-0,820	0,225	0,395
TOP2A	-0,005	0,444	0,173	0,059	0,055	0,328	0,151	0,261	0,354	0,329	-0,190	0,567	-0,369	0,272	-0,023
KIT	0,517	0,240	0,000	0,391	0,619	-0,062	0,239	0,413	0,825	-0,602	-0,687	0,000	-0,007	0,877	-0,281
PDGFRA	-0,036	0,332	0,071	-0,408	-0,290	0,000	-0,896	0,158	-0,792	0,128	-0,039	0,000	-0,083	-0,758	-0,586
ERCC1	-0,304	-0,327	0,049	0,102	0,245	0,402	0,242	-0,496	-0,006	0,525	0,487	-0,632	-0,292	0,015	0,678
XPA	-0,013	0,407	0,068	0,379	-0,062	0,471	-0,107	-0,450	0,193	0,076	-0,123	0,313	-0,585	0,240	0,217
XPC	0,454	-0,180	0,231	0,164	0,542	-0,307	-0,127	-0,331	-0,200	0,395	0,117	-0,168	-0,571	0,101	0,293
UDG	-0,069	0,105	0,170	-0,159	0,072	-0,102	0,371	0,316	0,259	0,234	0,276	-0,014	0,028	0,112	0,045
MLH1	-0,010	-0,157	-0,206	-0,232	-0,227	-0,238	0,607	0,201	0,816	0,185	0,517	-0,049	-0,250	0,578	0,253
PMS2	-0,175	-0,442	0,170	-0,049	0,441	0,307	0,417	-0,343	0,144	0,158	0,628	-0,451	0,070	0,081	0,663
MSH2	-0,441	0,202	0,349	-0,250	-0,188	0,090	0,198	0,072	0,263	0,091	0,057	-0,326	-0,046	0,060	0,085
MSH6	-0,455	0,215	0,162	-0,195	-0,166	0,061	0,299	0,184	0,281	0,172	0,102	-0,182	-0,082	0,045	0,074
GADD45	0,219	-0,365	0,221	-0,217	-0,084	-0,035	0,254	-0,388	0,307	0,491	0,409	-0,344	-0,211	0,236	0,374
BAX	0,152	0,002	0,212	0,177	0,146	0,304	0,094	-0,699	0,010	0,442	0,302	-0,384	-0,777	0,192	0,552
P21	0,439	0,169	0,080	0,005	0,178	0,185	0,182	-0,272	0,237	-0,026	-0,196	0,668	-0,179	0,562	0,163
FAS	-0,279	0,188	-0,270	0,021	-0,330	0,202	0,009	-0,571	-0,010	-0,119	0,174	-0,358	-0,281	-0,115	0,255
BCL2	-0,421	0,402	0,011	0,738	-0,137	0,703	-0,390	-0,366	-0,409	-0,004	-0,247	-0,321	-0,843	-0,455	-0,001
DIABLO	0,055	-0,229	-0,074	-0,136	0,032	0,057	0,393	-0,267	0,304	0,346	0,723	-0,476	-0,313	0,237	0,539
BIRC2	-0,235	-0,012	-0,055	-0,396	-0,053	-0,074	0,518	-0,034	0,420	0,241	0,237	0,015	0,102	0,325	0,265
XIAP	-0,099	0,068	0,293	0,255	0,367	0,643	0,359	-0,383	0,394	0,367	0,406	0,136	-0,485	0,311	0,660
BIRC5	0,026	0,063	-0,244	-0,151	-0,045	-0,111	0,564	0,153	0,543	0,261	0,293	0,306	-0,090	0,410	0,176
BIRC7	-0,076	0,127	-0,020	-0,203	0,116	-0,847	-0,238	0,253	-0,303	0,105	0,304	-0,453	-0,208	-0,231	0,027
CFLAR	0,272	0,322	0,007	0,130	-0,043	0,417	-0,198	-0,365	0,183	-0,097	-0,158	0,553	-0,205	0,308	0,106
EGFR	-0,506	-0,190	0,127	0,143	0,394	0,414	0,514	-0,346	0,154	0,197	0,108	-0,122	-0,016	0,100	0,551
MYC	0,021	0,274	0,365	0,337	0,236	0,312	0,084	-0,042	0,193	0,151	0,106	0,061	-0,590	0,209	0,194
MMP1	-0,375	0,477	-0,054	0,106	-0,195	0,830	-0,072	-0,619	-0,372	0,280	0,122	0,527	-0,487	-0,425	0,416
MMP2	0,000	-0,744	-0,886	-0,444	0,342	0,000	0,897	-0,188	0,267	0,169	0,614	0,000	0,539	-0,049	0,574
TIGAR	-0,147	-0,231	-0,168	-0,333	-0,066	-0,193	0,181	-0,535	-0,214	0,576	0,548	-0,703	-0,359	-0,252	0,495
NRF2	0,013	0,380	0,148	-0,004	0,288	0,201	0,105	-0,115	-0,414	0,390	0,164	0,089	-0,411	-0,276	0,177
KEAP1	0,278	0,202	0,073	0,311	0,105	0,391	0,378	-0,335	0,358	0,478	0,196	0,495	-0,667	0,432	0,392
ENT1n	-0,082	-0,022	-0,291	-0,087	0,131	0,364	0,280	-0,021	0,103	0,062	0,263	0,484	0,232	0,054	0,215
ENT2n	0,569	0,422	0,406	-0,139	-0,136	0,041	0,117	0,111	0,581	-0,167	0,072	0,359	-0,163	0,547	-0,165
CNT1n	-0,175	-0,014	0,024	-0,312	-0,088	-0,580	-0,153	0,399	-0,106	-0,033	0,155	-0,578	0,079	-0,357	-0,290
CNT2n	0,404	-0,184	-0,124	-0,013	-0,120	-0,100	0,212	-0,105	0,094	0,293	0,252	0,116	-0,026	0,007	0,020
CNT3n	-0,178	-0,002	0,258	0,021	0,162	0,254	0,610	-0,180	0,598	0,403	0,194	0,040	-0,451	0,504	0,472

P Values	AQP1	AQP3	AQP5	ABCA2	ABCA3	ABCB11	ABCC1	ABCC2	ABCC3	ABCC4	ABCC5	ABCC11	ABCG2	MVP	ATP7A
OATP1B1	1,000	0,593	0,663	0,098	0,111	0,596	0,038	0,997	0,025	0,756	0,694	1,000	0,306	0,128	0,227
OATP1B3	0,584	0,520	0,367	0,111	0,778	0,621	0,514	0,822	0,018	0,841	0,531	0,511	0,106	0,016	0,718
OATP2B1	0,179	0,512	0,060	0,423	0,384	1,000	0,557	0,716	0,359	0,492	0,511	0,823	0,572	0,852	0,472
OATP4A1	0,843	0,695	0,396	0,375	0,296	0,321	0,298	0,311	0,179	0,968	0,972	0,514	0,448	0,073	0,203
OCT1	0,409	0,792	0,415	0,993	0,978	0,239	0,087	0,247	0,471	0,262	0,064	0,288	0,629	0,811	0,046
OCT2	0,570	0,911	0,916	0,075	0,006	0,068	0,809	0,135	0,094	0,251	0,070	1,000	0,821	0,092	0,116
OCT3	0,298	0,589	0,718	0,622	0,098	0,237	0,516	0,522	0,435	0,903	0,815	0,344	0,751	0,975	0,431
OCTN1	0,911	0,563	0,907	0,288	0,720	0,237	0,023	0,955	0,000	1,000	0,616	0,405	0,690	0,000	0,189
OCTN2	0,644	0,879	0,902	0,633	0,649	0,881	0,048	0,687	0,000	0,801	0,887	0,239	0,278	0,000	0,446
CTR1	0,141	0,423	0,207	0,283	0,350	0,176	0,773	0,136	0,663	0,985	0,673	0,814	0,274	0,891	0,190
ENT1	0,815	0,533	0,761	0,649	0,412	0,261	0,087	0,644	0,328	0,303	0,092	0,966	0,762	0,492	0,094
ENT2	0,219	0,077	0,284	0,403	0,519	0,894	0,373	0,517	0,003	0,780	0,615	0,382	0,604	0,015	0,800
ENT3	0,257	0,481	0,522	0,042	0,794	0,975	0,466	0,870	0,291	0,982	0,827	0,885	0,668	0,912	0,773
ENT4	0,289	0,197	0,842	0,143	0,404	0,108	0,860	0,061	0,431	0,529	0,814	0,891	0,075	0,482	0,275
CNT3	0,836	0,896	0,261	0,776	0,643	0,540	0,061	0,700	0,006	0,760	0,570	0,755	0,340	0,008	0,217
AQP1	0,000	0,502	0,281	0,825	0,704	0,732	0,491	0,622	0,788	0,653	0,851	0,273	0,342	0,333	0,146
AQP3	0,502	0,000	0,569	0,860	0,146	0,388	0,043	0,879	0,307	0,554	0,185	0,074	0,177	0,596	0,097
AQP5	0,281	0,569	0,000	0,752	0,346	0,622	0,565	0,954	0,767	0,381	0,968	0,785	0,618	0,842	0,876
ABCA2	0,825	0,860	0,752	0,000	0,361	0,004	0,520	0,202	0,937	0,497	0,571	0,220	0,205	0,560	0,393
ABCA3	0,704	0,146	0,346	0,361	0,000	0,475	0,316	0,637	0,920	0,434	0,842	0,479	0,879	0,537	0,072
ABCB11	0,732	0,388	0,622	0,004	0,475	0,000	0,641	0,092	0,624	0,692	0,977	0,273	0,234	0,781	0,118
ABCC1	0,491	0,043	0,565	0,520	0,316	0,641	0,000	0,821	0,028	0,129	0,112	0,930	0,635	0,065	0,040
ABCC2	0,622	0,879	0,954	0,202	0,637	0,092	0,821	0,000	0,671	0,661	0,939	0,779	0,083	0,903	0,025
ABCC3	0,788	0,307	0,767	0,937	0,920	0,624	0,028	0,671	0,000	0,938	0,588	0,428	0,916	0,000	0,366
ABCC4	0,653	0,554	0,381	0,497	0,434	0,692	0,129	0,661	0,938	0,000	0,044	0,252	0,126	0,990	0,084
ABCC5	0,851	0,185	0,968	0,571	0,842	0,977	0,112	0,939	0,588	0,044	0,000	0,060	0,660	0,712	0,069
ABCC11	0,273	0,074	0,785	0,220	0,479	0,273	0,930	0,779	0,428	0,252	0,060	0,000	0,623	0,158	0,617
ABCG2	0,342	0,177	0,618	0,205	0,879	0,234	0,635	0,083	0,916	0,126	0,660	0,623	0,000	0,588	0,416
MVP	0,333	0,596	0,842	0,560	0,537	0,781	0,065	0,903	0,000	0,990	0,712	0,158	0,588	0,000	0,382
ATP7A	0,146	0,097	0,876	0,393	0,072	0,118	0,040	0,025	0,366	0,084	0,069	0,617	0,416	0,382	0,000
ATP7B	0,502	0,071	0,876	0,777	0,317	0,989	0,920	0,099	0,089	0,037	0,106	0,069	0,620	0,104	0,056
DPYD	0,353	0,145	0,548	0,010	0,208	0,215	0,354	0,141	0,278	0,331	0,539	0,749	0,910	0,113	0,086
TYMP	0,441	0,961	0,971	0,520	0,167	0,427	0,042	0,934	0,020	0,889	0,806	0,578	0,881	0,085	0,120
UPP1	0,460	0,457	0,755	0,995	0,768	0,357	0,014	0,891	0,027	0,891	0,219	0,902	0,477	0,105	0,134
EPHX1	0,349	0,358	0,879	0,832	0,186	0,507	0,067	0,305	0,283	0,719	0,357	0,714	0,582	0,204	0,672
DCK	0,923	0,693	0,534	0,345	0,206	0,214	0,336	0,091	0,976	0,127	0,336	0,925	0,069	0,716	0,041
RRM1	0,669	0,556	0,756	0,535	0,618	0,597	0,468	0,819	0,203	0,951	0,954	0,760	0,307	0,199	0,450
TYMS	0,062	0,886	0,820	0,309	0,834	0,952	0,807	0,455	0,610	0,294	0,630	0,128	0,905	0,520	0,284
TK1	0,596	0,140	0,994	0,575	0,616	0,898	0,249	0,766	0,148	0,508	0,819	0,793	0,125	0,350	0,785
UMPS	0,614	0,468	0,618	0,633	0,630	0,806	0,070	0,833	0,173	0,120	0,017	0,890	0,204	0,461	0,433
UCK2	0,972	0,841	0,357	0,332	0,510	0,779	0,072	0,624	0,472	0,098	0,028	0,533	0,400	0,798	0,322
FPGS	0,475	0,497	0,921	0,496	0,777	0,176	0,056	0,442	0,011	0,433	0,627	0,529	0,075	0,033	0,108
GCLC	0,939	0,692	0,792	0,730	0,794	0,374	0,013	0,947	0,001	0,945	0,739	0,250	0,526	0,002	0,278
UGTX	0,738	0,918	0,212	0,160	0,404	0,268	0,064	0,612	0,113	0,625	0,835	0,107	0,510	0,220	0,135
TOP1	0,943	0,495	0,304	0,814	0,960	0,544	0,339	0,409	0,250	0,029	0,134	0,643	0,001	0,440	0,162
TOP2A	0,990	0,128	0,611	0,841	0,859	0,428	0,607	0,368	0,214	0,250	0,515	0,185	0,238	0,346	0,938
KIT	0,373	0,647	1,000	0,443	0,265	0,921	0,648	0,416	0,043	0,206	0,131	1,000	0,989	0,022	0,590
PDGFRA	0,946	0,521	0,910	0,364	0,529	1,000	0,006	0,735	0,034	0,784	0,934	1,000	0,876	0,048	0,167
ERCC1	0,393	0,276	0,886	0,730	0,419	0,324	0,404	0,071	0,983	0,054	0,077	0,128	0,357	0,959	0,008
XPA	0,971	0,167	0,842	0,181	0,841	0,239	0,715	0,107	0,509	0,797	0,674	0,495	0,046	0,409	0,456
XPC	0,187	0,556	0,495	0,576	0,056	0,460	0,666	0,248	0,493	0,163	0,690	0,718	0,053	0,730	0,309
UDG	0,851	0,732	0,618	0,587	0,815	0,809	0,192	0,272	0,372	0,420	0,340	0,977	0,932	0,702	0,880
MLH1	0,977	0,608	0,543	0,424	0,456	0,570	0,021	0,490	0,000	0,526	0,059	0,918	0,434	0,030	0,382
PMS2	0,630	0,131	0,618	0,869	0,132	0,459	0,138	0,230	0,622	0,589	0,016	0,310	0,830	0,783	0,010
MSH2	0,202	0,530	0,292	0,409	0,559	0,833	0,516	0,816	0,386	0,768	0,854	0,476	0,893	0,847	0,783
MSH6	0,187	0,481	0,635	0,503	0,589	0,885	0,299	0,528	0,331	0,556	0,728	0,697	0,799	0,878	0,802
GADD45	0,543	0,220	0,514	0,457	0,784	0,935	0,380	0,170	0,285	0,075	0,147	0,450	0,510	0,417	0,188
BAX	0,676	0,994	0,532	0,545	0,633	0,463	0,750	0,005	0,974	0,114	0,294	0,395	0,003	0,511	0,041
P21	0,204	0,581	0,815	0,987	0,560	0,661	0,534	0,347	0,415	0,929	0,503	0,101	0,577	0,037	0,579
FAS	0,467	0,559	0,422	0,946	0,294	0,664	0,978	0,042	0,973	0,700	0,570	0,486	0,403	0,708	0,400
BCL2	0,299	0,220	0,976	0,006	0,688	0,078	0,210	0,243	0,187	0,990	0,439	0,534	0,002	0,137	0,997
DIABLO	0,879	0,451	0,828	0,644	0,917	0,894	0,165	0,356	0,291	0,226	0,004	0,280	0,322	0,415	0,046
BIRC2	0,512	0,968	0,872	0,161	0,863	0,862	0,058	0,909	0,135	0,406	0,415	0,974	0,752	0,257	0,360
XIAP	0,786	0,826	0,382	0,379	0,217	0,086	0,208	0,177	0,163	0,197	0,150	0,771	0,110	0,279	0,010
BIRC5	0,944	0,839	0,470	0,606	0,883	0,794	0,036	0,601	0,045	0,368	0,310	0,505	0,781	0,145	0,548
BIRC7	0,871	0,745	0,966	0,600	0,785	0,070	0,538	0,511	0,428	0,788	0,426	0,443	0,621	0,550	0,946
CFLAR	0,448	0,284	0,983	0,657	0,890	0,304	0,499	0,199	0,530	0,740	0,590	0,198	0,523	0,283	0,717
EGFR	0,136	0,535	0,711	0,626	0,183	0,308	0,060	0,226	0,599	0,499	0,713	0,795	0,960	0,733	0,041
MYC	0,955	0,366	0,269	0,239	0,439	0,452	0,776	0,887	0,510	0,605	0,718	0,896	0,043	0,474	0,507
MMP1	0,360	0,117	0,875	0,742	0,566	0,021	0,824	0,032	0,233	0,377	0,705	0,362	0,129	0,168	0,179
MMP2	1,000	0,090	0,045	0,378	0,507	1,000	0,015	0,721	0,609	0,748	0,194	1,000	0,270	0,927	0,233
TIGAR	0,686	0,448	0,622	0,245	0,829	0,647	0,536	0,049	0,462	0,031	0,043	0,078	0,251	0,385	0,072
NRF2	0,971	0,200	0,663	0,989	0,339	0,634	0,722	0,695	0,141	0,168	0,576	0,850	0,184	0,340	0,544
KEAP1	0,437	0,509	0,832	0,280	0,733	0,338	0,183	0,242	0,209	0,084	0,501	0,259	0,018	0,123	0,166
ENT1n	0,823	0,944	0,386	0,766	0,669	0,376	0,332	0,944	0,725	0,834	0,364	0,271	0,468	0,855	0,460
ENT2n	0,086	0,151	0,216	0,634	0,659	0,923	0,691	0,706	0,029	0,568	0,807	0,429	0,613	0,043	0,573
CNT1n	0,628	0,964	0,945	0,277	0,776	0,131	0,601	0,157	0,720	0,910	0,596	0,175	0,808	0,210	0,315
CNT2n	0,247	0,548	0,715	0,965	0,696	0,813	0,467	0,722	0,749	0,310	0,385	0,805	0,935	0,981	0,946
CNT3n	0,623	0,995	0,444	0,943	0,597	0,544	0,020	0,539	0,024	0,153	0,507	0,931	0,141	0,066	0,088

Correlat.	ATP7B	DPYD	TYMP	UPP1	EPHX1	DCK	RRM1	TYMS	TK1	UMPS	UCK2	FPGS	GCLC	UGTX	TOP1
OATP1B1	0,340	-0,710	-0,781	-0,588	-0,628	-0,580	-0,514	0,703	-0,349	-0,549	-0,545	-0,586	-0,470	-0,666	-0,474
OATP1B3	-0,383	0,419	0,649	0,264	0,481	0,438	0,590	0,146	0,451	0,361	0,281	0,691	0,468	0,231	0,512
OATP2B1	0,165	-0,684	-0,133	-0,769	-0,355	-0,346	-0,576	0,004	-0,409	0,231	0,082	-0,433	0,217	-0,119	-0,042
OATP4A1	-0,248	0,473	0,654	0,748	0,053	0,800	0,875	0,336	0,608	0,514	0,525	0,695	0,288	0,012	0,551
OCT1	0,119	0,261	0,468	0,762	-0,128	0,713	0,508	0,468	0,447	0,729	0,649	0,655	0,316	0,005	0,658
OCT2	-0,245	0,918	0,628	0,647	0,378	0,431	0,503	0,038	-0,016	-0,603	-0,479	0,697	0,619	0,517	-0,397
OCT3	-0,283	0,137	0,527	0,201	0,519	0,221	0,282	-0,055	0,360	0,015	0,318	0,291	0,121	0,422	0,121
OCTN1	-0,477	0,564	0,766	0,729	0,423	0,285	0,609	-0,125	0,477	0,471	0,301	0,820	0,788	0,491	0,423
OCTN2	-0,547	0,300	0,637	0,344	0,559	0,099	0,376	-0,225	0,465	0,314	0,265	0,660	0,688	0,583	0,365
CTR1	0,089	0,266	0,106	0,328	-0,230	0,438	0,482	0,386	0,431	0,215	0,039	0,537	0,009	0,092	0,404
ENT1	0,151	0,135	0,406	0,800	-0,212	0,660	0,545	0,477	0,385	0,611	0,559	0,438	0,305	-0,130	0,389
ENT2	-0,575	-0,124	0,380	0,558	-0,158	0,163	0,431	-0,065	0,534	0,620	0,454	0,506	0,604	-0,082	0,375
ENT3	-0,206	-0,257	0,093	0,164	0,124	-0,064	0,041	0,015	0,401	0,181	0,343	0,208	0,290	0,038	0,162
ENT4	0,216	-0,472	-0,425	-0,357	0,009	-0,468	-0,579	-0,311	-0,499	-0,280	-0,203	-0,736	-0,207	-0,091	-0,586
CNT3	-0,379	0,404	0,725	0,758	0,222	0,607	0,814	0,216	0,712	0,665	0,641	0,844	0,527	-0,012	0,711
AQP1	-0,241	-0,329	-0,295	-0,265	-0,332	-0,035	-0,155	-0,608	-0,192	0,183	0,013	-0,256	-0,028	-0,131	0,026
AQP3	-0,516	-0,428	-0,015	-0,227	-0,278	0,121	0,180	-0,044	0,433	0,221	0,062	0,207	-0,122	0,033	0,208
AQP5	0,054	-0,204	-0,012	-0,107	-0,052	0,211	0,106	0,078	-0,003	0,170	0,308	-0,034	-0,090	-0,409	0,342
ABCA2	-0,083	0,664	0,196	0,002	0,062	0,273	0,182	-0,293	-0,164	-0,140	-0,280	0,199	-0,101	0,432	0,069
ABCA3	0,301	0,374	0,426	0,091	0,391	0,376	0,153	-0,065	-0,154	-0,148	0,201	-0,087	-0,080	0,280	-0,016
ABCB11	0,006	0,492	0,329	0,377	-0,277	0,494	0,222	0,026	-0,055	0,104	-0,119	0,530	0,365	0,446	0,254
ABCC1	-0,030	0,268	0,570	0,640	0,502	0,278	0,212	0,072	0,330	0,498	0,494	0,521	0,643	0,550	0,276
ABCC2	-0,459	-0,415	-0,026	-0,040	0,295	-0,468	-0,068	-0,218	0,088	0,062	0,144	-0,224	0,019	-0,164	-0,240
ABCC3	-0,471	0,311	0,635	0,587	0,309	0,009	0,362	-0,150	0,408	0,386	0,210	0,653	0,806	0,481	0,329
ABCC4	0,561	-0,281	0,043	-0,040	0,106	0,428	0,018	0,302	0,193	0,435	0,460	0,228	0,020	0,158	0,583
ABCC5	0,450	-0,179	0,076	0,350	-0,267	0,278	-0,017	0,141	0,067	0,625	0,584	0,143	0,098	0,067	0,421
ABCC11	-0,718	0,150	0,289	0,058	0,171	0,044	0,143	-0,631	0,123	-0,065	-0,287	0,290	0,503	0,719	-0,216
ABCG2	-0,160	0,037	-0,048	0,228	0,177	-0,541	-0,322	-0,039	-0,468	-0,395	-0,268	-0,533	0,203	-0,223	-0,820
MVP	-0,453	0,442	0,496	0,451	0,361	0,107	0,365	-0,188	0,270	0,215	0,075	0,570	0,749	0,383	0,225
ATP7A	0,521	0,475	0,453	0,421	0,124	0,552	0,220	0,308	0,080	0,228	0,286	0,449	0,312	0,457	0,395
ATP7B	1,000	-0,090	-0,244	-0,262	-0,277	0,184	-0,294	0,418	-0,404	-0,162	-0,028	-0,322	-0,386	-0,158	0,062
DPYD	-0,090	1,000	0,374	0,432	0,386	0,260	0,399	-0,036	-0,006	-0,177	-0,180	0,389	0,202	0,215	0,047
TYMP	-0,244	0,374	1,000	0,679	0,450	0,556	0,609	0,345	0,512	0,408	0,550	0,688	0,611	0,466	0,301
UPP1	-0,262	0,432	0,679	1,000	0,083	0,498	0,636	0,281	0,504	0,623	0,537	0,672	0,586	0,130	0,355
EPHX1	-0,277	0,386	0,450	0,083	1,000	-0,050	0,243	-0,016	0,276	-0,146	0,082	0,316	0,235	0,299	0,060
DCK	0,184	0,260	0,556	0,498	-0,050	1,000	0,699	0,432	0,560	0,603	0,651	0,597	-0,024	0,168	0,714
RRM1	-0,294	0,399	0,609	0,636	0,243	0,699	1,000	0,463	0,802	0,465	0,556	0,742	0,113	-0,156	0,658
TYMS	0,418	-0,036	0,345	0,281	-0,016	0,432	0,463	1,000	0,352	0,161	0,317	0,298	-0,021	-0,405	0,356
TK1	-0,404	-0,006	0,512	0,504	0,276	0,560	0,802	0,352	1,000	0,657	0,689	0,793	0,209	0,012	0,732
UMPS	-0,162	-0,177	0,408	0,623	-0,146	0,603	0,465	0,161	0,657	1,000	0,834	0,633	0,337	0,154	0,726
UCK2	-0,028	-0,180	0,550	0,537	0,082	0,651	0,556	0,317	0,689	0,834	1,000	0,486	0,112	-0,000	0,701
FPGS	-0,322	0,389	0,688	0,672	0,316	0,597	0,742	0,298	0,793	0,633	0,486	1,000	0,562	0,350	0,742
GCLC	-0,386	0,202	0,611	0,586	0,235	-0,024	0,113	-0,021	0,209	0,337	0,112	0,562	1,000	0,641	0,074
UGTX	-0,158	0,215	0,466	0,130	0,299	0,168	-0,156	-0,405	0,012	0,154	-0,000	0,350	0,641	1,000	-0,049
TOP1	0,062	0,047	0,301	0,355	0,060	0,714	0,658	0,356	0,732	0,726	0,701	0,742	0,074	-0,049	1,000
TOP2A	-0,360	-0,053	0,193	0,084	0,461	0,235	0,448	0,069	0,609	0,243	0,207	0,532	0,188	0,209	0,449
KIT	-0,872	0,380	0,440	-0,022	0,816	-0,062	0,239	-0,788	0,313	-0,195	-0,037	0,169	0,441	0,724	-0,544
PDGFRA	0,710	-0,779	-0,434	-0,842	-0,644	-0,582	-0,892	0,777	-0,710	-0,472	-0,382	-0,764	-0,575	-0,256	-0,581
ERCC1	0,646	0,237	0,263	0,401	-0,205	0,667	0,418	0,727	0,153	0,330	0,323	0,356	0,011	-0,164	0,508
XPA	-0,118	0,337	0,213	0,364	-0,124	0,711	0,788	0,362	0,621	0,354	0,224	0,669	-0,023	-0,101	0,660
XPC	0,497	0,002	0,026	-0,324	-0,105	0,338	0,065	0,072	-0,140	-0,084	0,134	-0,170	-0,365	-0,073	0,241
UDG	-0,238	0,017	0,454	0,670	0,165	0,591	0,786	0,426	0,755	0,687	0,741	0,549	0,085	-0,260	0,580
MLH1	-0,308	0,046	0,605	0,661	0,124	0,195	0,466	0,112	0,617	0,714	0,585	0,682	0,608	0,100	0,562
PMS2	0,364	0,263	0,408	0,645	-0,256	0,538	0,289	0,292	0,072	0,419	0,553	0,188	0,166	-0,027	0,266
MSH2	-0,216	0,084	0,462	0,551	0,310	0,381	0,713	0,681	0,734	0,422	0,597	0,612	0,149	-0,376	0,611
MSH6	-0,265	0,072	0,445	0,529	0,374	0,430	0,747	0,545	0,841	0,511	0,602	0,685	0,140	-0,218	0,636
GADD45	0,439	0,044	-0,325	0,296	-0,334	0,280	0,136	0,313	0,063	0,323	0,130	0,231	0,177	-0,411	0,427
BAX	0,422	0,118	0,254	0,068	-0,231	0,619	0,255	0,312	0,180	0,342	0,357	0,348	0,003	0,079	0,604
P21	-0,168	0,026	0,460	0,204	-0,114	0,243	0,102	0,055	0,036	0,138	0,071	0,197	0,518	0,351	-0,047
FAS	0,061	0,212	0,138	0,482	-0,452	0,609	0,484	0,315	0,459	0,413	0,310	0,432	-0,079	-0,118	0,391
BCL2	0,046	0,332	-0,052	-0,377	0,138	0,281	0,178	-0,020	0,174	-0,112	-0,097	0,182	-0,571	0,162	0,347
DIABLO	0,308	-0,000	0,356	0,566	-0,381	0,532	0,354	0,404	0,287	0,658	0,599	0,389	0,272	-0,039	0,509
BIRC2	-0,081	0,018	0,469	0,774	-0,023	0,535	0,633	0,594	0,647	0,617	0,562	0,598	0,450	-0,218	0,438
XIAP	0,055	0,336	0,515	0,634	-0,003	0,839	0,720	0,292	0,606	0,630	0,646	0,730	0,217	0,171	0,784
BIRC5	-0,293	0,081	0,421	0,744	0,100	0,542	0,685	0,246	0,759	0,743	0,599	0,691	0,376	0,069	0,549
BIRC7	0,238	-0,264	0,284	0,074	-0,124	0,275	0,554	0,651	0,423	0,145	0,370	0,083	-0,393	-0,466	0,301
CFLAR	-0,047	0,111	0,100	0,343	-0,474	0,428	0,471	0,349	0,226	0,165	-0,022	0,302	0,177	-0,184	0,189
EGFR	0,025	0,536	0,503	0,598	0,385	0,671	0,572	0,276	0,496	0,330	0,477	0,566	0,114	0,175	0,455
MYC	-0,227	0,286	0,551	0,411	0,219	0,727	0,875	0,287	0,709	0,517	0,652	0,636	-0,087	-0,089	0,771
MMP1	0,259	-0,204	0,099	-0,006	-0,351	0,429	-0,017	0,182	0,244	0,268	0,095	0,420	0,203	0,514	0,317
MMP2	0,506	0,289	0,860	0,942	-0,137	0,773	0,615	0,770	0,191	0,820	0,722	0,318	0,700	-0,099	0,008
TIGAR	0,754	-0,279	-0,148	-0,049	-0,427	0,305	-0,205	0,367	-0,038	0,248	0,234	-0,025	-0,100	0,018	0,268
NRF2	0,153	-0,257	0,579	0,106	-0,061	0,717	0,304	0,335	0,384	0,455	0,614	0,171	-0,215	0,335	0,341
KEAP1	-0,081	0,252	0,356	0,463	0,050	0,813	0,653	0,165	0,641	0,683	0,492	0,768	0,210	0,263	0,784
ENT1n	0,016	0,062	0,314	0,697	-0,300	0,538	0,459	0,387	0,307	0,470	0,368	0,276	0,188	-0,059	0,130
ENT2n	-0,565	-0,054	0,197	0,531	-0,265	0,253	0,477	-0,120	0,479	0,590	0,439	0,407	0,400	-0,245	0,369
CNT1n	-0,033	-0,179	-0,219	-0,037	0,098	-0,016	0,310	0,108	0,385	0,090	0,354	-0,079	-0,552	-0,601	0,264
CNT2n	0,129	-0,084	-0,579	-0,029	-0,256	-0,071	-0,399	-0,479	-0,220	0,181	-0,158	-0,107	0,042	0,168	-0,025
CNT3n	-0,196	0,345	0,541	0,585	0,461	0,613	0,706	0,228	0,786	0,598	0,632	0,865	0,391	0,170	0,807

P Values	ATP7B	DPYD	TYMP	UPP1	EPHX1	DCK	RRM1	TYMS	TK1	UMPS	UCK2	FPGS	GCLC	UGTX	TOP1
OATP1B1	0,509	0,114	0,066	0,220	0,182	0,227	0,297	0,119	0,498	0,259	0,263	0,222	0,346	0,149	0,343
OATP1B3	0,220	0,175	0,022	0,407	0,113	0,154	0,043	0,652	0,141	0,250	0,376	0,013	0,125	0,495	0,089
OATP2B1	0,695	0,061	0,754	0,026	0,388	0,401	0,135	0,992	0,315	0,583	0,847	0,284	0,606	0,780	0,921
OATP4A1	0,393	0,087	0,015	0,002	0,857	0,001	0,000	0,240	0,021	0,060	0,054	0,006	0,318	0,971	0,041
OCT1	0,698	0,390	0,125	0,002	0,678	0,006	0,076	0,107	0,126	0,005	0,016	0,015	0,293	0,989	0,014
OCT2	0,639	0,010	0,182	0,165	0,460	0,394	0,309	0,942	0,976	0,205	0,336	0,124	0,190	0,294	0,436
OCT3	0,399	0,687	0,096	0,554	0,102	0,513	0,401	0,871	0,277	0,964	0,341	0,386	0,724	0,196	0,723
OCTN1	0,099	0,045	0,004	0,005	0,150	0,344	0,027	0,684	0,099	0,104	0,317	0,001	0,001	0,125	0,150
OCTN2	0,043	0,298	0,019	0,228	0,038	0,738	0,186	0,439	0,093	0,274	0,361	0,010	0,007	0,047	0,200
CTR1	0,762	0,358	0,729	0,252	0,430	0,117	0,081	0,173	0,124	0,460	0,896	0,048	0,976	0,777	0,152
ENT1	0,607	0,645	0,168	0,001	0,468	0,010	0,044	0,084	0,174	0,020	0,038	0,118	0,290	0,687	0,169
ENT2	0,031	0,672	0,200	0,038	0,589	0,578	0,124	0,825	0,049	0,018	0,103	0,065	0,022	0,800	0,186
ENT3	0,480	0,376	0,763	0,575	0,672	0,827	0,890	0,958	0,155	0,535	0,231	0,475	0,314	0,907	0,581
ENT4	0,478	0,103	0,169	0,231	0,977	0,107	0,038	0,301	0,083	0,355	0,505	0,004	0,497	0,790	0,035
CNT3	0,201	0,171	0,008	0,003	0,465	0,028	0,001	0,478	0,006	0,013	0,018	0,000	0,064	0,972	0,006
AQP1	0,502	0,353	0,441	0,460	0,349	0,923	0,669	0,062	0,596	0,614	0,972	0,475	0,939	0,738	0,943
AQP3	0,071	0,145	0,961	0,457	0,358	0,693	0,556	0,886	0,140	0,468	0,841	0,497	0,692	0,918	0,495
AQP5	0,876	0,548	0,971	0,755	0,879	0,534	0,756	0,820	0,994	0,618	0,357	0,921	0,792	0,212	0,304
ABCA2	0,777	0,010	0,520	0,995	0,832	0,345	0,535	0,309	0,575	0,633	0,332	0,496	0,730	0,160	0,814
ABCA3	0,317	0,208	0,167	0,768	0,186	0,206	0,618	0,834	0,616	0,630	0,510	0,777	0,794	0,404	0,960
ABCB11	0,989	0,215	0,427	0,357	0,507	0,214	0,597	0,952	0,898	0,806	0,779	0,176	0,374	0,268	0,544
ABCC1	0,920	0,354	0,042	0,014	0,067	0,336	0,468	0,807	0,249	0,070	0,072	0,056	0,013	0,064	0,339
ABCC2	0,099	0,141	0,934	0,891	0,305	0,091	0,819	0,455	0,766	0,833	0,624	0,442	0,947	0,612	0,409
ABCC3	0,089	0,278	0,020	0,027	0,283	0,976	0,203	0,610	0,148	0,173	0,472	0,011	0,001	0,113	0,250
ABCC4	0,037	0,331	0,889	0,891	0,719	0,127	0,951	0,294	0,508	0,120	0,098	0,433	0,945	0,625	0,029
ABCC5	0,106	0,539	0,806	0,219	0,357	0,336	0,954	0,630	0,819	0,017	0,028	0,627	0,739	0,835	0,134
ABCC11	0,069	0,749	0,578	0,902	0,714	0,925	0,760	0,128	0,793	0,890	0,533	0,529	0,250	0,107	0,643
ABCG2	0,620	0,910	0,881	0,477	0,582	0,069	0,307	0,905	0,125	0,204	0,400	0,075	0,526	0,510	0,001
MVP	0,104	0,113	0,085	0,105	0,204	0,716	0,199	0,520	0,350	0,461	0,798	0,033	0,002	0,220	0,440
ATP7A	0,056	0,086	0,120	0,134	0,672	0,041	0,450	0,284	0,785	0,433	0,322	0,108	0,278	0,135	0,162
ATP7B	0,000	0,760	0,421	0,366	0,338	0,530	0,308	0,137	0,153	0,579	0,925	0,262	0,173	0,624	0,834
DPYD	0,760	0,000	0,208	0,123	0,173	0,370	0,157	0,904	0,985	0,546	0,538	0,169	0,489	0,503	0,872
TYMP	0,421	0,208	0,000	0,011	0,123	0,048	0,027	0,249	0,074	0,166	0,052	0,009	0,027	0,127	0,318
UPP1	0,366	0,123	0,011	0,000	0,778	0,070	0,014	0,330	0,066	0,017	0,048	0,008	0,028	0,687	0,213
EPHX1	0,338	0,173	0,123	0,778	0,000	0,865	0,402	0,957	0,339	0,618	0,781	0,271	0,419	0,345	0,839
DCK	0,530	0,370	0,048	0,070	0,865	0,000	0,005	0,123	0,037	0,023	0,012	0,024	0,935	0,601	0,004
RRM1	0,308	0,157	0,027	0,014	0,402	0,005	0,000	0,096	0,001	0,094	0,039	0,002	0,699	0,629	0,011
TYMS	0,137	0,904	0,249	0,330	0,957	0,123	0,096	0,000	0,218	0,583	0,270	0,301	0,945	0,191	0,211
TK1	0,153	0,985	0,074	0,066	0,339	0,037	0,001	0,218	0,000	0,011	0,006	0,001	0,474	0,969	0,003
UMPS	0,579	0,546	0,166	0,017	0,618	0,023	0,094	0,583	0,011	0,000	0,000	0,015	0,239	0,633	0,003
UCK2	0,925	0,538	0,052	0,048	0,781	0,012	0,039	0,270	0,006	0,000	0,000	0,078	0,704	1,000	0,005
FPGS	0,262	0,169	0,009	0,008	0,271	0,024	0,002	0,301	0,001	0,015	0,078	0,000	0,037	0,265	0,002
GCLC	0,173	0,489	0,027	0,028	0,419	0,935	0,699	0,945	0,474	0,239	0,704	0,037	0,000	0,025	0,801
UGTX	0,624	0,503	0,127	0,687	0,345	0,601	0,629	0,191	0,969	0,633	1,000	0,265	0,025	0,000	0,880
TOP1	0,834	0,872	0,318	0,213	0,839	0,004	0,011	0,211	0,003	0,003	0,005	0,002	0,801	0,880	0,000
TOP2A	0,207	0,858	0,527	0,775	0,097	0,420	0,109	0,815	0,021	0,403	0,478	0,050	0,519	0,515	0,107
KIT	0,024	0,458	0,382	0,967	0,048	0,908	0,648	0,063	0,545	0,711	0,945	0,748	0,381	0,166	0,265
PDGFRA	0,074	0,039	0,389	0,017	0,119	0,170	0,007	0,040	0,074	0,285	0,398	0,045	0,177	0,625	0,171
ERCC1	0,013	0,414	0,385	0,156	0,483	0,009	0,137	0,003	0,602	0,249	0,260	0,211	0,970	0,610	0,064
XPA	0,689	0,239	0,484	0,200	0,672	0,004	0,001	0,204	0,018	0,215	0,441	0,009	0,939	0,755	0,010
XPC	0,071	0,995	0,932	0,258	0,721	0,237	0,826	0,808	0,634	0,774	0,647	0,561	0,199	0,821	0,407
UDG	0,413	0,954	0,119	0,009	0,573	0,026	0,001	0,129	0,002	0,007	0,002	0,042	0,773	0,414	0,030
MLH1	0,284	0,875	0,029	0,010	0,673	0,503	0,093	0,704	0,019	0,004	0,028	0,007	0,021	0,757	0,037
PMS2	0,201	0,364	0,167	0,013	0,377	0,047	0,317	0,310	0,807	0,136	0,040	0,520	0,571	0,933	0,357
MSH2	0,479	0,786	0,130	0,051	0,303	0,199	0,006	0,010	0,004	0,151	0,031	0,026	0,627	0,229	0,026
MSH6	0,360	0,806	0,128	0,052	0,187	0,125	0,002	0,044	0,000	0,062	0,023	0,007	0,633	0,497	0,014
GADD45	0,116	0,880	0,278	0,305	0,243	0,332	0,643	0,276	0,832	0,261	0,657	0,427	0,545	0,184	0,128
BAX	0,132	0,689	0,403	0,819	0,427	0,018	0,380	0,278	0,539	0,231	0,210	0,223	0,992	0,807	0,022
P21	0,567	0,930	0,114	0,484	0,699	0,403	0,729	0,851	0,904	0,637	0,810	0,500	0,058	0,264	0,874
FAS	0,844	0,486	0,668	0,095	0,121	0,027	0,094	0,295	0,115	0,161	0,303	0,141	0,798	0,729	0,186
BCL2	0,886	0,292	0,878	0,226	0,669	0,376	0,580	0,950	0,589	0,728	0,764	0,570	0,053	0,655	0,269
DIABLO	0,285	0,999	0,232	0,035	0,179	0,050	0,214	0,152	0,321	0,011	0,024	0,169	0,347	0,904	0,063
BIRC2	0,783	0,952	0,106	0,001	0,937	0,049	0,015	0,025	0,012	0,019	0,036	0,024	0,106	0,497	0,117
XIAP	0,853	0,239	0,071	0,015	0,991	0,000	0,004	0,312	0,022	0,016	0,013	0,003	0,456	0,594	0,001
BIRC5	0,310	0,783	0,152	0,002	0,734	0,045	0,007	0,397	0,002	0,002	0,024	0,006	0,185	0,831	0,042
BIRC7	0,538	0,493	0,459	0,849	0,751	0,474	0,122	0,058	0,257	0,709	0,328	0,833	0,295	0,244	0,431
CFLAR	0,874	0,706	0,745	0,230	0,087	0,127	0,089	0,222	0,437	0,572	0,942	0,294	0,545	0,566	0,519
EGFR	0,932	0,048	0,080	0,024	0,174	0,009	0,032	0,340	0,072	0,250	0,085	0,035	0,698	0,587	0,102
MYC	0,435	0,322	0,051	0,144	0,451	0,003	0,000	0,321	0,004	0,058	0,011	0,014	0,768	0,784	0,001
MMP1	0,416	0,524	0,759	0,986	0,264	0,164	0,958	0,571	0,445	0,400	0,770	0,174	0,527	0,106	0,316
MMP2	0,306	0,578	0,028	0,005	0,795	0,071	0,193	0,074	0,717	0,046	0,106	0,540	0,122	0,875	0,987
TIGAR	0,002	0,334	0,629	0,869	0,128	0,289	0,483	0,197	0,897	0,393	0,420	0,933	0,734	0,957	0,354
NRF2	0,601	0,375	0,038	0,719	0,835	0,004	0,291	0,241	0,175	0,102	0,019	0,559	0,459	0,287	0,232
KEAP1	0,783	0,385	0,232	0,096	0,864	0,000	0,011	0,573	0,013	0,007	0,074	0,001	0,472	0,409	0,001
ENT1n	0,956	0,833	0,296	0,006	0,298	0,047	0,099	0,172	0,286	0,090	0,195	0,340	0,519	0,856	0,657
ENT2n	0,035	0,854	0,519	0,051	0,359	0,383	0,084	0,684	0,083	0,026	0,116	0,148	0,157	0,442	0,194
CNT1n	0,912	0,540	0,472	0,900	0,740	0,957	0,281	0,714	0,175	0,760	0,215	0,787	0,041	0,039	0,362
CNT2n	0,659	0,775	0,038	0,921	0,377	0,809	0,158	0,083	0,450	0,535	0,591	0,717	0,885	0,602	0,931
CNT3n	0,501	0,226	0,056	0,028	0,098	0,020	0,005	0,433	0,001	0,024	0,015	0,000	0,167	0,597	0,000

Correlat.	TOP2A	KIT	PDGFRA	ERCC1	XPA	XPC	UDG	MLH1	PMS2	MSH2	MSH6	GADD45	BAX	P21	FAS
OATP1B1	-0,625	0,000	0,000	-0,025	-0,135	-0,459	-0,586	-0,848	-0,429	0,163	0,045	0,315	-0,424	-0,303	0,595
OATP1B3	0,296	0,578	-0,392	0,157	0,429	0,210	0,301	0,483	-0,087	0,374	0,334	-0,185	0,415	0,390	-0,143
OATP2B1	-0,252	0,000	0,000	-0,096	-0,511	0,338	-0,497	-0,076	-0,193	-0,204	-0,411	0,007	0,290	0,406	-0,561
OATP4A1	0,251	0,250	-0,764	0,470	0,747	0,133	0,658	0,387	0,513	0,505	0,487	0,253	0,392	0,418	0,635
OCT1	0,006	-0,526	-0,583	0,667	0,433	-0,200	0,583	0,444	0,678	0,630	0,568	0,452	0,408	0,061	0,551
OCT2	0,157	0,000	0,000	0,166	0,441	0,003	-0,435	-0,252	0,390	0,063	-0,193	-0,256	0,485	0,717	0,446
OCT3	0,621	0,792	-0,515	-0,260	0,049	-0,260	0,303	-0,042	0,043	0,301	0,402	-0,607	-0,399	-0,202	-0,206
OCTN1	0,391	0,551	-0,843	0,138	0,329	-0,189	0,429	0,702	0,263	0,439	0,517	0,186	0,134	0,320	0,063
OCTN2	0,428	0,921	-0,681	-0,163	0,153	0,037	0,146	0,652	-0,044	0,226	0,229	-0,062	0,179	0,402	-0,190
CTR1	0,281	-0,393	-0,398	0,478	0,730	-0,153	0,265	0,226	0,132	0,273	0,377	0,227	0,183	-0,155	0,648
ENT1	0,112	-0,294	-0,882	0,686	0,438	-0,019	0,707	0,424	0,706	0,528	0,389	0,558	0,184	0,221	0,465
ENT2	0,230	0,667	-0,522	-0,059	0,299	-0,122	0,423	0,752	0,229	0,317	0,288	0,251	0,118	0,449	0,243
ENT3	0,214	0,018	-0,105	-0,305	-0,100	-0,312	0,078	0,304	0,162	0,438	0,363	-0,060	-0,089	-0,049	0,170
ENT4	-0,103	0,123	0,558	-0,273	-0,674	0,100	-0,140	-0,298	-0,174	-0,618	-0,462	0,006	-0,509	-0,144	-0,596
CNT3	0,299	0,391	-0,768	0,309	0,562	0,058	0,604	0,734	0,461	0,625	0,579	0,292	0,410	0,339	0,388
AQP1	-0,005	0,517	-0,036	-0,304	-0,013	0,454	-0,069	-0,010	-0,175	-0,441	-0,455	0,219	0,152	0,439	-0,279
AQP3	0,444	0,240	0,332	-0,327	0,407	-0,180	0,105	-0,157	-0,442	0,202	0,215	-0,365	0,002	0,169	0,188
AQP5	0,173	0,000	0,071	0,049	0,068	0,231	0,170	-0,206	0,170	0,349	0,162	0,221	0,212	0,080	-0,270
ABCA2	0,059	0,391	-0,408	0,102	0,379	0,164	-0,159	-0,232	-0,049	-0,250	-0,195	-0,217	0,177	0,005	0,021
ABCA3	0,055	0,619	-0,290	0,245	-0,062	0,542	0,072	-0,227	0,441	-0,188	-0,166	-0,084	0,146	0,178	-0,330
ABCB11	0,328	-0,062	0,000	0,402	0,471	-0,307	-0,102	-0,238	0,307	0,090	0,061	-0,035	0,304	0,185	0,202
ABCC1	0,151	0,239	-0,896	0,242	-0,107	-0,127	0,371	0,607	0,417	0,198	0,299	0,254	0,094	0,182	0,009
ABCC2	0,261	0,413	0,158	-0,496	-0,450	-0,331	0,316	0,201	-0,343	0,072	0,184	-0,388	-0,699	-0,272	-0,571
ABCC3	0,354	0,825	-0,792	-0,006	0,193	-0,200	0,259	0,816	0,144	0,263	0,281	0,307	0,010	0,237	-0,010
ABCC4	0,329	-0,602	0,128	0,525	0,076	0,395	0,234	0,185	0,158	0,091	0,172	0,491	0,442	-0,026	-0,119
ABCC5	-0,190	-0,687	-0,039	0,487	-0,123	0,117	0,276	0,517	0,628	0,057	0,102	0,409	0,302	-0,196	0,174
ABCC11	0,567	0,000	0,000	-0,632	0,313	-0,168	-0,014	-0,049	-0,451	-0,326	-0,182	-0,344	-0,384	0,668	-0,358
ABCG2	-0,369	-0,007	-0,083	-0,292	-0,585	-0,571	0,028	-0,250	0,070	-0,046	-0,082	-0,211	-0,777	-0,179	-0,281
MVP	0,272	0,877	-0,758	0,015	0,240	0,101	0,112	0,578	0,081	0,060	0,045	0,236	0,192	0,562	-0,115
ATP7A	-0,023	-0,281	-0,586	0,678	0,217	0,293	0,045	0,253	0,663	0,085	0,074	0,374	0,552	0,163	0,255
ATP7B	-0,360	-0,872	0,710	0,646	-0,118	0,497	-0,238	-0,308	0,364	-0,216	-0,265	0,439	0,422	-0,168	0,061
DPYD	-0,053	0,380	-0,779	0,237	0,337	0,002	0,017	0,046	0,263	0,084	0,072	0,044	0,118	0,026	0,212
TYMP	0,193	0,440	-0,434	0,263	0,213	0,026	0,454	0,605	0,408	0,462	0,445	-0,325	0,254	0,460	0,138
UPP1	0,084	-0,022	-0,842	0,401	0,364	-0,324	0,670	0,661	0,645	0,551	0,529	0,296	0,068	0,204	0,482
EPHX1	0,461	0,816	-0,644	-0,205	-0,124	-0,105	0,165	0,124	-0,256	0,310	0,374	-0,334	-0,231	-0,114	-0,452
DCK	0,235	-0,062	-0,582	0,667	0,711	0,338	0,591	0,195	0,538	0,381	0,430	0,280	0,619	0,243	0,609
RRM1	0,448	0,239	-0,892	0,418	0,788	0,065	0,786	0,466	0,289	0,713	0,747	0,136	0,255	0,102	0,484
TYMS	0,069	-0,788	0,777	0,727	0,362	0,072	0,426	0,112	0,292	0,681	0,545	0,313	0,312	0,055	0,315
TK1	0,609	0,313	-0,710	0,153	0,621	-0,140	0,755	0,617	0,072	0,734	0,841	0,063	0,180	0,036	0,459
UMPS	0,243	-0,195	-0,472	0,330	0,354	-0,084	0,687	0,714	0,419	0,422	0,511	0,323	0,342	0,138	0,413
UCK2	0,207	-0,037	-0,382	0,323	0,224	0,134	0,741	0,585	0,553	0,597	0,602	0,130	0,357	0,071	0,310
FPGS	0,532	0,169	-0,764	0,356	0,669	-0,170	0,549	0,682	0,188	0,612	0,685	0,231	0,348	0,197	0,432
GCLC	0,188	0,441	-0,575	0,011	-0,023	-0,365	0,085	0,608	0,166	0,149	0,140	0,177	0,003	0,518	-0,079
UGTX	0,209	0,724	-0,256	-0,164	-0,101	-0,073	-0,260	0,100	-0,027	-0,376	-0,218	-0,411	0,079	0,351	-0,118
TOP1	0,449	-0,544	-0,581	0,508	0,660	0,241	0,580	0,562	0,266	0,611	0,636	0,427	0,604	-0,047	0,391
TOP2A	1,000	0,576	-0,767	-0,056	0,448	-0,184	0,480	0,205	-0,402	0,398	0,575	-0,032	-0,215	-0,126	-0,194
KIT	0,576	1,000	0,000	-0,664	-0,085	0,266	-0,073	0,003	-0,336	-0,685	-0,461	-0,778	-0,446	0,565	-0,581
PDGFRA	-0,767	0,000	1,000	-0,157	-0,848	0,175	-0,852	-0,596	-0,492	-0,456	-0,683	-0,391	0,038	0,037	-0,377
ERCC1	-0,056	-0,664	-0,157	1,000	0,481	0,366	0,359	0,196	0,580	0,291	0,238	0,648	0,587	0,103	0,391
XPA	0,448	-0,085	-0,848	0,481	1,000	0,125	0,491	0,209	0,100	0,430	0,485	0,342	0,402	0,106	0,638
XPC	-0,184	0,266	0,175	0,366	0,125	1,000	-0,169	-0,139	0,228	-0,273	-0,372	0,205	0,684	0,316	-0,037
UDG	0,480	-0,073	-0,852	0,359	0,491	-0,169	1,000	0,500	0,298	0,743	0,808	0,199	-0,052	-0,115	0,291
MLH1	0,205	0,003	-0,596	0,196	0,209	-0,139	0,500	1,000	0,327	0,445	0,477	0,338	0,194	0,122	0,247
PMS2	-0,402	-0,336	-0,492	0,580	0,100	0,228	0,298	0,327	1,000	0,194	0,086	0,373	0,433	0,196	0,461
MSH2	0,398	-0,685	-0,456	0,291	0,430	-0,273	0,743	0,445	0,194	1,000	0,936	0,099	0,091	-0,208	0,267
MSH6	0,575	-0,461	-0,683	0,238	0,485	-0,372	0,808	0,477	0,086	0,936	1,000	0,071	-0,046	-0,283	0,286
GADD45	-0,032	-0,778	-0,391	0,648	0,342	0,205	0,199	0,338	0,373	0,099	0,071	1,000	0,394	0,040	0,332
BAX	-0,215	-0,446	0,038	0,587	0,402	0,684	-0,052	0,194	0,433	0,091	-0,046	0,394	1,000	0,440	0,441
P21	-0,126	0,565	0,037	0,103	0,106	0,316	-0,115	0,122	0,196	-0,208	-0,283	0,040	0,440	1,000	0,107
FAS	-0,194	-0,581	-0,377	0,391	0,638	-0,037	0,291	0,247	0,461	0,267	0,286	0,332	0,441	0,107	1,000
BCL2	0,203	0,012	0,856	-0,026	0,417	0,070	-0,085	-0,346	-0,334	0,262	0,210	-0,308	0,296	-0,717	0,212
DIABLO	-0,272	-0,452	-0,219	0,692	0,267	0,335	0,347	0,643	0,751	0,185	0,126	0,539	0,644	0,350	0,513
BIRC2	0,259	-0,259	-0,708	0,526	0,469	-0,162	0,744	0,580	0,445	0,701	0,598	0,511	0,149	0,306	0,489
XIAP	0,379	-0,083	-0,822	0,568	0,697	0,174	0,583	0,463	0,608	0,491	0,516	0,366	0,484	0,099	0,510
BIRC5	0,477	0,141	-0,886	0,348	0,538	-0,182	0,836	0,693	0,267	0,450	0,610	0,395	0,030	0,108	0,427
BIRC7	0,094	0,000	0,000	0,477	0,348	0,464	0,432	0,382	0,192	0,375	0,351	-0,049	0,175	0,004	0,121
CFLAR	0,135	-0,108	-0,480	0,462	0,707	0,160	0,258	0,112	0,205	0,057	0,047	0,436	0,271	0,504	0,496
EGFR	0,265	0,025	-0,823	0,342	0,422	-0,136	0,516	0,146	0,479	0,529	0,592	0,141	0,160	-0,122	0,434
MYC	0,434	0,381	-0,701	0,323	0,687	0,223	0,692	0,352	0,250	0,647	0,665	-0,019	0,372	-0,019	0,313
MMP1	0,216	-0,604	0,657	0,216	0,385	-0,057	-0,128	-0,102	0,102	0,027	0,061	0,096	0,388	0,258	0,461
MMP2	-0,761	0,000	0,000	0,763	-0,156	-0,029	0,834	0,724	0,881	0,744	0,555	0,661	0,152	0,242	0,533
TIGAR	-0,368	-0,834	0,701	0,562	0,003	0,393	-0,145	0,088	0,427	-0,144	-0,167	0,542	0,630	0,123	0,481
NRF2	0,144	0,220	0,416	0,291	0,241	0,281	0,408	-0,114	0,258	0,139	0,232	-0,202	0,374	0,288	0,283
KEAP1	0,489	0,215	-0,802	0,495	0,776	0,210	0,562	0,422	0,192	0,257	0,408	0,431	0,510	0,241	0,472
ENT1n	0,095	-0,196	-0,606	0,513	0,408	-0,159	0,657	0,232	0,510	0,206	0,283	0,345	-0,049	0,215	0,474
ENT2n	0,128	0,641	-0,595	-0,051	0,389	-0,032	0,453	0,602	0,273	0,275	0,236	0,277	0,156	0,412	0,348
CNT1n	0,125	-0,255	-0,159	-0,094	0,081	0,001	0,436	0,176	0,002	0,446	0,470	-0,032	-0,210	-0,682	0,202
CNT2n	0,010	-0,414	-0,400	-0,046	-0,072	-0,143	-0,102	-0,006	-0,053	-0,483	-0,302	0,485	-0,126	-0,199	0,071
CNT3n	0,550	0,331	-0,895	0,297	0,545	-0,019	0,596	0,612	0,281	0,668	0,720	0,314	0,343	0,030	0,312

P Values	TOP2A	KIT	PDGFRA	ERCC1	XPA	XPC	UDG	MLH1	PMS2	MSH2	MSH6	GADD45	BAX	P21	FAS
OATP1B1	0,185	1,000	1,000	0,963	0,799	0,360	0,221	0,033	0,396	0,758	0,933	0,543	0,402	0,559	0,290
OATP1B3	0,351	0,230	0,442	0,625	0,164	0,512	0,341	0,112	0,787	0,257	0,288	0,565	0,180	0,210	0,674
OATP2B1	0,547	1,000	1,000	0,821	0,195	0,414	0,210	0,859	0,647	0,628	0,312	0,987	0,486	0,319	0,190
OATP4A1	0,386	0,632	0,045	0,090	0,002	0,649	0,010	0,172	0,061	0,078	0,078	0,383	0,165	0,136	0,020
OCT1	0,984	0,284	0,225	0,013	0,139	0,512	0,036	0,128	0,011	0,028	0,043	0,121	0,166	0,843	0,063
OCT2	0,767	1,000	1,000	0,753	0,381	0,996	0,389	0,630	0,445	0,906	0,714	0,624	0,330	0,109	0,451
OCT3	0,042	0,110	0,375	0,439	0,887	0,441	0,365	0,902	0,900	0,368	0,221	0,048	0,224	0,551	0,568
OCTN1	0,186	0,257	0,017	0,653	0,273	0,537	0,143	0,008	0,385	0,153	0,070	0,543	0,661	0,287	0,847
OCTN2	0,127	0,009	0,092	0,579	0,601	0,900	0,619	0,012	0,882	0,458	0,431	0,832	0,540	0,155	0,533
CTR1	0,331	0,441	0,377	0,084	0,003	0,601	0,360	0,438	0,653	0,367	0,184	0,435	0,531	0,596	0,017
ENT1	0,704	0,572	0,009	0,007	0,117	0,950	0,005	0,130	0,005	0,064	0,169	0,038	0,528	0,448	0,110
ENT2	0,429	0,148	0,230	0,841	0,299	0,678	0,131	0,002	0,431	0,292	0,319	0,386	0,688	0,108	0,424
ENT3	0,463	0,973	0,823	0,289	0,733	0,277	0,790	0,291	0,581	0,135	0,202	0,838	0,763	0,869	0,579
ENT4	0,737	0,817	0,249	0,367	0,012	0,746	0,648	0,323	0,569	0,032	0,112	0,983	0,076	0,638	0,041
CNT3	0,320	0,444	0,044	0,305	0,046	0,851	0,029	0,004	0,113	0,030	0,038	0,333	0,164	0,257	0,213
AQP1	0,990	0,373	0,946	0,393	0,971	0,187	0,851	0,977	0,630	0,202	0,187	0,543	0,676	0,204	0,467
AQP3	0,128	0,647	0,521	0,276	0,167	0,556	0,732	0,608	0,131	0,530	0,481	0,220	0,994	0,581	0,559
AQP5	0,611	1,000	0,910	0,886	0,842	0,495	0,618	0,543	0,618	0,292	0,635	0,514	0,532	0,815	0,422
ABCA2	0,841	0,443	0,364	0,730	0,181	0,576	0,587	0,424	0,869	0,409	0,503	0,457	0,545	0,987	0,946
ABCA3	0,859	0,265	0,529	0,419	0,841	0,056	0,815	0,456	0,132	0,559	0,589	0,784	0,633	0,560	0,294
ABCB11	0,428	0,921	1,000	0,324	0,239	0,460	0,809	0,570	0,459	0,833	0,885	0,935	0,463	0,661	0,664
ABCC1	0,607	0,648	0,006	0,404	0,715	0,666	0,192	0,021	0,138	0,516	0,299	0,380	0,750	0,534	0,978
ABCC2	0,368	0,416	0,735	0,071	0,107	0,248	0,272	0,490	0,230	0,816	0,528	0,170	0,005	0,347	0,042
ABCC3	0,214	0,043	0,034	0,983	0,509	0,493	0,372	0,000	0,622	0,386	0,331	0,285	0,974	0,415	0,973
ABCC4	0,250	0,206	0,784	0,054	0,797	0,163	0,420	0,526	0,589	0,768	0,556	0,075	0,114	0,929	0,700
ABCC5	0,515	0,131	0,934	0,077	0,674	0,690	0,340	0,059	0,016	0,854	0,728	0,147	0,294	0,503	0,570
ABCC11	0,185	1,000	1,000	0,128	0,495	0,718	0,977	0,918	0,310	0,476	0,697	0,450	0,395	0,101	0,486
ABCG2	0,238	0,989	0,876	0,357	0,046	0,053	0,932	0,434	0,830	0,893	0,799	0,510	0,003	0,577	0,403
MVP	0,346	0,022	0,048	0,959	0,409	0,730	0,702	0,030	0,783	0,847	0,878	0,417	0,511	0,037	0,708
ATP7A	0,938	0,590	0,167	0,008	0,456	0,309	0,880	0,382	0,010	0,783	0,802	0,188	0,041	0,579	0,400
ATP7B	0,207	0,024	0,074	0,013	0,689	0,071	0,413	0,284	0,201	0,479	0,360	0,116	0,132	0,567	0,844
DPYD	0,858	0,458	0,039	0,414	0,239	0,995	0,954	0,875	0,364	0,786	0,806	0,880	0,689	0,930	0,486
TYMP	0,527	0,382	0,389	0,385	0,484	0,932	0,119	0,029	0,167	0,130	0,128	0,278	0,403	0,114	0,668
UPP1	0,775	0,967	0,017	0,156	0,200	0,258	0,009	0,010	0,013	0,051	0,052	0,305	0,819	0,484	0,095
EPHX1	0,097	0,048	0,119	0,483	0,672	0,721	0,573	0,673	0,377	0,303	0,187	0,243	0,427	0,699	0,121
DCK	0,420	0,908	0,170	0,009	0,004	0,237	0,026	0,503	0,047	0,199	0,125	0,332	0,018	0,403	0,027
RRM1	0,109	0,648	0,007	0,137	0,001	0,826	0,001	0,093	0,317	0,006	0,002	0,643	0,380	0,729	0,094
TYMS	0,815	0,063	0,040	0,003	0,204	0,808	0,129	0,704	0,310	0,010	0,044	0,276	0,278	0,851	0,295
TK1	0,021	0,545	0,074	0,602	0,018	0,634	0,002	0,019	0,807	0,004	0,000	0,832	0,539	0,904	0,115
UMPS	0,403	0,711	0,285	0,249	0,215	0,774	0,007	0,004	0,136	0,151	0,062	0,261	0,231	0,637	0,161
UCK2	0,478	0,945	0,398	0,260	0,441	0,647	0,002	0,028	0,040	0,031	0,023	0,657	0,210	0,810	0,303
FPGS	0,050	0,748	0,045	0,211	0,009	0,561	0,042	0,007	0,520	0,026	0,007	0,427	0,223	0,500	0,141
GCLC	0,519	0,381	0,177	0,970	0,939	0,199	0,773	0,021	0,571	0,627	0,633	0,545	0,992	0,058	0,798
UGTX	0,515	0,166	0,625	0,610	0,755	0,821	0,414	0,757	0,933	0,229	0,497	0,184	0,807	0,264	0,729
TOP1	0,107	0,265	0,171	0,064	0,010	0,407	0,030	0,037	0,357	0,026	0,014	0,128	0,022	0,874	0,186
TOP2A	0,000	0,231	0,044	0,850	0,108	0,528	0,082	0,482	0,154	0,178	0,032	0,914	0,461	0,669	0,526
KIT	0,231	0,000	1,000	0,151	0,873	0,611	0,891	0,995	0,515	0,202	0,358	0,069	0,375	0,243	0,304
PDGFRA	0,044	1,000	0,000	0,736	0,016	0,707	0,015	0,158	0,262	0,303	0,091	0,386	0,935	0,938	0,461
ERCC1	0,850	0,151	0,736	0,000	0,082	0,198	0,208	0,502	0,030	0,335	0,413	0,012	0,027	0,726	0,186
XPA	0,108	0,873	0,016	0,082	0,000	0,671	0,074	0,474	0,735	0,142	0,079	0,231	0,155	0,719	0,019
XPC	0,528	0,611	0,707	0,198	0,671	0,000	0,563	0,635	0,434	0,367	0,190	0,481	0,007	0,271	0,904
UDG	0,082	0,891	0,015	0,208	0,074	0,563	0,000	0,069	0,301	0,004	0,000	0,495	0,860	0,694	0,334
MLH1	0,482	0,995	0,158	0,502	0,474	0,635	0,069	0,000	0,254	0,127	0,085	0,237	0,506	0,677	0,416
PMS2	0,154	0,515	0,262	0,030	0,735	0,434	0,301	0,254	0,000	0,525	0,770	0,188	0,122	0,502	0,113
MSH2	0,178	0,202	0,303	0,335	0,142	0,367	0,004	0,127	0,525	0,000	0,000	0,748	0,767	0,495	0,401
MSH6	0,032	0,358	0,091	0,413	0,079	0,190	0,000	0,085	0,770	0,000	0,000	0,810	0,876	0,326	0,343
GADD45	0,914	0,069	0,386	0,012	0,231	0,481	0,495	0,237	0,188	0,748	0,810	0,000	0,164	0,892	0,268
BAX	0,461	0,375	0,935	0,027	0,155	0,007	0,860	0,506	0,122	0,767	0,876	0,164	0,000	0,116	0,131
P21	0,669	0,243	0,938	0,726	0,719	0,271	0,694	0,677	0,502	0,495	0,326	0,892	0,116	0,000	0,728
FAS	0,526	0,304	0,461	0,186	0,019	0,904	0,334	0,416	0,113	0,401	0,343	0,268	0,131	0,728	0,000
BCL2	0,528	0,985	0,064	0,936	0,178	0,828	0,792	0,271	0,288	0,436	0,513	0,329	0,351	0,009	0,508
DIABLO	0,346	0,368	0,638	0,006	0,356	0,242	0,224	0,013	0,002	0,544	0,668	0,047	0,013	0,220	0,073
BIRC2	0,371	0,620	0,075	0,053	0,090	0,580	0,002	0,030	0,111	0,008	0,024	0,062	0,610	0,287	0,090
XIAP	0,182	0,876	0,023	0,034	0,006	0,553	0,029	0,095	0,021	0,088	0,059	0,198	0,079	0,735	0,075
BIRC5	0,085	0,790	0,008	0,223	0,047	0,533	0,000	0,006	0,357	0,123	0,021	0,162	0,918	0,714	0,145
BIRC7	0,811	1,000	1,000	0,194	0,358	0,208	0,246	0,310	0,620	0,360	0,354	0,901	0,652	0,991	0,775
CFLAR	0,646	0,839	0,275	0,097	0,005	0,585	0,372	0,702	0,481	0,854	0,872	0,119	0,349	0,066	0,085
EGFR	0,360	0,962	0,023	0,231	0,133	0,642	0,059	0,618	0,083	0,063	0,026	0,632	0,584	0,677	0,138
MYC	0,121	0,456	0,079	0,260	0,007	0,444	0,006	0,218	0,389	0,017	0,010	0,949	0,190	0,948	0,298
MMP1	0,500	0,280	0,229	0,500	0,216	0,861	0,691	0,753	0,753	0,936	0,850	0,766	0,213	0,419	0,131
MMP2	0,079	1,000	1,000	0,078	0,768	0,956	0,039	0,104	0,020	0,150	0,253	0,153	0,774	0,645	0,276
TIGAR	0,196	0,039	0,079	0,037	0,991	0,164	0,620	0,764	0,128	0,638	0,568	0,045	0,016	0,676	0,096
NRF2	0,623	0,675	0,353	0,313	0,406	0,331	0,148	0,699	0,374	0,651	0,424	0,488	0,188	0,317	0,349
KEAP1	0,076	0,683	0,030	0,072	0,001	0,472	0,036	0,133	0,510	0,397	0,147	0,124	0,063	0,406	0,104
ENT1n	0,748	0,710	0,149	0,061	0,148	0,587	0,011	0,424	0,063	0,500	0,326	0,227	0,867	0,460	0,102
ENT2n	0,664	0,170	0,159	0,862	0,169	0,912	0,104	0,023	0,345	0,363	0,416	0,338	0,593	0,143	0,244
CNT1n	0,671	0,626	0,734	0,750	0,783	0,998	0,119	0,547	0,994	0,127	0,090	0,913	0,472	0,007	0,508
CNT2n	0,973	0,414	0,374	0,875	0,807	0,625	0,729	0,985	0,856	0,095	0,294	0,079	0,669	0,495	0,817
CNT3n	0,042	0,522	0,006	0,303	0,044	0,950	0,025	0,020	0,330	0,013	0,004	0,274	0,230	0,920	0,300

Correlat.	BCL2	DIABLO	BIRC2	XIAP	BIRC5	BIRC7	CFLAR	EGFR	MYC	MMP1	MMP2	TIGAR	NRF2	KEAP1	ENT1n
OATP1B1	-0,198	-0,390	0,306	-0,567	-0,577	0,000	0,182	-0,608	-0,749	0,271	0,000	0,685	-0,530	-0,620	0,083
OATP1B3	0,497	0,129	0,118	0,306	0,255	0,187	0,111	0,187	0,693	-0,170	-0,260	-0,332	0,306	0,575	-0,124
OATP2B1	-0,710	0,201	-0,582	-0,493	-0,743	0,057	-0,151	-0,828	-0,298	-0,015	0,000	0,197	0,156	-0,296	-0,842
OATP4A1	-0,028	0,470	0,676	0,784	0,650	0,232	0,621	0,615	0,744	0,126	0,920	-0,100	0,374	0,715	0,603
OCT1	0,020	0,597	0,633	0,723	0,527	-0,017	0,202	0,684	0,488	0,307	0,986	0,294	0,363	0,621	0,519
OCT2	0,482	-0,210	0,173	0,655	-0,127	-0,258	0,472	0,562	0,260	0,649	0,000	-0,379	-0,157	0,187	0,220
OCT3	0,309	-0,433	-0,051	0,435	0,116	0,139	-0,232	0,497	0,363	0,268	0,000	-0,475	0,414	0,031	0,035
OCTN1	-0,258	0,328	0,406	0,549	0,548	-0,289	0,189	0,384	0,500	-0,176	0,425	-0,326	-0,194	0,525	0,196
OCTN2	-0,155	0,145	0,183	0,326	0,359	-0,122	-0,007	0,141	0,353	-0,129	-0,496	-0,294	-0,123	0,400	-0,180
CTR1	0,357	0,300	0,350	0,539	0,405	0,598	0,526	0,291	0,316	0,579	0,241	0,197	0,075	0,449	0,410
ENT1	-0,431	0,671	0,858	0,673	0,752	0,278	0,572	0,494	0,331	0,152	0,926	0,268	0,345	0,539	0,915
ENT2	-0,499	0,463	0,562	0,402	0,594	0,193	0,448	-0,018	0,315	0,036	0,094	-0,136	-0,047	0,371	0,321
ENT3	-0,155	-0,014	0,215	0,233	0,093	-0,233	-0,179	0,301	-0,000	0,408	-0,055	0,086	-0,016	-0,142	-0,106
ENT4	-0,580	-0,254	-0,185	-0,547	-0,127	-0,108	-0,278	-0,396	-0,591	-0,464	0,147	0,009	-0,100	-0,460	0,044
CNT3	-0,138	0,526	0,631	0,759	0,653	0,234	0,365	0,560	0,730	-0,106	0,712	-0,141	0,112	0,700	0,302
AQP1	-0,421	0,055	-0,235	-0,099	0,026	-0,076	0,272	-0,506	0,021	-0,375	0,000	-0,147	0,013	0,278	-0,082
AQP3	0,402	-0,229	-0,012	0,068	0,063	0,127	0,322	-0,190	0,274	0,477	-0,744	-0,231	0,380	0,202	-0,022
AQP5	0,011	-0,074	-0,055	0,293	-0,244	-0,020	0,007	0,127	0,365	-0,054	-0,886	-0,168	0,148	0,073	-0,291
ABCA2	0,738	-0,136	-0,396	0,255	-0,151	-0,203	0,130	0,143	0,337	0,106	-0,444	-0,333	-0,004	0,311	-0,087
ABCA3	-0,137	0,032	-0,053	0,367	-0,045	0,116	-0,043	0,394	0,236	-0,195	0,342	-0,066	0,288	0,105	0,131
ABCB11	0,703	0,057	-0,074	0,643	-0,111	-0,847	0,417	0,414	0,312	0,830	0,000	-0,193	0,201	0,391	0,364
ABCC1	-0,390	0,393	0,518	0,359	0,564	-0,238	-0,198	0,514	0,084	-0,072	0,897	0,181	0,105	0,378	0,280
ABCC2	-0,366	-0,267	-0,034	-0,383	0,153	0,253	-0,365	-0,346	-0,042	-0,619	-0,188	-0,535	-0,115	-0,335	-0,021
ABCC3	-0,409	0,304	0,420	0,394	0,543	-0,303	0,183	0,154	0,193	-0,372	0,267	-0,214	-0,414	0,358	0,103
ABCC4	-0,004	0,346	0,241	0,367	0,261	0,105	-0,097	0,197	0,151	0,280	0,169	0,576	0,390	0,478	0,062
ABCC5	-0,247	0,723	0,237	0,406	0,293	0,304	-0,158	0,108	0,106	0,122	0,614	0,548	0,164	0,196	0,263
ABCC11	-0,321	-0,476	0,015	0,136	0,306	-0,453	0,553	-0,122	0,061	0,527	0,000	-0,703	0,089	0,495	0,484
ABCG2	-0,843	-0,313	0,102	-0,485	-0,090	-0,208	-0,205	-0,016	-0,590	-0,487	0,539	-0,359	-0,411	-0,667	0,232
MVP	-0,455	0,237	0,325	0,311	0,410	-0,231	0,308	0,100	0,209	-0,425	-0,049	-0,252	-0,276	0,432	0,054
ATP7A	-0,001	0,539	0,265	0,660	0,176	0,027	0,106	0,551	0,194	0,416	0,574	0,495	0,177	0,392	0,215
ATP7B	0,046	0,308	-0,081	0,055	-0,293	0,238	-0,047	0,025	-0,227	0,259	0,506	0,754	0,153	-0,081	0,016
DPYD	0,332	-0,000	0,018	0,336	0,081	-0,264	0,111	0,536	0,286	-0,204	0,289	-0,279	-0,257	0,252	0,062
TYMP	-0,052	0,356	0,469	0,515	0,421	0,284	0,100	0,503	0,551	0,099	0,860	-0,148	0,579	0,356	0,314
UPP1	-0,377	0,566	0,774	0,634	0,744	0,074	0,343	0,598	0,411	-0,006	0,942	-0,049	0,106	0,463	0,697
EPHX1	0,138	-0,381	-0,023	-0,003	0,100	-0,124	-0,474	0,385	0,219	-0,351	-0,137	-0,427	-0,061	0,050	-0,300
DCK	0,281	0,532	0,535	0,839	0,542	0,275	0,428	0,671	0,727	0,429	0,773	0,305	0,717	0,813	0,538
RRM1	0,178	0,354	0,633	0,720	0,685	0,554	0,471	0,572	0,875	-0,017	0,615	-0,205	0,304	0,653	0,459
TYMS	-0,020	0,404	0,594	0,292	0,246	0,651	0,349	0,276	0,287	0,182	0,770	0,367	0,335	0,165	0,387
TK1	0,174	0,287	0,647	0,606	0,759	0,423	0,226	0,496	0,709	0,244	0,191	-0,038	0,384	0,641	0,307
UMPS	-0,112	0,658	0,617	0,630	0,743	0,145	0,165	0,330	0,517	0,268	0,820	0,248	0,455	0,683	0,470
UCK2	-0,097	0,599	0,562	0,646	0,599	0,370	-0,022	0,477	0,652	0,095	0,722	0,234	0,614	0,492	0,368
FPGS	0,182	0,389	0,598	0,730	0,691	0,083	0,302	0,566	0,636	0,420	0,318	-0,025	0,171	0,768	0,276
GCLC	-0,571	0,272	0,450	0,217	0,376	-0,393	0,177	0,114	-0,087	0,203	0,700	-0,100	-0,215	0,210	0,188
UGTX	0,162	-0,039	-0,218	0,171	0,069	-0,466	-0,184	0,175	-0,089	0,514	-0,099	0,018	0,335	0,263	-0,059
TOP1	0,347	0,509	0,438	0,784	0,549	0,301	0,189	0,455	0,771	0,317	0,008	0,268	0,341	0,784	0,130
TOP2A	0,203	-0,272	0,259	0,379	0,477	0,094	0,135	0,265	0,434	0,216	-0,761	-0,368	0,144	0,489	0,095
KIT	0,012	-0,452	-0,259	-0,083	0,141	0,000	-0,108	0,025	0,381	-0,604	0,000	-0,834	0,220	0,215	-0,196
PDGFRA	0,856	-0,219	-0,708	-0,822	-0,886	0,000	-0,480	-0,823	-0,701	0,657	0,000	0,701	0,416	-0,802	-0,606
ERCC1	-0,026	0,692	0,526	0,568	0,348	0,477	0,462	0,342	0,323	0,216	0,763	0,562	0,291	0,495	0,513
XPA	0,417	0,267	0,469	0,697	0,538	0,348	0,707	0,422	0,687	0,385	-0,156	0,003	0,241	0,776	0,408
XPC	0,070	0,335	-0,162	0,174	-0,182	0,464	0,160	-0,136	0,223	-0,057	-0,029	0,393	0,281	0,210	-0,159
UDG	-0,085	0,347	0,744	0,583	0,836	0,432	0,258	0,516	0,692	-0,128	0,834	-0,145	0,408	0,562	0,657
MLH1	-0,346	0,643	0,580	0,463	0,693	0,382	0,112	0,146	0,352	-0,102	0,724	0,088	-0,114	0,422	0,232
PMS2	-0,334	0,751	0,445	0,608	0,267	0,192	0,205	0,479	0,250	0,102	0,881	0,427	0,258	0,192	0,510
MSH2	0,262	0,185	0,701	0,491	0,450	0,375	0,057	0,529	0,647	0,027	0,744	-0,144	0,139	0,257	0,206
MSH6	0,210	0,126	0,598	0,516	0,610	0,351	0,047	0,592	0,665	0,061	0,555	-0,167	0,232	0,408	0,283
GADD45	-0,308	0,539	0,511	0,366	0,395	-0,049	0,436	0,141	-0,019	0,096	0,661	0,542	-0,202	0,431	0,345
BAX	0,296	0,644	0,149	0,484	0,030	0,175	0,271	0,160	0,372	0,388	0,152	0,630	0,374	0,510	-0,049
P21	-0,717	0,350	0,306	0,099	0,108	0,004	0,504	-0,122	-0,019	0,258	0,242	0,123	0,288	0,241	0,215
FAS	0,212	0,513	0,489	0,510	0,427	0,121	0,496	0,434	0,313	0,461	0,533	0,481	0,283	0,472	0,474
BCL2	1,000	-0,383	-0,433	0,143	-0,246	-0,308	-0,230	0,278	0,434	0,346	-0,673	-0,101	0,208	0,240	-0,422
DIABLO	-0,383	1,000	0,583	0,549	0,480	0,461	0,392	0,116	0,284	0,179	0,776	0,604	0,266	0,432	0,485
BIRC2	-0,433	0,583	1,000	0,530	0,846	0,347	0,555	0,442	0,315	0,146	0,911	0,226	0,283	0,534	0,782
XIAP	0,143	0,549	0,530	1,000	0,587	0,249	0,405	0,688	0,735	0,456	0,468	0,167	0,369	0,745	0,460
BIRC5	-0,246	0,480	0,846	0,587	1,000	0,269	0,417	0,434	0,461	0,053	0,822	0,034	0,253	0,727	0,714
BIRC7	-0,308	0,461	0,347	0,249	0,269	1,000	0,357	-0,213	0,452	-0,151	0,000	0,090	0,359	0,023	0,288
CFLAR	-0,230	0,392	0,555	0,405	0,417	0,357	1,000	-0,002	0,217	0,317	0,475	0,082	0,114	0,452	0,635
EGFR	0,278	0,116	0,442	0,688	0,434	-0,213	-0,002	1,000	0,512	0,219	0,615	0,039	0,332	0,489	0,346
MYC	0,434	0,284	0,315	0,735	0,461	0,452	0,217	0,512	1,000	0,010	-0,012	-0,221	0,432	0,637	0,196
MMP1	0,346	0,179	0,146	0,456	0,053	-0,151	0,317	0,219	0,010	1,000	-0,221	0,520	0,461	0,361	0,141
MMP2	-0,673	0,776	0,911	0,468	0,822	0,000	0,475	0,615	-0,012	-0,221	1,000	0,586	0,481	0,215	0,825
TIGAR	-0,101	0,604	0,226	0,167	0,034	0,090	0,082	0,039	-0,221	0,520	0,586	1,000	0,289	0,172	0,128
NRF2	0,208	0,266	0,283	0,369	0,253	0,359	0,114	0,332	0,432	0,461	0,481	0,289	1,000	0,421	0,380
KEAP1	0,240	0,432	0,534	0,745	0,727	0,023	0,452	0,489	0,637	0,361	0,215	0,172	0,421	1,000	0,422
ENT1n	-0,422	0,485	0,782	0,460	0,714	0,288	0,635	0,346	0,196	0,141	0,825	0,128	0,380	0,422	1,000
ENT2n	-0,389	0,423	0,510	0,413	0,558	0,077	0,503	0,039	0,398	-0,088	0,054	-0,175	0,002	0,409	0,359
CNT1n	0,256	-0,032	0,039	0,071	0,187	0,434	-0,258	0,134	0,356	-0,409	0,032	-0,079	-0,039	-0,096	-0,055
CNT2n	-0,111	-0,038	-0,015	-0,035	0,201	-0,689	-0,052	0,014	-0,402	0,127	-0,096	0,264	-0,201	0,243	0,135
CNT3n	0,162	0,298	0,548	0,771	0,643	-0,067	0,075	0,746	0,672	0,207	0,297	0,026	0,183	0,721	0,156

P Values	BCL2	DIABLO	BIRC2	XIAP	BIRC5	BIRC7	CFLAR	EGFR	MYC	MMP1	MMP2	TIGAR	NRF2	KEAP1	ENT1n
OATP1B1	0,749	0,444	0,556	0,241	0,231	1,000	0,730	0,200	0,087	0,659	1,000	0,133	0,280	0,189	0,876
OATP1B3	0,144	0,689	0,716	0,333	0,425	0,658	0,732	0,561	0,012	0,616	0,619	0,292	0,333	0,050	0,702
OATP2B1	0,114	0,633	0,130	0,215	0,035	0,914	0,721	0,011	0,473	0,974	1,000	0,639	0,713	0,477	0,009
OATP4A1	0,931	0,090	0,008	0,001	0,012	0,547	0,018	0,019	0,002	0,696	0,009	0,733	0,188	0,004	0,023
OCT1	0,954	0,031	0,020	0,005	0,064	0,966	0,507	0,010	0,091	0,359	0,002	0,329	0,223	0,023	0,069
OCT2	0,411	0,690	0,743	0,158	0,810	0,675	0,344	0,246	0,619	0,236	1,000	0,459	0,767	0,723	0,675
OCT3	0,386	0,183	0,882	0,181	0,735	0,767	0,492	0,120	0,272	0,453	1,000	0,140	0,206	0,928	0,920
OCTN1	0,443	0,273	0,168	0,052	0,053	0,488	0,536	0,195	0,082	0,604	0,401	0,277	0,525	0,066	0,522
OCTN2	0,630	0,620	0,532	0,255	0,207	0,754	0,980	0,631	0,216	0,689	0,317	0,308	0,675	0,157	0,539
CTR1	0,255	0,298	0,221	0,046	0,150	0,089	0,053	0,312	0,270	0,048	0,645	0,499	0,800	0,108	0,146
ENT1	0,162	0,009	0,000	0,008	0,002	0,469	0,033	0,072	0,248	0,637	0,008	0,355	0,227	0,047	0,000
ENT2	0,099	0,095	0,036	0,154	0,025	0,618	0,108	0,951	0,273	0,910	0,859	0,643	0,874	0,192	0,263
ENT3	0,631	0,963	0,460	0,423	0,752	0,546	0,541	0,296	1,000	0,188	0,917	0,770	0,958	0,628	0,718
ENT4	0,061	0,402	0,545	0,053	0,680	0,782	0,357	0,180	0,034	0,151	0,814	0,977	0,744	0,114	0,887
CNT3	0,687	0,065	0,021	0,003	0,016	0,577	0,220	0,047	0,005	0,757	0,113	0,645	0,715	0,008	0,316
AQP1	0,299	0,879	0,512	0,786	0,944	0,871	0,448	0,136	0,955	0,360	1,000	0,686	0,971	0,437	0,823
AQP3	0,220	0,451	0,968	0,826	0,839	0,745	0,284	0,535	0,366	0,117	0,090	0,448	0,200	0,509	0,944
AQP5	0,976	0,828	0,872	0,382	0,470	0,966	0,983	0,711	0,269	0,875	0,045	0,622	0,663	0,832	0,386
ABCA2	0,006	0,644	0,161	0,379	0,606	0,600	0,657	0,626	0,239	0,742	0,378	0,245	0,989	0,280	0,766
ABCA3	0,688	0,917	0,863	0,217	0,883	0,785	0,890	0,183	0,439	0,566	0,507	0,829	0,339	0,733	0,669
ABCB11	0,078	0,894	0,862	0,086	0,794	0,070	0,304	0,308	0,452	0,021	1,000	0,647	0,634	0,338	0,376
ABCC1	0,210	0,165	0,058	0,208	0,036	0,538	0,499	0,060	0,776	0,824	0,015	0,536	0,722	0,183	0,332
ABCC2	0,243	0,356	0,909	0,177	0,601	0,511	0,199	0,226	0,887	0,032	0,721	0,049	0,695	0,242	0,944
ABCC3	0,187	0,291	0,135	0,163	0,045	0,428	0,530	0,599	0,510	0,233	0,609	0,462	0,141	0,209	0,725
ABCC4	0,990	0,226	0,406	0,197	0,368	0,788	0,740	0,499	0,605	0,377	0,748	0,031	0,168	0,084	0,834
ABCC5	0,439	0,004	0,415	0,150	0,310	0,426	0,590	0,713	0,718	0,705	0,194	0,043	0,576	0,501	0,364
ABCC11	0,534	0,280	0,974	0,771	0,505	0,443	0,198	0,795	0,896	0,362	1,000	0,078	0,850	0,259	0,271
ABCG2	0,002	0,322	0,752	0,110	0,781	0,621	0,523	0,960	0,043	0,129	0,270	0,251	0,184	0,018	0,468
MVP	0,137	0,415	0,257	0,279	0,145	0,550	0,283	0,733	0,474	0,168	0,927	0,385	0,340	0,123	0,855
ATP7A	0,997	0,046	0,360	0,010	0,548	0,946	0,717	0,041	0,507	0,179	0,233	0,072	0,544	0,166	0,460
ATP7B	0,886	0,285	0,783	0,853	0,310	0,538	0,874	0,932	0,435	0,416	0,306	0,002	0,601	0,783	0,956
DPYD	0,292	0,999	0,952	0,239	0,783	0,493	0,706	0,048	0,322	0,524	0,578	0,334	0,375	0,385	0,833
TYMP	0,878	0,232	0,106	0,071	0,152	0,459	0,745	0,080	0,051	0,759	0,028	0,629	0,038	0,232	0,296
UPP1	0,226	0,035	0,001	0,015	0,002	0,849	0,230	0,024	0,144	0,986	0,005	0,869	0,719	0,096	0,006
EPHX1	0,669	0,179	0,937	0,991	0,734	0,751	0,087	0,174	0,451	0,264	0,795	0,128	0,835	0,864	0,298
DCK	0,376	0,050	0,049	0,000	0,045	0,474	0,127	0,009	0,003	0,164	0,071	0,289	0,004	0,000	0,047
RRM1	0,580	0,214	0,015	0,004	0,007	0,122	0,089	0,032	0,000	0,958	0,193	0,483	0,291	0,011	0,099
TYMS	0,950	0,152	0,025	0,312	0,397	0,058	0,222	0,340	0,321	0,571	0,074	0,197	0,241	0,573	0,172
TK1	0,589	0,321	0,012	0,022	0,002	0,257	0,437	0,072	0,004	0,445	0,717	0,897	0,175	0,013	0,286
UMPS	0,728	0,011	0,019	0,016	0,002	0,709	0,572	0,250	0,058	0,400	0,046	0,393	0,102	0,007	0,090
UCK2	0,764	0,024	0,036	0,013	0,024	0,328	0,942	0,085	0,011	0,770	0,106	0,420	0,019	0,074	0,195
FPGS	0,570	0,169	0,024	0,003	0,006	0,833	0,294	0,035	0,014	0,174	0,540	0,933	0,559	0,001	0,340
GCLC	0,053	0,347	0,106	0,456	0,185	0,295	0,545	0,698	0,768	0,527	0,122	0,734	0,459	0,472	0,519
UGTX	0,655	0,904	0,497	0,594	0,831	0,244	0,566	0,587	0,784	0,106	0,875	0,957	0,287	0,409	0,856
TOP1	0,269	0,063	0,117	0,001	0,042	0,431	0,519	0,102	0,001	0,316	0,987	0,354	0,232	0,001	0,657
TOP2A	0,528	0,346	0,371	0,182	0,085	0,811	0,646	0,360	0,121	0,500	0,079	0,196	0,623	0,076	0,748
KIT	0,985	0,368	0,620	0,876	0,790	1,000	0,839	0,962	0,456	0,280	1,000	0,039	0,675	0,683	0,710
PDGFRA	0,064	0,638	0,075	0,023	0,008	1,000	0,275	0,023	0,079	0,229	1,000	0,079	0,353	0,030	0,149
ERCC1	0,936	0,006	0,053	0,034	0,223	0,194	0,097	0,231	0,260	0,500	0,078	0,037	0,313	0,072	0,061
XPA	0,178	0,356	0,090	0,006	0,047	0,358	0,005	0,133	0,007	0,216	0,768	0,991	0,406	0,001	0,148
XPC	0,828	0,242	0,580	0,553	0,533	0,208	0,585	0,642	0,444	0,861	0,956	0,164	0,331	0,472	0,587
UDG	0,792	0,224	0,002	0,029	0,000	0,246	0,372	0,059	0,006	0,691	0,039	0,620	0,148	0,036	0,011
MLH1	0,271	0,013	0,030	0,095	0,006	0,310	0,702	0,618	0,218	0,753	0,104	0,764	0,699	0,133	0,424
PMS2	0,288	0,002	0,111	0,021	0,357	0,620	0,481	0,083	0,389	0,753	0,020	0,128	0,374	0,510	0,063
MSH2	0,436	0,544	0,008	0,088	0,123	0,360	0,854	0,063	0,017	0,936	0,150	0,638	0,651	0,397	0,500
MSH6	0,513	0,668	0,024	0,059	0,021	0,354	0,872	0,026	0,010	0,850	0,253	0,568	0,424	0,147	0,326
GADD45	0,329	0,047	0,062	0,198	0,162	0,901	0,119	0,632	0,949	0,766	0,153	0,045	0,488	0,124	0,227
BAX	0,351	0,013	0,610	0,079	0,918	0,652	0,349	0,584	0,190	0,213	0,774	0,016	0,188	0,063	0,867
P21	0,009	0,220	0,287	0,735	0,714	0,991	0,066	0,677	0,948	0,419	0,645	0,676	0,317	0,406	0,460
FAS	0,508	0,073	0,090	0,075	0,145	0,775	0,085	0,138	0,298	0,131	0,276	0,096	0,349	0,104	0,102
BCL2	0,000	0,219	0,160	0,658	0,440	0,502	0,471	0,382	0,158	0,297	0,213	0,756	0,517	0,453	0,172
DIABLO	0,219	0,000	0,029	0,042	0,082	0,211	0,166	0,693	0,325	0,577	0,069	0,022	0,357	0,123	0,078
BIRC2	0,160	0,029	0,000	0,051	0,000	0,361	0,040	0,114	0,273	0,652	0,012	0,437	0,327	0,049	0,001
XIAP	0,658	0,042	0,051	0,000	0,027	0,518	0,151	0,007	0,003	0,136	0,350	0,568	0,194	0,002	0,098
BIRC5	0,440	0,082	0,000	0,027	0,000	0,483	0,138	0,121	0,097	0,870	0,045	0,908	0,383	0,003	0,004
BIRC7	0,502	0,211	0,361	0,518	0,483	0,000	0,346	0,583	0,221	0,721	1,000	0,818	0,343	0,954	0,453
CFLAR	0,471	0,166	0,040	0,151	0,138	0,346	0,000	0,994	0,455	0,316	0,341	0,780	0,698	0,105	0,015
EGFR	0,382	0,693	0,114	0,007	0,121	0,583	0,994	0,000	0,061	0,494	0,194	0,894	0,247	0,076	0,226
MYC	0,158	0,325	0,273	0,003	0,097	0,221	0,455	0,061	0,000	0,975	0,982	0,448	0,123	0,014	0,502
MMP1	0,297	0,577	0,652	0,136	0,870	0,721	0,316	0,494	0,975	0,000	0,674	0,083	0,132	0,250	0,663
MMP2	0,213	0,069	0,012	0,350	0,045	1,000	0,341	0,194	0,982	0,674	0,000	0,222	0,334	0,682	0,043
TIGAR	0,756	0,022	0,437	0,568	0,908	0,818	0,780	0,894	0,448	0,083	0,222	0,000	0,316	0,557	0,662
NRF2	0,517	0,357	0,327	0,194	0,383	0,343	0,698	0,247	0,123	0,132	0,334	0,316	0,000	0,134	0,180
KEAP1	0,453	0,123	0,049	0,002	0,003	0,954	0,105	0,076	0,014	0,250	0,682	0,557	0,134	0,000	0,133
ENT1n	0,172	0,078	0,001	0,098	0,004	0,453	0,015	0,226	0,502	0,663	0,043	0,662	0,180	0,133	0,000
ENT2n	0,211	0,132	0,062	0,142	0,038	0,843	0,067	0,895	0,159	0,786	0,919	0,550	0,996	0,146	0,207
CNT1n	0,422	0,915	0,894	0,808	0,522	0,243	0,373	0,647	0,212	0,187	0,952	0,789	0,894	0,743	0,852
CNT2n	0,731	0,898	0,959	0,906	0,491	0,040	0,859	0,962	0,154	0,695	0,856	0,361	0,490	0,402	0,646
CNT3n	0,614	0,301	0,043	0,001	0,013	0,865	0,798	0,002	0,009	0,518	0,567	0,930	0,531	0,004	0,595

Correlat.	ENT2n	CNT1n	CNT2n	CNT3n
OATP1B1	-0,252	0,340	0,144	-0,735
OATP1B3	0,335	-0,271	-0,454	0,507
OATP2B1	0,192	-0,414	-0,132	-0,460
OATP4A1	0,609	-0,048	-0,223	0,651
OCT1	0,332	-0,055	0,039	0,639
OCT2	0,031	-0,627	-0,473	0,405
OCT3	-0,159	0,143	-0,343	0,395
OCTN1	0,524	-0,304	0,001	0,705
OCTN2	0,437	-0,183	-0,153	0,620
CTR1	0,019	0,081	-0,027	0,281
ENT1	0,425	-0,030	0,125	0,417
ENT2	0,943	-0,005	-0,023	0,426
ENT3	0,247	0,249	-0,098	0,395
ENT4	-0,267	0,067	0,429	-0,533
CNT3	0,724	0,063	-0,278	0,892
AQP1	0,569	-0,175	0,404	-0,178
AQP3	0,422	-0,014	-0,184	-0,002
AQP5	0,406	0,024	-0,124	0,258
ABCA2	-0,139	-0,312	-0,013	0,021
ABCA3	-0,136	-0,088	-0,120	0,162
ABCB11	0,041	-0,580	-0,100	0,254
ABCC1	0,117	-0,153	0,212	0,610
ABCC2	0,111	0,399	-0,105	-0,180
ABCC3	0,581	-0,106	0,094	0,598
ABCC4	-0,167	-0,033	0,293	0,403
ABCC5	0,072	0,155	0,252	0,194
ABCC11	0,359	-0,578	0,116	0,040
ABCG2	-0,163	0,079	-0,026	-0,451
MVP	0,547	-0,357	0,007	0,504
ATP7A	-0,165	-0,290	0,020	0,472
ATP7B	-0,565	-0,033	0,129	-0,196
DPYD	-0,054	-0,179	-0,084	0,345
TYMP	0,197	-0,219	-0,579	0,541
UPP1	0,531	-0,037	-0,029	0,585
EPHX1	-0,265	0,098	-0,256	0,461
DCK	0,253	-0,016	-0,071	0,613
RRM1	0,477	0,310	-0,399	0,706
TYMS	-0,120	0,108	-0,479	0,228
TK1	0,479	0,385	-0,220	0,786
UMPS	0,590	0,090	0,181	0,598
UCK2	0,439	0,354	-0,158	0,632
FPGS	0,407	-0,079	-0,107	0,865
GCLC	0,400	-0,552	0,042	0,391
UGTX	-0,245	-0,601	0,168	0,170
TOP1	0,369	0,264	-0,025	0,807
TOP2A	0,128	0,125	0,010	0,550
KIT	0,641	-0,255	-0,414	0,331
PDGFRA	-0,595	-0,159	-0,400	-0,895
ERCC1	-0,051	-0,094	-0,046	0,297
XPA	0,389	0,081	-0,072	0,545
XPC	-0,032	0,001	-0,143	-0,019
UDG	0,453	0,436	-0,102	0,596
MLH1	0,602	0,176	-0,006	0,612
PMS2	0,273	0,002	-0,053	0,281
MSH2	0,275	0,446	-0,483	0,668
MSH6	0,236	0,470	-0,302	0,720
GADD45	0,277	-0,032	0,485	0,314
BAX	0,156	-0,210	-0,126	0,343
P21	0,412	-0,682	-0,199	0,030
FAS	0,348	0,202	0,071	0,312
BCL2	-0,389	0,256	-0,111	0,162
DIABLO	0,423	-0,032	-0,038	0,298
BIRC2	0,510	0,039	-0,015	0,548
XIAP	0,413	0,071	-0,035	0,771
BIRC5	0,558	0,187	0,201	0,643
BIRC7	0,077	0,434	-0,689	-0,067
CFLAR	0,503	-0,258	-0,052	0,075
EGFR	0,039	0,134	0,014	0,746
MYC	0,398	0,356	-0,402	0,672
MMP1	-0,088	-0,409	0,127	0,207
MMP2	0,054	0,032	-0,096	0,297
TIGAR	-0,175	-0,079	0,264	0,026
NRF2	0,002	-0,039	-0,201	0,183
KEAP1	0,409	-0,096	0,243	0,721
ENT1n	0,359	-0,055	0,135	0,156
ENT2n	1,000	0,069	0,030	0,380
CNT1n	0,069	1,000	-0,135	0,168
CNT2n	0,030	-0,135	1,000	-0,006
CNT3n	0,380	0,168	-0,006	1,000

P Values	ENT2n	CNT1n	CNT2n	CNT3n
OATP1B1	0,630	0,510	0,786	0,096
OATP1B3	0,288	0,394	0,139	0,093
OATP2B1	0,648	0,307	0,755	0,251
OATP4A1	0,021	0,869	0,444	0,012
OCT1	0,268	0,859	0,900	0,019
OCT2	0,953	0,182	0,344	0,425
OCT3	0,642	0,676	0,302	0,230
OCTN1	0,066	0,313	0,997	0,007
OCTN2	0,118	0,531	0,601	0,018
CTR1	0,948	0,783	0,926	0,331
ENT1	0,129	0,919	0,670	0,138
ENT2	0,000	0,985	0,939	0,129
ENT3	0,395	0,390	0,740	0,163
ENT4	0,378	0,828	0,144	0,061
CNT3	0,005	0,837	0,357	0,000
AQP1	0,086	0,628	0,247	0,623
AQP3	0,151	0,964	0,548	0,995
AQP5	0,216	0,945	0,715	0,444
ABCA2	0,634	0,277	0,965	0,943
ABCA3	0,659	0,776	0,696	0,597
ABCB11	0,923	0,131	0,813	0,544
ABCC1	0,691	0,601	0,467	0,020
ABCC2	0,706	0,157	0,722	0,539
ABCC3	0,029	0,720	0,749	0,024
ABCC4	0,568	0,910	0,310	0,153
ABCC5	0,807	0,596	0,385	0,507
ABCC11	0,429	0,175	0,805	0,931
ABCG2	0,613	0,808	0,935	0,141
MVP	0,043	0,210	0,981	0,066
ATP7A	0,573	0,315	0,946	0,088
ATP7B	0,035	0,912	0,659	0,501
DPYD	0,854	0,540	0,775	0,226
TYMP	0,519	0,472	0,038	0,056
UPP1	0,051	0,900	0,921	0,028
EPHX1	0,359	0,740	0,377	0,098
DCK	0,383	0,957	0,809	0,020
RRM1	0,084	0,281	0,158	0,005
TYMS	0,684	0,714	0,083	0,433
TK1	0,083	0,175	0,450	0,001
UMPS	0,026	0,760	0,535	0,024
UCK2	0,116	0,215	0,591	0,015
FPGS	0,148	0,787	0,717	0,000
GCLC	0,157	0,041	0,885	0,167
UGTX	0,442	0,039	0,602	0,597
TOP1	0,194	0,362	0,931	0,000
TOP2A	0,664	0,671	0,973	0,042
KIT	0,170	0,626	0,414	0,522
PDGFRA	0,159	0,734	0,374	0,006
ERCC1	0,862	0,750	0,875	0,303
XPA	0,169	0,783	0,807	0,044
XPC	0,912	0,998	0,625	0,950
UDG	0,104	0,119	0,729	0,025
MLH1	0,023	0,547	0,985	0,020
PMS2	0,345	0,994	0,856	0,330
MSH2	0,363	0,127	0,095	0,013
MSH6	0,416	0,090	0,294	0,004
GADD45	0,338	0,913	0,079	0,274
BAX	0,593	0,472	0,669	0,230
P21	0,143	0,007	0,495	0,920
FAS	0,244	0,508	0,817	0,300
BCL2	0,211	0,422	0,731	0,614
DIABLO	0,132	0,915	0,898	0,301
BIRC2	0,062	0,894	0,959	0,043
XIAP	0,142	0,808	0,906	0,001
BIRC5	0,038	0,522	0,491	0,013
BIRC7	0,843	0,243	0,040	0,865
CFLAR	0,067	0,373	0,859	0,798
EGFR	0,895	0,647	0,962	0,002
MYC	0,159	0,212	0,154	0,009
MMP1	0,786	0,187	0,695	0,518
MMP2	0,919	0,952	0,856	0,567
TIGAR	0,550	0,789	0,361	0,930
NRF2	0,996	0,894	0,490	0,531
KEAP1	0,146	0,743	0,402	0,004
ENT1n	0,207	0,852	0,646	0,595
ENT2n	0,000	0,814	0,919	0,180
CNT1n	0,814	0,000	0,646	0,566
CNT2n	0,919	0,646	0,000	0,982
CNT3n	0,180	0,566	0,982	0,000

Table 25. Values of Pearson coefficient and statistic P-value in correlations between genes.

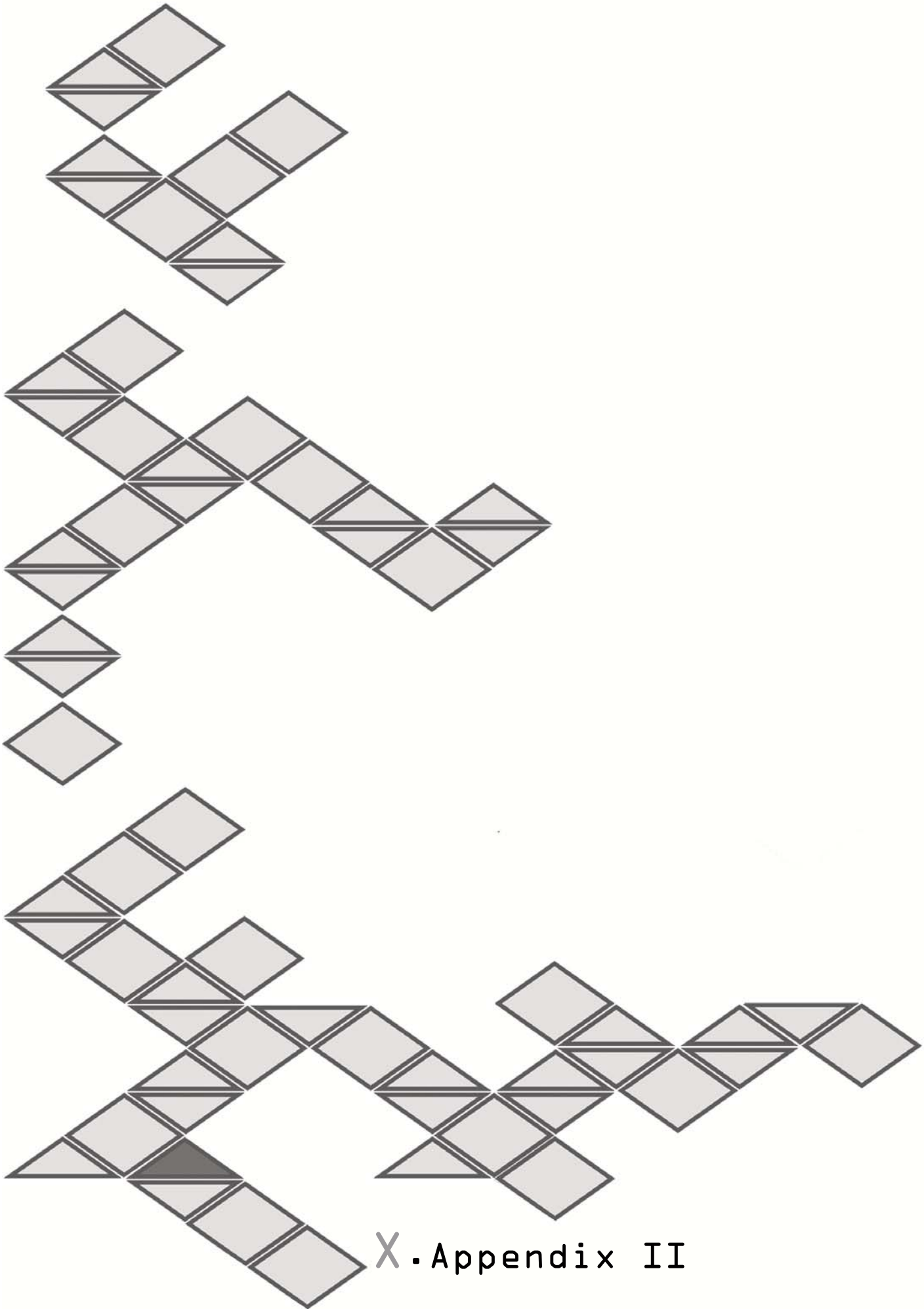

X. Appendix II

23 RECIPES FOR SOLUTIONS AND BUFFERS

- Ampicillin 1000x: Ampicillin 100 mg/ml in dd$H_2$0 and autoclaved by 0.22 µm filtering.
- Biotinylation washing buffer 2: Tris-HCl 50 mM (pH 7.5), NaCl 500 mM and NP-40 0.001% buffer.
- Biotinylation washing buffer 3: Tris-HCl 10 mM (pH 7.5)
- Crude membranes lysis buffer: Tris-HCl 10mM (pH 7.5), EDTA 1 mM, NaCl 0.1 mM.
- Crude membranes solubilizing buffer: Tris-HCl (pH 7.5) 50 mM, EDTA 1 mM, Triton X-100 1% and SDS 0.5%.
- Dropout mix 10x: Dissolve 400 mg adenine, 200 mg arginine, 200 mg histidine, 300 mg isoleucine, 1,000 mg leucine, 300 mg lysine, 1,500 mg methionine, 500 mg phenylalanine, 2,000 mg threonine, 400 mg tryptophan, 300 mg tyrosine, 200 mg uracil and 1,500 mg valine in a total volume of 1 litre ddH_2O and autoclave. Store at 4 °C for up to 6 months. Remove the components indicated for specific selection.
- Electrophoresis Solution A: see Acrylamide solution in commercial references.
- Electrophoresis Solution B: Tris-HCl 1.5 M (pH 8.8) and SDS 0.4%
- Electrophoresis Solution C: Tris-HCl 0.5 M (pH 6.8) and SDS 0.4%
- Kanamycin 1000x: Kanamycin 50 mg/ml in dd$H_2$0 and autoclaved by 0.22 µm filtering.
- LB (Luria-Broth) liquid medium: Bacto-tryptone 1% (w/v), yeast extract 0.5% (w/v) and NaCl 1% (w/v), pH 7 adjusted by adding NaOH. Autoclaving.
- LB-agar medium: Bacto-tryptone 1% (w/v), yeast extract 0.5% (w/v) and NaCl 1% (w/v), pH 7 adjusted by adding NaOH. Agar 1.5% added before autoclaving.
- M9 Minimal medium: D-glucose 0.5 M, $Na_2HPO_4 \cdot 7H_2O$ 0.02 M, KH_2PO_4 0.02 M, NaCl 0.01 M, NH_4Cl 0.02 M supplemented with $CaCl_2$ 0.1 mM, $MgSO_4$ 1 mM, 50 µg/ml kanamycin and 200 µl/l trace metals.
- ND96 medium: NaCl 96 mM, KCl 2 mM and Hepes 5 mM supplemented with gentamicin sulphate (50 µg/ml), penicillin G (100 µg/ml), pyruvic acid 2mM, theophylline 90 mg, $MgCl_2$ 1mM and $CaCl_2$ 1.8 mM
- NP-40 buffer: Tris-HCl 50 mM pH=8, NaCl 150 mM, NP-40 1% (v/v), $Na_4P_2O_7$ 5 mM and NaF 50 mM.
- PBS: NaCl 140 mM, KCl 2.7 mM, KH_2PO_4 1.5 mM and Na_2HPO_4 8.1 mM.
- PBS-Ca/Mg: PBS supplemented with $CaCl_2$ 1mM and $MgCl_2$ 1mM.
- Ponceau solution: Acetic acid 5% (v/v) and Ponceau S 0.1% (w/v)

- Protein Loading Buffer 5x (PLB 5x): Tris-HCl 60 mM (pH 6.8), glycerol 25%, SDS 2%, β-mercaptoethanol 0.05% and BrPheOH Blue 0.1%
- Running buffer 10x: Tris-HCl 25 mM (pH 8.3), glycine 192 mM and SDS 0.1%.
- Synthetic Dropout media (liquid and solid): Dissolve 6.7 g yeast nitrogen base, 20 g d-glucose and 20 g agar (omit if preparing liquid medium) in a total volume of 900 ml ddH_2O. Add 100 ml of the appropriate 10× Dropout Mix (if preparing SD-Trp medium, use 10× Dropout Mix prepared without tryptophan) and autoclave. For solid medium, allow to cool to 55 °C and pour into sterile Petri dishes. Note that if you wish to include 3-AT in the solid medium, reduce the initial volume of ddH_2O by the volume of 1 M 3-AT solution needed to obtain the desired concentration. Add 3-AT solution after autoclaving, once the medium has cooled to 55 °C.
- T300: Tris-HCL 10 mM, NaCl 0.5 M; pH8
- TBS 10x: Tris-HCl 2 M (pH 7.5) NaCl 4 M
- TBS-T: TBS 1x and Tween-20 0.1%
- Transfection calcium buffer: 500 mM $CaCl_2$ and 100 mM BES, pH=6.95. Sterilized by 0.22 µm membrane-filtering. pH is adjusted with NaOH. pH was optimized for HeLa cells transfection, other cell lines might need another pH.
- Transfection phosphate buffer: 280 mM NaCl, 0.75 mM Na_2HPO_4, 0.75 mM NaH_2PO_4 and 50 mM BES. Sterilized by 0.22 µm membrane-filtering.
- Transfer buffer 1x: Tris base 25 mM, Glycine 192 mM and Methanol 20%.
- Transport Choline buffer: Choline-chloride 137 mM, KCl 5.4 mM, $CaCl_2$ 1.8 mM, $MgSO_4$ 1.2 mM, and Hepes 10 mM. pH adjusted to 7.4 with Tris base 1M.
- Transport Lysis buffer: Triton-X100 0.5%, NaOH 100 mM.
- Transport STOP buffer: NaCl 137 mM and Hepes 10 mM. pH adjusted to 7.4 with Tris base 1M.
- Yeast transformation buffer: For 110 μl of reaction add 80 μl of PEG-3350 50%, 10 μl of LiOAc 1 M, 10 μl of DTT 0.1 M and 10 μl of commercial single-stranded DNA 2 mg/ml.
- YPAD media (liquid and solid): Dissolve 10 g yeast extract, 20 g peptone, 20 g d-glucose, 40 mg adenine sulphate and 20 g agar (omit if preparing liquid medium) in a total volume of 1 litre ddH_2O and autoclave. For solid medium, allow to cool to 50 °C and pour into sterile Petri dishes.

24 COMMERCIAL REFERENCES

- 3-AT (Bioshop - ATT124): 3-amino-1,2,4-triazole
- [γ-^{32}P]-ATP (Perkin elmer - BLU002H250UC): ATP, [γ-^{32}P]- 3000Ci/mmol 5mCi/ml
- Acrylamide solution (Bio-rad - 1610148): 40% Acrylamide/Bis Solution, 37.5:1.
- Antibiotic-antimycotic 100x (GIBCO - 15240062): contains penicillin G, streptomycin sulfate and amphotericin B in 0.85% NaCl.
- Antibodies:
    - Anti-ENT2 (Abcam - ab48595): Rabbit polyclonal.
    - Anti-FLAG (Abcam - ab106218): Mouse monoclonal, HRP conjugated.
    - Anti-HA (Roche - 11867423001): High affinity, rat monoclonal, clone 3F10.
    - Anti-NPC (Abcam - ab50008): Mouse monoclonal, clone 414.
    - Donkey anti-mouse Alexa Fluor® 555 (Invitrogen - A31570): anti IgG (H+L).
    - Donkey anti-rat Alexa Fluor® 488 (Invitrogen - A21208): anti IgG (H+L).
    - Goat anti-mouse Alexa Fluor® 488 (Invitrogen - A11001): anti IgG (H+L).
    - Goat anti-mouse Alexa Fluor@ 456 (Invitrogen - A11003): IgG (H+L).
    - Goat anti-mouse HRP (BioRad - 170-6516): anti IgG (H+L), HRP conjugated.
    - Goat anti-rabbit HRP (BioRad - 170-6516): anti IgG (H+L), HRP conjugated.
    - Goat anti-rat HRP (Abcam - ab7097): anti IgG (H+L), HRP conjugated.

- BCA protein assay (Thermo Scientific - 23227): Pierce BCA protein assay kit.
- BigDye® Terminator v3.1 Cycle Sequencing Kit (Applied Biosystems - 4337455)
- Bradford protein assay (Bio-Rad - 500-0205): Quick Start Bradford 1x dye reagent.
- CamKII (Calbiochem - 208707): Ca^{2+}/Calmodulin Kinase II, rat brain.
- cDNA library for MYTH screening (Dual-systems P02234): mouse embryo on day 11.
- CKII (Calbiochem - 218701): Casein Kinase II, human.
- Collagenase Type I (Sigma-Aldrich - C1639): form *Clostridium histolyticum*.
- Competent cell (Invitrogen - 18265-017): Subcloning Efficiency™ DH5α™.
- Cycloheximide (Sigma-Aldrich - C4859): 100 mg/ml in DMSO, 0.2 µm filtered.
- DAPI (Invitrogen - D1306): Nucleic acid stain, excitation/emission: 358/461 nm.
- DMEM (GIBCO - 11965-118): Dulbecco's Modified Eagle Medium with high glucose.
- DMEM - F12 (GIBCO - 11320-033): Dulbecco's Modified Eagle Medium:Ham's F12 (1:1).
- DNA ladder 1 Kb (New England Biolabs - N3231)

- DNA ladder 100 bp (New England Biolabs - N3232)
- ECL Solution (Thermo Scientific - 32106): Pierce ECL Western-Blot substrate.
- F12-K (GIBCO - 21127-022): Kaighn's modification of Ham's F-12 Nutrient Mixture.
- FBS (GIBCO - 12483-020): Fetal Bovine Serum, qualified.
- Films for autoradiography (Amersham - 28906835): Amersham Hyperfilm ECL.
- Gel extraction kit (Qiagen - 28704): DNA extraction from agarose gels.
- Gel loading dye 6x (New England Biolabs - B70216S)
- GlutaMAX™-1 100x (GIBCO - 35050061): 200 mM L-alanyl-L-glutamine dipeptide in 0.85% NaCl.
- Histone H1 (Calbiochem - 382150): Histone H1 from Calf Thymus.
- IMDM (GIBCO - 12440-053): Iscove's Modified Dulbecco's Medium.
- IPTG (Calbiochem - 420322): Isopropyl-β-D-thiogalactopyranoside, dioxane - free.
- L-Glutamine 200 mM 100x (GIBCO - 25030-081): supplied at 29.2 mg/ml in 0.85% NaCl.
- Lipofectamine® 2000 (Invitrogen - 11668-019): solution in membrane-filtered water.
- Maxi-prep Kit (Qiagen - 12163): QIAGEN Plasmid Maxi Kit.
- MEM non-essential aminoacids 100x (GIBCO: 11140-050): 10 mM in MEM-alpha medium.
- Mini-prep kit (Sigma-Aldrich - PLN70): GenElute™ Plasmid Mini-prep kit.
- Microcon YM-3 columns (Millipore - 42403): Ultracel YM-3 membrane.
- MitoTracker® (Invitrogen - M7510): Orange CMTMRos in methanol.
- mMessage mMachine® Kit (Ambion - AM1344)
- Mounting medium (MP Biomedicals - ICN622701): Immuno-fluore 25 ml.
- MTT (Invitrogen: M-6494): 3-(4,5-Dimethylthiazol-2-yl)-2,5diphenyltetrazolium bromide.
- Multiple tissue CDNA panel (Clontech - 636742/636743)
- Nitrocellulose membrane (Bio-Rad - 1620090): Supported Nitrocellulose Membrane 0.45 micron.
- NP-40 (Bioshop - NON505): Nonidet P40
- PageBlue™ Protein Staining solution (Thermo Scientific - R0571).
- PDD (Sigma-Aldrich - P9018): Phorbol 12,13-didecanoate.
- Penicillin-Streptomycin 100x (GIBCO - 15070-063): contains 5000 units of penicillin and 5000 µg of streptomycin per ml.
- PfuTurbo® DNA polymerase (Roche - 600250): High fidelity polymerase.
- pGemT® Easy vector (Promega - A1360)

- PKA (Calbiochem - 539481): PKA, catalytic subunit from mouse.
- PKC (Calbiochem - 539513): PKC, catalytic subunit from rat brain.
- Protease inhibitors cocktail (Roche - 11836153001): Complete, Mini; Tablets.
- Protein marker (New England Biolabs - P7709): ColorPlus Prestained Protein Marker.
- Reverse transcription kit (Applied biosystems - 4374966): High Capacity cDNA reverse transcription kit.
- RPMI 1640 (GIBCO - A10491-01): Roswell Park Memorial Institute 1640.
- Single-stranded DNA (Sigma-Aldrich - D7656): ssDNA from salmon testes.
- Sodium Pyruvate 100 mM (GIBCO - 11360-070): The final concentration used in most cell culture medium is 1 mM.
- Streptavidin-agarose beads (Sigma-Aldrich - s1638): from *Streptomyces avidinii*.
- Sulfo-NHS-LC-Biotin (Thermo scientific - 127062-22-0): EZ-Link Sulfo-NHS-LC-Biotin.
- SV Total RNA isolation System (Promega - Z3100)
- SYBR® Green PCR Master Mix (Applied-Biosystems - 4309155)
- SYBR® Safe (Invitrogen - S33102): DNA gel stain.
- T4 DNA ligase (New ENgland Biolabs - M0202)
- Taq DNA polymerase (New England Biolabs - M0273S)
- TaqMan@ Universal PCR master mix (Applied-Biosystems - 4324018)
- TEMED (Sigma-Aldrich - T9281): N,N,N',N'-Tetramethylethylenediamine.
- TO-PRO@-3 Iodide (Invitrogen - T3605): 1 mM in DMSO, excitation/emission: 642/661 nm.
- TRITON® X-100 (Bioshop - TRX506)
- Trypsin-EDTA (GIBCO - 25200-072): 0,25% trypsin with EDTA 1mM and phenol red.
- WGA (Invitrogen - W11262): Wheat germ agglutinin Alexa Fluor® 594 conjugated.

25 EXTERNAL LINKS FROM INTERNET

A. GenBank: http://www.ncbi.nlm.nih.gov/genbank

B. Clone Manager: http://www.scied.com

C. TMHMM 2.0: http://www.cbs.dtu.dk/services/TMHMM

D. ORF Finder - NCBI: http://www.ncbi.nlm.nih.gov/gorf.html

E. NCBI: http://www.ncbi.nlm.nih.gov

F. BLAST: http://blast.ncbi.nlm.nih.gov

G. DNA 2.0: http://www.dna20.com

H. NetPhosK: http://www.cbs.dtu.dk/services/NetPhosK

I. R-Project: http://www.r-project.org

J. CIBERehd Bioinformatics Platform: http://bioinfo.ciberehd.org

K. ATCC: http://www.atcc.org

L. DSMZ: http://www.dsmz.de

M. CCiTUB: http://www.ccit.ub.edu